Interdisciplinary Cardiovascular Health Research: Quantitative Methods, Heliogeophysical Influence, Demographics, and Spatial Trends

by

Joseph M. Caswell

A thesis submitted in partial fulfillment
of the requirements for the degree of
Doctor of Philosophy (PhD) in Human Studies

The Faculty of Graduate Studies
Laurentian University
Sudbury, Ontario, Canada

THESIS DEFENCE COMMITTEE/COMITÉ DE SOUTENANCE DE THÈSE
Laurentian Université/Université Laurentienne

Faculty of Graduate Studies/Faculté des études supérieures

Title of Thesis Titre de la thèse	Interdisciplinary Cardiovascular Health Research: Quantitative Methods, Heliogeophysical Influence, Demographics, and Spatial Trends	
Name of Candidate Nom du candidat	Caswell, Joseph	
Degree Diplôme	Doctor of Philosophy	
Department/Program Département/Programme	Human Studies	Date of Defence Date de la soutenance January 13, 2017

APPROVED/APPROUVÉ

Thesis Examiners/Examinateurs de thèse:

Dr. Michael Persinger
(Supervisor/Directeur(trice) de thèse)

Dr. Cynthia Whissell
(Committee member/Membre du comité)

Dr. John Lewko
(Committee member/Membre du comité)

Approved for the Faculty of Graduate Studies
Approuvé pour la Faculté des études supérieures
Dr. David Lesbarrères
Monsieur David Lesbarrères
Dean, Faculty of Graduate Studies
Doyen, Faculté des études supérieures

Dr. Borislav Dimitrov
(External Examiner/Examinateur externe)

Dr. Frank Mallory
(Internal Examiner/Examinateur interne)

ACCESSIBILITY CLAUSE AND PERMISSION TO USE

Abstract

The study of cardiovascular health involves myriad scientific disciplines associated with diverse factors that contribute to health which further necessitates interdisciplinary endeavors. The current series of studies concern cardiovascular health from multiple interdisciplinary perspectives including biomedical signal processing, heliobiology, and public health, with a particular focus on quantitative methods throughout. The first study examined heart rate variability (HRV) derived from healthy and arrhythmia human electrocardiograph records. Data processed using wavelet entropy was quantitatively novel compared to traditional indices of HRV and also demonstrated significant accuracy for prediction and classification of arrhythmia. Next, heliobiological perspectives of cardiovascular physiology were examined beginning with experimental verification of previous correlational results. Artificially simulated geomagnetic impulses were associated with significant increases in participant HRV, particularly for frequency-based components. An additional pilot case study demonstrated similar effects for natural geomagnetic storms, while a nonlinear relationship was observed overall for HRV and geomagnetic activity. National data regarding mortalities due to hypertensive diseases in Canada from 1979 to 2009 were aggregated and investigated for periodic components and relationships with space weather parameters. Time-lagged linear correlations were observed along with conspicuously overlapping temporal trends, for which geomagnetic activity and solar wind pressures were identified as central sources of variance. Finally, three ecological cross-sectional studies investigated sub-provincial cardiovascular concerns across Canada at the health region level with emphasis on demography and spatial statistics. Hospitalizations due to myocardial infarction demonstrated significant relationships with socioeconomic and behavioral factors as well as significant geospatial clustering of high rates in Northern Ontario and Quebec. Aggregate rates of self-reported hypertension were similarly related to income and demographics with spatial results demonstrating high rates clustered in the North Atlantic, particularly Newfoundland. Furthermore, analyses for hypertension specifically among older adult Canadians ($\geq$ 65 years of age) suggested that education was the strongest contributor at the health region level and there were no significant spatial relationships, in contrast to age-standardized rates. Various implications and other relevant associations are discussed throughout.

Keywords

Cardiovascular health, multivariate statistics, signal processing, spatial statistics, public health, demographics, heart rate variability, generalized linear models, time series analysis, heliobiology, space weather, nonlinear models, solar activity, geomagnetic activity, arrhythmia, hypertension, myocardial infarction, socioeconomic determinants of health

Co-Authorship Statement

Chapter 2: Sample A (healthy sample) data were collected during study from Chapter 3.

Chapter 3: Manraj Singh and Suzanne Fleming assisted with laboratory data collection; Dr. Michael A. Persinger assisted with magnetic field measurement, contributed introduction and discussion sections on electromagnetic field theory, and designed magnetic field equipment with Stan Koren.

Chapter 5: Trevor N. Carniello provided non-statistical calculations of physical dimensions in results section and assisted with writing discussion; Dr. Nirosha J. Murugan assisted with writing introduction and discussion.

Original Chapter Citations

Chapter 2:

In submission

Chapter 3:

Caswell, J. M., Singh, M., & Persinger, M. A. (2016). *Life Sciences in Space Research*, 10: 47-52. DOI: 10.1016/j.lssr.2016.08.001

Chapter 5:

Caswell, J. M., Carniello, T. N., & Murugan N. J. (2016). *International Journal of Biometeorology*, 60: 9-20. DOI: 10.1007/s00484-015-1000-3

Chapter 6:

Caswell, J. M. (2016). *Public Health*, in press. DOI: 10.1016/j.puhe.2016.07.006

Chapter 7:

Caswell, J. M. (2016). *Journal of Public Health*, in press. DOI: 10.1007/s10389-016-0761-4

Acknowledgments

I would first like to thank Dr. Michael A. Persinger for his mentorship and support over many years, as well as his friendship, and for allowing me the freedom to pursue my own research interests during all stages of my studies.

I would also like to extend gratitude to Dr. Cynthia Whissell, a kindred spirit in quantification who has helped as an academic guide and member of thesis committees over a number of years, always with a great deal of support and enthusiasm.

Many thanks are owed to Dr. John Lewko for assistance and support in myriad forms, especially for providing important opportunities in earlier graduate studies, and for wading outside of more familiar territory as part of the current dissertation committee.

Thanks are also extended to the Neuroscience Research Group (NRG) at Laurentian University for their friendship over many years. Special thanks are owed to Lucas W. E. Tessaro, Trevor N. Carniello, Nicolas Rouleau, and Dr. Nirosha J. Murugan of the NRG, as well as Suzanne Fleming and Manraj Singh for additional contributions and assistance, and to Prof. Stan Koren for engineering experimental equipment.

The accelerated completion of this dissertation would not have been possible without the support of many scientific colleagues at home and abroad.

This work is dedicated to the memory of Alexander Chizhevsky (1897-1964), John Snow (1813-1858), Franz Halberg (1919-2013), Ronald Fisher (1890-1962), and Karl Pearson (1857-1936).

Table of Contents

List of Tables

List of Figures

Chapter 1 – Introduction

1. General Introduction

The current series of studies incorporate methods and perspectives from a diverse and wide array of scientific disciplines integrated in an overall framework of inherent “interdisciplines”, biomedical signal processing, heliobiology, and public health, with a focus on quantitative methodologies for cardiovascular health research. The analyses and experiments, as well as the associated background material, overtly include facets of biology, psychology, physics, statistics and signal processing, astronomy, sociology, epidemiology, and geography. More specifically, a number of experimental, correlational, and ecological designs are discussed, converging upon a central theme: human cardiovascular health. The current project also includes empirical investigation of quantitative methods and their use in cardiovascular health research of particular interest to biomedical engineering, demography, and statistics. Furthermore, the primary research procedures discussed herein feature both correlational and experimental protocols exploring the relationship between physiological indicators of autonomic-cardiovascular state with geomagnetic activity, as well as additional explorations of various quantitative methodologies for cardiovascular health including risk stratification, socioeconomic factors, and geospatial considerations. In order to cover a more inclusive spectrum of dependent measures, epidemiological data pertaining to cardiovascular features has also been assessed for potential relationships with heliogeophysical factors along with demographic and spatial trends across Canada. The diversity of previous research and the related number of (inter)disciplines relevant to the current studies cover a number of both theoretical and empirical positions along with seemingly disparate areas of scientific exploration. However, all major topics contributing to the current discussion are integrated in a manner reflective of the immense amount of inherent interconnection between the concepts that form the basis of the current research. There are many questions remaining in the interdisciplinary field of heliobiology, some of which have been investigated in the current studies and explored in the associated discussions that follow. Emerging areas of cardiovascular signal processing and spatial epidemiology are also considered from quantitative, clinical, demographic, and geographic perspectives with particular importance for public health.

1.1. Cardiovascular Physiology

1.1.1. The Human Heart

Cardiovascular function is important for maintaining many biological systems in a wide array of lifeforms with the heart serving as the central organ. As commonly known, the heart's primary function is to pump blood through the circulatory system in order to provide itself and the rest of the body with oxygen and other biochemical factors, as well as playing a role in removing metabolic waste from the body. Aside from its functional overlap across species, the anatomy of the heart tends to be similar in most mammals such as humans. There are four major chambers into which the heart is typically divided including the left and right atria which are the upper divisions, along with the left and right ventricles which are the lower divisions, while the valves of the heart ensure unidirectional blood flow. As blood is pumped through the lungs, hemoglobin within red blood cells becomes saturated in oxygen to be carried throughout the body while also discarding carbon dioxide which is then expelled back into the external atmosphere through the lungs. Each beat of the heart pumps blood through the left ventricle to the rest of the body to be metabolized by other organs as the right ventricle pumps blood to the respiratory system to continue the cycle of discarding carbon dioxide and subsequent re-oxygenation.

There is an integral electrical component to cardiovascular function with about $\sim 2.5 \cdot 10^9$ electrically active cells (Alder & Costabel, 1974) largely controlled by the sinoatrial node (SA node) (Joyner & van Capelle, 1986) which is found in the right atrium of the heart. This region stimulates the upper heart chambers to contract. From this point the signal originating from the SA node proceeds to the atrioventricular node (AV node) before eventually passing through Purkinje fibers of the heart (James, 1961) which are similar to those found in the cerebellum of the brain. Each electrical signal conducted this way eventually converges upon a number of cardiovascular regions including the ventricular epicardium through a depolarization wave that passes from cell to cell through gap junctions (Conrath et al., 2004), again similar to cellular neurophysiology. Myocytes (cardiac cells) also demonstrate action potentials with negative resting membrane potentials (Conrath et al., 2004; Joyner & van Capelle, 1986) like neurons (neural cells). The electrical potentials exhibited by the heart are mostly associated with pacemaker cells that help mediate heart rate through connections with contractile cells via gap junctions (DiFrancesco & Tortora, 1991). This enables the entire heart to function in a highly unified manner allowing activity to quickly and synchronously propagate through the organ where electrical stimulation of non-pacemaker cells causes the heart contractions that maintain blood flow in a rhythmic manner (Cerbai & Mugelli, 2006). The electrical signal originating from the SA node stimulates the myocardium (i.e., major cardiac muscle) which then contracts, pumping blood through the internal chambers and outward to the rest of the body (Joyner & van Capelle, 1986).

1.1.2. Autonomic Nervous System

The autonomic branch of the human nervous system is a vital and dynamic part of human biology and psychology in terms of both its wide-ranging physiological effects and its contribution to overt manifestations of human behavior. The autonomic nervous system (ANS) is itself a branch of the wider peripheral nervous system composed of connections external to the central nervous system (CNS; i.e., brain and spine) that facilitate the transfer of information between the CNS and the rest of the body. The ANS in particular is responsible for innervation of the internal organs, including the heart (Shin et al., 1988), through myriad ascending and descending fibers and is involved in physiological regulation such as respiration (Saul et al., 1989), as well as overall homeostasis in general (Benzinger, 1969). This system is also responsible for the well-known "fight-or-flight" response in which the internal state of the organism is automatically prepared to deal with a perceived threat (i.e., either to fight or escape) in the most bio-energetically efficient manner. As such, ANS activity is also physiologically representative of many important psychological states related to arousal and vigilance and those involving emotion (Ekman et al., 1983; Kreibig, 2010; Levenson et al., 1990; Porges, 1997).

The physiologically-mediating effects of the ANS are processed through two separate divisions: the sympathetic nervous system (SNS) and parasympathetic nervous system (PSNS). The sympathetic branch is typically involved in activation related to preparation in response to environmental and other external stimuli, particularly those that may be threatening. As an example, ANS connections can affect aspects of digestive activity (Rogers et al., 1995) in order to better utilize biological energy to adequately respond to a threat, or dilate the pupils (Bradley et al., 2008; Steinhauer et al., 2004) to accommodate enhanced vision, particularly in a darkened environment. Modulation of cardiovascular activity originating from the SNS results in increased heart rate (Akselrod et al., 1981; Pomeranz et al., 1985). By contrast, the parasympathetic branch of the nervous system is typically involved in “resting” behavioral states including digestion and elimination of biological waste (Goyal & Avery, 2005), although sexual arousal is also largely mediated by the PSNS (Zuckerman, 1971) with associated SNS contributions. This branch of the ANS also includes a number of important cranial nerves including the vagus nerve which is strongly related to PSNS contributions to cardiovascular activity (Paintal, 1953).

1.1.3. Electrocardiography

The electrical activity produced within the heart can be measured for many features of amplitude or temporal structure as a quantitative indicator of autonomic and cardiovascular function. One of the most commonly used tools in this regard is electrocardiography (ECG). This non-invasive technique simply employs electrodes applied to the chest that measure minute changes in electrical activity detectable at the surface of the skin occurring as a result of depolarization within the cells of the heart (Goldman, 1976). The waveform of a typical ECG is often referred to as a PQRST complex or QRS complex according to labels applied to the most prominent features (Figure 1), each of which is explained by a specific physiological component of heart activity and the resultant beat itself.

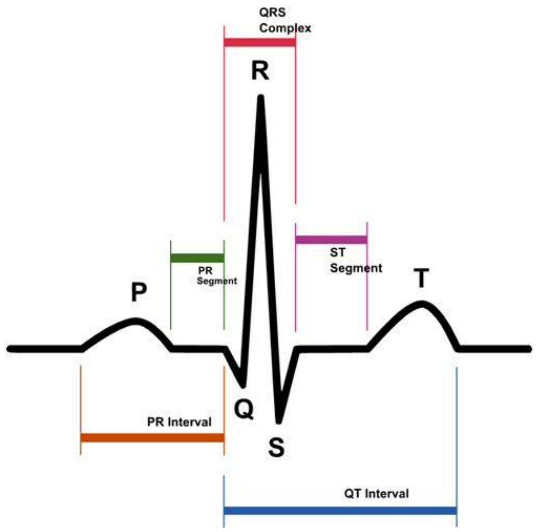

Figure 1: (P)QRS(T) complex from a typical electrocardiogram (ECG) waveform (image acquired from http://www.ing.unitn.it/~melganif/research.html)

The first component of an ECG waveform is the P wave which is a result of SA node electrical activity traveling from the right to the left atria. This electrical depolarization subsequently causes the myocardium to contract, producing the observed P component. In order to ensure the atria and ventricles of the heart do not contract simultaneously, the AV node exhibits a conduction delay as the electrical signal is received from the SA node (Wit et al., 1970). The electrically quiet PR component of an ECG reflects this important delay. Ventricular depolarization then occurs as the original signal travels through the Purkinje fibers to stimulate other cells involved in contraction of the ventricular myocardium (Wit et al., 1970). The major component of interest in most ECG investigations, the QRS complex, results from the spread of electrical activity throughout the ventricular regions (Goldman, 1976). As the ventricular myocardium becomes repolarized there is another brief moment of quiet ECG activity during the ST phase, followed by the final peak, referred to as the T wave, as the ventricles return to baseline activation. Thus, the QRS component reflects the actual beat of the heart from which numerous additional quantitative measures can be derived regarding heart rate accelerations and decelerations or general indices of variability.

1.1.4. Cardiovascular Disease

There are many forms of cardiovascular disease (CVD) and related health issues, including myocardial infarction (i.e., heart attack), contributing to an overwhelming number of illnesses and deaths around the world. Hypertension (i.e., high blood pressure) is a particularly prominent adjustable risk factor for CVD with alarmingly high prevalence. The Global Burden of Disease database (http://healthdata.org/gbd/) indicated that hypertensive disease was the greatest risk factor for both disability and mortality in 2010 with ischemic heart disease remaining one of the highest risks in Canada for years lost due to premature death in 2013. One of the most alarming factors related to CVD is that an estimated ~90% of cases may be preventable by making healthier lifestyle choices (McGill et al., 2008) including regular exercise and properly balanced diet. The prevention of hypertension in particular is possible through tighter regulation of arterial blood pressure (Bertoia et al. 2012; Lloyd-Jones et al. 2002; Williams et al. 2006), while atherosclerosis (thickening of the artery wall) is another leading cause of various CVDs with a strong aging component (Kavey et al., 2003). According to an earlier study by Joffres et al. (1997) up to ~20% of Canadians demonstrated hypertension placing them at an increased risk for developing further heart disease and stroke. The use of non-invasive ECG and additional autonomic-cardiovascular indices has identified a wide range of relationships with risk factors for CVD, particularly through well-established psychophysiological techniques such as heart rate variability (Thayer et al., 2010; Tsuji et al., 1994).

1.2. Heart Rate Variability

1.2.1. Overview

Along with investigation of amplitude and other characteristics of an ECG recording, this type of data can also be used to calculate measures of heart rate variability (HRV). A large number of contemporary studies have demonstrated the potential of HRV as an important indicator for a wide array of conditions including many physiological pathologies (Cheng et al., 2014; Dekker et al., 2000; Thayer et al., 2010), psychological pathologies (Hagit et al., 1998; Kemp et al., 2012) and various mood states (Lane et al., 2009; McCraty et al., 1995), as well as for cognitive performance (Durantin et al., 2014), and autonomic-cardiovascular function in general (Billman, 2013; Task Force, 1996). The measures of HRV itself are simply derived from the time in between beats (e.g., Figure 2) which are referred to as R-R intervals according to the R portion (peak) of the ECG QRS complex. However, R-R measures have also been labelled N-N intervals to denote normal (sinus rhythm) beats, as well as inter-beat intervals (IBI).

Figure 2: Filtered sample (6 seconds) from a single ECG recording; dark horizontal line above indicates a single R-R interval

There are a number of standard guidelines that have been published by the Task Force of the European Society of Cardiology and the North American Society of Pacing and Electrophysiology (Task Force, 1996) outlining proper procedures for ECG recording and standardized analysis of HRV measures along with a number of relatively recent methods developed for research in this area using signal processing and information theory (Işler & Kuntalp, 2007). As an example of a HRV guideline, the minimum recording length for analyzing such data should be approximately five minutes in order to allow application of frequency-domain decomposition. This is because the longer cycle lengths that are generally of interest for cardiovascular activity assessed this way require a data record of length at least equivalent to the periodicity of interest. Furthermore, it should be noted that an R-R interval time series (e.g., Figure 3) will be inherently unevenly sampled given that the subsequent series is based upon the length between heart beats rather than a defined temporal interval (e.g., 1/s). Therefore, appropriate resampling procedures are required prior to application of certain quantitative techniques employed in HRV analyses for which evenly sampled time series are assumed, although alternative methods are also available for such analyses.

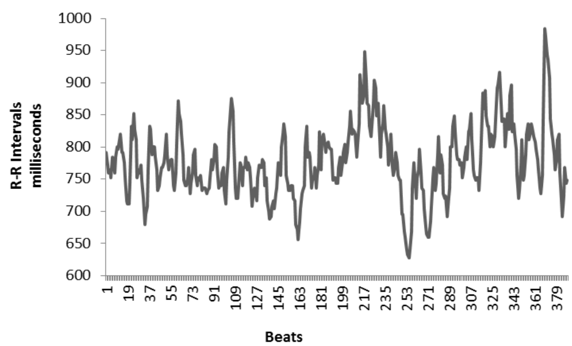

Figure 3: Sample short-term (5 minutes) R-R interval time series

1.2.2. Time Domain Analysis

The simplest and most prominently used statistics for HRV analysis are computed in the time domain using the first two statistical moments of central tendency and variance. The mean value of R-R intervals in a series (*mNN*) is typically computed in seconds (s) or milliseconds (ms), although more useful indicators of HRV include the standard deviation of R-R intervals (*SDNN*) and the root mean square (i.e., $\sqrt{m}(x_i^2)$ where m = mean and x = variable of interest) of successive differences between adjacent R-R intervals (*RMSSD*), both typically in values of s or ms. The *SDNN* and *RMSSD* of a series reflect long- and short-term variability respectively. *SDNN* indicates the contribution from long-term changes in heart rate and more generally represents the overall contribution of temporal dynamics (i.e., periodicities) to the total variability in heart rate. In contrast, *RMSSD* reflects short-term changes in heart rate that are thought to result largely from parasympathetic control (Nunan et al., 2009). An additional measure of HRV that may be calculated for a given R-R interval time series is the standard coefficient of variation (*cvNN*) as a further indicator of general variability:

$$cvNN = \frac{SDNN}{mNN}$$

While the previous time domain indices of HRV follow more general descriptive statistical formats (i.e., the first two statistical moments of central tendency and variance), the number of consecutive R-R interval pairs that differ by more than 50 ms (*NN50*) have also often been included in studies examining HRV along with *NN50* expressed as a percentage of the total number of R-R intervals (*pNN50*). Although these particular variables may not be as intuitive as those in the preceding discussion, they provide an additional measure of short-term changes in HRV thought to be associated with PSNS activity.

1.2.3. Frequency Domain Analysis

In order to examine the periodic components of HRV in greater detail, R-R interval time series require additional analysis using various signal processing methods of spectral decomposition in the frequency domain. This allows identification of the series as relative “power” spectra indicating how strongly a given time series demonstrates cyclic dynamics or oscillations within a particular frequency or range of frequencies. The methods of Fourier transform have arguably been among the most prominent general methods of signal processing for all scientific areas.

As expected, the popularity of Fourier-based spectral analyses, especially the fast Fourier transform (FFT), is also clear within the realm of HRV quantitative methodology. However, it should be noted that the FFT method of frequency decomposition requires an evenly sampled time series (e.g., 1/s). Given that R-R intervals indicate the time between heart beats, the sampling rate is inherently uneven and thus resampling and detrending procedures are required prior to analysis with FFT in order to adjust the data such that it can be interpreted according to a given increment of time. Following the appropriate data processing procedures, a resampled HRV series is decomposed into the frequency domain using FFT for which the discrete Fourier transform is described by:

$$X_k = \sum_{\mathrm{n}=0}^{\mathrm{N}-1} x_{\mathrm{n}} e^{-i2\pi k \frac{\mathrm{n}}{\mathrm{N}}}$$

where k = 1, 2, 3, …, N-1, and N = total sample size of the signal. Subsequently, a series of power spectral density values (i.e., the “strength” of a given periodicity) are derived for a range of frequencies up to the Nyquist limit (N/2). Of particular interest for the analysis of HRV (Task Force, 1996) are the overall components (usually in power spectral density units of ms^2) of very low frequency (*VLF* = 0.003 to 0.04 Hz), low frequency (*LF* = 0.04 to 0.15 Hz), and high frequency power (*HF* = 0.15 to 0.40 Hz) obtained by summing the respective frequency bins contained within each specified band (e.g., Figure 4). Furthermore, the values for *LF* and *HF* are often expressed as proportional normalized units (LF_{nu} and HF_{nu}) according to:

$$LF_{\mathrm{nu}} = \frac{LF}{(LF + HF)}$$

$$HF_{\mathrm{nu}} = \frac{HF}{(HF + LF)}$$

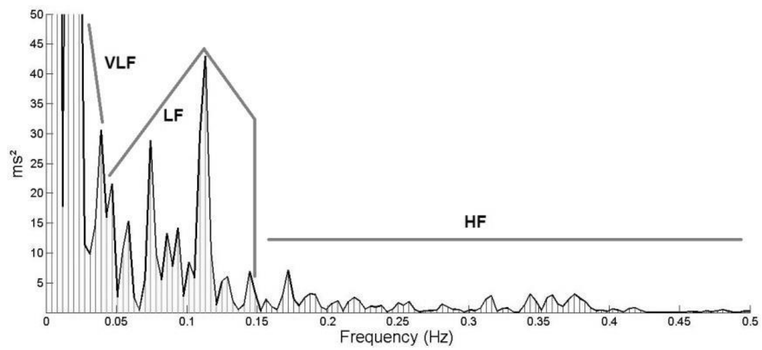

Figure 4: Sample heart rate variability frequency spectrum including very low frequency (*VLF*), low frequency (*LF*), and high frequency (*HF*) components; note *y*-axis has been truncated

The unitless ratio between *LF* and *HF* (*LF/HF*) has also often been employed in previous research as an indicator of sympathovagal balance (Dimitrova et al., 2013; Durantin et al., 2014; Montano et al., 1994; Pagani et al., 1986; 1997; Saboul et al., 2014) or the balance between sympathetic and parasympathetic nervous system activation. However, the validity for this interpretation of the *LF/HF* index has been criticized (Billman, 2013; Eckberg, 1997; Reyes del Paso et al., 2013) and it has been further stated that the HRV theory of sympathovagal balance inferred by *LF/HF* is based on an inaccurate interpretation of how the ANS actually functions. Simply stated, the traditional and long-standing physiological interpretation of *LF* and *HF*, and the ratio between these values in particular, appears to imply that the autonomic division of the nervous system works in a neatly counterbalanced manner with regard to the actions of the sympathetic and parasympathetic branches where increased activity of one branch is associated with a concomitant decrease in activity of the opposing branch. It should also be noted that LF_{nu}, HF_{nu}, and *LF/HF* are algebraically redundant (Burr, 2007) given that they are calculated in relation to one another and as such will present similar effect sizes with the same exogenous variable(s) with only the direction of the effect (i.e., sign) changing between measures (positive or negative). However, the overall consensus including opinion from those that have criticized previous interpretations evidently remains in favor of attributing more general autonomic-mediated activations to the frequency-based components of HRV analyses and the use of the *LF/HF* index remains popular. In an effort to better quantify the autonomic dynamics represented by *LF/HF*, Billman (2013) conducted a thorough review of published results from experimental studies that employed HRV indices in the frequency domain. Through interpretation of the various effects found throughout the literature, a weighting scheme and associated equation was compiled for sympathetic and parasympathetic nerve activity contributions to *LF/HF* according to the observed experimental effects in arbitrary units where a value of 1 indicated baseline activation. When the derived values for *LF/HF* were plotted against varied activity of the SNS and PSNS, a complicated and nonlinear image emerged further indicating the potential complexity of the *LF/HF* index following the relationship (Billman, 2013):

$$\frac{LF}{HF} = \frac{0.5\ \text{PSNS} + 0.25\ \text{SNS}}{0.9\ \text{PSNS} + 0.1\ \text{SNS}}$$

1.2.4. Nonlinear Dynamics

Nonlinear systems are those that display polynomial trends of a second order or higher, or some other non-polynomial trend. Stated alternatively and with utmost simplicity, any system that does not follow a simple linear trend may fall under the umbrella term of nonlinear. Although in reality many human systems display complicated dynamics involving nonlinearity, many standard statistical procedures are based on the assumption of linear effects while a number of the more prominent calculations associated with standard HRV analyses may only capture linear components rather than alternate nonlinear dimensions that could help explain various processes and effects determined by chaotic physiological signals.

One of the original and still popular techniques applied to HRV time series to examine nonlinear dimensions is Poincaré plot analysis (PPA) (Kemp et al., 2012; Saranya et al., 2015; Stein et al., 2005). This method has also been applied in many other areas of research and can be considered a form of geometric analysis. A simple scattergram is constructed by plotting a time series of interest (x_i) against itself leading by a specified number of cases (e.g., Figure 5), although a lead of 1 is generally used for analysis of HRV (x_{i+1}). By plotting the data, PPA also enables easy visual identification of ectopic beats (i.e., those originating from fibres outside the major cardiac muscles) and other ECG artifacts, along with particular features associated with distinct pathologies (Kleiger et al., 2005). Among the most common methods of quantifying PPA results, particularly for analysis of HRV, involves fitting an ellipse to the scattergram distribution and calculating its geometric properties according to width and length. The first PPA statistic (*SD1*) can be computed using:

$$SD1 = \sqrt{\left(\left(\frac{1}{2}\right) \cdot SDSD^2\right)}$$

where *SDSD* = standard deviation of successive differences between adjacent R-R intervals. The second PPA statistic (*SD2*) can be derived with:

$$SD2 = \sqrt{\left(2 \cdot SDNN^2 - \left(\frac{1}{2}\right) \cdot SDSD^2\right)}$$

Interpretation of these measures is relatively simple where *SD1* indicates the width of the ellipse following the dispersion of data perpendicular to the line of identity which reflects short-term variability similar to the standard HRV measure of *RMSSD*; note that both indices are derived with a form of *SDSD*. Conversely, *SD2* indicates the ellipse length following the dispersion of data along the line of identity. Similar to the standard measure of *SDNN*, *SD2* represents long-term variability. Additionally, the ratio of ellipse width to length (*SD1*/*SD2*) has been suggested as a cardiac sympathetic index (*CSI*) mediated by the SNS while the product of width and length (*SD1·SD2*) has similarly been suggested to reflect a cardiac vagal index (*CVI*) of parasympathetic origin (Petković & Ćojbašić, 2011; Tochi et al., 1997).

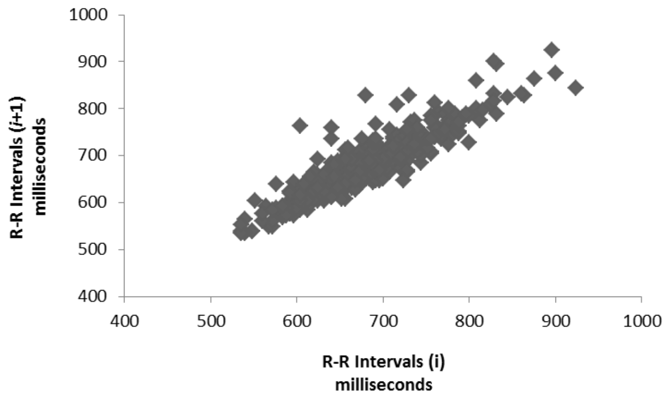

Figure 5: Sample Poincaré plot for a single R-R interval time series

1.2.5. Pathology and Heart Rate Variability

Although there are a multitude of significant relationships that may exist between the reduction of HRV measures and various pathological conditions (Cheng et al., 2014; Griffin & Moorman, 2001; Mani et al., 2009), those of particular interest for the current discussion include apparent associations between HRV and especially prominent factors in disability and mortality including myocardial infarction (for a thorough account of experimental associations of HRV frequency components with particular biochemical manipulations of the ANS refer to the comprehensive reviews by Billman, 2013 and Reyes del Paso et al., 2013). As an example of the association between HRV dynamics and cardiovascular risk factors, Tsuji et al. (1994) analyzed ECG records obtained from an elderly cohort using methods of HRV for which proportional hazards models indicated significant predictive capacity for all causes of mortality in a four year follow-up (n = 74 deaths) with major frequency domain measures (i.e., *VLF*, *LF*, *HF*, and total power) and total variability (*SDNN*). Review of many studies over time has consistently indicated that reductions in HRV can predict the risk for cardiovascular disease in general (Thayer et al., 2010) including myocardial infarction, congestive heart failure, and coronary heart disease (Dekker et al., 2000; Tsuji et al., 1996).

In addition to demonstrating predictive validity for cardiovascular risk factors in otherwise cardiovascular-healthy groups, one of the primary clinical applications for the use of HRV that has remained popular over many years is for prognostic purposes in patients following cardiac events such as myocardial infarction. Even HRV indices derived from short-term ECG recordings have demonstrated the capacity to predict mortality following chronic heart failure, particularly the *LF* spectral component of variability (La Rovere et al., 2003). Similarly, significant reductions in time domain HRV as inferred by *SDNN* have also been found to significantly predict cardiac death in cases of chronic heart failure (Nolan et al., 1998) and after myocardial infarction (Cripps et al., 1991). Subsequent studies have further suggested that previously identified links between mortality following myocardial infarction and depression or anxiety could be related to the psychophysiological ANS effects reflected in the correlation between depressive or anxious states and HRV (Carney et al., 2001; Kemp et al., 2012). Stemming directly from a sample of the literature in clinical utility of HRV, it is clear that a greater understanding of the associations between autonomic-cardiovascular variability and environmental parameters could help our understanding of how exogenous factors might influence the risk for cardiovascular disease and how these relationships manifest psychologically in terms of mood, psychopathology, and cognitive performance.

1.2.6. Psychology and Heart Rate Variability

While the use of HRV as an indicator of physiology is obvious, it is also intuitive to expect a relationship between HRV indices and psychological measures given the role of autonomic activity in both. However, the use of HRV to infer potential autonomic influence has revealed a surprising range of relationships with psychological measures including control and overall performance on cognitive tasks, the occurrence of specific psychopathologies, and reports of mood. Although ANS activity is largely associated with arousal in general, those who reported a greater degree of worry throughout the day demonstrated reductions in HRV (Brosschot et al., 2007) which is also an indicator for cardiovascular disease risk (Thayer et al., 2010). As previously discussed, the role of negative emotional states (e.g., depression, anxiety, etc.) has been shown to relate to reduced HRV with associated cardiovascular risk (Kemp et al., 2012). Furthermore, a similar relationship has been observed in post-traumatic stress disorder (PTSD) patients regarding reduction in cardiovascular variation and a strikingly conspicuous effect was observed for comorbid disorders concerning reductions in both short-term (*RMSSD*) and long-term variability (*SDNN*), as well as the *HF* spectral component that linearly decreased between mentally healthy controls, major depressive disorder (MDD), MDD with PTSD, and MDD with generalized anxiety disorder (Kemp et al., 2012) that could suggest a linearity between the degree of HRV reduction and severity of psychological illness. Although no such effect was reported for the *LF* spectral component of HRV with depressive and anxious disorders and related comorbidities, Hagit et al. (1998) had earlier observed that ECG records of patients diagnosed with PTSD demonstrated increased *LF* power compared to control participants for which an increase in sympathetic activation has been attributed. However, it is important to note that the validity of the *LF* index of HRV as an indicator of purely SNS activity has been questioned (Billman, 2013; Eckberg, 1997; Reyes del Paso et al., 2013). Despite the criticisms of *LF* power as a clear indicator of sympathetic contributions to HRV, the evidence for *HF* power as a measure of vagal-cardiac influence remains relatively clearer and generally supported by many diverse studies (Berntson et al., 1997; Billman, 2013; Reyes del Paso et al., 2013).

Rather than only being identified with depression and anxiety, a small pilot study recently demonstrated that healthy participants reporting symptoms of physical pain not otherwise diagnosed was also related to reduced PSNS activity as inferred by short-term HRV indices of *pNN50*, *RMSSD*, and *HF* power, with concomitant increases in *LF* power and associated *LF/HF* ratio (Koenig et al., 2014). Regarding positive emotional states or behaviors, Sakuragi et al. (2002) identified significantly increased *LF/HF* index when participants watched comedy videos which then returned to baseline levels once viewing had ceased. Furthermore, HRV measures have been suggested to reflect the ability to produce appropriate emotional responses with regard to the timing and overall degree of the response (Appelhans & Luecken, 2006) and the use of emotion regulation strategies (Geisler et al., 2010). Additional support for the relationship between autonomic-cardiovascular activity and emotion in general was also derived from positron emission tomography (PET) research in which regional cerebral blood flow (rCBF) of participants was measured during various states of emotional induction (i.e., happy, sad, disgusted) compared to neutral recordings while concurrent ECG measurements were acquired (Lane et al., 2009). Although a number of significant results were reported, an example of the more intriguing findings included a marked relationship between rCBF from the medial prefrontal cortex and caudate nucleus, which strongly contribute to emotional processing (Aron et al., 2005; Cardinal et al., 2002; Lane et al., 1997; Wager et al., 2008), with the *HF* spectral index of HRV (Lane et al., 2009). This particularly revealing research may also help explain the efficacy of HRV use in applications of biofeedback therapy (Lehrer et al., 2003; Nolan et al., 2005; Siepmann et al., 2008), as well as for the induction of positive mood for which increases in *HF* power have also been associated using short-term ECG records (McCraty et al., 1995).

Although not as prolific as the number of previous studies on HRV and aspects of psychology, there is some evidence for a link between cardiovascular variability indices and dimensions of cognition with associated task performance. Durantin et al. (2014) recently employed functional near infrared spectroscopy (fNIRS) to measure the oxygenation associated with neuronal activity of participants' prefrontal cortices along with ECG-derived measures of HRV to detect conditions of cognitive overload determined by performance and accuracy on rudimentary aircraft operation simulation tasks with varied cognitive processing load requirements and overall levels of difficulty. The authors (Durantin et al., 2014) observed an interaction for cognitive load and difficulty with both prefrontal brain activity and the *LF/HF* index of HRV. This is further indicative of the general association between the activations of the frontal lobes, overall autonomic-cardiovascular state, and psychological conditions as previously discussed (Lane et al., 2009). Further to these findings, it has been demonstrated that differences in HRV of healthy individuals may be related to a range of tasks associated with prefrontal brain activity and that performance levels on cognitive tasks can actually be affected through experimental alteration of HRV (Thayer et al., 2009).

1.3. Space Weather

1.3.1. The Sun and Solar Wind

Our local star exerts a tremendous influence over the entire heliosphere and can directly influence activity of the geosphere through a range of geoeffective solar processes. The study of space weather focuses on the various forms of solar activity as well as their influence on other local astro- and geophysical phenomena such as the geomagnetic field and cosmic rays (Kudela et al., 2000). The sun itself is a massive sphere of nuclear fusion that provides a great deal of the energy necessary to sustain a wide spectrum of life on Earth. Human interest in studying solar activity has persisted for millennia (Schove, 1955) where indices of sunspots have often been employed and remain in common use even today. Sunspots themselves appear to be isolated dark regions of the solar surface that are a result of extreme magnetic activity. This remains an important indicator of overall solar activity given the association between sunspots and coronal mass ejections (CME), although these events can also occur due to other solar phenomena (Hundhausen, 1993). CMEs are enormous bursts of energetic solar material ejected from the sun that often originate from regions close to sunspots or other intense magnetic processes. This particular type of volatile solar activity is largely responsible for influencing storm conditions of the Earth's magnetic field which protects terrestrial systems from their potentially destructive effects. Along with producing auroras, CMEs sweeping across the geomagnetic surface also increase the local magnetic activity which can then influence terrestrial systems, including a wide range of biological effects (Babayev & Allahverdiyeva, 2007; Dimitrova et al., 2013; Mulligan et al., 2010; Papailiou, 2011; Saroka et al., 2014) that could manifest behaviorally.

The sun produces its own magnetic field with a well-established and predictable dominant periodicity of ~22 years with an approximately ~11 year sunspot cycle (Friis-Christensen & Lassen, 1991). Streams of charged particles emanating from the sun (i.e., solar wind) are also responsible for distributing the solar magnetic field throughout the wider heliosphere (Lepping et al., 1993). This is because solar wind is actually plasma that is sufficiently electrically conductive to carry an embedded magnetic field along its path thus producing the interplanetary magnetic field (IMF). As a result of solar rotation along the sun's axis and the vast distance to which the IMF extends, there is a distinct warping of this field forming a spiral shape over the space it occupies with variations in intensity throughout. Aside from a strong correlation between geomagnetic and interplanetary magnetic fields, additional charged particle emissions originating from the sun (i.e., solar proton storms) can also affect the Earth's magnetic field (Pieper et al., 1962).

1.3.2. Geomagnetic Field

The Earth, like the sun, produces a magnetic field of its own. The geomagnetic field is a result of a magnetohydrodynamic effect from the rotating liquid metal core of the planet (Gubbins & Roberts, 1987). This field extends from the centre of the Earth to the magnetopause where the magnetic field reaches the solar wind (Tsyganenko, 1987) and is responsible for shielding the surface of the planet from harmful effects of solar radiation and a great deal of hazardous cosmic rays. While Earth-directed CMEs and proton storms can give some indication of potential geomagnetic activity, the ring current of the magnetosphere that surrounds the Earth is affected by incoming solar particles and the ring current itself has a magnetic field, typically measured using the disturbance storm time (*DST*) index, that is anti-correlated to the planetary magnetic field such that a *DST* decrease will be associated with a concomitant increase in geomagnetic activity (Akasofu & Chapman, 1961). Following the strong correlations between solar and geomagnetic phenomena, the planet's magnetic field similarly demonstrates predictable dominant cycles of ~22 years and ~11 years. Although the geomagnetic field protects the planet from a majority of harmful space weather, storm level activity within the geosphere itself can produce undesirable effects for terrestrial systems. However, the more immediately relevant influence of geomagnetic activity is on terrestrial biology, both in humans (Cornélissen et al., 2002; Dimitrova et al., 2013; Saroka et al., 2014) and elsewhere in nature (e.g., Lohmann et al., 2007; Walker et al., 2002; Wiltschko & Wiltschko, 2005). This type of sensitivity and potential electromagnetic coupling is to be expected when considering the role of adaptation to surrounding environmental conditions as *zeitgeber* and other temporal or spatial reference that takes place throughout the course of evolution, including the synchronization of menstrual and lunar cycles or 24-hour circadian rhythms in biochemistry as prominent examples.

1.3.3. Cosmic Rays

Along with the study of solar and geomagnetic processes, cosmic rays are also typically of interest to those examining space weather dynamics and helio- or cosmobiologists studying the effects of space weather on living systems (Lim, 2002; Papailiou et al., 2012; Singh et al., 2011). Cosmic rays are essentially high-energy particles (mostly protons) of extragalactic origin, some of which are able to penetrate the Earth's atmosphere through the process of ionization (Lowder & Beck, 1966). As a result of this process, cosmic rays are thought to be capable of affecting weather conditions (Carslaw et al., 2002; Svensmark & Friis-Christensen, 1997) and atmospheric radiation levels, particularly at higher altitudes (O'Brien et al., 1996). Because of this property, there has been a number of health risk concerns associated with cosmic radiation, especially at higher altitudes such as those typically experienced by aviators (Lim, 2002; Papailiou et al., 2012). Despite the potential negative issues presented by cosmic rays, more general studies involving effects of space weather may neglect the fact that terrestrial cosmic ray observatories and other monitoring stations for this type of heliophysical activity are strongly influenced by local solar conditions. Through what is referred to as Forbush decreases, enhanced solar activity (e.g., CMEs) can actually remove incoming cosmic radiation from the heliosphere as the magnetic field of the incoming plasma will force cosmic rays out of the solar system (Barouch & Burlaga, 1975). Therefore, general measures of cosmic ray activity will tend to be strongly and negatively correlated with overall solar activity and, by extension, geomagnetic activity, and follow similar periodicities (Kudela et al., 2000).

1.4. Heliobiology

1.4.1. Overview

One of the lesser known pioneers of modern interdisciplinary science, Alexander Chizhevsky, was a Russian biophysicist in the Soviet era widely regarded as the founder of heliobiology. This inherently "interdiscipline" integrates methods and perspectives from solar physics, biology, psychology, and even history, among other potential candidates for inclusion such as epidemiology. Heliobiology is the study of the sun's influence on terrestrial systems, particularly biological as many common labels for the field suggest, although Chizhevsky also became greatly interested in how human behavior and, in particular, "mass excitability" could be related to solar activity and the ~11 year sunspot cycle (Chizhevsky, 1926; 1936). This latter interest of heliobehavioral investigation largely emerged as a result of observations Chizhevsky made during World War I for which the occurrence of violent battles appeared to oscillate with contemporary solar flare activity and geomagnetic storms (Chizhevsky, 1936). Through historiometric investigations, Chizhevsky (1926) determined that revolutionary cycles tended to correlate with solar cycles, a claim which would later result in being sent to a gulag for eight years as this statement clashed with Soviet ideology regarding the true origins of their revolution.

These observations were later reaffirmed by subsequent researchers in similar contexts (Ertel, 1996; Grigoryev et al., 2009; Persinger, 1999; Putilov, 1992), some also adopting the methods of quantitative historiometry. The field of heliobiology may also be related to or essentially synonymous with cosmobiology through inclusion of various other space weather parameters such as galactic cosmic rays, as well as the more general labels of space biology or astrobiology, although these latter two are more often associated with organic terrestrial systems in extraplanetary space and the search for biology outside of Earth respectively. The work of Chizhevsky has further led to the closely related development of biometeorology which is more immediately concerned with effects of the planetary atmosphere on terrestrial biology and behavior.

Although the field of heliobiology and related scientific endeavors have remained somewhat controversial in some circles, the empirical links identified between human systems and the geomagnetic field in particular have increased in both quantity and quality in recent decades with especially strong evidence accumulating for a coupling between the Earth-ionosphere and geomagnetic activity with the human brain (Persinger, 2014; Saroka & Persinger, 2014). However, a vast majority of contemporary research in heliobiology has essentially been correlational in nature. While the growing convergence of evidence is promising, there is still a great need for experimental verification.

1.4.2. Cardiovascular Heliobiology

In direct relation to the psychophysiological study of heart rate variability measures, there have been a number of studies conducted on the potential influence of heliogeophysical parameters on cardiovascular state although most previous research has focused on blood pressure indices. One particular study investigating cosmobiological effects specifically on aviators in Slovakia revealed that cosmic ray activity could be related to both diastolic and systolic measures of blood pressure (Papailiou et al., 2012) while it was also observed that Slovakian aviators demonstrated changes in arterial blood pressure on the day of a geomagnetic storm (Papailiou et al., 2011). Similar to these findings, Dimitrova et al. (2009) had previously found increases in arterial blood pressure in healthy samples from Bulgaria and Azerbaijan up to two days before and after a geomagnetic storm although the use of raw heart rate (HR) was not particularly revealing in this regard. Later research employing a smaller population of healthy participants in Bulgaria again identified significant increases in blood pressure associated with geomagnetic storms (Dimitrova et al., 2013).

Despite the number of studies that have explored potential heliogeophysical effects on human cardiovascular state, especially in Eastern Europe and the Middle East, there have been very few investigations into relationships with measures of HRV or other autonomic indices employed in contemporary psychophysiology. The relatively more recent work conducted by Dimitrova et al. (2013) incorporated a number of HRV parameters from the time and frequency domain and found, as an example, an increase in *SDNN* values the day prior to geomagnetic storm activity decreasing over the following two to three days. Additionally, the *LF/HF* index was observed to significantly decrease on the day of a geomagnetic storm after which an increase was observed up to three days later (Dimitrova et al., 2013). While a large number of the aforementioned results were obtained from particular geographic regions, Otsuka et al. (2001) had much earlier conducted preliminary analyses on ECG records obtained from eight healthy participants in subarctic Norway showing that decreases in HRV, including spectral characteristics, were observed during increased geomagnetic activity for which the authors speculated mechanisms other than those mediated by parasympathetic activation were likely involved. Cornélissen et al. (2002) further examined this finding and again identified decreases in HRV characteristics associated with magnetic storms. However, these latter studies (Cornélissen et al., 2002; Dimitrova et al., 2013; Otsuka et al., 2001) are among the relatively fewer investigations to employ indices of HRV in the context of heliogeophysical activity. Additionally, the relationships between human cardiovascular state and geomagnetic activity have not yet been confirmed with experimental verification.

1.4.3. Heliopsychology

The study of heliobiology also presents a number of associated behavioral concerns linked to biological underpinnings. The association between aggressive behavior and limbic structures of the brain (e.g., amygdala) could be of great interest for the field of heliobiology when considering previous links between geomagnetic activity with temporal lobe and limbic regions. Of particular note, Saroka et al. (2014) identified enhanced coherence between the left and right temporal lobes as measured by quantitative EEG during periods of geomagnetic storms. The same relationship was also identified for left and right parahippocampal gyri (PHG), while overall differences in left- and right-hemispheric activation for PHG were significantly correlated with geomagnetic activity (Saroka et al., 2014). This could be important for the heliobiological study of human aggression and other behavior not only due to the relationships observed specifically with temporal lobe structures that include the amygdala, but also given the role these particular areas may play in mediating anomalous subjective experiences and altered states of consciousness in general (Booth et al., 2005; Persinger, 1983; Persinger et al., 1991;

Ruttan et al., 1990; Saroka et al., 2014). There are many additional published studies demonstrating relationships between various measures of space weather and human brain activity (Mulligan et al., 2010; Saroka & Persinger, 2014) with some including psychological indicators such as anxiety and depression (Babayev & Allahverdiyeva, 2007; Dzvoník et al., 2006) which may help investigators determine the more specific neurophysiological role of aggression and other harmful behaviors including suicide incidence over time in the context of heliogeophysical variations (Kancírová & Kudela, 2014; Berk et al., 2006). As an example, one study demonstrated results suggesting that increases in geomagnetic activity are related to frequency-specific decreases in right frontal lobe activity (Mulligan et al., 2010), which is involved in behavioral inhibition and estimating the future consequences of current actions.

On a much larger but related scale of analysis, Persinger (1999) previously identified heliogeophysical correlations with species-wide aggression related to complex social phenomena (i.e., war). Similarly, space weather factors were statistically related to historic events of aggression and violence that appeared to vary as a function of solar cycle activity (Chao et al., 1996). Later studies examined the relationship between space weather and more specific acts of violence such as terrorist suicide attacks which determined a strong effect of geomagnetic activity (Grigoryev et al., 2009). Additional research has concluded many of these results may be in part related to subjective experiences of “pleasantness” being negatively correlated with geomagnetic parameters (Persinger, 2004). Finally, supporting experimental evidence has been obtained regarding the role of geomagnetic perturbations in neuroelectrical function using laboratory simulations of sudden increases in geomagnetic activity (Mulligan & Persinger, 2012).

1.4.4. Epidemiological Heliobiology

As an extension of the various physiological relationships with space weather, it should be expected that similar dynamics might appear regarding human disease. Along with physiology and psychology, an influence of heliogeophysical parameters on epidemiology was suggested by Chizhevsky (1936). A wide array of research has subsequently supported this general contention by identifying many heliobiological relationships with various diseases. Although linear methods common to standard inferential statistics have been relatively typical, there have also been many nonlinear dynamics revealed, particularly when examining frequency domain characteristics.

As an example of the current findings in this area of study, Dimitrov (1993) earlier identified solar cycle rhythmicity of ~11 years for malignant melanoma in former Czechoslovakia that was correlated with solar activity. More directly relevant for the current discussions, however, are the findings presently available for cardiovascular events. In this regard, the reported incidence of myocardial infarction in association with magnetic storms has been noted by researchers in Mexico, Israel, Italy, and Russia (Cornélissen et al., 2002). A large sample of myocardial infarction events in Russia and Bulgaria similarly suggested a correlation with increased geomagnetic activity, especially occurrences of Pc1 geomagnetic pulsations (~0.20 to 4 Hz) (Fraser & McNabb, 1984), for which the authors (Kleimenova et al., 2007) concluded that this particular class of magnetic perturbation could be responsible for the observed effects on infarction incidence given their potential periodicities in range of those observed for the human cardiovascular system. Specifically at low geomagnetic latitude, Mendoza and Diaz-Sandoval (2004) revealed similar findings of association between increased occurrence of deaths due to myocardial infarction in Mexico and geomagnetic disturbances, although Messner et al. (2002)

found no such relationship between infarction and geomagnetic indices in the higher latitude polar region of northern Sweden. Although there is relative convergence of inferences derived from empirical investigations regarding cardiovascular incidents and space weather factors, some ambiguity and controversy remains over the exact nature of these findings that are inherently correlational.

1.5. Population Sciences

1.5.1. Early Epidemiology

In the mid-19th century a number of cholera outbreaks occurred in London, England. The prevailing theory of disease at the time was that of miasma or “bad air”, thought to result from proximity or exposure to organic decay (e.g., cess pit or open grave). John Snow, a pioneer in early anesthesiology (Snow, 1847), rightfully believed that microscopic organisms were the culprit. However, to avoid outright dismissal by his contemporaries, Snow suggested some form of “self-replicating poison” was responsible for the outbreaks of cholera. For his efforts toward the study of this epidemic, John Snow is commonly considered the father of epidemiology as he was not only able to identify the site of cholera exposure as a specific drinking well but also to track the source to its probable origin (Snow, 1855). Furthermore, the means through which the site was contaminated by a nearby cess pool was found as well. One of the primary tools Snow employed in his investigations was spatial mapping. By plotting the sites of individuals that had contracted cholera on a street-level map of London and conducting interviews with residents, it was hypothesized early on in his investigation that a particular well was likely involved in spreading the contaminant. Since this early research, quantitative spatial methods have become considerably more advanced and rooted in statistics where spatial analyses are now employed within a wide range of population sciences including public health and epidemiology (Auchincloss et al., 2012).

1.5.2. A Brief Introduction to Public Health

The field of public health incorporates methods and perspectives from many interdisciplinary sciences including statistics, epidemiology, environmental and social sciences, as well as medicine. Many physical, social, and environmental aspects that are known or suspected to contribute to health are considered by researchers in an effort to better promote health and prevent disease at the population level and this can also include economics, biology, behavior, policy, or other facets of human sciences (de Castro, 2007; Edwards et al., 2013; Lazzarino et al., 2013; Lustig et al., 2012). General public health surveillance is often conducted for a range of indices related to both physical and mental health in an effort to better focus and organize appropriate programs for optimal treatment and prevention of diseases or other relevant health issues within specific communities or wider geographic regions (CDC, 2012; Kelsey et al., 2012; Pearson et al., 2013). However, where epidemiology is generally concerned with determining the patterns and potential source(s) of a particular health concern, one of the primary goals of public health is to employ this information in the monitoring and prevention of disease or other illness rather than a focus on treatment or pathology, and to apply research-derived evidence to inform policy, educate the public, and assess healthcare systems (de Castro, 2007; Grotto et al., 2008; Pearson et al., 2013).

1.5.3. The Role of Demography

The field of demography is often considered a branch of sociology although subdiscipline and discipline can be differentiated by some key features. Demographers' research is typically more focused on statistical aspects and related to studying larger populations or groups rather than smaller groups or individuals. This focus makes demography an integral component of other population sciences including epidemiology and public health endeavors (Gruebner et al., 2011; Sparks et al., 2013; Sparks & Sparks, 2010) as well as for healthcare services and policy making (de Castro, 2007; Tao et al., 2013; Voss, 2007) through the study of prominent population characteristics including age, sex, cultural background, dynamics of births and deaths, religious affiliations, and a range of additional features that are often associated with wider population dynamics related to social, economic, or health factors and from both spatial and temporal perspectives (Sasson, 2016; Sparks et al., 2013; Sparks & Sparks, 2010; Zorlu & Mulder, 2011). These factors also present interactions where, as an example, socioeconomic factors including income, occupation, and education are known contributors to a number of health concerns including hypertension (de Gaudemaris et al., 2002; Grotto et al., 2008; Pickering, 1999) and heart disease (Lazzarino et al., 2013; Pickering, 1999) given that socioeconomic status may also be associated with varied knowledge about (cardiovascular) health (Gazmararian et al., 2003; van der Heide et al., 2013), greater difficulties obtaining necessary healthcare services (Millman, 1993; Talwar et al., 2016), and increased psychological stress (Lazzarino et al., 2013; Pickering, 1999). These trends may also vary significantly between developed and still-developing nations (Ploubidis, 2013). By examining or controlling for the known effects of demographic factors in further epidemiological or public health analyses, the accuracy of subsequent results is greatly enhanced along with associated inferences and their applicability.

1.5.4. Spatial Trends

The development of geographic information systems (GIS) and associated spatial statistics has greatly contributed to the advancement of myriad population sciences from alternative perspectives that take into account spatial information and processes. The study of spatial statistics typically employs a spatial weight matrix (Getis, 2009) in order to identify neighboring regions within a larger area under investigation according to rules of contiguity (e.g., queen or rook rules) or distance (e.g., *k*-nearest neighbors approach) and this information is then employed in subsequent exploratory spatial data analyses (ESDA) or more advanced methods for multivariate modeling (Anselin, 1994). Techniques for ESDA typically include the concept of global spatial autocorrelation (Anselin, 1994; Moran, 1950) which indicates that the spatial distribution of data under investigation is non-random. This may reflect either high or low values for a variable of interest tending to simultaneously occur for a group(s) of neighboring regions (positive autocorrelation) or extreme spatial separation of regions with high or low values (negative autocorrelation). Although global spatial statistics do not provide more specific information regarding where such autocorrelation might be occurring and among which regions, numerous methods for testing local measures of spatial association have been developed which can be used to assess local spatial clustering of low or high values, commonly referred to as hot spots (Pouliou & Elliott, 2009; Songchitruksa & Zeng, 2010), and the presence of spatial outliers where regions with low values may be surrounded by neighbors with high values or vice versa (Anselin, 1995). Various methods of spatial analysis can also be employed to study diffusive processes (Dall'erba & Le Gallo, 2008; Le Gallo et al., 2005) or applied to much more novel predictive analyses (Hauge et al., 2016).

The identification of spatial trends has been considered an important tool for general public health surveillance (Rushton, 2003; Waller & Gotway, 2004) in order to better identify problematic regions and to discern the importance of geographic space as a potential contributing factor to diverse health concerns, often integrated with perspectives from demography (Sparks & Sparks, 2010). As an example, Pouliou and Elliott (2009) had previously found that rates of overweight and obesity across Canada tended toward east-west disparities with higher prevalence clustered in north Atlantic regions of the country. Additionally, many inferential statistical procedures assume independence among samples where the presence of spatial dependence or autocorrelation may violate this assumption. Therefore, the identification of and control for spatial information in subsequent statistical modelling can help researchers better discern epidemiological effects of interest including environmental (Bayentin et al., 2010) and demographics factors (Sparks et al., 2013).

1.5.5. Caveats of Aggregation

Although population sciences often employ aggregate data out of either necessity or simplicity, there are potential caveats related to both the interpretation and calculation of results derived from aggregate measures rather than individual-level data (i.e., ecological analyses). Arguably the more widely discussed issue among the social sciences and epidemiology is the ecological fallacy which concerns interpretation of results using aggregate data. A conceptually similar issue specific to spatial analyses is the modifiable areal unit problem (MAUP). Although these potential issues may not necessarily hinder a particular research endeavor or the accuracy of subsequent empirical results, they are worth noting in order to better clarify the appropriate interpretation of population level data.

The ecological fallacy refers to the logical error of using results from aggregate data to make inferences about individuals or other smaller units of aggregation (Freedman, 2002). As an example, it would be incorrect to employ a group average to make inferences about a random individual from that group, especially when data are non-normally distributed. Correlations among variables within an ecological study do not necessarily represent effects at the individual level as the latter do not involve cross-sectional effects that result from aggregation (Robinson, 1950; Freedman, 2002). In an early study on literacy and immigration conducted by Robinson (1950), it was demonstrated that correlations obtained using either individual or population data can even have opposite sign (i.e., positive or negative) where cross-sectional effects of aggregation may influence the outcome and subsequent inferences. However, when asking questions or making decisions at a particular scale, such as for many public health concerns associated with specifically defined regional boundaries, the use of aggregate data and ecological analyses remain important tools. The role of population dynamics is also an important consideration with respect to investigating diverse emergent properties of group behavior, further necessitating or favoring the use of ecological studies (Lubinski & Humphreys, 1996).

The MAUP was first discussed by Gehlke & Biehl (1934). In their seminal manuscript it was shown that level of aggregation and the arbitrary regional boundaries applied to spatial data can affect the results of statistical analyses (Gehlke & Biehl, 1934). Essentially, the choice of scale for grouping data can affect the outcome of analyses and subsequent inferences depending on the choice of spatial or “areal” units (e.g., neighborhoods, districts, cities, provinces, etc.) which is further complicated by the inherent capriciousness of unit definition and scale selection. Additionally, there is no widely accepted solution to the MAUP (Horner & Murray, 2002; King, 1979). However, similar to the ecological fallacy and potential inconsistencies between group and individual data, there are many research questions specifically concerned with investigating phenomena at a standardized or otherwise defined spatial scale that require or favor analyses using appropriate spatial units (Hauge et al., 2016).

1.6. Current Studies

1.6.1. Issues in Heart Rate Variability Quantification

Despite the fact that PPA remains a popular tool for assessing nonlinear dynamics of HRV (Kemp et al., 2012; Saranya et al., 2015; Stein et al., 2005), some empirical evaluations of the validity for this interpretation have been critical (Brennan et al., 2001; Hoshi et al., 2013). More specifically, some research has suggested that the standard statistics derived from PPA may not indicate nonlinear dimensions and may actually reflect similar content to the predominant time and frequency domain measures of HRV. As an example, Hoshi et al. (2013) found no strong correlations ($r \geq 0.70$) between *SD1* and *SD2* with any additional indices of nonlinearity they examined including sample entropy (*SampEn*), largest Lyapunov exponent (*LLE*), Hurst exponent, correlation dimension (*CD*), and indices from detrended fluctuation analysis (DFA). Furthermore, there were strongly significant correlations identified between PPA statistics with standard time and frequency domain measures of HRV (Hoshi et al., 2013). Previous empirical investigation similarly concluded that Poincaré indices actually reflect linear dimensions already contained within traditional measures of HRV (Brennan et al., 2001). Contrary to these conclusions, Cardoso et al. (2014) identified a significant correlation for a specific short-term index (α1) derived from the nonlinear method of DFA with the geometric *SD1* statistic from PPA.

However, there are a multitude of procedures available for quantification of nonlinear dynamics in apparently chaotic time series aside from those employed by Hoshi et al. (2013) including the few additional examples of Higuchi fractal dimension (Cervantes-De la Torre et al., 2013; Higuchi, 1988) and the increasingly popular method of wavelet entropy (Işler & Kuntalp, 2007; Sharma et al., 2015). Finally, many studies continue to interpret PPA values as inferences of nonlinearity (Kemp et al., 2012; Saranya et al., 2015; Stein et al., 2005) even though there are a number of empirical evaluations of the validity of Poincaré geometry as nonlinear dimensionality for HRV analysis with conflicting or entirely contrary inferences (Brennan et al., 2001; Cardoso et al., 2014; Hoshi et al., 2013). Therefore, one of the goals for the current research involved the accumulation of sample databases of ECG records for processing and analysis with various methods along with both Poincaré plot indices and additional measures of nonlinearity that have not yet been compared with PPA results to further empirically assess these descriptors. The risk stratification capacity of additional nonlinear dimensions was also assessed for cardiac arrhythmias compared to cardiovascular healthy volunteers from a biomedical signal processing perspective.

1.6.2. Heart Rate Variability and Geomagnetism

From the preceding discussions, it is clear that cardiovascular function is of general interest to heliobiological investigation for both physical and mental health concerns. However, the previous research remains somewhat controversial. Furthermore, while there has been interest in general cardiovascular function measured by blood pressure indices in heliobiology, there are fewer studies that have examined overall autonomic state as inferred by HRV measures (Cornélissen et al., 2002; Dimitrova et al., 2013; Otsuka et al., 2001). This particular state of affairs is also hindered by the relatively limited sampling available, especially with regard to longitudinal research for which individual case studies have typically had to suffice. As aptly stated by Dimitrova et al. (2013), this is simply a result of the inherent difficulty in enlisting participants to contribute their time over extended periods without prior motivation or subsequent compensation. However, the gradual accumulation of convergent empirical evidence over multiple studies can contribute to a general consensus regarding potential heliobiological influences. As such, it remains important to continue longitudinal studies in this respect with any sample size capacities. This statement carries even more salience in heliobiology where overall shifts in occurrence of solar activity, and therefore geoeffective solar phenomena, will vary over longer periods of time according to solar minima and maxima of various intensities. In order to contribute to the growing body of evidence for relationships between autonomic-cardiovascular state and heliogeophysical factors, one of the projects involved in the current research was a simple longitudinal pilot observation of HRV. A single participant contributed daily ECG recordings that were assessed for *post hoc* statistical relationships with concomitant geomagnetic parameters to determine if any observed relationships overlapped with previous findings in this area of inquiry.

One of the primary issues for the overall validity of contemporary heliobiological investigation is the excessive use of correlational evidence (Babayev & Allahverdiyeva, 2007; Mulligan et al., 2010; Dimitrova et al., 2013). As previously stated, the convergence of evidence across studies, even correlational in nature, can provide some confidence in the inferences derived from subsequent quantification. However, further experimental verification would certainly bolster the insights associated with heliobiological research. There have already been preliminary efforts to investigate these findings in the context of the brain's neuroelectrical activity (Mulligan & Persinger, 2012), although autonomic and cardiovascular state have not yet been subjected to the same verification procedure with humans across a range of magnetic field configurations outside of ultra-low frequency (ULF) fields (Mitsutake et al., 2004). Therefore, an additional study regarding HRV and geomagnetic activity was included in the current research in order to address this particular demand. Similar protocols used by previous verification of neuroelectrical-geomagnetic dynamics (Mulligan & Persinger, 2012) were applied to the experimental simulation of sudden increases in fast-frequency geomagnetic activity with associated measurement of participants' HRV from various perspectives. It was hoped that this particular study would not only overlap with the previously discussed longitudinal case study, but also converge with correlational findings obtained by other researchers.

1.6.3. Cardiovascular Disease and Heliogeophysical Activity

Contrary to heliobiology related to physiology or psychology, epidemiological investigations of heliogeophysical influence are by their very nature limited to correlational methods. However, the application of a wider variety of quantitative techniques from statistical, signal processing, and artificial machine learning methods is still emerging with many new promising avenues of empirical exploration being applied within the fields of biostatistics and demography. One particular approach that has increasingly been used in epidemiology is the examination of time series within the frequency and time-frequency domains through various spectral methods (Cornélissen, 2014; Dimitrov, 1993) and associated coherence measures (Cazelles et al., 2005;

2007). Furthermore, the investigation of periodic components inherent to disease incidence and mortality has also indicated additional relationships with heliogeophysical processes that may be mediated by temporal dynamics (Dimitrov, 1993; Dimitrov & Babayev, 2015; Dimitrov et al., 2011; 2013). Thus, it remains paramount to continue pursuing the relevance of heliobiological inference with regard to disease prevalence and progression and to simultaneously expand the range of geographical, pathological, temporal, and heliogeophysical variability under assessment to further cement these inferences.

As previously discussed, even when empirical evidence is correlational, the gradual accumulation of convergent quantification can enhance the confidence associated with observed results (i.e., replicability). This is especially accurate when mechanistic candidates can be identified by quantitative means. To further address this area of interest, an alternate approach was taken regarding epidemiological measures where the annual numbers of mortalities associated with hypertensive disease were assessed. Both traditional linear relationships and nonlinear periodic components were explored for hypertensive disease mortality in Canada with a number of contemporary heliogeophysical factors to demonstrate the potential role of space weather and geophysics across levels of discourse from individuals to larger population trends. This particular area of study as a whole also remains somewhat controversial and misunderstood with the continuing need for further research.

Additionally, many earlier studies have examined concurrent relationships for dependent health measures of interest with many aspects of space weather including geophysical, solar, interplanetary, and extragalactic (Cornélissen et al., 2002; Mulligan et al., 2010; Singh et al., 2011) while some studies have seemingly little regard for the mutual influence these parameters have upon one another, largely originating from a central source of variance (i.e., the sun). In contrast, the current study quantitatively considered the interconnections between independent measures to better determine their most likely source of influence on hypertensive mortality temporal trends. On a final note, although relatively small effects may be observed in similar studies, Vares and Persinger (2015) have aptly noted that seemingly minute effect sizes, such as might be observed in population-based sciences including sociology, epidemiology, and even biometeorology, can have substantial impact when applied over such large groups.

1.6.4. Cardiovascular Health Trends

A number of previous studies of Canadian populations have considered spatial processes and regional clustering in the investigation of public health concerns such as overweight and obesity rates (Katzmarzyk, 2002; Pouliou & Elliot, 2009). However, similar research employing standard ESDA techniques and spatial regression for indicators of cardiovascular health and healthcare in Canada have not yet been as prevalent (Bayentin et al., 2010). Despite this gap, researchers in other countries have examined indicators of cardiovascular health from spatial epidemiological and demographic perspectives. For example, Ahmadi et al. (2015) used methods of ESDA to study spatial variations in hospitalization due to myocardial infarction across the regions of Iran for which significant spatial trends were observed indicating regional disparities and autocorrelation. One of the primary perspectives for the current series of studies involved integration of spatial statistical analyses for Canadian public health with perspectives employed by researchers elsewhere in the world in order to identify the presence of spatial properties for cardiovascular health among the sub-provincial administrative health regions of Canada.

Furthermore, the role of additional health determinants was also investigated in these analyses including behavioral and socioeconomic factors.

Following previous work by Ahmadi et al. (2015), the first spatial public health study in the current research focused on identification of various spatial processes present for Canadian hospitalizations due to myocardial infarction along with demographic, behavioral, socioeconomic, and other determinants of health. Although this hospitalization variable is a more direct indicator of healthcare usage associated with issues of cardiovascular health, the second spatial public health study focused on self-reported high blood pressure (i.e., hypertension). This is a particularly important consideration given that hypertension may be a risk factor for developing further cardiovascular health issues including heart disease (Campbell et al., 2012; Joffres et al., 2007). Although the spatial parameter of interest for this second spatial public health study was largely concerned with the presence of spatial clustering among neighboring regions, standard demographic factors were also considered in greater detail and with additional demographic investigation at the individual-level including age, gender, and household income. Finally, the presence of diagnosed high blood pressure among older adult (≥ 65 years of age) Canadians was assessed independent of previous results for spatial processes and contributions from a range of additional health determinants with a focus on socioeconomic factors.

1.7. Discussion

As delineated throughout the preceding series of discussions, the current project addresses important areas of study and interdisciplinary knowledge production that are relevant to many different fields, and does so by integrating a diverse array of disciplines and “interdisciplines” including biology, geography, physics, demography, statistics, and epidemiology. It is hoped that by beginning to fill present gaps in the knowledge discerned through heliobiology additional problems can be addressed by future researchers in relation to environmental psychophysiology. Among other potential applications, these results can then be translated into enhanced neuroergonomic or health and safety guidelines following additional research that expands upon the current findings. Furthermore, signal processing and public health perspectives contribute to better understanding clinical, socioeconomic, behavioral, and demographic factors involved in cardiovascular issues for risk stratification and prediction, as well as general public health surveillance, which are important aspects of health sciences.

The current project features a wide range of methods and perspectives in order to address the relevant questions outlined in previous discussions. The continued use of HRV measures without regard for empirical evidence questioning the validity of their interpretation needs to be addressed further and the first study in this project contributes to investigation of this issue along with exploring potential clinical utility of novel nonlinear indices. In the primary context of potential heliogeophysical influences, a greater number of longitudinal studies are required for heliobiological assessment of temporal dynamics and generalizability, particularly regarding autonomic-cardiovascular function that contributes to both physiological and psychological well-being. Thus, the current pilot case study was meant to further explore a basis from which to continue the collection of relevant data. Of even greater importance, there has not yet been experimental verification of potential fast-frequency geomagnetic effects on human cardiovascular activity despite a number of correlational studies and some preliminary experimental results for lower frequency magnetic fields (Mitsutake et al., 2004). The current experimental study on HRV and geomagnetic simulation serves as an important step forward in providing such verification as well as a potential comparison for the subsequent longitudinal pilot investigation. Similar concepts from these studies were applied to epidemiological data at the population level regarding disease mortality associated with the cardiovascular system. Therefore, the potential role of heliogeophysical factors in human systems is presented across multiple levels of discourse including individuals as well as within populations. Finally, geographic, demographic, behavioral, and socioeconomic considerations were also included by means of both spatial and non-spatial statistics with application to public health surveillance of cardiovascular health issues in Canada.

References

Ahmadi, A., Soori, H., Mehrabi, Y., & Etemad, K. (2015). Spatial analysis of myocardial infarction in Iran: National report from the Iranian myocardial infarction registry. *Journal of Research in Medical Sciences*, 20(5): 434-439.

Akasofu, S.-I., & Chapman, S. (1961). The ring current, geomagnetic disturbance, and the Van Allen radiation belts. *Journal of Geophysical Research*, 66(5): 1321-1350.

Akselrod, S., Gordon, D., Ubel, F. A., Shannon, D. C., Berger, A. C., & Cohen, R. J. (1981). Power spectrum analysis of heart rate fluctuation: a quantitative probe of beat-to-beat cardiovascular control. *Science*, 213(4504): 220-222.

Alder, C. P., & Costabel, U. (1974). Cell number in human heart in atrophy, hypertrophy, and under the influence of cytostatics. *Recent Advances in Studies of Cardiac Structure and Metabolism*, 6: 343-355.

Anselin, L. (1994). Exploratory spatial data analysis and geographic information systems. In Longley P, Brooks S, Macmillan B, McDonnell R (eds.) pp. 77-94, *GeoComputation: A Primer*. New York: Wiley.

Anselin, L. (1995). Local indicators of spatial association – LISA. *Geographical Analysis*, 27: 93-115.

Appelhans, B. M., & Luecken, L. J. (2006). Heart rate variability as an index of regulated emotional responding. *Review of General Psychology*, 10(3): 229-240.

Aron, A., Fisher, H., Mashek, D. J., Strong, G., Li, H., & Brown, L. L. (2005). Reward, motivation, and emotion systems associated with early-stage intense romantic love. *Journal of Neurophysiology*, 94(1): 327-337.

Auchincloss, A. H., Gebreab, S. Y., Mair, C., Diez Roux, A. V. (2012). A review of spatial methods in epidemiology, 2000-2010. *Annual Review of Public Health*, 33: 107-122.

Babayev, E. S., and Allahverdiyeva, A. A. (2007). Effects of geomagnetic activity variations on the physiological and psychological state of functionally healthy humans: Some results of Azerbaijani studies. *Advances in Space Research*, 40(12): 1941-1951.

Barouch, E., & Burlaga, L. F. (1975). Causes of Forbush decreases and other cosmic ray variations. *Journal of Geophysical Research*, 80: 449-456.

Bayentin, L., El Adlouni, S., Ouarda, T. B. M. J., Gosselin, P., Doyon, B., & Chebana, F. (2010). Spatial variability of climate effects on ischemic heart disease hospitalization rates for the period 1989-2006 in Quebec, Canada. *International Journal of Health Geographics*, 9(5).

Berntson, G. G., Bigger, J. T., Eckberg, D. L., Grossman, P., Kaufmann, P. G., Malik, M., Nagaraja, H. N., Porges, S. W., Saul, J. P., Stone, P. H., & van der Molen, M. W. (1997). Heart rate variability: Origins, methods, and interpretive caveats. *Psychophysiology*, 34: 623-648.

Benzinger, T. H. (1969). Heat regulation: Homeostasis of central temperature in man. *Physiological Reviews*, 49(4): 671-759.

Berk, M., Dodd, S., & Henry, M. (2006). Do ambient electromagnetic fields affect behaviour? A demonstration of the relationship between geomagnetic storm activity and suicide. *Bioelectromagnetics*, 27(2): 151-155.

Bertoia, M. L., Waring, M. E., Gupta, P. S., Roberts, M. B., & Eaton, C. B. (2012). Implications of new hypertension guidelines in the United States. *Hypertension*, 60(3): 639-644.

Billman, G. E. (2013). The LF/HF ratio does not accurately measure cardiac sympatho-vagal balance. *Frontiers in Physiology*, 4(26): 1-5.

Booth, J. N., Koren, S. A., & Persinger, M. A. (2005). Increased feelings of the sensed presence and increased geomagnetic activity at the time of the experience during exposures to transcerebral weak complex magnetic fields. *International Journal of Neuroscience*, 115(7): 1053-1079.

Bradley, M. M., Miccoli, L., Escrig, M. A., & Lang, P. J. (2008). The pupil as a measure of emotional arousal and autonomic activation. *Psychophysiology*, 45(4): 602-607.

Brennan, M., Palaniswami, M., & Kamen, P. (2001). Do existing measures of Poincaré plot geometry reflect nonlinear features of heart rate variability? *IEEE Transactions on Biomedical Engineering*, 48(11): 1342-1347.

Brosschot, J. F., van Dijk, E., & Thayer, J. F. (2007). Daily worry is related to low heart rate variability during waking and the subsequent nocturnal sleep period. *International Journal of Psychophysiology*, 63(1): 39-47.

Burr, R. L. (2007). Interpretation of normalized spectral heart rate variability indices in sleep research: A critical review. *Sleep*, 30(7): 913-919.

Campbell, N., Young, E. R., Drouin, D., Legowski, B., Adams, M. A., Farrell, J., Kaczorowski, J., Lewanczuk, R., Lum-Kwong, M. M., & Tobe, S. (2012). A framework for discussion on how to improve prevention, management, and control of hypertension in Canada. *Canadian Journal of Cardiology*, 28(3): 262-269.

Cardinal, R. N., Parkinson, J. A., Hall, J., Everitt, B. J. (2002). Emotion and motivation: The role of the amygdala, ventral striatum, and prefrontal cortex. *Neuroscience & Biobehavioral Reviews*, 26(3): 321-352.

Cardoso, M. A., Dos Santos, M. A., de Abreu, L. C., Fontes, A. M. G., da Silva, A. G., Ogata, C. M., de Oliveira, L. S., Sousa, F. H., do Amaral, J. A. T., Cano, A. S., Plassa, B. O., Milan, R., & Valenti, V. E. (2014). Fractal scaling exponents of heart rate variability association with linear indices and Poincaré plot. *Experimental and Clinical Cardiology*, 20(1): 2444-2456.

Carney, R. M., Blumenthal, J. A., Stein, P. K., Watkins, L., Catellier, D., Berkman, L. F., Czajkowski, S. M., O'Connor, C., Stone, P. H., & Freedland, K. E. (2001). Depression, heart rate variability, and acute myocardial infarction. *Circulation*, 104: 2024-2028.

Carslaw, K. S., Harrison, R. G., & Kirby, J. (2002). Cosmic rays, clouds, and climate. *Science*, 298(5599): 1732-1737.

de Castro, M. C. (2007). Spatial demography: An opportunity to improve policy making at diverse decision levels. *Population Research and Policy Review*, 26: 477-509.

Cazelles, B., Chavez, M., McMichael, A. J., & Hales, S. (2005). Nonstationary influence of El Niño on the synchronous dengue epidemics in Thailand. *PLoS Medicine*, 2(4): e106.

Cazelles, B., Chavez, M., de Magny, G. C., Guégan, J.-F., & Hales, S. (2007). Time-dependent spectral analysis of epidemiological time-series with wavelets. *Journal of the Royal Society Interface*, 4: 625-636.

CDC, Centers for Disease Control and Prevention. (2012). Integrated prevention services for HIV infection, viral hepatitis, sexually transmitted diseases, and tuberculosis for persons who use drugs illicitly: Summary guidance from CDC and the U.S. Department of Health and Human Services. *MMWR Recommendation Report*, 61(RR-5): 1-40.

Cerbai, E., & Mugelli, A. (2006). I_f in non-pacemaker cells: Role and pharmacological implications. *Pharmacological Research*, 53(5): 416-423.

Cervantes-De la Torre, F., González-Trejo, J. I., Real-Ramírez, C. A., & Hoyos-Reyes, L. F. (2013). Fractal dimension algorithms and their application to time series associated with natural phenomena. *Journal of Physics: Conference Series*, 475(conference 1).

Chao, S., Zhengxing, L., Hongchun, Z., & Hong, Z. (1996). Relationship between solar-terrestrial environments and spontaneous collective aggressive events. *Journal of Catastrophology*, 1996-04.

Cheng, S.-T., Wu, Y.-K., Yang, M.-C., Huang, C.-Y., Huang, H.-C., Chu, W.-H., & Lan, C.-C. (2014). Pulmonary rehabilitation improves heart rate variability at peak exercise, exercise capacity and health-related quality of life in chronic obstructive pulmonary disease. *Heart & Lung*, 43: 249-255.

Chizhevsky, A. L. alternately Tchijevsky, A. L. (1926). Physical factors of the historical process. *Annual Meeting of the American Meteorological Society, 1926*.

Chizhevsky, A. L. alternately Tchijevsky, A. L. (1936). *The Terrestrial Echo of Solar Storms* (translated). Moscow: Mysl'Press.

Conrath, C. E., Wilders, R., Coronel, R., de Bakker, M. T., Taggart, P., de Groot, J. R., & Opthof, T. (2004). Intercellular coupling through gap junctions masks M cells in the human heart. *Cardiovascular Research*, 62(2): 407-414.

Cornélissen, G. (2014). Cosinor-based rhythmometry. *Theoretical Biology and Medical Modelling*, 11(1): 16-40.

Cornélissen, G., Halberg, F., Breus, T., Syutkina, E. V., Baevsky, R., Weydahl, A., Watanabe, Y., Otsuka, K., Siegelova, J., Fiser, B., & Bakken, E. E. (2002). Non-photic solar associations of heart rate variability and myocardial infarction. *Journal of Atmospheric and Solar-Terrestrial Physics*, 64(5-6): 707-720.

Cripps, T. R., Malik, M., Farrell, T. G., & Camm, A. J. (1991). Prognostic value of reduced heart rate variability after myocardial infarction: Clinical evaluation of a new analysis method. *British Heart Journal*, 65: 14-19.

Dall'erba, S., & Le Gallo, J. (2008). Regional convergence and the impact of European structural funds over 1989-1999: A spatial econometric analysis. *Papers in Regional Science*, 87(2): 219-244.

Dekker, J. M., Crow, R. S., Folsom, A. R., Hannan, P. J., Liao, D., Swenne, C. A., & Schouten, E. G. (2000). Low heart rate variability in a 2-minute rhythm strip predicts risk of coronary heart disease and mortality from several causes. *Circulation*, 102: 1239-1244.

DiFrancesco, D., & Tortora, P. (1991). Direct activation of cardiac pacemaker channels by intracellular cyclic AMP. *Nature*, 351: 145-147.

Dimitrov, B. D. (1993). Heliophysical activity and incidence variations of skin malignant melanoma in Czechoslovakia: A regional study. *International Journal of Biometeorology*, 37: 68-71.

Dimitrov, B. D., & Babayev, E. S. (2015). Cyclic variations in the dynamics of flu incidence in Azerbaijan, 1976-2000. *Epidemiology and Infection*, 143(1): 13-22.

Dimitrov, B. D., Valev, D., Werner, R., Atanassova, P. A. (2011). Cyclic patterns of malaria incidence in Burundi. *Central European Journal of Biology*, 6(1): 58-67.

Dimitrov, B. D., Valev, D., Werner, R., Atanassova, P. A. (2013). Cyclic patterns of malaria admissions in Papua New Guinea for the years 1987-1996. *Epidemiology and Infection*, 141(11): 2317-2327.

Dimitrova, S., Mustafa, F. R., Stoilova, I., Babayev, E. S., & Kazimov, E. A. (2009). Possible influence of solar extreme events and related geomagnetic disturbances on human cardiovascular state: Results of collaborative Bulgarian–Azerbaijani studies. *Advances in Space Research*, 43(4): 641-648.

Dimitrova, S., Angelov, I., & Petrova, E. (2013). Solar and geomagnetic activity effects on heart rate variability. *Natural Hazards*, 69: 25-37.

Durantin, G., Gagnon, J.-F., Tremblay, S., & Dehais, F. (2014). Using near infrared spectroscopy and heart rate variability to detect mental overload. *Behavioural Brain Research*, 259: 16-23.

Dzvoník, O., Stetiarova, J., Kudela, K., & Daxner, P. (2006). A monitoring of space weather effects on some parameters of mental performance and health in aviation personnel. *Studia Psychologica*, 48(4): 273-291.

Eckberg, D. L. (1997). Sympathovagal balance: A critical appraisal. *Circulation*, 96: 3224-3232.

Edwards, R. T., Charles, J. M., & Lloyd-Williams, H. (2013). Public health economics: A systematic review of guidance for the economic evaluation of public health interventions and discussion of key methodological issues. *BMC Public Health*, 13.

Ekman, P., Levenson, R. W., & Friesen, W. V. (1983). Autonomic nervous system activity distinguishes among emotions. *Science*, 221(4616): 1208-1210.

Ertel, S. (1996). Space weather and revolutions: Chizevsky's (sic) heliobiological claim scrutinized. *Studia Psychologica*, 38: 1-2.

Fraser, B. J., & McNabb, P. W. (1984). The recording of Pc1 geomagnetic pulsations using a microcomputer preprocessing system. *Geophysical Surveys*, 6: 249-258.

Freedman, D. A. (2002). *The Ecological Fallacy*. California: University of California Press.

Friis-Christensen, E., & Lassen, K. (1991). Length of the solar cycle: An indicator of solar activity closely associated with climate. *Science*, 254(5032): 698-700.

de Gaudemaris, R., Lang, T., Chatellier, G., Larabi, L., Lauwers-Cancès, V., Maître, A., & Diène, E. (2002). Socioeconomic inequalities in hypertension prevalence and care: The IHPAF study. *Hypertension*, 39: 1119-1125.

Gazmararian, J. A., Williams, M. V., Peel, J., & Baker, D. W. (2003). Health literacy and knowledge of chronic disease. *Patient Education and Counseling*, 51(3): 267-275.

Gehlke, C. E., & Biehl, K. (1934). Certain effects of grouping upon the size of the correlation coefficient in census tract material. *Journal of the American Statistical Association*, 29(185A): 169-170.

Geisler, F. C. M., Vennewald, N., Kubiak, T., & Weber, H. (2010). The impact of heart rate variability on subjective well-being is mediated by emotion regulation. *Personality and Individual Differences*, 49(7): 723-728.

Getis, A. (2009). Spatial weights matrices. *Geographical Analysis*, 41(4): 404-410.

Goldman, M. J. (1976). *Principles of Electrocardiography*. Los Altes: Lange.

Goyal, M., & Avery, J. A. (2005). Paroxysmal disorders and the autonomic nervous system in pediatrics. *American Journal of Electroneurodiagnostic Technology*, 45(4): 240-247.

Griffin, M. P., & Moorman, J. R. (2001). Toward the early diagnosis of neonatal sepsis and sepsis-like illness using novel heart rate analysis. *Pediatrics*, 107(1): 97-104.

Grigoryev, P., Rozanov, V., Vaiserman, A., & Vladimirskiy, B. (2009). Heliogeophysical factors as possible triggers of suicide terroristic acts. *Health*, 1: 294-297.

Grotto, I., Huerta, M., & Sharabi, Y. (2008). Hypertension and socioeconomic status. *Current Opinion in Cardiology*, 23(4): 335-339.

Gruebner, O., Khan, M. M. H., Lautenbach, S., Müller, D., Kraemer, A., Lakes, T., & Hostert, P. (2011). A spatial epidemiological analysis of self-rated mental health in the slums of Dhaka. *International Journal of Health Geographics*, 10.

Gubbins, D., & Roberts, P. H. (1987). Magnetohydrodynamics of the Earth's core. *Geomagnetism*, 2: 1-183.

Hagit, C., Kotler, M., Matar, M. A., Kaplan, Z., Loewenthal, U., Miodownik, H., & Cassuto, Y. (1998). Analysis of heart rate variability in posttraumatic stress disorder patients in response to a trauma-related reminder. *Biological Psychiatry*, 44(10): 1054-1059.

Hauge, M. V., Stevenson, M. D., Rossmo, D. K., & Le Comber, S. C. (2016). Tagging Banksy: Using geographic profiling to investigate a modern art mystery. *Journal of Spatial Science*, 61(1): 185-190.

Higuchi, T. (1988). Approach to an irregular time series on the basis of the fractal theory. *Physica D: Nonlinear Phenomena*, 31(2): 277-283.

Horner, M. W., & Murray, A. T. (2002). Excess commuting and the modifiable areal unit problem. *Urban Studies*, 39(1): 131-139.

Hoshi, R. A., Pastre, C. M., Vanderlei, L. C. M., & Godoy, M. F. (2013). Poincaré plot indexes of heart rate variability: Relationships with other nonlinear variables. *Autonomic Neuroscience: Basic and Clinical*, 177: 271-274.

Hundhausen, A. J. (1993). Sizes and locations of coronal mass ejections: SMM observations from 1980 and 1984-1989. *Journal of Geophysical Research*, 98(A8): 13177-13200.

Işler, Y., & Kuntalp, M. (2007). Combining classical HRV indices with wavelet entropy measures improves to performance in diagnosing congestive heart failure. *Computers in Biology and Medicine*, 37(10): 1502-1510.

James, T. N. (1961). Morphology of the human atrioventricular node, with remarks pertinent to its electrophysiology. *American Heart Journal*, 62(6): 756-771.

Joffres, M. R., Ghadirian, P., Fodor, J. G., Petrasovits, A., Chockalingam, A., & Hamet, P. (1997). Awareness, treatment, and control of hypertension in Canada. *American Journal of Hypertension*, 10(10): 1097-1102.

Joffres, M. R., Campbell, N. R. C., Manns, B., & Tu, K. (2007). Estimate of the benefits of a population-based reduction in dietary sodium additives on hypertension and its related health care costs in Canada. *Canadian Journal of Cardiology*, 23(6): 437-443.

Joyner, R. W., & van Capelle, F. J. (1986). Propagation through electrically coupled cells: How a small SA node drives a large atrium. *Biophysical Journal*, 50(6): 1157-1164.

Kancírová, M., & Kudela, K. (2014). The relationship between suicide incidents in Slovakia and the Czech Republic and heliophysical parameters: Empirical results. *Journal of Astrobiology & Outreach*, 2(2): 1-5.

Katzmarzyk, P. T. (2002). The Canadian obesity epidemic, 1985-1998. *Journal of the Canadian Medical Association*, 166: 1039-1040.

Kavey, R.-E. W., Daniels, S. R., Lauer, R. M., Atkins, D. L., Hayman, L. L., & Taubert, K. (2003). American heart association guidelines for primary prevention of atherosclerotic cardiovascular disease beginning in childhood. *Journal of Pediatrics*, 142(4): 368-372.

Kelsey, J. L., Procter-Gray, E., Hannan, M. T., & Li, W. (2012). Heterogeneity of falls among older adults: Implications for public health prevention. *American Journal of Public Health*, 102(11): 2149-2156.

Kemp, A. H., Quintana, D. S., Felmingham, K. L., Matthews, S., & Jelinek, H. F. (2012). Depression, comorbid anxiety disorders, and heart rate variability in physically healthy, unmedicated patients: Implications for cardiovascular risk. *PLoS ONE*, 7(2).

King, P. E. (1979). Problems of spatial analysis in geographical epidemiology. *Social Science and Medicine*, 13D: 249-252.

Kleiger, R. E., Stein, P. K., & Bigger Jr., J. T. (2005). Heart rate variability: Measurement and clinical utility. *Annals of Noninvasive Electrocardiology*, 10(1): 88-101.

Kleimenova, N. G., Kozyreva, O. V., Breus, T. K., & Rapoport, S. I. (2007). Pc1 geomagnetic pulsations as a potential hazard of the myocardial infarction. *Journal of Atmospheric and Solar-Terrestrial Physics*, 69(14): 1759-1764.

Kreibig, S. D. (2010). Autonomic nervous system activity in emotion: A review. *Biological Psychology*, 84(3): 394-421.

Kudela, K., Storini, M., Hofer, M. Y., & Belov, A. (2000). Cosmic rays in relation to space weather. *Space Science Reviews*, 93: 153-174.

La Rovere, M. T., Pinna, G. D., Maestri, R., Mortara, A., Capomolla, S., Febo, O., Ferrari, R., Franchini, M., Gnemmi, M., Opasich, C., Riccardi, P. G., Traversi, E., & Cobelli, F. (2003). Short-term heart rate variability strongly predicts sudden cardiac death in chronic heart failure patients. *Circulation*, 107: 565-570.

Lane, R. D., Reiman, E. M., Bradley, M. M., Lang, P. J., Ahern, G. L., Davidson, R. J., & Schwartz, G. E. (1997). Neuroanatomical correlates of pleasant and unpleasant emotion. *Neuropsychologia*, 35(11): 1437-1444.

Lane, R. D., McRae, K., Reiman, E. M., Chen, K., Ahern, G. L., & Thayer, J. F. (2009). Neural correlates of heart rate variability during emotion. *NeuroImage*, 44(1): 213-222.

Lazzarino, A. I., Hamer, M., Stamatakis, E., & Steptoe, A. (2013). Low socioeconomic status and psychological distress as synergistic predictors of mortality from stroke and coronary heart disease. *Psychosomatic Medicine*, 75(3): 311-316.

Le Gallo, J., Baumont, C., Dall'erba, S., & Ertur, C. (2005). On the property of diffusion in the spatial error model. *Applied Economic Letters*, 12(9): 533-536.

Lehrer, P. M., Vaschillo, E., Vaschillo, B., Lu, S.-E., Eckberg, D. L., Edelberg, R., Shih, W. J., Lin, Y., Kuusela, T. A., Tahvanainen, K. U. O., & Hamer, R. M. (2003). Heart rate variability biofeedback increases baroreflex gain and peak expiratory flow. *Psychosomatic Medicine*, 65(5): 796-805.

Lepping, R. P., Acũna, M. H., Burlaga, L. F., Farrell, W. M., Slavin, J. A., Schatten, K. H., Mariani, F., Ness, N. F., Neubauer, F. M., Whang, Y. C., Byrnes, J. B., Kennon, R. S., Panetta, P. V., Scheifele, J., & Worley, E. M. (1995). The WIND magnetic field investigation. *Space Science Reviews*, 71(1): 207-229.

Levenson, R. W., Ekman, P., & Friesen, W. V. (1990). Voluntary facial action generates emotion-specific autonomic nervous system activity. *Psychophysiology*, 27(4): 363-384.

Lim, M. K. (2002). Cosmic rays: Are air crew at risk? *Occupational & Environmental Medicine*, 59: 428-432.

Lloyd-Jones, D. M., Larson, M. G., Leip, E. P., Beiser, A., D'Agostino, R. B., Kannel, W. B., Murabito, J. M., Vasan, R. S., Benjamin, E. J., & Levy, D. (2002). Lifetime risk for developing congestive heart failure: The Framingham heart study. *Circulation*, 106: 3068-3072.

Lohmann, K. J., Lohmann, C. M. F., & Putnam, N. F. (2007). Magnetic maps in animals: Nature's GPS. *Journal of Experimental Biology*, 210: 3697-3705.

Lowder, W. M., & Beck, H. L. (1966). Cosmic-ray ionization in the lower atmosphere. *Journal of Geophysical Research*, 71(19): 4661-4668.

Lubinski, D., & Humphreys, L. G. (1996). Seeing the forest from the trees: When predicting the behavior or status of groups, correlate means. *Psychology, Public Policy, and Law*, 2(2): 363-376.

Lustig, R. H., Schmidt, L. A., & Brindis, C. D. (2012). Public health: The toxic truth about sugar. *Nature*, 482(7383): 27-29.

Mani, A. R., Montagnese, S., Jackson, C. D., Jenkins, C. W., Head, I. M., Stephens, R. C., Moore, K. P., & Morgan, M. Y. (2009). Decreased heart rate variability in patients with cirrhosis relates to the presence and degree of hepatic encephalopathy. *American Journal of Physiology – Gastrointestinal and Liver Physiology*, 296(2): G330-G338.

McCraty, R., Atkinson, M., Tiller, W. A., Rein, G., & Watkins, A. D. (1995). The effects of emotions on short-term power spectrum analysis of heart rate variability. *American Journal of Cardiology*, 76(14): 1089-1093.

McGill, H. C., McMahan, C. A., & Gidding, S. S. (2008). Preventing heart disease in the 21st century: Implications of the Pathobiological Determinants of Atherosclerosis in Youth (PDAY) study. *Circulation*, 117(9): 1216-1227.

Mendoza, B., & Diaz-Sandoval, R. (2004). Effects of solar activity on myocardial infarction deaths in low geomagnetic latitude regions. *Natural Hazards*, 32: 25-36.

Messner, T., Häggström, I., Sandahl, I., & Lundberg, V. (2002). No covariation between the geomagnetic activity and the incidence of acute myocardial infarction in the polar area of northern Sweden. *International Journal of Biometeorology*, 46: 90-94.

Millman, M. (1993). *Access to Health Care in America*. Washington, DC: National Academic Press.

Mitsutake, G., Otsuka, K., Oinuma, S., Ferguson, I., Cornélissen, G., Wanliss, J., Halberg, F. (2004). Does exposure to an artificial ULF magnetic field affect blood pressure, heart rate variability and mood? *Biomedical Pharmacotherapy*, 58: 20-27.

Montano, N., Ruscone, T. G., Lombardi, F., Pagani, M., & Malliani, A. (1994). Power spectrum analysis of heart rate variability to assess the changes in sympathovagal balance during graded orthostatic tilt. *Circulation*, 90: 1826-1831.

Moran, P. A. P. (1950). Notes on continuous stochastic phenomena. *Biometrika*, 37(1): 17-23.

Mulligan, B. P., & Persinger, M. A. (2012). Experimental simulation of the effects of sudden increases in geomagnetic activity upon quantitative measures of human brain activity: Validation of correlational studies. *Neuroscience Letters*, 516(1): 54-56.

Mulligan, B. P., Hunter, M. D., & Persinger, M. A. (2010). Effects of geomagnetic activity and atmospheric power variations on quantitative measures of brain activity: Replication of the Azerbaijani studies. *Advances in Space Research*, 45(7): 940-948.

Nolan, J., Batin, P. D., Andrews, R., Lindsay, S. J., Brooksby, P., Mullen, M., Baig, W., Flapan, A. D., Cowley, A., Prescott, R. J., Neilson, J. M. M., & Fox, K. A. A. (1998). Prospective study of heart rate variability and mortality in chronic heart failure. *Circulation*, 98: 1510-1516.

Nolan, R. P., Kamath, M. V., Floras, J. S., Stanley, J., Pang, C., Picton, P., & Young, Q. R. (2005). Heart rate variability biofeedback as a behavioral neurocardiac intervention to enhance vagal heart rate control. *American Heart Journal*, 149(6): 1137e1-1137e7.

Nunan, D., Donovan, G., Jakovljevic, D. G., Hodges, L. D., Sandercock, G. R. H., & Brodie, D. A. (2009). Validity and reliability of short-term heart-rate variability from the Polar S810. *Medicine and Science in Sports and Exercise*, 41(1): 243-250.

O'Brien, K., Friedberg, W., Sauer, H. H., & Smart, D. F. (1996). Atmospheric cosmic rays and solar energetic particles at aircraft altitudes. *Environment International*, 22(supplement 1): 9-44.

Otsuka, K., Cornélissen, G., Weydahl, A., Holmeslet, B., Hansen, T. L., Shinagawa, M., Kubo, Y., Nishimura, Y., Omori, K., Yano, S., & Halberg, F. (2001). Geomagnetic disturbance associated with decrease in heart rate variability in a subarctic area. *Biomedical Pharmacotherapy*, 55: 51-56.

Pagani, M., Lombardi, F., Guzzetti, S., Rimoldi, O., Furlan, R., Pizzinelli, P., Sandrone, G., Malfatto, G., Dell'Orto, S., & Piccaluga, E. (1986). Power spectral analysis of heart rate and arterial pressure variabilities as a marker of sympatho-vagal interaction in man and conscious dog. *Circulation Research*, 59(2): 178-193.

Pagani, M., Montano, N., Porta, A., Malliani, A., Abboud, F. M., Birkett, C., & Somers, V. K. (1997). Relationship between spectral components of cardiovascular variabilities and direct measures of muscle sympathetic nerve activity in humans. *Circulation*, 95: 1441-1448.

Paintal, A. S. (1953). The conduction velocities of respiratory and cardiovascular afferent fibres in the vagus nerve. *Journal of Physiology*, 121: 341-359.

Papailiou, M., Mavromichalaki, H., Kudela, K., Stetiarova, J., & Dimitrova, S. (2011). Effect of geomagnetic disturbances on physiological parameters: An investigation on aviators. *Advances in Space Research*, 48: 1545-1550.

Papailiou, M., Mavromichalaki, H., Kudela, K., Stetiarova, J., & Dimitrova, S. (2012). Cosmic radiation influence on the physiological state of aviators. *Natural Hazards*, 61: 719-727.

Pearson, T. A., Palaniappan, L. P., Artinian, N. T., Carnethon, M. R., Criqui, M. H., Daniels, S. R., Fonarow, G. C., Fortmann, S. P., Franklin, B. A., Galloway, J. M., Goff Jr., D. C., Heath, G. W., Holland, F. A. T., Kris-Etherton, P. M., Labarthe, D. R., Murabito, J. M., Sacco, R. L., Sasson, C., & Turner, M. B.; on behalf of the American Heart Association Council on Epidemiology and Prevention. (2013). American Heart Association guide for improving cardiovascular health at the community level, 2013 update: A scientific statement for public health practitioners, healthcare providers, and health policy makers. *Circulation*.

Persinger, M. A. (1983). Religious and mystical experiences as artifacts of temporal lobe function: A general hypothesis. *Perceptual and Motor Skills*, 57: 1255-1262.

Persinger, M. A. (1999). Wars and increased solar-geomagnetic activity: Aggression or change in intraspecies dominance? *Perceptual and Motor Skills*, 88: 1351-1355.

Persinger, M. A. (2004). Weak-to-moderate correlations between global geomagnetic activity and reports of diminished pleasantness: A nonspecific source for multiple behavioral correlates? *Perceptual and Motor Skills*, 98: 78-80.

Persinger, M. A. (2014). Schumann resonance frequencies found within quantitative electroencephalographic activity: Implications for Earth-brain interactions. *International Letters of Chemistry, Physics and Astronomy*, 11(1): 24-32.

Persinger, M. A., Koren, S. A., Makarec, K., Richards, P., & Youlton, S. (1991). Differential effects of wave form and the subject's possible temporal lobe signs upon experiences during cerebral exposure to weak intensity magnetic fields. *Electromagnetic Biology and Medicine*, 10(1-2): 141-184.

Petković, D., & Ćojbašić, Ž. (2011). Adaptive neuro-fuzzy estimation of autonomic nervous system parameters effect on heart rate variability. *Neural Computing and Applications*, 21(8): 2065-2070.

Pickering, T. (1999). Cardiovascular pathways: Socioeconomic status and stress effects on hypertension and cardiovascular function. *Annals of the New York Academy of Sciences*, 896: 262-277.

Pieper, G. F., Zmuda, A. J., Bostrom, C. O., & O'Brien, B. J. (1962). Solar protons and magnetic storms in July 1961. *Journal of Geophysical Research*, 67(13); 4959-4981.

Ploubidis, G. B., Mathenge, W., de Stavola, B., Grundy, E., Foster, A., & Kuper, H. (2013). Socioeconomic position and later life prevalence of hypertension, diabetes and visual impairment in Nakuru, Kenya. *International Journal of Public Health*, 58(1): 133-141.

Pomeranz, B., Macaulay, R. J., Caudill, M. A., Kutz, I., Adam, D., Gordon, D., Kilborn, K. M., Barger, A. C., Shannon, D. C., & Cohen, R. J. (1985). Assessment of autonomic function in humans by heart rate spectral analysis. *American Journal of Physiology – Heart and Circulatory Physiology*, 248(1): H151-H153.

Porges, S. W. (1997). Emotion: An evolutionary by-product of the neural regulation of the autonomic nervous system. *Annals of the New York Academy of Sciences*, 807: 62-77.

Pouliou, T., & Elliott, S. J. (2009). An exploratory spatial analysis of overweight and obesity in Canada. *Preventive Medicine*, 48: 362-367.

Putilov, A. A. (1992). Unevenness of distribution of historical events throughout an 11-year solar cycle. *Biofizika*, 37(4): 629-635.

Reyes del Paso, G. A., Langewitz, W., Mulder, L. J. M., van Roon, A., & Duschek, S. (2013). The utility of low frequency heart rate variability as an index of sympathetic cardiac tone: A review with emphasis on a reanalysis of previous studies. *Psychophysiology*, 50: 477-487.

Robinson, W. S. (1950). Ecological correlations and the behavior of individuals. *American Sociological Review*, 15(3): 351-357.

Rogers, R. C., McTigue, D. M., & Hermann, G. E. (1995). Vagovagal reflex control of digestion: Afferent modulation by neural and “endoneurocrine” factors. *American Journal of Physiology – Gastrointestinal and Liver Physiology*, 268(1): G1-G10.

Rushton, G. (2003). Public health, GIS, and spatial analytic tools. *Annual Review of Public Health*, 24: 43-56.

Ruttan, L. A., Persinger, M. A., & Koren, S. (1990). Enhancement of temporal lobe-related experiences during brief exposures to milliGauss intensity extremely low frequency magnetic fields. *Electromagnetic Biology and Medicine*, 9(1): 33-54.

Saboul, D., Pialoux, V., & Hautier, C. (2014). The breathing effect of the LF/HF ratio in the heart rate variability measurements of athletes. *European Journal of Sport Sciences*, 14(S1): S282-S288.

Sakuragi, S., Sugiyama, Y., & Takeuchi, K. (2002). Effects of laughing and weeping on mood and heart rate variability. *Journal of Physiological Anthropology and Applied Human Science*, 21(3): 159-165.

Saranya, K., Pal, G. K., Habeebullah, S., & Pal, P. (2015). Analysis of Poincaré plot of heart rate variability in the assessment of autonomic dysfunction in patients with polycystic ovary syndrome. *International Journal of Clinical and Experimental Physiology*, 2(1): 34-39.

Saroka, K. S., & Persinger, M. A. (2014). Quantitative evidence for direct effects between Earth-ionosphere Schumann resonances and human cerebral cortical activity. *International Letters of Chemistry, Physics and Astronomy*, 20(2): 166-194.

Saroka, K. S., Caswell, J. M., Lapointe, A., & Persinger, M. A. (2014). Greater electroencephalographic coherence between left and right temporal lobe structures during increased geomagnetic activity. *Neuroscience Letters*, 560: 126-130.

Sasson, I. (2016). Trends in life expectancy and lifespan variation by educational attainment: United States, 1990-2010. *Demography*, 53(2): 269-293.

Saul, J. P., Berger, R. D., Chen, M. H., & Cohen, R. J. (1989). Transfer function analysis of autonomic regulation II: Respiratory sinus arrhythmia. *American Journal of Physiology – Heart and Circulatory Physiology*, 256(1): H153-H161.

Schove, D. J. (1955). The sunspot cycle, 649 BC to AD 2000. *Journal of Geophysical Research*, 60(2): 127–146.

Sharma, R., Pachori, R. B., & Acharya, U. R. (2015). An integrated index for the identification of focal electroencephalogram signals using discrete wavelet transform and entropy measures. *Entropy*, 17(8): 5218-5240.

Shin, S., Reisman, S. S., Tapp, W. N., & Natelson, B. H. (1988). Assessment of autonomic regulation to heart rate variability by the method of complex demodulation. *Computers in Cardiology Conference Proceedings*: 147-150.

Siepmann, M., Aykae, V., Unterdörfer, J., Petrowski, K., & Mueck-Weymann, M. (2008). A pilot study on the effects of heart rate variability biofeedback in patients with depression and in healthy subjects. *Applied Psychophysiology and Biofeedback*, 33: 195-201.

Singh, A. K., Siingh, D., & Singh, R. P. (2011). Impact of galactic cosmic rays on Earth's atmosphere and human health. *Atmospheric Environment*, 45(23): 3806-3818.

Snow, J. (1847). *On the Inhalation of the Vapour of Ether in Surgical Operations*. London: John Churchill, Princes Street, Soho.

Snow, J. (1855). *On the Mode of Communication of Cholera*. London: John Churchill, New Burlington Street.

Songchitruksa, P., & Zeng, X. (2010). Getis-Ord spatial statistics to identify hot spots by using incident management data. *Transportation Research Record*, 2165.

Sparks, P. J., & Sparks, C. S. (2010). An application of spatially autoregressive models to the study of US county mortality rates. *Population, Space and Place*, 16(6): 465-481.

Sparks, P. J., Sparks, C. S., & Campbell, J. J. A. (2013). An application of Bayesian spatial statistical methods to the study of racial and poverty segregation and infant mortality rates in the US. *GeoJournal*, 78(2): 389-405.

Stein, P. K., Domitrovich, P. P., Huikuri, H. V., & Kleiger, R. E. (2005). Traditional and nonlinear heart rate variability are each independently associated with mortality after myocardial infarction. *Journal of Cardiovascular Electrophysiology*, 16(1): 13-20.

Steinhauer, S. R., Siegle, G. J., Condray, R., & Pless, M. (2004). Sympathetic and parasympathetic innervation of pupillary dilation during sustained processing. *International Journal of Psychophysiology*, 52(1): 77-86.

Svensmark, H., & Friis-Christensen, E. (1997). Variation of cosmic ray flux and global cloud coverage: A missing link in solar-climate relationships. *Journal of Atmospheric and Solar-Terrestrial Physics*, 59(11): 1225-1232.

Talwar, A., Sahni, S., Talwar, A., Kohn, N., & Klinger, J. R. (2016). Socioeconomic status affects pulmonary hypertension disease severity at time of first evaluation. *Pulmonary Circulation*, 6(2): 191-195.

Tao, L., Liu, J., & Xiao, B. (2013). Effects of geodemographic profiles on healthcare service utilization: A case study on cardiac care in Ontario, Canada. *BMC Health Services Research*, 13.

Task Force of the European Society of Cardiology. (1996). The North American Society of Pacing and Electrophysiology – Heart rate variability: Standards of measurement, physiological interpretation and clinical use. *Circulation*, 93.5: 1043-1065.

Thayer, J. F., Hansen, A. L., Saus-Rose, E., & Johnsen, B. H. (2009). Heart rate variability, prefrontal neural function, and cognitive performance: The neurovisceral integration perspective on self-regulation, adaptation, and health. *Annals of Behavioral Medicine*, 37: 141-153.

Thayer, J. F., Yamamoto, S. S., & Brosschot, J. F. (2010). The relationship of autonomic imbalance, heart rate variability and cardiovascular disease risk factors. *International Journal of Cardiology*, 141(2): 122-131.

Tochi, M., Sugiura, T., Murai, T., & Sengoku, A. (1997). A new method of assessing cardiac autonomic function and its comparison with spectral analysis and coefficient of variation of R-R interval. *Journal of Autonomic Nervous System*, 62: 79-84.

Tsuji, H., Venditti Jr., F. J., Manders, E. S., Evans, J. C., Larson, M. G., Feldman, C. L., & Levy, D. (1994). Reduced heart rate variability and mortality risk in an elderly cohort: The Framingham heart study. *Circulation*, 90: 878-883.

Tsuji, H., Larson, M. G., Venditti Jr., F. J., Manders, E. S., Evans, J. C., Feldman, C. L., & Levy, D. (1996). Impact of reduced heart rate variability on risk for cardiac events: The Framingham heart study. *Circulation*, 94: 2850-2855.

Tsyganenko, N. A. (1987). Global quantitative models of the geomagnetic field in the cislunar magnetosphere for different disturbance levels. *Planetary and Space Science*, 35(11): 1347-1358.

van der Heide, I., Wang, J., Droomers, M., Spreeuwenberg, P., Rademakers, J., & Uiters, E. (2013). The relationship between health, education, and health literacy: Results from the Dutch Adult Literacy and Life Skills Survey. *Journal of Health Communication: International Perspectives*, 18(S1): 172-184.

Vares, D. A. E., & Persinger, M. A. (2015). Correlations between a new daily global indicator of human behavior, threshold seismicity, and solar activity: Congruence of energy and implications. *Global Journal of Human-Social Science Research*: 15(1).

Voss, P. R. (2007). Demography as a spatial social science. *Population Research and Policy Review*, 26: 457-476.

Wager, T. D., Davidson, M. L., Hughes, B. L., Lindquist, M. A., & Ochsner, K. N. (2008). Prefrontal-subcortical pathways mediating successful emotion regulation. *Neuron*, 59(6): 1030-1050.

Walker, M. M., Dennis, T. E., & Kirschvink, J. L. (2002). The magnetic sense and its use in long-distance navigation by animals. *Current Opinion in Neurobiology*, 12(6): 735-744.

Waller, L. A., & Gotway, C. A. (2004). *Applied Spatial Statistics for Public Health Data*. New Jersey: Wiley.

Williams, B., Lacy, P. S., Thom, S. M., Cruickshank, K., Stanton, A., Collier, D., Hughes, A. D., Thurston, H., & O'Rourke, M. (2006). Differential impact of blood pressure-lowering drugs on central aortic pressure and clinical outcomes. *Circulation*, 113: 1213-1225.

Wiltschko, W., & Wiltschko, R. (2005). Magnetic orientation and magnetoreception in birds and other animals. *Journal of Comparative Physiology A*, 191(8): 675-693.

Wit, A. L., Weiss, M. B., Berkowitz, W. D., Rosen, K. M., Steiner, C., & Damato, A. N. (1970). Patterns of atrioventricular conduction in the human heart. *Circulation Research*, 27: 345-359.

Zorlu, A., & Mulder, C. H. (2011). Ethnic differences in leaving home: Timing and pathways. *Demography*, 48(1): 49-72.

Zuckerman, M. (1971). Physiological measures of sexual arousal in the human. *Psychological Bulletin*, 75(5): 297-329.

Chapter 2 – Assessing Nonlinear Descriptors for Heart Rate Variability and Discrimination of Cardiac Arrhythmia

In submission

2. Abstract

Many studies on heart rate variability continue to employ Poincaré plot analysis to derive nonlinear information. As shown by some studies, however, this may not be an accurate inference. Furthermore, numerous overlapping relationships have been identified between Poincaré descriptors and standard measures of heart rate variability computed in the time and frequency domains. Many additional nonlinear descriptors are available for exploration in the context of heart rate variability with some remaining relatively novel for this area. Using two samples (healthy and arrhythmia), the current study further emphasizes the information redundancy inherent to Poincaré statistics and also assesses three other nonlinear measures for similar overlap with traditional variables. In particular, calculations of average wavelet entropy were shown to present information not contained within other variables that were assessed. Finally, the use of time-frequency complexity derived from a combination of discrete wavelet transform and information entropy was applied to the discrimination of healthy or arrhythmia recordings, indicating potential usefulness of this method for future investigation.

2.1. Introduction

Nonlinear dimensions of heart rate variability (HRV) continue to interest researchers and clinicians as alternate indicators of autonomic-cardiovascular state stemming from chaotic physiological activity (Voss et al., 2009). In this regard, the method of Poincaré plot analysis (PPA) has been a particularly popular technique (Kemp et al., 2012; Saranya et al., 2015; Stein et al., 2005) which may be partly attributable to its ease of use. A scattergram is produced for a time series of heart rate R-R intervals (x_i) with itself leading by a single case (x_{i+1}), as demonstrated in Figure 6, which is typically quantified using a geometric technique of fitting an ellipse to the scatter distribution along its line of identity. The associated width and length of the ellipse are then obtained, which reflect short- and long-term variability respectively, that result from cardiac modulation mediated by activity of the parasympathetic and sympathetic nervous system (Huikuri et al., 2003). As an example of autonomic contribution to PPA dynamics, Karmakar et al. (2011) identified decreases in Poincaré indices associated with experimentally manipulated decreases in parasympathetic activity while indices also increased with concomitant parasympathetic increases.

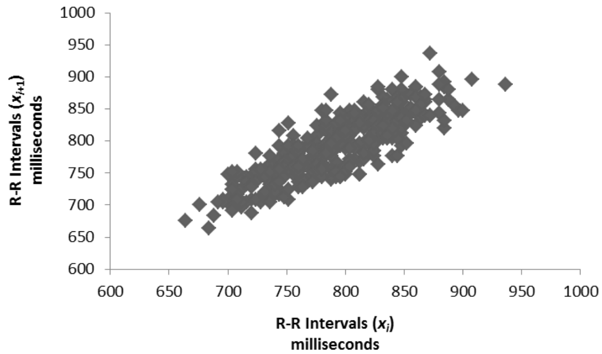

Figure 6: Example Poincaré plot of short-term (~5 minutes) R-R interval time series from healthy volunteer

The use of PPA and other nonlinear dimensions for quantifying HRV has also been effective in clinical applications including risk stratification of sudden cardiac death in cardiomyopathy patients, where traditional linear techniques of quantifying HRV did not demonstrate a similar predictive capacity (Voss et al., 2007). Previous research by Stein et al. (2005) had also shown important relationships between both linear and nonlinear indices of HRV with patient mortality following myocardial infarction. In a particularly interesting study it was shown that the short-term component derived from PPA was significantly lower in patients with major depressive disorder compared to control participants, while this difference further extended to an intriguing linear decrease in HRV across psychological comorbidities of various magnitudes (Kemp et al., 2012). However, there are also strong correlations between Poincaré indices with standard time and frequency domain measures of HRV (Huikuri et al., 2003). For the current example of depressive disorders (Kemp et al., 2012), the same results shown for the short-term PPA index were also identified for short-term HRV calculated by standard time domain methods.

The inter-subject reliability and prognostic capability of various nonlinear HRV dimensions has been assessed with positive indications in this regard, perhaps even more reliable than traditional indicators of HRV (Carrasco et al., 2001; Huikuri & Stein, 2013). However, Brennan et al. (2001) have questioned whether values derived from PPA actually reflect nonlinear HRV dynamics. While one study (Cardoso et al., 2014) identified a statistically significant correlation between the short-term PPA index and a nonlinear coefficient obtained from detrended fluctuation analysis (DFA $\alpha 1$), Hoshi et al. (2013) found no strong relationship for PPA width and length with a wide range of nonlinear dimensions including DFA. The authors found further strong overlap between PPA indices and standard HRV measures including their respective variables for short-term variability which demonstrated correlations of $\rho = 0.99$ for both databases investigated (Hoshi et al., 2013).

Previous use of alternate nonlinear descriptors of HRV for risk stratification suggests that these various indicators, typically derived through application of signal processing techniques and information theories, present significant predictive capacity for the identification of patients who are at high-risk for sudden cardiac death (SCD) following myocardial infarction (Gang, 2013). In this specific context, Fujita et al. (2016) recently applied various nonlinear measures to the prediction of SCD up to four minutes prior to the event. A number of nonlinear measures were tested for classification accuracy between SCD risk and healthy controls including variables derived from discrete wavelet transform (DWT) which simultaneously reflect time and frequency domains. The wavelet energies employed by Fujita et al. (2016) were found to be significant predictors of SCD with a high degree of sensitivity and specificity.

The aim of the current study was to extend the results of Hoshi et al. (2013) considering the myriad nonlinear indices available for HRV (Huikuri et al., 2003) and their potential overlap with traditional time and frequency domain measures (Voss et al., 2009). Alternate nonlinear methods that have not yet been thoroughly assessed in the specific context of HRV inter-correlation were employed for the current analyses including Higuchi (1988) fractal dimension (*HFD*), mutual information (*MI*), and average wavelet entropy (*wH*). The previous study (Hoshi et al., 2013) also separately assessed two databases including either healthy participants or those with coronary artery disease. A similar approach was taken for the current study which also included two separate databases with varied characteristics (arrhythmia or cardiovascular healthy). Finally, HRV data were investigated for the potential to discriminate between healthy ECG records and those containing cardiac arrhythmia. This is particularly important given the relatively fewer number of studies examining HRV indices during arrhythmia, particularly those using nonlinear qualities, compared to other cardiac health issues such as SCD or myocardial infarction. An optimal model was sought for the discrimination of healthy or arrhythmia HRV using standard indicators and relatively novel nonlinear descriptors after controlling for participant age.

2.2. Methods

Two separate databases of different characteristics were first analyzed independently for the current study. The first set of results (Sample A) were obtained from a healthy sample of n = 20 volunteers (n = 11 males, n = 9 females) during normal breathing while seated comfortably and facing forward with minimal movement (age range of 18 to 55 years). After a brief rest period (~5 minutes) short-term electrocardiograph (ECG) recordings were obtained for ~5 minutes using single lead (two electrodes) Covidien Kendall H135SG disposable ECG electrodes connected to a Mitsar-201 amplifier with a laptop computer and WinEEG v2.103.7 software. Recordings were exported for further processing and analysis. ARTiiFACT v2.05 (Kaufmann et al., 2011) was used for automatic QRS peak detection with additional visual verification from which R-R intervals were obtained in msec. Where necessary, artifacts were corrected using cubic spline interpolation.

The second set of ECG records (Sample B) were derived from the MIT-BIH Arrhythmia Database (Goldberger et al., 2000; Moody & Mark, 2001) which is a widely used standard collection of n = 48 typical arrhythmia ECG records from in- and outpatients, each of ~30 minutes in duration. The original recordings were digitized at 360 Hz with independent annotation by at least two cardiologists for each record (for a thorough description of this database see Moody & Mark, 2001). ECG annotations were accessed directly from PhysioNet using the WFDB Toolbox for Matlab (Goldberger et al., 2000; Silva & Moody, 2014) and converted to R-R intervals in msec. One individual contributed two ECG records and the latter was removed for the current study, along with an additional two records missing ages or other necessary information. From the remaining records we selected the 15 individuals within the age range of Sample A (i.e., ages 20 to 60). The next five youngest individuals were also selected for inclusion in order to produce equal sample sizes for the two groups. This filtered case selection was undertaken to reduce the overall age discrepancy between groups. After case selection, Sample B consisted of n = 20 individuals aged 23 to 64 years (n = 11 males, n = 9 females) from which HRV samples of ~5 minutes were acquired.

ARTiiFACT software was employed with both samples for computation of standard time and frequency domain HRV variables including necessary resampling (4 Hz interpolation) and detrending procedures for the latter. All other indicators of HRV were computed using Matlab v7.12 which was also used for wavelet techniques. Popular time domain measures used for the current study included an estimate of long-term or total variability as indicated by the standard deviation of R-R intervals (*SDNN*), as well as short-term variability as indicated by the root mean square of successive differences between adjacent R-R intervals (*RMSSD*). Standard frequency domain indices acquired through resampled fast Fourier transform (FFT) included low frequency (*LF* = 0.04 to 0.15 Hz) and high frequency components (*HF* = 0.15 to 0.40 Hz) in spectral power units of ms^2, as well as the unitless *LF/HF* ratio. Poincaré plot ellipse measures were computed according to:

$$SD1 = \sqrt{\left(\left(\frac{1}{2}\right) \cdot SDSD^2\right)}$$

where *SDSD* = standard deviation of successive differences between R-R intervals. This value indicates the ellipse width and follows the data dispersion perpendicular to the line of identity. This particular variable also reflects short-term variability. Similarly, the second Poincaré measure was obtained with:

$$SD2 = \sqrt{\left(2 \cdot SDNN^2 - \left(\frac{1}{2}\right) \cdot SDSD^2\right)}$$

This indicates the ellipse length following the data dispersion along the line of identity and reflects long-term variability.

The Higuchi (1988) fractal dimension (*HFD*) of each R-R interval series was calculated with the following procedure: First, a finite series of data is represented as $x(1)$, $x(2)$, $x(3)$, …, $x(\mathrm{N})$. A new time series (x^{t}_{k}) is created from the original such that:

$$x_k^{\mathrm{t}}; x(\mathrm{t}), x(\mathrm{t}+k), x(\mathrm{t}+2k), \ldots, \left(\mathrm{t}+\left[\frac{\mathrm{n}-\mathrm{t}}{k}\right]k\right)$$

where t = initial time (t = 1, 2, 3, …, k), k = time interval (both t and k are integers), and [·] = Gauss notation or floor function from which [x] is the largest integer that does not exceed x. Through this process k new series are derived. As previously demonstrated by others including Cervantes-De la Torre et al. (2013), for an example where k = 4 and n = 100, the following set of new series would be produced:

$$x_4^1 = x(1), x(5), x(9), \ldots, x(97)$$

$$x_4^2 = x(2), x(6), x(10), \ldots, x(98)$$

$$x_4^3 = x(3), x(7), x(11), \ldots, x(99)$$

$$x_4^4 = x(4), x(8), x(12), \ldots, x(100)$$

A curve is then fit to each new series ($x_{\mathrm{t}k}$) where the respective lengths (L) are calculated according to:

$$L_{\mathrm{t}}(k) = \frac{1}{k}\left(\sum_{i=1}^{\left[\frac{\mathrm{n}-\mathrm{t}}{k}\right]}\big(x(\mathrm{t}+ik) - x(\mathrm{t}+(i-1)k)\big)\right)\left(\frac{\mathrm{n}-1}{\left[\frac{\mathrm{n}-\mathrm{t}}{k}\right]k}\right)$$

for which the final set of parentheses indicate a normalization factor. Finally, the average of the series lengths (<$L(k)$>) is then obtained from which the fractal dimension can be derived by comparing <$L(k)$> with a power law satisfying the following proportional condition:

$$\langle L(k) \rangle \propto k^{-HFD}$$

If <$L(k)$> follows a power equation then the derived curve is considered to be a fractal dimension described by *HFD*. This index reflects the complexity of a signal through the changes of detail with scale ("self-similarity") or the general irregularity of a time series (Higuchi, 1988) while also being particularly useful with signals consisting of fewer data points (Accardo et al., 1997). Corresponding values computed for *HFD* generally lie within an interval of [1, 2] (Cervantes-De la Torre et al., 2013) which reflects the idea that fractal dimensions are too complicated to be one-dimensional while they are not quite two-dimensional. However, this is more of a theoretical boundary as particularly noisy signals can produce *HFD* values beyond a limit of 2. The optimal maximum interval (k_{max}) was determined by plotting a range of k with corresponding *HFD* values and identifying the point at which *HFD* plateaus (Doyle et al., 2004). In the current study, k_{max} = 25 was identified as the optimal value based on examination of normal ECG records.

Wavelet entropy is a relatively more recent method of analyzing ECG based on time-frequency complexity that has been used in neuroelectrical studies (e.g., more recently in Sharma et al., 2015) and successfully applied to HRV data (Işler & Kuntalp, 2007). The wavelet entropy technique begins with one-dimensional decomposition of an R-R interval time series using wavelet analysis which applies a mother wavelet to dilate and shift a signal with:

$$\psi_{a,b} = \frac{1}{\sqrt{a}} \psi \left(\frac{\mathrm{t} - b}{a} \right)$$

where ψ = basis function or wavelet family, t = time, a = scaling parameter, and b = shifting parameter. Unlike traditional Fourier transform analyses (e.g., FFT), this allows decomposition of a signal in both time- and frequency-space simultaneously. Subsequently, the base transformation employed in wavelet analysis (*W*) of a discrete signal (*x*) is an integral of the form:

$$W(a, b) = \int_{-\infty}^{\infty} x(\mathrm{t})\psi_{a,b}(\mathrm{t})\mathrm{dt}$$

Low- and high-pass filters are then applied in multiple iterations in order to extract low frequency approximation coefficients (a_i) and high frequency detail coefficients (d_1, …, d_i) as demonstrated in Figure 7. A scale of analysis is indicated prior to transformation which dictates the decomposition level (i.e., number of additional filter passes and relevant resampling of each iteration) and associated number of frequency coefficient series to be extracted (*i*). For wavelet decomposition of physiological time series, the suggested form (Işler & Kuntalp, 2007) uses a db4 mother wavelet function (Daubechies, 1992) with a scale of 7. All R-R interval series were standardized (*z*-scores) prior to DWT.

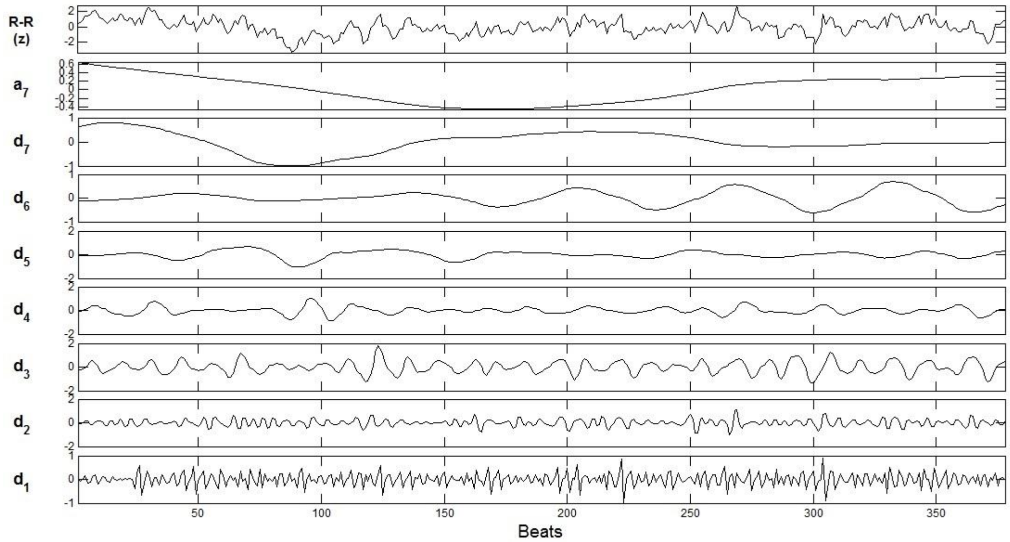

Figure 7: Example one-dimensional decomposition of sample short-term (5 minute) R-R interval time series using discrete wavelet transform (DWT) with db4 mother wavelet function at scale (level) 7; Standardized (*z*-score) R-R interval series with wavelet coefficients a_7 to d_1

After extraction of relevant coefficients, wavelet packet energies (E_i) are obtained according to:

$$E_i = |C_i|$$

where C_i = *i*th coefficient in a series. The total energy (E_{tot}) is simply the summation of $|C_i|$ or $\sum E_i$ (Sharma et al., 2015). Using these indices, normalized values of relative wavelet energy equivalent to a probability distribution (P_i) are computed with:

$$P_i = \frac{E_i}{E_{tot}}$$

where $\sum P_i = 1$. Finally, P_i is entered into Shannon's (1948) equation for information entropy (*H*) with a base 2 logarithm typically employed in order to derive values in bits:

$$H = -\sum \left(\mathrm{P}_i \cdot \log_2(\mathrm{P}_i) \right)$$

Higher entropy reflects a greater number of different values found in a signal along with how evenly distributed those values are. Following this, time series with lower entropy are more predictable and ordered while higher entropy indicates a more chaotic signal. Once this procedure was applied, the average wavelet entropy (*wH*) was obtained by simply averaging the individual *H* values from each decomposition scale within a given time series.

Computation of results obtained through mutual information concepts (Li, 1990; Wells et al., 1996) can be used to describe the interdependence between two signals similar to cross-correlation, or autocorrelation in the case of a signal related to itself over time. Despite this conceptual overlap, mutual information calculations do not present the same limitations as standard correlation analyses and instead solve for the similarity of the joint probability distribution ($\mathrm{P}(x, y)$) with the marginal probability distributions of each variable ($\mathrm{P}(x)$ and $\mathrm{P}(y)$) using the primary discrete equation:

$$MI(x;y) = \sum_{y} \sum_{x} \mathrm{P}(x,y) \log \left(\frac{\mathrm{P}(x,y)}{\mathrm{P}(x)\mathrm{P}(y)} \right)$$

where the same calculation would be applied in a continuous scenario by simply substituting a definite double integral function ($\int y \int x$) for the summation functions. To simplify this concept, mutual information can be considered a combination of joint entropy and correlation. This calculation provides some insight into the degree to which knowledge of signals *x* and *y* reduce the uncertainty of each other. For analysis of HRV in the current study, lead+1 mutual information values (*MI*) were simply calculated for each R-R interval series (x_i) with itself shifted by one case (x_{i+1}) following the basis of a standard Poincaré plot.

Additional statistical analyses were conducted using SPSS v17 software. This included Shapiro-Wilks distribution testing and nonparametric linear correlations. Factor analysis was applied using the principal components method with Varimax rotation for optimal factor solutions. All variable loadings < 0.70 were suppressed to better compensate for the relatively small overall sample. A series of binary logistic models were also assessed according to the standard logistic regression:

$$p_y = \frac{1}{1 + e^{(A+B_1x_1+,\dots,+B_ix_i)}}$$

where p_y = probability of dependent variable y being 1 (i.e., arrhythmia), A = regression constant, B_1 to B_i = regression coefficients, and x_1 to x_i = predictor variables. Similarly, the logit of p_y can be expressed according to a linear regression following:

$$\text{logit}_{p_y} = \log\left(\frac{p_y}{1 - p_y}\right) = A + B_1x_1+, \dots, +B_ix_i$$

Along with additional standard regression model appraisal, Hosmer-Lemeshow goodness-of-fit testing (Hosmer & Lemeshow, 2013), which follows a chi-square (χ^2) distribution with degrees of freedom (df) equal to the number of predictor variables, was applied to assess how well each logistic regression model fit the data. Regression coefficients from this type of model are exponentiated in order to obtain odds ratios (OR) where OR = 1 indicates no effect, OR > 1 suggests that an increase in the predictor variable is associated with increased odds of arrhythmia, and OR < 1 similarly shows a decrease in the independent measure predicts increased odds of arrhythmia. Where OR < 1, values were also inverted (1/OR) to better reflect the actual strength of the relationship although with respect to the odds of having healthy ECG rather than arrhythmia. Any inverted values are noted as such and original values are also provided with 95% confidence intervals (CI). Age was controlled for as a covariate in each analysis. All regression analyses were conducted in two blocks where age was entered in the first block and HRV predictor variables were entered in the second block with a backward conditional variable selection procedure. This nested-modelling allowed comparison between regression blocks to better determine if HRV variables improved accuracy beyond the age-only model. Finally, sensitivity and specificity of logistic regression models were tested using receiver operating characteristics (ROC) and associated area under the curve (AUC) statistics.

2.3. Results

All variables were assessed for normality using Shapiro-Wilk tests for which a majority were not normally distributed. Thus, to avoid the use of varied data transformation across databases, nonparametric techniques were employed for correlation analyses. In order to investigate the presence of inter-correlation among HRV indices of interest, a series of linear Spearman (ρ) correlations were conducted for each nonlinear descriptor with all other standard HRV variables following previous research (Hoshi et al., 2013). Only strong coefficients ($\rho > 0.70$) were considered as adequate evidence for potential information overlap between variables with respect to their relationship with a third variable. Furthermore, correlations of $\rho > 0.90$ potentially indicated that the associated variables likely convey very similar information. Note that nonlinear descriptors that were not calculated in time units (*HFD*, *wH*, and *MI*) were standardized (*z*-scores) to allow easier interpretation of subsequent results.

Nonparametric correlations for Sample A (healthy) indicated a very strong relationship between both Poincaré descriptors (*SD1* and *SD2*) and *SDNN*, particularly with *SD2* ($\rho = 0.982$, $p < 0.001$). Similar to previous research (Hoshi et al., 2013), a perfect correlation was observed between *SD1* and *RMSSD* ($\rho = 1.00$, $p < 0.001$). These results were anticipated considering *SD1* and *RMSSD* both reflect short-term variability while *SD2* and *SDNN* indicate long-term variability. Conversely, none of the alternate nonlinear descriptors (*HFD*, *wH*, *MI*) demonstrated strong correlations (all $\rho < 0.70$) with standard indices of HRV (Table 1). A similar pattern of correlations was observed for Sample B (arrhythmia) although some coefficients varied slightly. However, *SD2* remained particularly strongly associated with SDNN ($\rho = 0.961$, $p < 0.001$) and the correlation between *SD1* and *RMSSD* was again perfect and positive ($\rho = 1.00$, $p < 0.001$). For this second sample, the additional nonlinear *MI* was also very strongly associated with many standard HRV descriptors including *SDNN*, *RMSSD*, *HF*, and *LF* (Table 2).

Table 1: Spearman correlation coefficients (ρ) for nonlinear descriptors with all other variables using Sample A (healthy)

Variable	***SD1***	***SD2***	***HFD***	***wH***	***MI***
SDNN	0.808	0.982	0.170	-0.465	0.696
RMSSD	1.0	0.746	0.635	-0.448	0.674
LF	0.565	0.749	-0.057	-0.614	0.580
HF	0.956	0.704	0.693	-0.344	0.656

Variable	SD1	SD2	HFD	wH	MI
LF/HF	-0.337	0.039	-0.612	-0.192	-0.036

Table 2: Spearman correlation coefficients (ρ) for nonlinear descriptors with all other variables using Sample B (arrhythmia)

Variable	SD1	SD2	HFD	wH	MI
SDNN	0.913	0.961	0.020	-0.423	0.931
RMSSD	1.0	0.833	0.260	-0.486	0.848
LF	0.753	0.946	-0.317	-0.203	0.931
HF	0.902	0.877	0.033	-0.386	0.905
LF/HF	-0.268	0.143	-0.564	0.373	0.129

Factor analysis was conducted on the combined datasets. Descriptors derived from PPA were excluded given the perfect or near-perfect overlap observed with standard time-domain HRV variables. Factor loadings < 0.70 were suppressed to help compensate for the relatively small sample. Two components emerged with eigenvalues > 1 after rotation which together explained 72.427% of the total variance. According to the rotated component matrix (Table 3), factor 1 consisted of *SDNN*, *RMSSD*, *HF*, *LF*, and MI_z, while factor 2 included *LF/HF*, which loaded negatively, and HFD_z. The variable wH_z did not strongly load onto either component. Factor scores were extracted and saved for subsequent analysis.

Table 3: Factor analysis for all included descriptors of heart rate variability (HRV); includes rotated components with factor loading scores for each variable as well as the eigenvalue and total variance explained (%) by each component (loadings < 0.70 suppressed)

Variable	Component 1	Component 2
SDNN	0.943	-
RMSSD	0.826	-
LF	0.760	-
HF	0.712	-
LF/HF	-	-0.918
HFD_z	-	0.883
wH_z	-	-
MI_z	0.875	-
Eigenvalue	3.523	2.271
Variance Explained (%)	44.038	28.389

Logistic regression models were constructed for each subset of HRV predictors (time, frequency, nonlinear descriptors) according to previously described two-block modelling. When regression analysis was conducted with time domain HRV variables as additional independent measures, only participant age was a significant predictor of healthy or arrhythmia ECG records. No additional HRV variables entered the regression model when using frequency domain descriptors. The nonlinear descriptor model ($\chi^2_{(2)}$ = 30.502, p < 0.001) produced a significant change from the age-only block ($\chi^2_{(1)}$ = 6.788, p = 0.009) and included age (OR = 1.148, CI 95% = 1.044 to 1.263, p = 0.004) as well as wH_z (OR = 0.240, CI 95% = 0.066 to 0.867, p = 0.029) indicating that a decrease of one wH_z standard deviation was associated with being about four times more likely to present with an arrhythmia (1/OR = 4.167) with 82.50% accuracy according to the equation:

$$\text{logit}_{p_y} = -5.019 - 1.428 \cdot wH_z + 0.138 \cdot \text{age}$$

The associated confusion matrix is provided in Table 4. Finally, the components derived from factor analysis were also assessed as independent variables in binary logistic regression analysis. However, only age entered as a significant predictor. Gender did not enter as a significant predictor in any models examined. Probabilities predicted by age and wH_z were assessed with ROC plot analysis for sensitivity and specificity which further suggested a high degree of model accuracy (AUC = 0.943, SE = 0.033, p < 0.001) as shown in Figure 8.

Table 4: Confusion matrix of logistic regression prediction outcome using age and average wavelet entropy (wH_z) to classify healthy or arrhythmia heart rate variability (HRV)

Observed		**Predicted**	
	Healthy (n)	**Arrhythmia (n)**	**Correct (%)**
Healthy	17	3	85
Arrhythmia	4	16	80

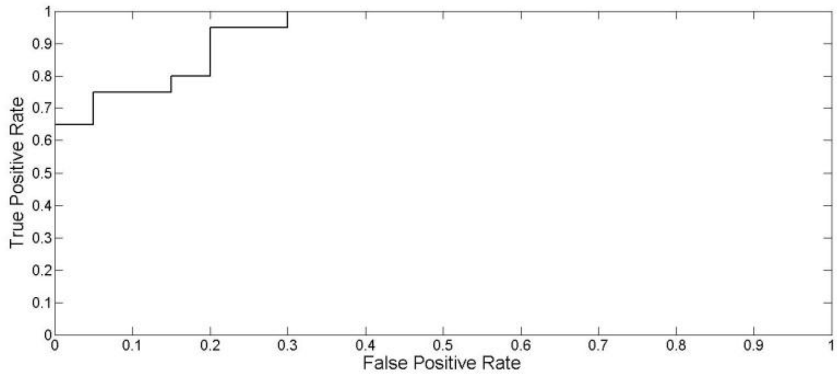

Figure 8: Receiver operating characteristic (ROC) plot for sensitivity and specificity of age with average wavelet entropy (*wH_z*) logistic regression model predicting between arrhythmia and healthy ECG records

2.4. Discussion

Although the current results for PPA descriptors of HRV tended to coincide with those obtained by other researchers (Hoshi et al., 2013), the present study also extends these results to examination of additional nonlinear variables with associated pathology discrimination. Specifically, the *SD1* descriptor appeared to be practically useless in analysis of short-term recordings whether cardiac anomalies were present or not. This inference was simply due to the perfect correlation shown between *SD1* and the standard time domain *RMSSD* variable in both cases (i.e., healthy or arrhythmia) after which *SD1* was excluded from subsequent analyses. This finding is consistent with that observed by Hoshi et al. (2013) where healthy individuals' HRV and that acquired from those with coronary artery disease similarly overlapped between *SD1* and *RMSSD* values, while Huikuri et al. (2003) had also identified information overlap between PPA descriptors and standard time domain calculations of HRV. Although not quite as strong as short-term descriptor correlations, *SD2* derived from PPA was also very strongly correlated with *SDNN* for both short-term databases and similarly excluded from further investigation.

While previous authors (Hoshi et al., 2013) examined relationships between PPA descriptors and a range of nonlinear dimensions, a number of the alternate methods employed require particularly large signals (e.g., DFA and correlation dimension). However, additional nonlinear indices not often employed in previous analysis are more amenable to relatively smaller samples including *HFD* (Accardo et al., 1997). Measures of *wH* revealed even greater potential as a promising alternate dimension of HRV given the lack of correlation with traditional indices and the solitary loading of *wH* within principle component exploration. The use of *wH* in research of HRV has been slowly increasing (Fujita et al., 2016; Işler & Kuntalp, 2007) with positive indication of significant risk stratification capability in specific contexts, although more work is required in order to better discern the physiological process(es) underlying variations in *wH* values and the use of entropy averaged across wavelet bands. Future research should also further assess the applicability of *wH* as a predictor of cardiac arrhythmia compared to healthy ECG records according to the regression models previously discussed in which age and *wH* were the only significant predictors identified with positive and negative associations to arrhythmia respectively. Although age was controlled for in the regression analyses, the overall age discrepancy between samples should be addressed in future studies through the use of case-control research design with conditional regression where appropriate data are available.

It was observed that PPA calculations appear to be redundant in terms of the information they contain compared to traditional measures of HRV, although information redundancy is an issue for other areas of HRV research. As an example, Burr (2007) has noted that the normalized values for *LF* and *HF* (LF_{nu} and HF_{nu} respectively) and *LF/HF* are algebraically redundant where a relationship with a third variable will produce the same effect but with opposite direction (positive or negative coefficient) between LF_{nu} and HF_{nu} with *LF/HF* also following the same results. Although Brennan et al. (2001) had earlier questioned the nonlinear dimensionality of PPA descriptors, few studies have sought to explicitly explore this issue and researchers continue to infer unique nonlinear dimensionality through PPA. However, the investigations that have been conducted appear to converge upon similar conclusions of information redundancy and a continuing interest in the identification of alternate nonlinear descriptors applied to discrimination of pathological conditions (Hoshi et al., 2013; Huikuri et al., 2003; Huikuri & Stein, 2013), particularly with the use of time-frequency information complexity as discerned by measures of entropy (Fujita et al., 2016).

References

Accardo, A., Affinito, M., Carrozzi, M., & Bouquet, F. (1997). Use of the fractal dimension for the analysis of electroencephalographic time series. *Biological Cybernetics*, 77: 339-350.

Brennan, M., Palaniswami, M., & Kamen, P. (2001). Do existing measures of Poincaré plot geometry reflect nonlinear features of heart rate variability? *IEEE Transactions on Biomedical Engineering*, 48(11): 1342-1347.

Burr, R. L. (2007). Interpretation of normalized spectral heart rate variability indices in sleep research: A critical review. *Sleep*, 30(7): 913-919.

Cardoso, M. A., Dos Santos, M. A., de Abreu, L. C., Fontes, A. M. G., da Silva, A. G., Ogata, C. M., de Oliveira, L. S., Sousa, F. H., do Amaral, J. A. T., Cano, A. S., Plassa, B. O., Milan, R., & Valenti, V. E. (2014). Fractal scaling exponents of heart rate variability association with linear indices and Poincaré plot. *Experimental and Clinical Cardiology*, 20(1): 2444-2456.

Carrasco, S., Gaitán, M. J., González, R., & Yánez, O. (2001). Correlation among Poincaré plot indexes and time and frequency domain measures of heart rate variability. *Journal of Medical Engineering and Technology*, 25(6): 240-248.

Cervantes-De la Torre, F., González-Trejo, J. I., Real-Ramírez, C. A., & Hoyos-Reyes, L. F. (2013). Fractal dimension algorithms and their application to time series associated with natural phenomena. *Journal of Physics: Conference Series*, 475(conference 1).

Daubechies, I. (1992). *Ten Lectures on Wavelets*. Philadelphia: Society for Industrial and Applied Mathematics.

Doyle, T. L. A., Dugan, E. L., Humphries, B., & Newton, R. U. (2004). Discriminating between elderly and young using a fractal dimension analysis of centre of pressure. *International Journal of Medical Sciences*, 1(1): 11-20.

Fujita, H., Acharya, U. R., Sudarshan, V. K., Ghista, D. N., Sree, S. V., Eugene, L. W. J., & Koh, J. E. W. (2016). Sudden cardiac death (SCD) prediction based on nonlinear heart rate variability features and SCD index. *Applied Soft Computing*, 43: 510-519.

Gang, Y. (2013). Heart rate variability: Measurements and risk stratification. In Gussak, I., & Antzelevitch, C. (eds.) *Electrical Diseases of the Heart*. London: Springer-Verlag.

Goldberger, A. L., Amaral, L. A. N., Glass, L., Hausdorff, J. M., Ivanov, P. C., Mark, R. G., Mietus, J. E., Moody, G. B., Peng, C.-K., & Stanley, H. E. (2000). PhysioBank, PhysioToolkit, and PhysioNet: Components of a new research resource for complex physiologic signals. *Circulation*, 101(23): e215-e220.

Higuchi, T. (1988). Approach to an irregular time series on the basis of the fractal theory. *Physica D: Nonlinear Phenomena*, 31(2): 277-283.

Hoshi, R. A., Pastre, C. M., Vanderlei, L. C. M., & Godoy, M. F. (2013). Poincaré plot indexes of heart rate variability: Relationships with other nonlinear variables. *Autonomic Neuroscience: Basic and Clinical*, 177: 271-274.

Hosmer, D. W., & Lemeshow, S. (2013). *Applied Logistic Regression*. New York: Wiley.

Huikuri, H. V., Mäkikallio, T. H., & Perkiömäki, J. (2003). Measurement of heart rate variability by methods based on nonlinear dynamics. *Journal of Electrocardiology*, 36: 95-99.

Huikuri, H. V., & Stein, P. K. (2013). Heart rate variability in risk stratification of cardiac patients. *Progress in Cardiovascular Diseases*, 56(2): 153-159.

Işler, Y., & Kuntalp, M. (2007). Combining classical HRV indices with wavelet entropy measures improves to performance in diagnosing congestive heart failure. *Computers in Biology and Medicine*, 37(10): 1502-1510.

Kaufmann, T., Sütterlin, S., Schulz, S. M., & Vögele, C. (2011). ARTiiFACT: A tool for heart rate artifact processing and heart rate variability analysis. *Behavior Research Methods*, 43(4): 1161-1170.

Karmakar, C. K., Khandoker, A. H., Voss, A., & Palaniswami, M. (2011). Sensitivity of temporal heart rate variability in Poincaré plot to changes in parasympathetic nervous system activity. *BioMedical Engineering OnLine*, 10(17).

Kemp, A. H., Quintana, D. S., Felmingham, K. L., Matthews, S., & Jelinek, H. F. (2012). Depression, comorbid anxiety disorders, and heart rate variability in physically healthy, unmedicated patients: Implications for cardiovascular risk. *PLoS ONE*, 7(2).

Li, W. (1990). Mutual information functions versus correlation functions. *Journal of Statistical Physics*, 60(5): 823-837.

Moody, G. B., & Mark, R. G. (2001). The impact of the MIT-BIH Arrhythmia Database. *IEEE Transactions on Engineering in Medicine and Biology*, 20(3): 45-50.

Saranya, K., Pal, G. K., Habeebullah, S., & Pal, P. (2015). Analysis of Poincaré plot of heart rate variability in the assessment of autonomic dysfunction in patients with polycystic ovary syndrome. *International Journal of Clinical and Experimental Physiology*, 2(1): 34-39.

Shannon, C. E. (1948). A mathematical theory of communication. *Bell Systems Technical Journal*, 27: 379-423, 623-656.

Sharma, R., Pachori, R. B., & Acharya, U. R. (2015). An integrated index for the identification of focal electroencephalogram signals using discrete wavelet transform and entropy measures. *Entropy*, 17(8): 5218-5240.

Silva, I., & Moody, G. (2014). An open-source toolbox for analysing and processing PhysioNet databases in MATLAB and Octave. *Journal of Open Research Software*, 2(1): e27.

Stein, P. K., Domitrovich, P. P., Huikuri, H. V., & Kleiger, R. E. (2005). Traditional and nonlinear heart rate variability are each independently associated with mortality after myocardial infarction. *Journal of Cardiovascular Electrophysiology*, 16(1): 13-20.

Voss, A., Schroeder, R. Truebner, S., Goernig, M., Figulla, H. R., & Schirdewan, A. (2007). Comparison of nonlinear methods symbolic dynamics, detrended fluctuation, and Poincaré plot analysis in risk stratification in patients with dilated cardiomyopathy. *Chaos*, 17.

Voss, A., Schulz, S., Schroeder, R., Baumert, M., & Caminal, P. (2009). Methods derived from nonlinear dynamics for analysing heart rate variability. *Philosophical Transactions of the Royal Society A*, 367: 277-296.

Wells, W. M., Viola, P., Atsumi, H., Nakajima, S., & Kikinis, R. (1996). Multi-modal volume registration by maximization of mutual information. *Medical Image Analysis*, 1(1): 35-51.

Chapter 3 – Simulated Sudden Increase in Geomagnetic Activity and its Effect on Heart Rate Variability: Experimental Verification of Correlation Studies

Published in Life Sciences in Space Research

3. Abstract

Previous research investigating the potential influence of geomagnetic factors on human cardiovascular state has tended to converge upon similar inferences although the results remain relatively controversial. Furthermore, previous findings have remained essentially correlational without accompanying experimental verification. An exception to this was noted for human brain activity in a previous study employing experimental simulation of sudden geomagnetic impulses in order to assess correlational results that had demonstrated a relationship between geomagnetic perturbations and neuroelectrical parameters. The present study employed the same equipment in a similar procedure in order to validate previous findings of a geomagnetic-cardiovascular dynamic with electrocardiography and heart rate variability measures. Results indicated that potential magnetic field effects on frequency components of heart rate variability tended to overlap with previous correlational studies where low frequency power and the ratio between low and high frequency components of heart rate variability appeared affected. In the present study, a significant increase in these particular parameters was noted during geomagnetic simulation compared to baseline recordings.

3.1. Introduction

The potential role of space weather, especially geomagnetic activity, in human physiological systems has been demonstrated across a range of phenomena including endocrine activity (Breus et al., 2015) and brain activity (Mulligan et al., 2010; Saroka et al., 2014). Particularly relevant to the current study, previous researchers have shown that the cardiovascular system may also be susceptible to variations resulting from geomagnetic perturbation (Dimitrova et al., 2004; 2009; Stoupel, 1999). From a pathological perspective, geomagnetic storms may actually result in an increased occurrence of myocardial infarction (Kleimenova et al., 2007; Stoupel, 1999) where the observed relationships may be associated with geophysically-mediated changes in arterial blood pressure (Dimitrova, 2006; Dimitrova et al., 2009; Papailiou et al., 2011).

Although indices of mean heart rate and blood pressure have typically been employed in heliobiological research on autonomic or cardiovascular activity, there have been relatively fewer studies using heart rate variability (HRV) (Cornélissen et al., 2002; Dimitrova et al., 2013; Otsuka et al., 2001a; 2001b). A number of earlier results presented by Otsuka and colleagues have indicated that HRV tended to decrease in response to increased geomagnetic activity for a subarctic sample of healthy males (Otsuka et al., 2001a), and that the observation of a gradation for this biological response to geomagnetic activity in a subarctic region could implicate a form of human magnetoreception (Oinuma et al., 2002). Furthermore, magnetoreception was also inferred from a light-dark-mediated response of human participants to ultra-low frequency (ULF) Pc5 geomagnetic pulsations (Otsuka et al., 2001b). Finally, the application of an artificial magnetic field simulating ULF (~0.0016 Hz) geomagnetic pulsations with a weak intensity of ~50 nT appeared to decrease participants' HRV although this particular field application was eight hours in duration (Mitsutake et al., 2004). However, additional research has also implicated higher frequency Pc1 pulsations in geomagnetic-modulated variations of HRV (Kleimenova et al., 2007) and the current study used applied magnetic fields within this range (~0.20 to 4 Hz). Of further interest are the results obtained by Dimitrova et al. (2013) which identified significant changes (often decreases) in total variability and various frequency components of HRV including the ratio between low frequency and high frequency power which was interpreted as the balance between autonomic branches (i.e., sympathetic and parasympathetic contributions to HRV). However, the authors (Dimitrova et al., 2013) also suggested that there was a degree of variation regarding how individuals accommodated geomagnetic changes with respect to autonomic-cardiovascular state.

Despite these conclusions, it should be noted that Billman (2013), after a thorough review of the relevant literature, determined that the low frequency to high frequency ratio of HRV does not reflect an evenly balanced system of influence. Rather, the low frequency component appears to be relatively ambiguous regarding specific autonomic contributions, which may be largely cholinergic in origin, while the high frequency component is more likely dominated by parasympathetic (e.g., vagal) effects. The author (Billman, 2013) derived an overall relationship of low frequency (*LF*) to high frequency (*HF*) activity with their relative autonomic contributions in arbitrary units (1 = baseline activity) following the relationship:

$$\frac{LF}{HF} = \frac{0.5\ \mathrm{PSNS} + 0.25\ \mathrm{SNS}}{0.9\ \mathrm{PSNS} + 0.1\ \mathrm{SNS}}$$

where PSNS = relative parasympathetic nervous system contribution, and SNS = relative sympathetic nervous system contribution.

Of greater importance for the field of heliobiology overall, a vast majority of relevant studies are inherently correlational in nature due to the independent measures of interest. Although related research has tended to converge upon similar conclusions regarding an effect of geomagnetic activity on human physiology, there is a persistent need for experimental verification of these effects. As an example, Mulligan et al. (2010) had earlier corroborated results revealed by Babayev and Allahverdiyeva (2007) regarding an influence of geomagnetic processes on neuroelectrical activity using correlational means. Following this, the inferences were validated through experimental simulation of sudden geomagnetic increases during electroencephalographic (EEG) recording (Mulligan & Persinger, 2012). Although cardiovascular activity has often demonstrated similar relationships throughout past investigations, there has yet to be experimental verification of this potential influence from a range of magnetic field configurations, particularly various frequency components.

One of the potential concerns regarding the use of magnetic fields in physiological research is the weak intensity of the applied field relative to other well-known electromagnetic sources such as magnetic resonance imaging (MRI) which employs much stronger fields in the Tesla range. However, imaging studies often required Tesla-level magnetic fields in order to discern sufficient detail from signals generated by the alterations in spin of protons. In contrast, the current experiment was involved with simulating natural conditions that disrupt essential physiological conditions (Dimitrova, 2006; Dimitrova et al., 2004). There are multiple correlational studies that have shown reliable associations between the types of cardiac features we measured and natural geomagnetic activity within the 20 to 200 nT range (Babayev & Allahverdiyeva, 2007; Breus et al., 2015; Cornélissen et al., 2002; Dimitrova et al., 2009;

Mulligan et al., 2010; Oinuma et al., 2002; Papailiou et al., 2011; Saroka et al., 2014). Furthermore, Mitsutake et al. (2004) similarly observed cardiovascular effects resulting from application of a temporally-patterned magnetic field of only 50 nT. The temporal pattern of the applied field used in the current study was constructed to optimally influence “physiological patterns”. We have found that the more proximal the temporal pattern of the applied field is to the intrinsic patterns of cellular electrical activity the less intensity that is required to produce measurable disruptions (Lagace et al., 2009; Mach & Persinger, 2009). For example, a similar phenomenon was described for the most effective simulation patterns for inducing neuronal long-term potentiation (LTP) across different layers of the entorhinal cortices (Yun et al., 2002). This is consistent with the concept of natural resonance.

There are mechanisms other than Faradic induction of potential differences by which weak, physiologically patterned (that is non-temporally symmetrical shapes such as sine waves and square waves) magnetic fields applied through the body can produce significant influence upon function. Persinger and Saroka (2013) showed that the types of experiences induced in patients whose temporal lobes were stimulated surgically by mA electric currents were comparable to normal volunteers who were exposed transcerebrally to μT magnetic fields. Estimates of the current induced within cerebral tissue by the surgical currents and the energy within the cerebral volume associated with the applied magnetic field produced almost identical effective values.

The integral duration and amplitude modulations of the field configuration we employed was simulated from the amplitude displacements associated with sudden storm commencements. The construct validity of this pattern was indicated by the similarity of the effect sizes for the onset of spontaneous seizures in epileptic rats when it was applied experimentally and the background values when natural fields occurred intermittently (Michaud & Persinger, 1985). The specificity of the shape and intensity of this experimentally generated field has been shown in other settings. For example rats developing experimental forms of a demyelinating disease displayed marked attenuation of symptoms when the base frequency of the applied field was 7 Hz and the serial changes in amplitude modulations was less than 40 nT with mHz intrinsic periodicities (Cook et al., 2000). Application of the same field at 400 nT or application of 40 nT with 40 Hz oscillations or the latter with 400 nT produced effects that did not differ from sham field exposures. The primary goal of the current study was to employ similar geomagnetic simulation hardware used in verification studies by Mulligan and Persinger (2012) and also recently applied elsewhere for geomagnetic simulation (Murugan et al., 2013) in order to verify the apparent effect of geomagnetic increases on autonomic-cardiovascular activity determined by HRV measures.

3.2. Methods

After receiving ethics approval from the Laurentian University Research Ethics Board (LU REB), a total of 23 individuals volunteered for the current study. Exclusion criteria included < 18 years of age, history of hypertension or other known cardiovascular health issues including arrhythmia or presence of a pacemaker (n = 2 excluded). Short-term electrocardiograph (ECG) recordings were obtained from a sample of 21 healthy volunteers (12 males, 9 females) from 18 to 55 years of age during both control and experimental conditions in a simple counterbalanced repeated-measures design. However, a single male ECG record was rejected for further analysis given the large number of artifacts (final sample of n = 20). Recording was done while participants were seated comfortably and during normal spontaneous breathing within a Faraday cage.

Single-lead (two electrodes) Covidien Kendall H135SG disposable ECG electrodes were used for all recordings with a Mitsar-201 amplifier connected to a laptop computer. WinEEG v2.103.7 software was used for data collection at a sampling rate of 250 Hz. All data were exported for further processing and analysis using additional software. Automatic QRS detection and computation of R-R intervals in msec was conducted with ARTiiFACT v2.05 (Kaufmann et al., 2011). All records were further verified manually for accurate identification of waveform peaks. Any artifacts were corrected using a cubic spline interpolation of R-R intervals.

The HRV analysis suite within ARTiiFACT was used to calculate standard time domain indices of interest in msec including the standard deviation of R-R intervals (*SDNN*) which indicates long-term variability, and the root mean square of successive differences between intervals (*RMSSD*) which indicates short-term variability. Time series resampling (4 Hz interpolation) and detrending was also conducted within ARTiiFACT along with fast Fourier transform (FFT) for very low frequency (*VLF* = 0.003 to 0.04 Hz), low frequency (*LF* = 0.04 to 0.15 Hz), and high frequency (*HF* = 0.15 to 0.40 Hz) components of HRV in power spectral densities of ms^2, as well as the commonly used *LF/HF* ratio.

Statistical analyses were conducted with SPSS v17 software including both parametric and nonparametric techniques, while Matlab v7.12 was employed for wavelet transform of magnetic field measures with a Morlet mother wavelet function using scripts created by Grinsted et al. (2004; Jevrejeva et al., 2003). Wavelet power probability estimates were also computed through comparison with red-noise (AR1) spectra. The appropriateness of this method for null hypothesis testing was verified by comparing the power decay of red-noise with that of a given time series of interest after Burg algorithm spectral analysis. Magnetic field data were standardized and zero-padded prior to time-frequency analysis with wavelet transform. Descriptive statistics of HRV variables were computed for each condition followed by application of Shapiro-Wilks test to check for normal distributions. Experimental conditions were compared using either paired *t*-test or Wilcoxon signed rank test as determined by the presence or absence of normally distributed data respectively, with statistical significance considered for $p < 0.05$. Median box-plots for significant results were produced using Matlab software. To further explore potential gender effects, data were transformed using a natural logarithm to accommodate parametric repeated-measures analysis of variance (ANOVA) in SPSS.

Sudden increases in geomagnetic activity were simulated using two custom rectangular coils (about 1.15 by 1.15 m) placed on either side of the participant seating area ~1 m apart and ~35 cm away from the body proper. The waveform used was designed to imitate sudden geomagnetic impulses with individual point durations of 69 ms each separated by 1 ms. The resultant magnetic field was produced using a DOS PC system with Complex2 software designed by Prof. Stan Koren. Each point in the waveform ranges from 0 to 256 and is converted to an equivalent voltage (-5 to +5 mV) through a custom digital-to-analogue converter (DAC). An associated current is then delivered through the rectangular coils to produce the field.

Further investigation of magnetic field dynamics was undertaken using a MEDA FVM-400 Vector Fluxgate Magnetometer measured on three axes (X, Y, and Z) at a sample rate of 0.10 Hz (10/s). The field recording was acquired from the approximate location of the chest of a seated participant where the X and Z components did not demonstrate discernible periodicities as determined by both FFT and wavelet transform. The horizontal (front-to-back) *X* plane had an average intensity of 4750 nT (minimum = 4743 nT, maximum = 4757 nT) during field presentation with no significant change from baseline activity. The vertical *Z* plane also did not show a prominent change from normal background conditions with an observed average intensity of 19343 nT (minimum = 19338 nT, maximum = 19349 nT). Although the average intensity of the horizontal (side-to-side) *Y* axis during magnetic field presentation remained relatively minimal (mean = 775 nT), there were distinct and periodic spikes above background levels by ~20 to 100 nT (approximately equivalent to a minor geomagnetic storm of K_p ~5) with a median variation of 20 nT in peak intensity resulting in a total *Y* value of ~870 nT when maximal. These intensity spikes presented a particularly strong cycle of ~5.50 to 5.70 s (within the range of Pc1 geomagnetic pulsations) as determined by FFT and wavelet transform with associated probability estimates. We also noted an average field declination of ~13.50° during baseline conditions that oscillated between ~12.70° to 13.80° during field presentation (inclination of ~77° remained unchanged). The sample time series of each magnetic field axis are presented in Figure 9. These measurements indicated that the geomagnetic simulation field would cross the minor axis of the heart (from side-to-side of participant) as a vector oscillating back and forth within the cardiac space.

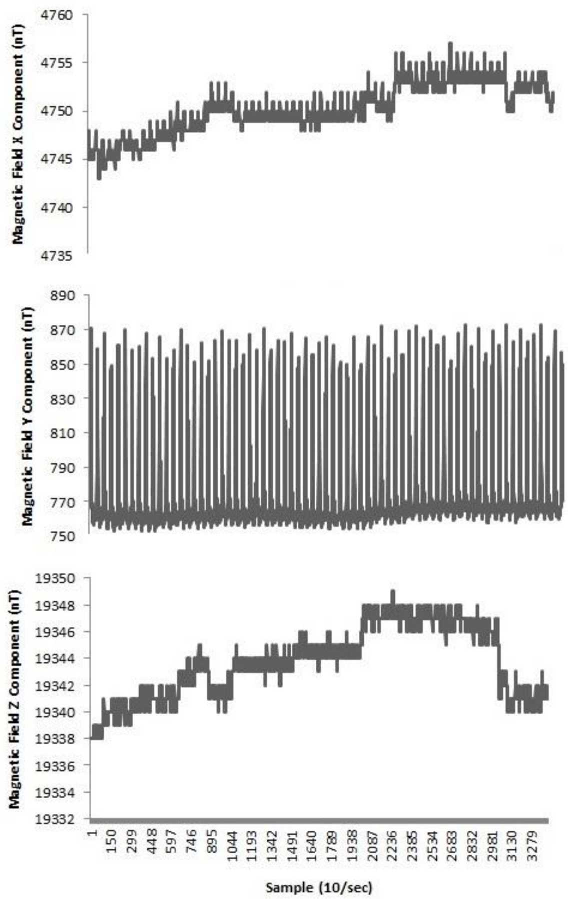

Figure 9: Raw time series of sample magnetic field recordings from *X*, *Y*, and *Z* axes

Participants contributed to both conditions (baseline and geomagnetic field) in a repeated-measures design for which each participant acted as their own control. The presentation order of these two conditions was counterbalanced in order to further account for potential differences in HRV that may simply occur over time. For order A, a baseline (BL) ECG recording was acquired for 5 minutes followed by 15 minutes of whole-body exposure to the geomagnetic field simulation (GM) and finally an additional 5 minute ECG recording during exposure. For order B, the GM condition was first applied for 15 minutes followed by the 5 minute ECG recording while the field was still active. Afterwards, the field was terminated and 10 minutes were allowed to pass. Finally, a 5 minute ECG recording was made for a BL condition. The procedure is further outlined in Figure 10 along with a flow chart outlining the study from recruitment to data analysis in Figure 11. Concomitant geomagnetic activity as indicated by three-hourly K_p index was noted for each test session. Geomagnetic data were acquired from the Solen Solar Terrestrial Activity Report (http://www.solen.info/solar/).

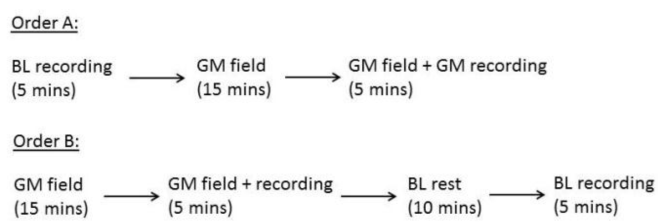

Figure 10: Outline of each condition with associated times for counterbalanced presentation; BL = baseline, GM = geomagnetic simulation

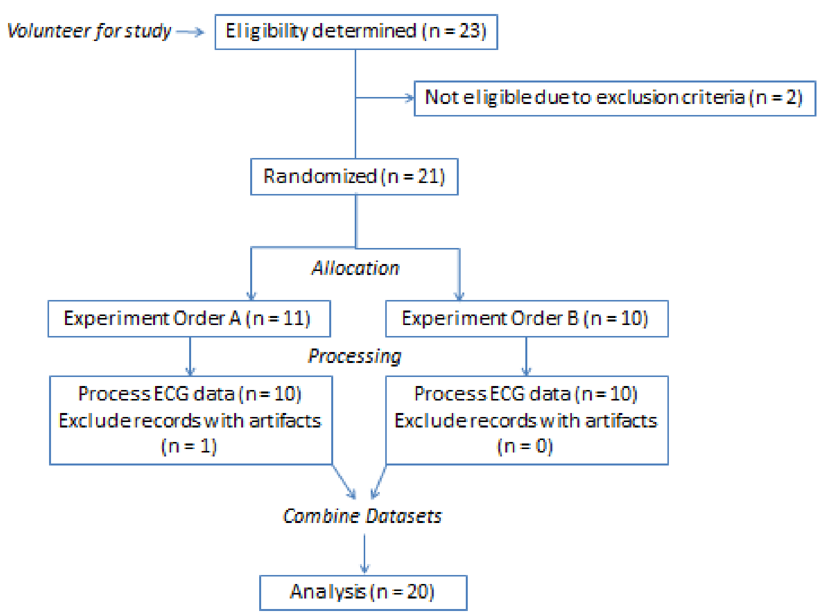

Figure 11: Flow chart of study stages from recruitment to data analysis

3.3. Results

All HRV variables were assessed for normality with Shapiro-Wilks test. Where normal distributions were observed, paired Student's *t*-tests were considered for comparing HRV between BL and GM conditions. However, practically all variables were non-normally distributed ($p < 0.05$) and nonparametric Wilcoxon signed rank test was instead used where associated estimates of effect size (*es*) were computed according to:

$$es = \frac{z}{\sqrt{\mathrm{n}_1 + \mathrm{n}_2}}$$

where n_1 and n_2 = sample size for each condition (BL + GM = 40).

Subsequent analyses revealed no significant difference between BL and GM conditions for variables *SDNN*, *RMSSD*, *VLF*, or *HF* (all $p > 0.05$). Statistically significant increases were observed for the *LF* component of HRV ($z = 2.651$, $p < 0.01$, $es = 0.419$) during the GM condition compared to BL measures with an associated relative increase for 15 out of 20 cases assessed (75%) (Figure 12). Similarly, the *LF/HF* ratio also tended to increase from BL to GM with a significant difference between conditions ($z = 2.875$, $p < 0.01$, $es = 0.456$) and the associated relative increase observed for 16 out of 20 cases (80%) (Figure 13).

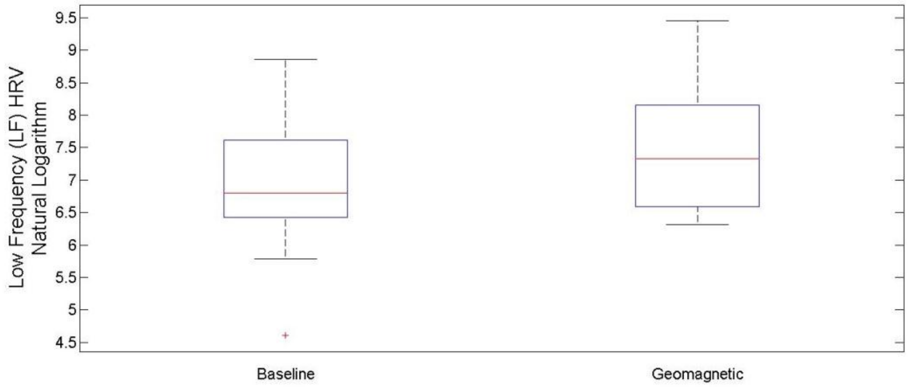

Figure 12: Box-and-whisker plot of median low frequency (*LF*) heart rate variability (HRV) for baseline and geomagnetic conditions; data transformed to natural logarithm to reduce outlier distances ('+' sign)

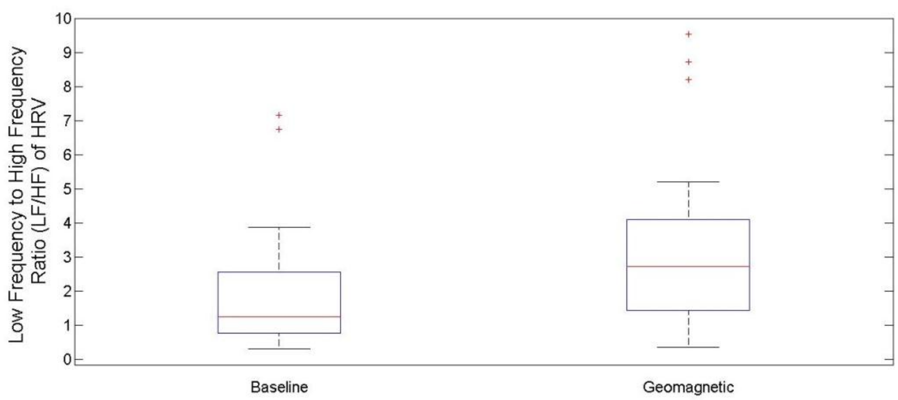

Figure 13: Box-and-whisker plot of median low frequency to high frequency ratio (*LF/HF*) heart rate variability (HRV) for baseline and geomagnetic conditions; outlier cases indicated by '+' sign

The effects identified remained significant ($p < 0.01$) after removing a single case recorded during a natural geomagnetic storm ($K_p \geq 5$). Following data transformation using the natural logarithm, repeated-measures ANOVA did not indicate any significant effect of gender ($p >$

0.05) for the differences between BL and GM among HRV parameters. Descriptive statistics of all variables were computed by experimental condition and are provided in Table 5.

Table 5: Descriptive statistics for all participant heart rate variability (HRV) measures by condition including mean, median, standard deviation (sd), and interquartile range (IQR)

Group	*Mean*	*Median*	*SD*	*IQR*
Baseline (BL)				
• ***SDNN***	63.98	60.57	26.37	38.20
• ***RMSSD***	47.08	36.49	27.67	31.73
• ***VLF***	1934.48	1073.37	2407.58	1834.82
• ***LF***	1596.79	895.86	1833.14	1547.05
• ***HF***	1148.07	625.28	1258.0	1359.21
• ***LF/HF***	2.0	1.26	1.94	1.86
Geomagnetic (GM)				
• ***SDNN***	71.91	66.98	30.36	34.86
• ***RMSSD***	52.48	42.87	32.68	35.03
• ***VLF***	2066.68	1407.35	2098.44	2231.79
• ***LF***	2877.21	1550.40	3361.70	3637.89
• ***HF***	1391.94	773.20	1590.71	1374.72
• ***LF/HF***	3.32	2.72	2.71	2.82

3.4. Discussion

While there have been a number of essentially correlational studies investigating the potential role of geomagnetic influence on autonomic-cardiovascular state (Cornélissen et al., 2002; Dimitrova et al., 2013; Papailiou et al., 2011), the present study is among the first to begin an experimental verification of similar effects using fast frequency pulsations rather than ULF artificial fields. Although the strength of the applied field was relatively weak, similar HRV effects have been noted for an applied ULF magnetic field of only ~50 nT (Mitsutake et al., 2004). However, these previous results conversely indicated a decrease in HRV associated with the much lower frequency field and significantly longer exposure time. Although additional replications are required, the current results remain informative and tend to overlap with other relatively recent correlational results (Dimitrova et al., 2013). While we employed magnetic field simulation of sudden geomagnetic impulses, the results are nonetheless revealing when considered in light of findings from other researchers. Specifically, Dimitrova et al. (2013) previously found that *LF/HF* measured longitudinally from two individuals' HRV tended to increase during the two days prior to geomagnetic storms. In addition to this, the dominant periodicity of our applied magnetic field was within range of Pc1 (~0.20 to 4 Hz) geomagnetic pulsations (Fraser & McNabb, 1984) which have also been implicated in geomagnetic-mediated variations of HRV (Kleimenova et al., 2007). While a time lag effect was not possible in the current experiment design, our results generally supported this contention through observation of significantly increased *LF/HF* values during the geomagnetic simulation compared to baseline recordings. Although earlier work had conversely found an overall decrease in *LF/HF* for a group of volunteers during the time of increased geomagnetic activity, the authors (Dimitrova et al., 2013) suggested that participants' physiological response to geophysical processes varied according to individual biology. Furthermore, an increase in *LF/HF* was also found to occur during the periods following storm-level activity in earlier results (Dimitrova et al., 2013).

Despite this relative discrepancy, the earlier study upon which the current experimental verification was largely based (Dimitrova et al., 2013) also found some evidence for significant increases in the *LF* component of HRV during geomagnetic storms which was similarly observed in the current results where participants' *LF* values tended to increase during geomagnetic simulation compared to baseline measures. This factor may also be partly responsible for the presently observed ratio effects as an increase in *LF* would result in a corresponding increase of *LF/HF*. Although induction artifacts were not suspected given the transformation from ECG to HRV and subsequent resampling procedures, it is also evident that the observed effect was not simply an induction artifact given the discrepancy between the dominant frequency of the applied magnetic field and the band of periodicities identified for HRV effects. However, varied field strengths should also be investigated in future studies to examine potential amplitude-mediated variations of the observed effect with human participants. For the current experiment, this would have required considerably longer participant recordings and additional magnetic field exposures or a further sample of available participants. Further research could address this concern using preliminary animal models of HRV (Supakul et al., 2014) prior to additional human testing.

Although applied magnetic fields within the Tesla range produce energies in the picoJoule (pJ) range within the volume of a typical cell, the specific energy within the much smaller volumetric shell that composes the plasma cell membrane is almost a billion times less or 10^{-20} J (Persinger, 2010). This is the energy associated with the forces over the averaged separation between potassium ions that contribute the resting membrane potential as well as to the action potential in neurons (Persinger, 2010). The results obtained in the present study are more consistent with direct effects upon the resting membrane conditions of aggregates of cells rather than direct interference with the metabolism and signaling pathways within the cells themselves.

The results of the current experiment support previous correlational work on the effects of geomagnetic influence on human cardiovascular state (Cornélissen et al., 2002; Dimitrova et al., 2009; 2013; Papailiou et al., 2011), specifically with regard to the overall state of the sympathetic and parasympathetic branches of the nervous system. In particular, the frequency components of HRV appear most susceptible to environmental electromagnetic factors, especially regarding frequencies ranging from 0.04 to 0.15 Hz. Further research is required to determine whether these apparent effects are due to geoeffective modulation of the central nervous system (Mulligan et al., 2010; Mulligan & Persinger, 2012; Saroka et al., 2014; 2016) or a direct product of autonomic-cardiovascular influence.

References

Babayev, E. S., & Allahverdiyeva, A. A. (2007). Effects of geomagnetic activity variations on the physiological and psychological state of functionally healthy humans: Some results of Azerbaijani studies. *Advances in Space Research*, 40(12): 1941-1951.

Billman, G. E. (2013). The LF/HF ratio does not accurately measure cardiac sympatho-vagal balance. *Frontiers in Physiology*, 4(26): 1-5.

Breus, T. K., Boiko, E. R., & Zenchenko, T. A. (2015). Magnetic storms and variations in hormone levels among residents of North Polar area – Svalbard. *Life Sciences in Space Research*, 4: 17-21.

Cook, L. L., Persinger, M. A., & Koren, S. A. (2000). Differential effects of low frequency, low intensity (<6 mG) nocturnal magnetic fields upon infiltration of mononuclear cells and numbers of mast cells in Lewis rat brains. *Toxicology Letters*, 118(1-2): 9-19.

Cornélissen, G., Halberg, F., Breus, T., Syutkina, E. V., Baevsky, R., Weydahl, A., Watanabe, Y., Otsuka, K., Siegelova, J., Fiser, B., & Bakken, E. E. (2002). Non-photic solar associations of heart rate variability and myocardial infarction. *Journal of Atmospheric and Solar-Terrestrial Physics*, 64(5-6): 707-720.

Dimitrova, S. (2006). Relationship between human physiological parameters and geomagnetic variations of solar origin. *Advances in Space Research*, 37(6): 1251-1257.

Dimitrova, S., Stoilova, I., & Cholakov, I. (2004). Influence of local geomagnetic storms on arterial blood pressure. *Bioelectromagnetics*, 25(6): 408-414.

Dimitrova, S., Mustafa, F. R., Stoilova, I., Babayev, E. S., & Kazimov, E. A. (2009). Possible influence of solar extreme events and related geomagnetic disturbances on human cardio-vascular state: Results of collaborative Bulgarian–Azerbaijani studies. *Advances in Space Research*, 43(4): 641-648.

Dimitrova, S., Angelov, I., & Petrova, E. (2013). Solar and geomagnetic activity effects on heart rate variability. *Natural Hazards*, 69(1): 25-37.

Fraser, B. J., & McNabb, P. W. (1984). The recording of Pc1 geomagnetic pulsations using a microcomputer preprocessing system. *Geophysical Surveys*, 6: 249-258.

Grinsted, A., Moore, J. C., & Jevrejeva, S. (2004). Application of the cross wavelet transform and wavelet coherence to geophysical time series. *Nonlinear Processes in Geophysics*, 11: 561-566.

Jevrejeva, S., Moore, J. C., & Grinsted, A. (2003). Influence of the Arctic Oscillation and El Niño-Southern Oscillation (ENSO) on ice conditions in the Baltic Sea: The wavelet approach. *Journal of Geophysical Research*, 108(D21): 4677.

Kaufmann, T., Sütterlin, S., Schulz, S. M., & Vögele, C. (2011). ARTiiFACT: A tool for heart rate artifact processing and heart rate variability analysis. *Behavior Research Methods*, 43(4): 1161-1170.

Kleimenova, N. G., Kozyreva, O. V., Breus, T. K., & Rapoport, S. I. (2007). Pc1 geomagnetic pulsations as a potential hazard of the myocardial infarction. *Journal of Atmospheric and Solar-Terrestrial Physics*, 69(14): 1759-1764.

Lagace, N., St-Pierre, L. S., & Persinger, M. A. (2009). Attenuation of epilepsy-induced brain damage in the temporal cortices of rats by exposure to LTP-patterned magnetic fields. *Neuroscience Letters*, 450(2): 147-151.

Mach, Q. H., & Persinger, M. A. (2009). Behavioral changes with brief exposures to weak magnetic fields patterned to stimulate long-term potentiation. *Brain Research*, 1261: 45-53.

Michaud, L. Y., & Persinger, M. A. (1985). Geophysical variables and behaviour XXV: Alterations in memory for a narrative following application of theta frequency electromagnetic fields. *Perceptual and Motor Skills*, 60: 416-418.

Mitsutake, G., Otsuka, K., Oinuma, S., Ferguson, I., Cornélissen, G., Wanliss, J., & Halberg, F. (2004). Does exposure to an artificial ULF magnetic field affect blood pressure, heart rate variability and mood? *Biomedical Pharmacotherapy*, 58: 20-27.

Mulligan, B. P., & Persinger, M. A. (2012). Experimental simulation of the effects of sudden increases in geomagnetic activity upon quantitative measures of human brain activity: Validation of correlational studies. *Neuroscience Letters*, 516(1): 54-56.

Mulligan, B. P., Hunter, M. D., & Persinger, M. A. (2010). Effects of geomagnetic activity and atmospheric power variations on quantitative measures of brain activity: Replication of the Azerbaijani studies. *Advances in Space Research*, 45(7): 940-948.

Murugan, N. J., Karbowski, L. M., Lafrenie, R. M., & Persinger, M. A. (2013). Temporally-patterned magnetic fields induce complete fragmentation in planaria. *PLOS One*. http://dx.doi.org/10.1371/journal.pone.0061714

Oinuma, S., Kubo, Y., Otsuka, K., Yamanaka, T., Murakami, S., Matsuoka, O., Ohkawa, S., Cornélissen, G., Weydahl, A., Holmeslet, B., Hall, C., & Halberg, F. (2002). On behalf of the "ICEHRV" Working Group: Graded response of heart rate variability associated with an alteration of geomagnetic activity in a subarctic area. *Biomedical Pharmacotherapy*, 56: 284-288.

Otsuka, K., Cornélissen, G., Weydahl, A., Holmeslet, B., Hansen, T. L., Shinagawa, M., Kubo, Y., Nishimura, Y., Omori, K., Yano, S., & Halberg, F. (2001a). Geomagnetic disturbance associated with decrease in heart rate variability in a subarctic area. *Biomedical Pharmacotherapy*, 55: 51-56.

Otsuka, K., Oinuma, S., Cornélissen, G., Weydahl, A., Ichimaru, Y., Kobayashi, M., Yano, S., Holmeslet, B., Hansen, T. L., Mitsutake, G., Engebretson, M. J., Schwartzkopff, O., & Halberg, F. (2001b). Alternating-light-darkness-influenced human electrocardiographic magnetoreception in association with geomagnetic pulsations. *Biomedical Pharmacotherapy*, 55: 63-75.

Papailiou, M., Mavromichalaki, H., Kudela, K., Stetiarova, J., & Dimitrova, S. (2011). Effect of geomagnetic disturbances on physiological parameters: An investigation on aviators. *Advances in Space Research*, 48: 1545-1550.

Persinger, M. A. (2010). 10^{-20} Joules as a neuromolecular quantum in medicinal chemistry: An alternative approach to myriad molecular pathways? *Current Medicinal Chemistry*, 17(27): 3094-3098.

Persinger, M. A., & Saroka, K. S. (2013). Comparable proportions of classes of experiences and intracerebral consequences for surgical stimulation and external application of weak magnetic field patterns: Implications for converging effects in complex partial seizures. *Epilepsy and Behavior*, 27(1): 220-224.

Saroka, K. S., Caswell, J. M., Lapointe, A., & Persinger, M. A. (2014). Greater electroencephalographic coherence between left and right temporal lobe structures during increased geomagnetic activity. *Neuroscience Letters*, 560: 126-130.

Saroka, K. S., Vares, D. E., & Persinger, M. A. (2016). Similar spectral power densities within the Schumann resonance and a large population of quantitative electroencephalographic profiles: Supportive evidence for Koenig and Pobachenko. *PLoS One*, 11(1).

Stoupel, E. (1999). Effect of geomagnetic activity on cardiovascular parameters. *Journal of Clinical and Basic Cardiology*, 2(1): 34-40.

Supakul, L., Pintana, H., Apaijai, N., Chattipakorn, S., Shinlapawittayatorn, K., & Chattipakorn, N. (2014). Protective effects of garlic extract on cardiac function, heart rate variability, and cardiac mitochondria in obese insulin-resistant rats. *European Journal of Nutrition*, 53: 919-928.

Yun, S. H., Mook-Jung, I., & Jung, M. W. (2002). Variation in effective stimulus patterns for induction of long-term potentiation across different layers of the rat entorhinal cortex. *Journal of Neuroscience*, 22: 1-5.

Chapter 4 – Pilot Observation of Daily Heart Rate Variability Samples and Relationship with Concomitant Geomagnetic Indices

4. Abstract

A small number of previous studies have investigated the potential influence of geomagnetic activity on human autonomic-cardiovascular state as inferred by heart rate variability. Recent results obtained by other researchers have indicated a relationship between geomagnetic factors and various parameters of heart rate variability, particularly with regard to frequency components. The aim of the present exploratory pilot study was to investigate the generalizability of previous longitudinal case studies on the relationship between geomagnetic activity and heart rate variability. Current results, which were severely limited due to their essentially anecdotal nature, corroborated previous findings to some degree with the identification of a significant nonlinear relationship between the low frequency component and the low frequency to high frequency ratio of heart rate variability with contemporary geomagnetic indices where decreases were observed during disturbed geomagnetic conditions and increases were observed for active storm conditions. Note that solar and temperature factors did not appear to contribute to heart rate variability. Although proper double-blind experimental design and additional research is required in order to better discern the exact nature of these effects, the gradual accumulation of convergent evidence provides some measure of confidence in the current inferences that may, at the least, provide a basis for further investigations.

4.1. Introduction

The use of heart rate variability (HRV) as an indicator of autonomic and cardiovascular activity has increased in recent decades with both clinical (Cheng et al., 2014; Dekker et al., 2000; Griffin & Moorman, 2001; Mani et al., 2009; Thayer et al., 2010) and experimental applications (Billman, 2013; Durantin et al., 2014; Sakuragi et al., 2002; Thayer et al., 2009). Rather than more traditional measures associated with electrocardiography (ECG) and blood pressure, HRV variables are derived from the time intervals between heart beats. These intervals are bound by the peaks (R component) in a typical ECG QRS complex. Variability in R-R intervals assessed from a number of quantitative perspectives reflects the various inputs that converge on the heart, particularly the sympathetic and parasympathetic branches of the autonomic nervous system (Cabiddu et al., 2012; Montano et al., 1994).

Despite the wealth of physiological research on HRV, there have been few studies of HRV rhythmicity over time beyond standard daily or circadian rhythms (Boudreau et al., 2012; Cornélissen et al., 1990; Valenza et al., 2014). The study of chronobiology has persistently indicated the importance of investigating significant cycles over time for biological and psychological phenomena where a better understanding of temporal structure and periodicity may contribute to identifying potential factors of influence (Caswell et al., 2016a; Simko, 2012; Cornélissen et al., 2002) or to inform better health policies (Halberg et al., 1990; Otsuka et al., 1996; Syutkina et al., 1997). Not only does a chronobiological understanding of daily cardiovascular variation benefit better management of pharmacological treatments (Ayala et al., 2013; Lemmer, 2001; 2012; Smolensky et al., 2011) but exploring longer cycles may also facilitate better management of additional medical services over time that can affect cardiovascular health (Cantwell et al., 2015; Čulić, 2014; Gun Song et al., 2013; Levandovski et al., 2012).

Heliobiology or cosmobiology, the study of the influence of space weather on terrestrial biology, has revealed myriad potential effects for the endocrine system (Breus et al., 2015), central nervous system (Mulligan et al., 2010; Saroka et al., 2014; 2016; Saroka & Persinger, 2014), and cardiovascular system (Dimitrova et al., 2004; 2009; 2013; Stoupel, 1999). Of particular relevance for the current study, Stoupel (1999) previously found that low levels of geomagnetic activity were correlated with cardiovascular mortalities that were not due to myocardial infarction, increased growth hormone levels, electrical instability of the cardiovascular system, and increased rates of tachycardia. Conversely, high levels of geomagnetic activity were correlated with increases in myocardial infarctions, increased diastolic blood pressure, and a range of other factors examined (Stoupel, 1999). Dimitrova et al. (2004) also identified relationships between geomagnetic activity and arterial, systolic, and diastolic blood pressures. However, it was later suggested that while arterial blood pressure appeared more varied in the context of geomagnetic disturbances, heart rate remained relatively stable under the same circumstances (Dimitrova, 2006; Dimitrova et al., 2009). Contrary to these results mostly obtained from middle latitudes, a subarctic population demonstrated decreased HRV in response to high geomagnetic activity (Otsuka et al., 2001) and more recent findings from Slovakia have also demonstrated relative ambiguity with regard to a relationship between blood pressure and geomagnetic activity with the exception of systolic pressure (Papailiou et al., 2011).

More relevant for the current investigation, Dimitrova et al. (2013) previously examined two individuals longitudinally and identified heart rate variability changes associated with geomagnetic storms, specifically a decrease in total variability on the day before and during storm-level activity. The authors (Dimitrova et al., 2013) also identified a potential influence of geomagnetic storms on frequency components of HRV including varied effects for both low and high frequency measures as well as the ratio between low and high frequencies which tended to be reduced during storms. However, the overall response of each participant varied suggesting individual accommodation to space weather parameters (Dimitrova et al., 2013). In addition to this, differing effects were observed across different geomagnetic intensities that might indicate nonlinearity in heliogeophysical-cardiovascular influence, although the potential nonlinear features were not discussed. Recent experimental verification of these effects (Caswell et al., 2016b) further indicated significant effects of simulated geomagnetic increases on specific frequency components of HRV.

Further research in this area is still required in order to solidify the nature of the largely correlational results. Although this type of study is inherently correlational due to the independent measures of interest, additional convergence of empirical results from a larger number of studies using different designs, sampling increments, populations, and geographic locations will help to improve confidence in these findings. In addition to this latter point, the case study may be an important tool in identifying the most likely candidates for a heliobiological relationship with cardiovascular function to better determine how the statistical results obtained from previous studies might apply to and persist across individuals (Watanabe et al., 1994). Finally, the use of HRV variables in heliogeophysical research (Cornélissen et al., 2002; Dimitrova et al., 2013; Otsuka et al., 2001) has generally been neglected as a dependent measure in the past where use of blood pressure and mean heart rate has been more prominent (Dimitrova, 2006; Dimitrova et al., 2009; Papailiou et al., 2011).

The current exploratory pilot study was undertaken in order to partially address some of the aforementioned points, particularly the expansion of HRV as a cardiovascular and autonomic indicator for investigations in current heliobiology, the diversification of geographical regions included in heliobiological investigation, and additional convergence of empirical findings. Measures of solar activity and temperature were also examined to better determine if any statistical relationships between geomagnetic and HRV variables could be related to a mutual third variable. An additional aim was to identify similar relationships found by previous researchers with larger populations and longer-term recordings for a single short-term case study in order to examine the generalizability of previous results (Dimitrova et al., 2013). It was reasoned that if previous researchers' findings were generalizable then a statistical relationship between HRV and geomagnetic indices should be apparent even when examining a single volunteer over a shorter period of time. However, note that the current exploration remains essentially anecdotal without empirical quantification of a significantly larger and more diverse sample of participants measured within a properly blinded experimental context. In addition to analyses for relationships with geomagnetic, solar, and temperature parameters, measures of HRV were also assessed for cyclic behavior over time, not only as this could aid identification of short-term geoeffective dynamics of autonomic-cardiovascular activity but also due to the additional insight gleaned from examining periodicities of any process for better organization of health care practices.

4.2. Methods

A single individual (the author) measured their HRV approximately daily in Sudbury, Ontario, Canada (46.5221° N, 80.9530° W) although the study ended earlier than anticipated due to the development of a seasonal illness. Some data recording sessions during the study also had to be cancelled due to other participant obligations. In total, there were 9 missing days from a span of 54 (n = 45). Because the investigator was also the subject, the current study essentially represents anecdotal empirical observations rather than a true scientific experiment with proper blind-conditions and controls. Furthermore, as only a single person was measured for a short time period the results may not be generalizable and merely represent an exploratory pilot investigation associated with additional experimental research (Caswell et al., 2016b). The individual measured for this study was a 30 year old male with no history of hypertension, diabetes, or obesity and a single prescription medication taken throughout the test period (daily 20 mg paroxetine, selective serotonin reuptake inhibitor or SSRI). Although the participant regularly smoked during the time investigated, they were otherwise healthy and caffeine was not consumed prior to daily recordings. Note that the presence cigarette smoking are both associated with changes in HRV (Hayano et al., 1990) although effects of SSRI treatment are not as well-established (Kemp et al., 2010) and, while these factors remained constant over the course of the study, present severe limitations for the current exploratory investigation that should be noted and further controlled for in future research. The individual's daily regime was consistent throughout the recording period following a personal academic research schedule with a routine that did not vary from day to day rather than a typical work week. Electrocardiograph (ECG) recording consistently occurred between 12:30 to 16:00 local time (Eastern Standard Time) in order to minimize the potential influence of HRV changes that are known to occur throughout the day (i.e., heart rate differences between morning and night). Recordings were taken while seated comfortably and facing forward.

All ECG data were recorded at a sample rate of 250 Hz through single lead (two sensors) Covidien Kendall H135SG disposable ECG electrodes connected to a Mitsar-201 amplifier with WinEEG v2.103.7 software on a laptop computer. Short-term (5 minute) segments were exported for further processing with ARTiiFACT v2.05 software (Kaufmann et al., 2011) before time series of R-R intervals in ms were extracted from each recording. Although the presence of artifacts was quite minimal throughout the investigation, artifact correction was accomplished using a cubic spline interpolation procedure where necessary. ARTiiFACT was also used to compute standard time domain measures of HRV followed by internal resampling (4 Hz interpolation) and detrending procedures for calculation of standard frequency domain variables through fast Fourier transform (FFT). Matlab v7.12 software was used for least-squares spectral analysis and preliminary cosinor analysis. All other statistical procedures were conducted with SPSS v17 software including tests of normality, linear and quadratic oneway analysis of variance (ANOVA) with Levene's (1960) test for homogeneity of variances, polynomial regression, Spearman (ρ) correlation, and detailed assessment of cosinor results. For ANOVA procedures, *post hoc* analyses were conducted using Tukey's (1949) method.

The primary HRV measures of interest included the standard deviation of R-R intervals (*SDNN*) indicating total variability, the root mean square of successive differences between R-R intervals (*RMSSD*) which reflects short-term variability, as well as the very low frequency (*VLF* = 0.003

to 0.04 Hz), low frequency (*LF* = 0.04 to 0.15 Hz), and high frequency components (*HF* = 0.15 to 0.40 Hz) of HRV obtained from spectral decomposition. The *LF/HF* ratio was also employed.

Because nonlinearity was anticipated for a relationship between HRV and geomagnetic indices, polynomial ANOVA and regression were performed. For regression procedures as an example, this constitutes a special form of linear regression that fits a higher order polynomial trend to the data rather than a straight line, where a quadratic (second order) fit with one predictor would follow the form:

$$y = a + B_1(x) + B_2(x^2)$$

where a = regression constant, B = coefficients, and x = independent measure. Essentially, x and x^2 are considered separate predictor variables for least-squares estimation with multiple regression analysis, although the final function derived from this technique is of greater interest than the individual coefficients.

Due to the presence of missing days from the composite daily time series, the Lomb-Scargle normalized periodogram method (Lomb, 1976; Scargle, 1982) of least-squares spectral analysis (Vaníček, 1971), which is amenable to investigating a series with missing samples, was used to explore potential periodicities with Matlab software. The first step determines a time delay at which relevant cosine and sine functions that describe a given cycle become orthogonal at time t with the equation:

$$\tan \cdot 2f\tau = \frac{\sum_i \sin \cdot 2f\mathrm{t}}{\sum_i \cos \cdot 2f\mathrm{t}}$$

where f = frequency, and τ = time delay between sinusoids. The periodogram power value (P) for each frequency f is subsequently calculated following:

$$\mathrm{P}(f) = \frac{1}{2}\left(\frac{\left(\sum_i x_i \cdot \cos f(\mathrm{t}-\tau)\right)^2}{\sum_i \cos^2 f(\mathrm{t}-\tau)} + \frac{\left(\sum_i x_i \cdot \sin f(\mathrm{t}-\tau)\right)^2}{\sum_i \sin^2 f(\mathrm{t}-\tau)}\right)$$

For additional verification of dominant rhythmic features observed using the Lomb-Scargle periodogram method, a cosinor technique was also applied by fitting a periodic regression to each time series (Cornélissen, 2014; Dimitrov, 1993) according to:

$$y(\mathrm{t}) = M + A \cdot \cos\left(\frac{2\pi\mathrm{t}}{T_{\mathrm{C}}}\right) + B \cdot \sin\left(\frac{2\pi\mathrm{t}}{T_{\mathrm{C}}}\right)$$

where M = regression constant equivalent to the midline estimating statistic of rhythm or *MESOR*, A and B = regression coefficients (cosine and sine periodic components respectively), and T_{C} = cycle length in days. Results obtained from this technique were employed to calculate amplitude or half of the predictable change over a cycle:

$$Amp = \sqrt{A^2 + B^2}$$

Coefficients of determination (R^2) were derived from linear regression with periodic components. Due to the parametric nature of this technique, any significant results were further verified after normalizing the data distribution (Cornélissen, 2014) with natural logarithmic transformation of variables. To further determine model accuracy, a procedure previously suggested by Barnett and Dobson (2010) was employed whereby rejecting a null hypothesis of $Amp = 0$ follows identification of statistical significance for either A or B regression coefficients after Bonferroni probability correction (p_A or $p_B \leq \alpha/2 = 0.025$). Model residuals were also examined for normal distributions (Cornélissen, 2014) using Shapiro-Wilks tests and visual techniques (i.e., Q-Q plot and histogram).

Planetary magnetic field variables included three-hourly K_p indices (quasi-logarithmic scale) during the time of recording (zero-lag) and for lag/lead periods up to three indices before and after recording. Daily average geomagnetic indices were also acquired at zero-lag and the day before recording with a focus on the auroral electrojet index (*AE*) which reflects a global measure of magnetic activity around the auroral zone associated with deviations in the horizontal component (H) of the magnetic field. Solar activity was also indicated by daily average sunspot numbers (*SSN*). Measures of geomagnetic and solar activity were accessed from the NASA OMNIWeb database (http://omniweb.gsfc.nasa.gov/form/dx1.html) and transformed to their natural logarithm. Finally, daily average temperature in °C was acquired (*TEMP*) for the city of Sudbury, Ontario, Canada (ECG recording location) during the day of and prior to recording and converted to K = °C + 273.15. Temperature data were accessed from the AccuWeather database (http://www.accuweather.com).

4.3. Results

Although previous research employed repeated-measures ANOVA (i.e., superposed epoch analysis) for testing the association between HRV parameters and geomagnetic activity (Dimitrova et al., 2013), the current sample was not amenable to this technique given the number of days missing from the composite time series (n = 9). Following the use of superposed epoch analysis, each missing case would also affect six neighboring cases (three prior to and three following), greatly reducing the overall sample. Therefore, analyses for the present study were based on an alternate statistical approach from which similar inferences could be made.

All HRV and geomagnetic variables were assessed for skew and kurtosis after which it was determined that frequency components of HRV (*VLF*, *LF*, *HF*, and *LF/HF*) required logarithmic transformation to better approximate normality for parametric testing. Because a strictly linear relationship was not anticipated according to the varied effects previously observed for different ranges of geomagnetic perturbation (Dimitrova et al., 2013), both linear and nonlinear trends were investigated (quadratic, second-order polynomial). All cases were aggregated according to lag/lead and zero-lag three-hour K_p indices where subsequent groups consisted of quiet (K_p = 0 to 2, n = 29), disturbed (K_p = 3 to 4, n = 11), or active ($K_p \geq 5$, n = 5) geomagnetic conditions. However, it should be noted that few cases were acquired during active storm conditions, a caveat also encountered by many geomagnetic health researchers including Dimitrova et al. (2013) over a considerably longer period of time.

Oneway ANOVA revealed a significant difference for the natural logarithm of *LF* ($F_{(2, 44)}$ = 6.799, p = 0.013, η^2 = 0.139) and *LF/HF* ($F_{(2, 44)}$ = 7.995, p = 0.007, η^2 = 0.160) between K_p lag -1 conditions with nonlinear quadratic terms (Figure 14 and Figure 15 respectively). After *post hoc* testing, a moderate difference was observed between disturbed and active conditions for *LF* (adjusted p = 0.063). A significant *post hoc* difference for *LF/HF* was identified between disturbed and active conditions (adjusted p = 0.046) with a moderate difference between quiet and disturbed conditions (adjusted p = 0.052).

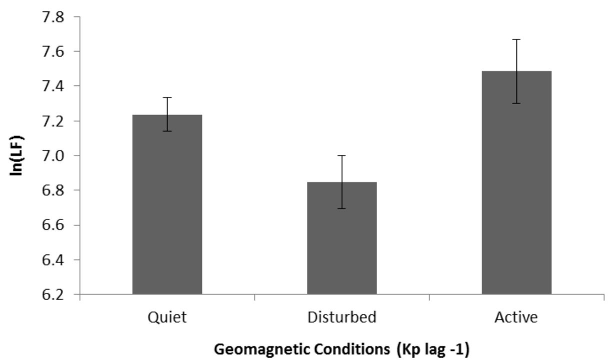

Figure 14: Mean values for low frequency component (*LF*) of heart rate variability from each geomagnetic condition according to lag -1 K_p indices; error bars indicate standard errors of the mean (SEM)

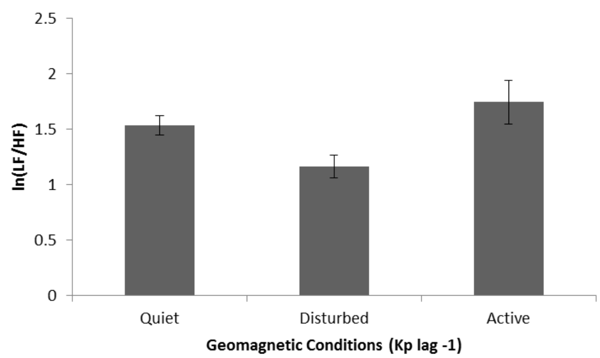

Figure 15: Mean values for low frequency to high frequency ratio (*LF/HF*) of heart rate variability from each geomagnetic condition according to lag -1 K_p indices; error bars indicate standard errors of the mean (SEM)

A set of polynomial regressions were assessed using the normally distributed natural logarithm of *LF* and *LF/HF* with appropriately transformed concomitant daily average geomagnetic and solar indices as well as temperature. The expected nonlinear relationship was most evident for the *LF/HF* ratio, as anticipated according to ANOVA *post hoc* testing, with zero-lag *AE* values

($F_{(2, 44)}$ = 4.541, p = 0.016, R^2 = 18%) which demonstrated an expected quadratic trend (Figure 16) according to the regression equation:

$$\log\left(\frac{LF}{HF}\right) = 8.769 - 2.614\big(\log(AE)\big) + 0.230(\log(AE)^2)$$

The residuals obtained were normally distributed (p > 0.05) and values predicted with this model were moderately correlated with their original values ($\rho_{(45)}$ = 0.441, p = 0.002). There were no significant relationships observed for HRV with either *SSN* or *TEMP*.

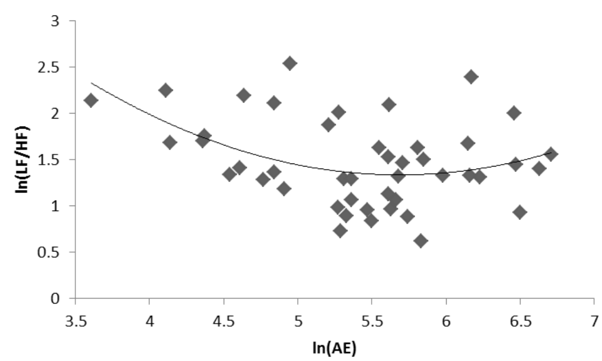

Figure 16: Scatter plot of low frequency to high frequency ratio (*LF/HF*) of heart rate variability and daily average geomagnetic activity (*AE* index) after natural logarithmic transformation with associated quadratic trend line

Time series of each HRV variable were assessed using Lomb-Scargle periodogram in order to explore potential rhythms over the period of observation. Conspicuous peak amplitudes were identified for *RMSSD* (2.437 days), *VLF* (11.158 days), *LF* (3.365 days), *HF* (2.465 days), and *LF/HF* (2.494 days). Verification of significant periodicities was conducted with cosinor analyses. Assessment of results followed previous procedures for model coefficients (Barnett & Dobson, 2010) which were further confirmed after variable distributions were normalized with natural logarithmic transformation. Values for *Amp* are presented in natural logarithm units as variables required transformation prior to parametric analysis. Cosinor zero-amplitude testing was significant for the *VLF* periodicity of 11.158 days (R^2 = 18%, *Amp* = 0.331, p = 0.014) with a particularly large deviation from the cycle observed from day 36 to 38 (Figure 17). The *LF* cycle was non-significant ($p > 0.05$) after normalizing the dependent variable distribution. The 2.465 day periodicity identified for the *HF* component of HRV (Figure 18) was statistically significant (R^2 = 25%, *Amp* = 0.424, p = 0.002). Note that the *HF* changes in HRV are conceptually similar to the short-term variability reflected in the time domain by *RMSSD* which had a similar periodicity of 2.437 days (R^2 = 23%, *Amp* = 0.136, p = 0.004). Finally, the cycle for *LF/HF* was not statistically significant ($p > 0.05$) after assessment of model coefficients.

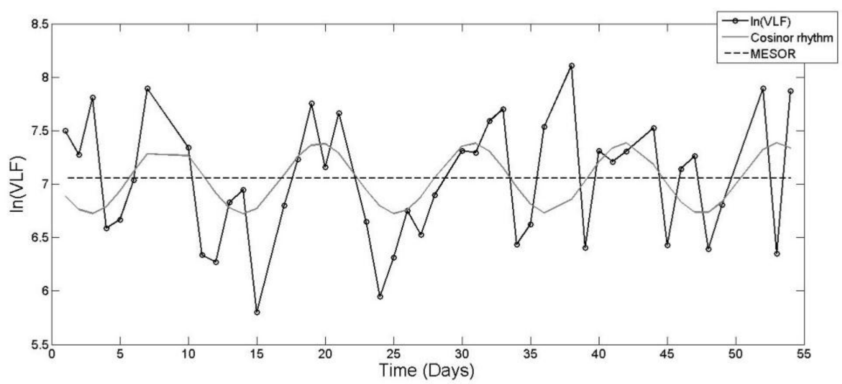

Figure 17: Cosinor rhythm (11.158 days) for natural logarithm of very low frequency (*VLF*) heart rate variability with rhythm-adjusted mean (*MESOR*)

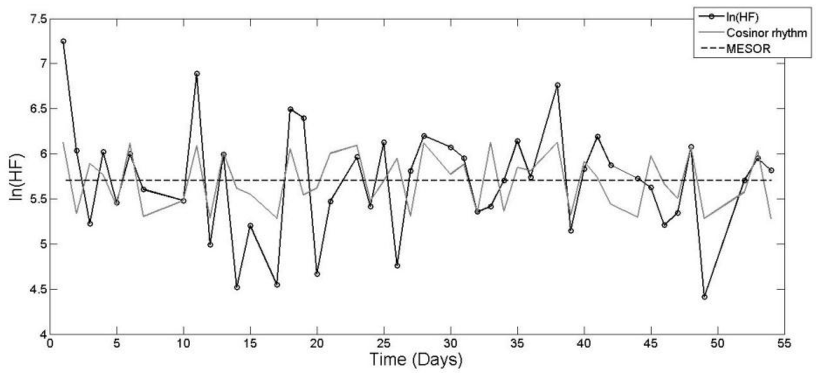

Figure 18: Cosinor rhythm (2.465 days) for natural logarithm of high frequency (*HF*) heart rate variability with rhythm-adjusted mean (*MESOR*)

Least-squares spectral analysis of geomagnetic factors followed by cosinor indicated dominant periodicities for the *AE* index natural logarithm of 7.570 days (R^2 = 15%, *Amp* = 0.394, p = 0.030) and 9.634 days (R^2 = 18%, *Amp* = 0.415, p = 0.014) that were considerably longer than those observed for HRV measures other than *VLF* which itself had a longer cycle than the observed geomagnetic variations. Due to missing samples and the relatively short time series available, additional measures of frequency and time-frequency cross-spectral density or coherence were not pursued.

4.4. Discussion

The current pilot investigation was undertaken in order to further examine the more recent findings of Dimitrova et al. (2013), particularly with regard to the authors' longitudinal analyses of two volunteers. The present results demonstrated a statistically significant relationship between *LF* and *LF/HF* with geomagnetic parameters of contemporary *AE* index and lag -1 K_p index but not with *SSN* or *TEMP*. The geomagnetic results revealed a nonlinear relationship between variables of interest such that apparent heliogeophysical effects on HRV varied according to geomagnetic intensity which corroborates previous research to some degree where different effects were observed for various ranges of geomagnetic intensity and often during periods prior to physiological recording (Dimitrova et al., 2013). Furthermore, previous researchers observed relatively varied effects between two volunteers and suggested that individuals might differentially accommodate environmental electromagnetic factors. However, it should again be noted that the current results are essentially anecdotal pilot statistics and an additional caveat of the current results was the particularly small sample size of recordings acquired during active ($K_p \geq 5$) geomagnetic conditions, although differences between quiet and unsettled conditions were also observed. Despite this limitation, the current results were also consistent with recent experimental verification of geomagnetic influence on HRV parameters (Caswell et al., 2016b) for which we had also identified *LF* and *LF/HF* as prominent indicators of increased geomagnetic activity ($K_p \geq 5$). Overall, the results obtained thus far appear to converge on similar inferences for a role of geomagnetic influence on overall autonomic balance between sympathetic and parasympathetic branches, although the influence of autonomic branches on HRV is itself nonlinear (Billman, 2013). While the time span of the present investigation was considerably shorter than that employed in previous research and assessed only a single person in a non-blind experimental setup, it appears that a weak but significant relationship between parameters of interest could be apparent even over a shorter period. However, proper experimentation and analysis is required in order to confidently explore these relationships beyond *post hoc* anecdotal convergence.

Aside from the general geomagnetic-physiological relationships observed, the fast frequency changes and short-term variability of HRV (*HF* and *RMSSD*) were also found to oscillate over time with cycles of approximately ~2.50 days that explained a significant amount of the total variance. However, the more dominant cycles for daily geomagnetic activity (*AE* index) were found to be longer than the most of the physiological periodicities identified with the exception of *VLF* which had a longer dominant cycle than *AE* index, suggesting that these particular cyclical components of sample HRV over time may not be coupled to concomitant geomagnetic cycles. Larger time series should be acquired in future research with a much larger, more diverse participant sample to better accommodate investigation of frequency or time-frequency coherence between measures of interest rather than simply identifying similar dominant periodicities through univariate or autospectral techniques, which was an additional limitation of the current pilot investigation.

While results from similar research have remained somewhat controversial in some circles, the gradual accumulation of convergent evidence has continued to enhance the confidence of associated inferences. The present study specifically demonstrated a relative generalizability of previous correlational results (Dimitrova et al., 2013) for a single individual examined over a more discrete time period although extreme caution is advised in over interpreting the current exploratory analyses. Additionally, the current results identified a nonlinear relationship with geomagnetic parameters of interest. As others have suggested, more investigations of this nature are still required in order to better support and understand the apparent relationship between human physiological processes and environmental factors including those related to geophysics and, in the case of cardiovascular variables of interest, whether the effects observed could be due to geomagnetic influence on the central nervous system (Mulligan et al., 2010; Saroka & Persinger, 2014; Saroka et al., 2014; 2016) or cardiovascular input/output proper.

References

Ayala, D. E., Hermida, R. C., Mojón, A., & Fernández, J. R. (2013). Cardiovascular risk of resistant hypertension: Dependence on treatment-time regimen of blood pressure-lowering medications. *Chronobiology International*, 30(1-2): 340-352.

Barnett, A. G., & Dobson, A. J. (2010). Cosinor. In: *Analysing seasonal health data*. Springer, pp 75-92.

Billman, G. E. (2013). The LF/HF ratio does not accurately measure cardiac sympatho-vagal balance. *Frontiers in Physiology*, 4(26): 1-5.

Boudreau, P., Hsien Yeh, W., Dumont, G. A., & Boivin, D. B. (2012). A circadian rhythm in heart rate variability contributes to the increased cardiac sympathovagal response to awakening in the morning. *Chronobiology International*, 29(6): 757-768.

Breus, T. K., Boiko, E. R., & Zenchenko, T. A. (2015). Magnetic storms and variations in hormone levels among residents of North Polar area – Svalbard. *Life Sciences in Space Research*, 4: 17-21.

Cabiddu, R., Cerutti, S., Viardot, G., Werner, S., & Bianchi, A. M. (2012). Modulation of the sympatho-vagal balance during sleep: Frequency domain study of heart rate variability and respiration. *Frontiers in Physiology*, 3.

Cantwell, K., Morgans, A., Smith, K., Livingston, M., & Dietze, P. (2015). Temporal trends in cardiovascular demand in EMS: Weekday versus weekend differences. *Chronobiology International*, 32(6): 731-738.

Caswell, J. M., Carniello, T. N., & Murugan, N. J. (2016a). Annual incidence of mortality related to hypertensive disease in Canada and associations with heliophysical parameters. *International Journal of Biometeorology*, 60: 9-20.

Caswell, J. M., Singh, M., & Persinger, M. A. (2016b). Simulated sudden increase in geomagnetic activity and its effect on heart rate variability: Experimental verification of correlation studies. *Life Sciences in Space Research*, 10: 47-52.

Cheng, S.-T., Wu, Y.-K., Yang, M.-C., Huang, C.-Y., Huang, H.-C., Chu, W.-H., & Lan, C.-C. (2014). Pulmonary rehabilitation improves heart rate variability at peak exercise, exercise capacity and health-related quality of life in chronic obstructive pulmonary disease. *Heart & Lung*, 43: 249-255.

Cornélissen, G. (2014). Cosinor-based rhythmometry. *Theoretical Biology and Medical Modelling*, 11(1): 16-40.

Cornélissen, G., Bakken, E., Delmore, P., Orth-Gomér, K., Âkerstedt, T., Carandente, O., Carandente, F., & Halberg, F. (1990). From various kinds of heart rate variability to chronocardiology. *American Journal of Cardiology*, 66(10): 863-868.

Cornélissen, G., Halberg, F., Breus, T., Syutkina, E. V., Baevsky, R., Weydahl, A., Watanabe, Y., Otsuka, K., Siegelova, J., Fiser, B., & Bakken, E. E. (2002). Non-photic solar associations of heart rate variability and myocardial infarction. *Journal of Atmospheric and Solar-Terrestrial Physics*, 64(5-6): 707-720.

Čulić, V. (2014). Chronobiological rhythms of acute cardiovascular events and underlying mechanisms. *International Journal of Cardiology*, 174(2): 417-419.

Dekker, J. M., Crow, R. S., Folsom, A. R., Hannan, P. J., Liao, D., Swenne, C. A., & Schouten, E. G. (2000). Low heart rate variability in a 2-minute rhythm strip predicts risk of coronary heart disease and mortality from several causes. *Circulation*, 102: 1239-1244.

Dimitrov, B. D. (1993). Heliophysical activity and incidence variations of skin malignant melanoma in Czechoslovakia: A regional study. *International Journal of Biometeorology*, 37: 67-71.

Dimitrova, S. (2006). Relationship between human physiological parameters and geomagnetic variations of solar origin. *Advances in Space Research*, 37(6): 1251-1257.

Dimitrova, S., Stoilova, I., & Cholakov, I. (2004). Influence of local geomagnetic storms on arterial blood pressure. *Bioelectromagnetics*, 25(6): 408-414.

Dimitrova, S., Mustafa, F. R., Stoilova, I., Babayev, E. S., & Kazimov, E. A. (2009). Possible influence of solar extreme events and related geomagnetic disturbances on human cardio-vascular state: Results of collaborative Bulgarian-Azerbaijani studies. *Advances in Space Research*, 43(4): 641-648.

Dimitrova, S., Angelov, I., & Petrova, E. (2013). Solar and geomagnetic activity effects on heart rate variability. *Natural Hazards*, 69(1): 25-37.

Durantin, G., Gagnon, J.-F., Tremblay, S., & Dehais, F. (2014). Using near infrared spectroscopy and heart rate variability to detect mental overload. *Behavioural Brain Research*, 259: 16-23.

Griffin, M. P., & Moorman, J. R. (2001). Toward the early diagnosis of neonatal sepsis and sepsis-like illness using novel heart rate analysis. *Pediatrics*, 107(1): 97-104.

Gun Song, B., Hyeon Oh, J., Kim, H.-J., Hea Kim, S., Man Chung, S., Lee, M., Hyun Kang, G., Hwan Park, Y., & Jung Chun, W. (2013). Chronobiological variation in the occurrence of Tako-tsubo cardiomyopathy: Experiences of two tertiary cardiovascular centers. *Heart & Lung*, 42(1): 40-47.

Halberg, F., Cornélissen, G., & Bakken, E. (1990). Caregiving merged with chronobiologic outcome assessment, research and education in health maintenance organizations (HMOs). *Progress in Clinical Biology Research*, 341B: 491-549.

Hayano, J., Yamada, M., Sakakibara, Y., Fujinami, T., Yokoyama, K., Watanabe, Y., & Takata, K. (1990). Short- and long-term effects of cigarette smoking on heart rate variability. *American Journal of Cardiology*, 65(1): 84-88.

Kaufmann, T., Sütterlin, S., Schulz, S. M., & Vögele, C. (2011). ARTiiFACT: A tool for heart rate artifact processing and heart rate variability analysis. *Behavior Research Methods*, 43(4): 1161-1170.

Kemp, A. H., Quintana, D. S., Gray, M. A., Felmingham, K. L., Brown, K., & Gatt, J. M. (2010). Impact of depression and antidepressant treatment on heart rate variability: A review and meta-analysis. *Biological Psychiatry*, 67(11): 1067-1074.

Lemmer, B. (2001). Cardiovascular chronobiology and chronopharmacology: Importance of timing of dosing. In: W. B. White (ed.) *Blood pressure monitoring in cardiovascular medicine and therapeutics*. Humana Press, pp 255-271.

Lemmer, B. (2012). The importance of biological rhythms in drug treatment of hypertension and sex-dependent modifications. *ChronoPhysiology and Therapy*, 2: 9-18.

Levandovski, R., Harb, A., Bernardi, F., Allebrandt, K. V., & Paz Loayza Hidalgo, M. (2012). A chronobiological policy to decrease the burden of hypertension and obesity in low- and middle-income population. *Biological Rhythm Research*, 43(1): 81-102.

Levene, H. (1960). Robust tests for equality of variances. In: Olkin, I., Ghurye, S. G., Hoeffding, W., Madow, W. G., & Mann, H. B. (eds.) *Contributions to probability and statistics: Essays in honor of Harold Hotelling*. California: Stanford University Press, pp. 278-292.

Lomb, N. R. (1976). Least-squares frequency analysis of unequally spaced data. *Astrophysics and Space Science*, 39(2): 447-462.

Mani, A. R., Montagnese, S., Jackson, C. D., Jenkins, C. W., Head, I. M., Stephens, R. C., Moore, K. P., & Morgan, M. Y. (2009). Decreased heart rate variability in patients with cirrhosis relates to the presence and degree of hepatic encephalopathy. *American Journal of Physiology – Gastrointestinal Liver Physiology*, 296(2): G330-G338.

Montano, N., Ruscone, T. G., Lombardi, F., Pagani, M., & Malliani, A. (1994). Power spectrum analysis of heart rate variability to assess the changes in sympathovagal balance during graded orthostatic tilt. *Circulation*, 90: 1826-1831.

Mulligan, B. P., Hunter, M. D., & Persinger, M. A. (2010). Effects of geomagnetic activity and atmospheric power variations on quantitative measures of brain activity: Replication of the Azerbaijani studies. *Advances in Space Research*, 45(7): 940-948.

Otsuka, K., Cornélissen, G., & Halberg, F. (1996). Predictive value of blood pressure dipping and swinging with regard to vascular disease risk. *Clinical Drug Investigation*, 11: 20-31.

Otsuka, K., Cornélissen, G., Weydahl, A., Holmeslet, B., Hansen, T. L., Shinagawa, M., Kubo, Y., Nishimura, Y., Omori, K., Yano, S., & Halberg, F. (2001). Geomagnetic disturbance associated with decrease in heart rate variability in a subarctic area. *Biomedical Pharmacotherapy*, 55(1): s51-s56.

Papailiou, M., Mavromichalaki, H., Kudela, K., Stetiarova, J., & Dimitrova, S. (2011). Effect of geomagnetic disturbances on physiological parameters: An investigation on aviators. *Advances in Space Research*, 48: 1545-1550.

Sakuragi, S., Sugiyama, Y., & Takeuchi, K. (2002). Effects of laughing and weeping on mood and heart rate variability. *Journal of Physiological Anthropology and Applied Human Science*, 21(3): 159-165.

Saroka, K. S., & Persinger, M. A. (2014). Quantitative evidence for direct effects between Earth-ionosphere Schumann resonances and human cerebral cortical activity. *International Letters of Chemistry, Physics and Astronomy*, 20(2): 166-194.

Saroka, K. S., Caswell, J. M., Lapointe, A., & Persinger, M. A. (2014). Greater electroencephalographic coherence between left and right temporal lobe structures during increased geomagnetic activity. *Neuroscience Letters*, 560: 126-130.

Saroka, K. S., Vares, D. E., & Persinger, M. A. (2016). Similar spectral power densities within the Schumann resonance and a large population of quantitative electroencephalographic profiles: Supportive evidence for Koenig and Pobachenko. *PLoS One*, 11(1).

Scargle, J. D. (1982). Studies in astronomical time series analysis II: Statistical aspects of spectral analysis of unevenly spaced data. *Astrophysical Journal*, 263: 835-853.

Simko, F. (2012). Chronobiology of blood pressure: Emerging implications of melatonin. *European Journal of Clinical Investigation*, 42(11): 1252-1254.

Smolensky, M. H., Siegel, R. A., Haus, E., Hermida, R., & Portaluppi, F. (2011). Biological rhythms, drug delivery, and chronotherapeutics. In: J Slepmann, RA Siegel, & MJ Rathbone (eds.), *Fundamentals and applications of controlled release drug delivery*. Springer US.

Stoupel, E. (1999). Effect of geomagnetic activity on cardiovascular parameters. *Journal of Clinical and Basic Cardiology*, 2(1): 34-40.

Syutkina, E. V., Cornélissen, G., Grigoriev, A. E., Mitish, M. D., Turti, T., Yatsyk, G. V., Pimenov, K., Breus, T. K., Studenikin, M. Y., Siegelova, J., Fiser, B., Dusek, J., Johnson, D., & Halberg, F. (1997). Neonatal intensive care may consider associations of cardiovascular rhythms with local magnetic disturbance. *Scripta Medica*, 70: 217-226.

Thayer, J. F., Hansen, A. L., Saus-Rose, E., & Johnsen, B. H. (2009). Heart rate variability, prefrontal neural function, and cognitive performance: The neurovisceral integration perspective on self-regulation, adaptation, and health. *Annals of Behavioral Medicine*, 37: 141-153.

Thayer, J. F., Yamamoto, S. S., & Brosschot, J. F. (2010). The relationship of autonomic imbalance, heart rate variability and cardiovascular disease risk factors. *International Journal of Cardiology*, 141(2): 122-131.

Tukey, J. (1949). Comparing individual means in the analysis of variance. *Biometrics*, 5(2): 99-114.

Valenza, G., Nardelli, M., Lanata, A., Gentili, C., Bertschy, G., Paradiso, R., & Scilingo, E. P. (2014). Wearable monitoring for mood recognition in bipolar disorder based on history-dependent long-term heart rate variability analysis. *IEEE Journal of Biomedical Health Informatics*, 18(5): 1625-1635.

Vaníček, P. (1971). Further development and properties of the spectral analysis by least-squares. *Astrophysics and Space Science*, 12: 10-33.

Watanabe, Y., Hillman, D. C., Otsuka, K., Bingham, C., Breus, T. K., Cornélissen, G., & Halberg, F. (1994). Cross-spectral coherence between geomagnetic disturbance and human cardiovascular variables at non-societal frequencies. *Chronobiologia*, 21(3-4): 265-272.

Chapter 5 – Annual Incidence of Mortality Related to Hypertensive Disease in Canada and Associations with Heliophysical Parameters

Published in International Journal of Biometeorology

5. Abstract

Increasing research into heliobiology and related fields has revealed a myriad of potential relationships between space weather factors and terrestrial biology. Additionally, many studies have indicated cyclicity in incidence of various diseases along with many aspects of cardiovascular function. The current study examined annual mortality associated with hypertensive diseases in Canada from 1979 to 2009 for periodicities and linear relationships with a range of heliophysical parameters. Analyses indicated a number of significant lagged correlations between space weather and hypertensive mortality, with solar wind plasma beta identified as the likely source of these relationships. Similar periodicities were observed for geomagnetic activity and hypertensive mortality. A significant rhythm was revealed for hypertensive mortality centered on a 9.6-year cycle length, while geomagnetic activity was fit with a 10.1-year cycle. Cross-correlograms of mortality with space weather demonstrated a 10.67-year periodicity coinciding with the average 10.6-year solar cycle length for the time period examined. Further quantification and potential implications are discussed.

5.1. Introduction

Hypertension is one of the most important adjustable risk factors for cardiovascular disease (CVD). Its prevalence is overwhelming in industrialized populations and a prominent risk factor for myocardial infarction, stroke, congestive heart failure, end-stage renal disease, and peripheral vascular disease (Johnson et al., 2003; Levy et al., 1996; Lloyd-Jones et al., 2002; O'Leary et al., 1999; Yusuf et al., 2004). There is an increasing body of literature from clinical trials that indicate the tight regulation of arterial pressure at < 140/90 mmHg markedly reduces CVD factors (Bertoia et al., 2012; Lloyd-Jones et al., 2002; McCubbin et al., 1989;Williams et al., 2006). However, this form of disease remains one of the top five risk factors for mortality around the world, with the Global Burden of Disease database (http://www.healthdata.org/gbd) placing hypertensive disease as the number one risk factor for disability and mortality as recently as 2010. Given the wide prevalence of hypertensive disease and risks associated with this form of disorder, increasing the general body of knowledge on time series characteristics of hypertension and external factors related to hypertension remains a necessary endeavor in order to aid in the prediction and reduction of this particularly important health issue.

Despite Canada having a health care system that is relatively inexpensive and easily accessible for the public, and in which a great proportion of the population have had regular blood pressure observations (Kaplan et al., 2010), the prevalence of hypertension remains high, particularly in males, with a low level of control (Gee et al., 2012; Joffres et al., 1997; Wolf-Maier, et al. 2004) along with associated mortality rates (Robitaille et al., 2011). According to one particular study (Joffres et al., 1997), about 4.1 million Canadians aged 18 to 74 years have presented clinical manifestations of hypertension and were at increased risk for coronary heart disease and stroke.

Of these, about 960,000 (23 %) were treated but did not have hypertension controlled, 757,000 (18 %) were not treated and not controlled, and 1.7 million (41 %) were not aware of their high arterial blood pressure. Surprisingly, most of these individuals with hypertension were not from the older age group (Joffres et al., 1997), a common factor often linked with the onset and treatment of hypertension and resulting comorbidities (Gee et al., 2012; Kaplan et al., 2010; Robitaille et al., 2011).

Accumulating evidence in the field of heliobiology has previously identified a potential role for space weather factors in the incidence of a number of diseases. While there may be subtle energies involved in the interaction between heliophysical parameters and terrestrial systems, there is a myriad of quantitative and experimental evidence to support the contention of heliobiological effects (Babayev & Allahverdiyeva, 2007; Dzvoník et al., 2006; Mulligan et al., 2010; Mulligan & Persinger, 2012; Saroka et al., 2014; Stoupel et al., 2006). In direct relation to the study of hypertensive disease, there are a number of space weather investigations which have specifically demonstrated relationships with human cardiovascular function (Dimitrova et al., 2004; 2009; Papailiou et al., 2011; 2012). As rigorously outlined in recent studies (Persinger, 2014; Saroka & Persinger, 2014), relatively minute environmental forces, including those outside the threshold for human perception, are sufficient to produce effects on biological systems.

Aside from the previously observed linear empirical relationships revealed for heliophysical factors and human physiology, there have also been a number of non-linear epidemiological studies conducted on the occurrence of various diseases which have shown significant rhythms in incidence for a number of cancers (Dimitrov, 1999; 2000; Dimitrov et al., 2008) and myocardial infarction (Cornélissen et al., 2002), with some results indicative of potential solar cycle (~11 years) rhythmicity (Dimitrov, 1993) in the occurrence of specific diseases. The closely related area of research, chronobiology, has proven effective in the identification of potential relationships between epidemiology and human behavior with space weather by expanding the methods of analysis from the simple identification of linear relationships into the examination of cyclicity coinciding with space weather cycles (Cornélissen et al., 2011; Dimitrov et al., 2009; Kancírová & Kudela, 2014).

The current study was undertaken in order to investigate the relationship between the incidence of mortality associated with hypertensive diseases (*HM*, hypertensive mortality) in Canada and a number of heliophysical parameters for the period 1979 to 2009. More traditional correlational analyses were applied to determine both the linear relationships between *HM* and space weather variables of interest, along with determining the inter-relatedness between heliophysical parameters under investigation and their main potential source of variance regarding relationships with *HM*. Furthermore, analyses to determine potential cyclicity were employed, including least-squares spectral analysis (Vaníček, 1971; Lomb, 1976; Scargle, 1982) and periodic regression (Dimitrov, 1993) based on the cosinor method (Halberg, 1969; Cornélissen, 2014). These analyses essentially consist of least-squares fitting of trigonometric functions at specific cycle lengths to the variable under examination. The inter-relatedness of space weather parameters is also often ignored in typical studies of heliobiology, and we have therefore chosen to examine these interconnections in detail as a further guide to the true source of the statistical effects observed. These investigations could prove particularly beneficial, given the use of regional data, when considering that cardiomyopathy (e.g., hypertension) is a leading cause of death in Canada (Joffres et al., 1997).

5.2. Methods

The annual total numbers of deaths (males and females, all ages) associated with hypertensive diseases in Canada (*HM*) were obtained for 1979 to 2009 from the World Health Organization (WHO) online mortality database (http://apps. who.int/healthinfo/statistics/mortality/whodpms/). The *HM* values were obtained directly from this resource without additional modification or aggregation. WHO mortality database category 4061 was used (number of deaths due to hypertensive disease, both sexes, all standardized age ranges from < 1 to ≥ 75 years) which provided data on ICD-10 categories I10 to I15 (I10, essential or primary hypertension; I11, hypertensive heart disease; I12, hypertensive renal disease; I13, hypertensive heart disease and renal disease; and I15, secondary hypertension). This information was acquired by the WHO from Canadian civil registration systems for medically certified deaths only. The aggregated variable employed in the current study was available as is from the mortality database. Additional descriptive information for *HM* data regarding age ranges and sexes are included in Table 6 and Table 7 respectively.

Table 6: Mean, standard deviation (st. dev.), and total numbers of deaths related to hypertensive disease (*HM*) for each age range from 1979 to 2009

Age Range	< 1 year	1 to 4	5 to 14	15 to 24	25 to 34	35 to 54	55 to 74	≥ 75
Mean	0.097	0.032	0.290	0.936	3.710	57.613	367.968	1156.452
St. Dev.	0.301	0.180	0.529	0.892	2.053	20.787	55.041	365.418
Total	3	1	9	29	115	1,786	11,407	33,850

Table 7: Mean, standard deviation (st. dev.), and total numbers of deaths related to hypertensive disease (*HM*) for males, females, and both sexes from 1979 to 2009

	Males	Females	Both
Mean	608.548	942.0	1587.226
St. Dev.	115.597	231.871	370.602
Total	18,865	29,202	49,204

All geomagnetic and solar variables of interest were accessed from the Goddard Space Flight Center/Space Physics Data Facility OMNIWeb database (http://omniweb.gsfc.nasa.gov/form/dx1.html). Values obtained were monthly averages which were subsequently converted to annual means for further analysis. Variables of interest included geomagnetic activity (A_p index), the vertical component of the interplanetary magnetic field (B_z) in nT, solar wind proton density (SW_d) in N·cm^{-3}, and the solar wind plasma beta (β) which refers to the ratio between plasma and magnetic pressures. Note that although the standard A_p index is an ordinal scale, the OMNIWeb database reports associated averages on a continuous scale in nT. As an additional heliophysical parameter, the annual average numbers of cosmic ray (*CR*) impulses per minute were retrieved from the Moscow Neutron Monitor (http://cr0.izmiran.rssi.ru/mosc/main.htm). The total sample of annual data examined for final analysis consisted of n = 31. All data were obtained during solar cycle 21 (10.3 years; May 1976 to March 1986), cycle 22 (9.7 years; March 1986 to June 1996), and cycle 23 (11.7 years; June 1996 to January 2008), with a single case (2009) from the ongoing solar cycle 24.

For cosinor investigation, regression analyses were employed using the equation (Dimitrov, 1993):

$$y(\mathrm{t}) = M + A\cos\left(\frac{2\pi\mathrm{t}}{T_{\mathrm{C}}}\right) + B\sin\left(\frac{2\pi\mathrm{t}}{T_{\mathrm{C}}}\right)$$

where M = constant coefficient equivalent to the *MESOR* or midline estimating statistic of rhythm, A and B = regression coefficients, t = point in time, and T_{C}=cycle length. Amplitude for each cosinor result was calculated according to (Cornélissen, 2014):

$$Amp = \sqrt{(A^2 + B^2)}$$

Data detrending and nonlinear analyses were conducted using Matlab v7.12. All other statistical techniques were performed using SPSS v17. Prior to analysis, all variables were subject to visual inspection of chronograms (raw time series), detrended where necessary, and tested for a normal distribution.

5.3. Results

Hypertensive mortality (*HM*) displayed a clear quadratic trend (Figure 19) and was therefore fit with a second order polynomial:

$$\mathrm{f}(x) = 3.022 \cdot x^2 + (-64.91) \cdot x + 1610$$

A normal distribution was observed following appropriate quadratic detrending. A_{p} index was chosen as the measure of geomagnetic activity in the current study (Figure 20a), which was linearly detrended with:

$$\mathrm{f}(x) = -2.495 \cdot x + 17.90$$

The B_z variable was not fit with a polynomial or power trend (Figure 20b) and did not require further data transformation. The SW_d was best fit by a third order polynomial (Figure 20c) and cubically detrended following:

$$\mathrm{f}(x) = 0.001 \cdot x^3 + (-0.045) \cdot x^2 + 0.668 \cdot x + 5.895$$

The ratio of plasma to magnetic pressure for solar winds (β) did not require detrending; however, further transformation was applied using Blom's (1958) ranking method for normalizing the distribution as suggested elsewhere (Cornélissen, 2014):

$$s_i = \phi \frac{\left(\rho_i - \frac{3}{8}\right)}{\left(\mathrm{n} + \frac{1}{4}\right)}$$

where s = normal score obtained, ϕ = inverse cumulative normal function, ρ = rank score, and n = sample size, following which no further data treatment of β was required given the lack of accuracy observed for general curve fitting procedures (Figure 20d). As with the B_z component of the interplanetary magnetic field, the annual *CR* values could not be fit using low order polynomials or power equations, and data were normally distributed (Figure 20e). The overall raw mean of each variable was added to the residuals of the associated data after detrending.

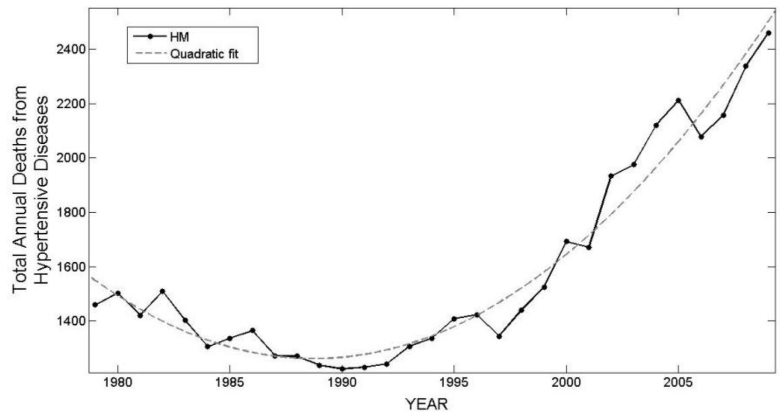

Figure 19: Chronograph of raw data for total annual deaths associated with hypertensive diseases (*HM*) in Canada with quadratic fit

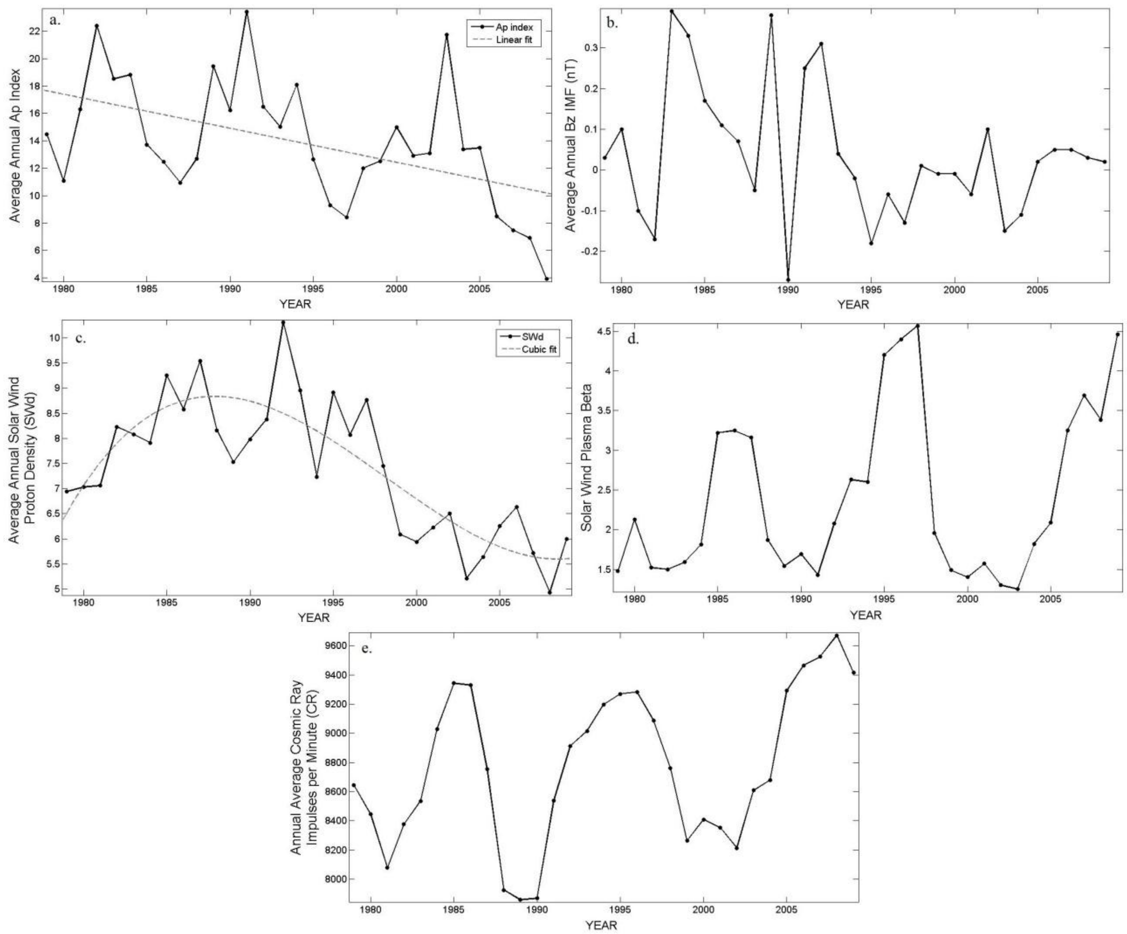

Figure 20: Chronographs of raw annual data for (a) geomagnetic activity (A_p index) with linear fit, (b) vertical (B_z) component of the interplanetary magnetic field in nT, (c) solar wind proton density (SW_d) in N·cm^{-3} with cubic fit, (d) solar wind plasma beta (β), and (e) cosmic ray impulses (*CR*)

Following preliminary data processing procedures, heliophysical parameters were symmetrically time-shifted with a maximum step (lag/lead) of 12 years (11-year solar cycle +1). Results for A_p index with *HM* (Figure 21a) suggested a phase relationship of 11 years ($r_{(20)} = 0.715$, $p < 0.001$) with the geomagnetic cycle preceding that of *HM* (Figure 22a). There were no significant relationships observed between *HM* and B_z. However, SW_d cross-correlation with *HM* suggested a possible phase shift of ∼8 years (Figure 21b) with significant Pearson coefficients computed for SW_d lag -8 ($r_{(23)} = 0.512$, $p < 0.05$) with *HM* (Figure 22b) and an additional peak coefficient leading by 10 years ($r_{(21)} = 0.586$, $p < 0.01$). Symmetrical lag/lead correlations for *HM* with β demonstrated the greatest relative number of significant relationships (Figure 21c), with a phase shift of 8 years ($r_{(23)} = 0.742$, $p < 0.001$) and a strongly positive correlation (Figure 22c). Finally, *CR* data were correlated with *HM* which suggested a phase shift of ∼8 to 9 years (Figure 21d). Pearson coefficients were obtained for *CR* lag -9 ($r_{(22)} = 0.627$, $p < 0.01$) and *CR* lag -8 ($r_{(23)} = 0.626$, $p < 0.01$) with *HM* (e.g., Figure 22d). Additionally, least-squares spectral analysis (Vaníček, 1971; Lomb, 1976; Scargle, 1982) of lag/lead correlation coefficients for *HM* with A_p index, β, and *CR* all displayed a ∼10.67-year periodicity, or approximately the average solar cycle length for the data examined, while the dominant periodicity for SW_d correlations was ∼9.6 years (Figure 23).

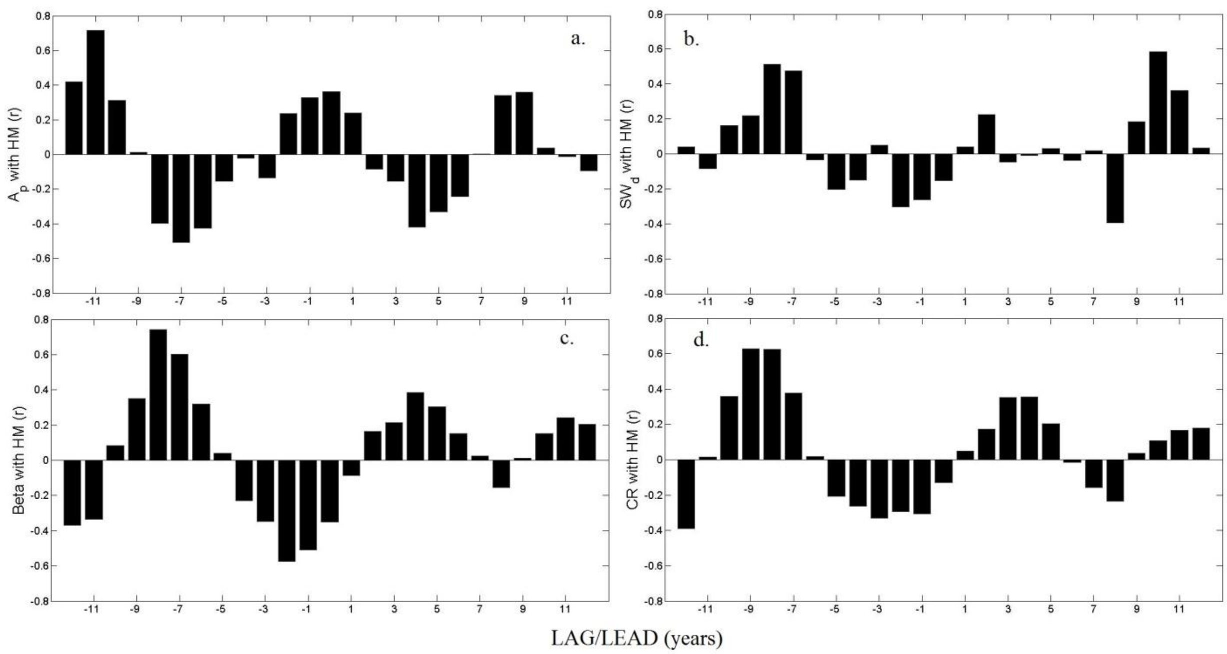

Figure 21: Cross-correlograms of correlation coefficients (*r*) across lag/lead time for hypertensive mortality (*HM*) with (a) geomagnetic activity (A_p index), (b) solar wind proton density (SW_d), (c) solar wind plasma beta (β), and (d) cosmic rays (*CR*)

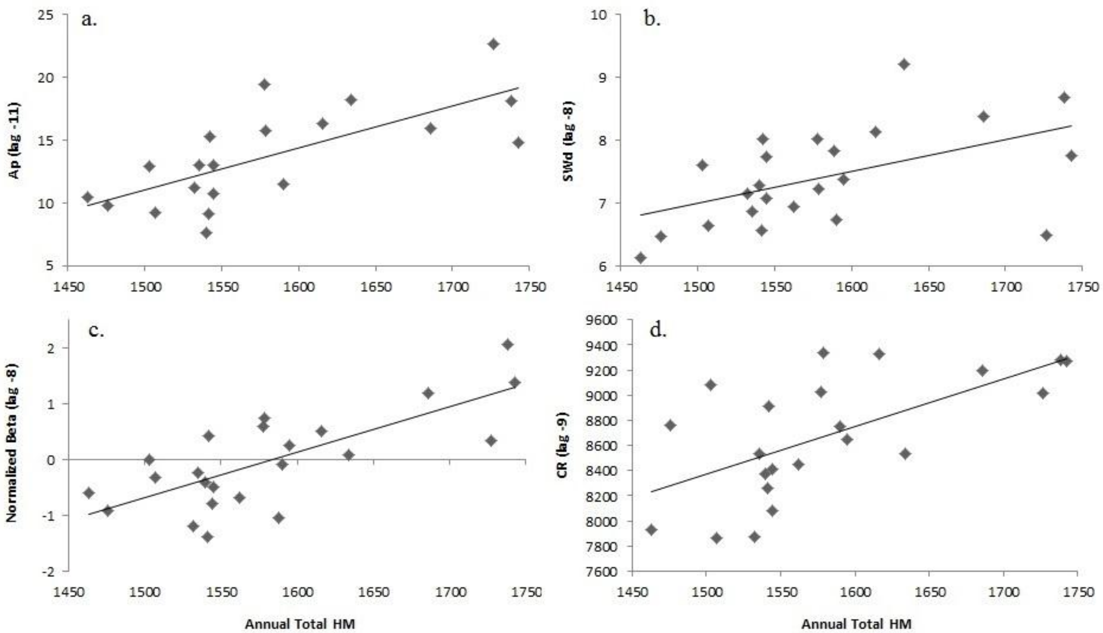

Figure 22: Scatterplots of linear (Pearson *r*) correlations between annual total deaths from hypertensive diseases in Canada (*HM*) with (a) geomagnetic activity (A_p index) lagged by 11 years, (b) solar wind proton density (SW_d) index lagged by 8 years, (c) solar wind plasma beta (β) lagged by 8 years, and (d) cosmic rays (*CR*) lagged by 9 years

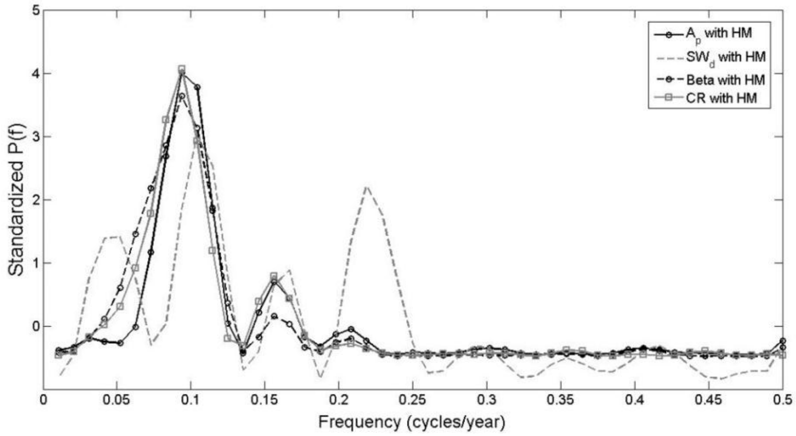

Figure 23: Periodogram for least-squares spectral analysis of lag/lead correlation coefficients for hypertensive mortality (*HM*) with space weather variables with standardized (*z*-scores) power; *HM* with geomagnetic activity (A_p index), solar wind proton density (SW_d), solar wind plasma beta (β), and cosmic rays (*CR*)

A high degree of inter-correlation was revealed among heliophysical parameters at both zero-lag, and the appropriate time-lags for which the greatest respective lagged relationships with *HM* were observed (Table 8). Additionally, calculation of correlation standard errors (SE) was conducted with:

$$\mathrm{SE} = \sqrt{\frac{(1 - r^2)}{\mathrm{n} - 2}}$$

for which the relative lowest values were found for correlations of β with A_p, SW_d, and *CR*. The relative lowest SE for β was identified for the correlation with *CR* (Table 8). A series of partial correlations were conducted for *HM* with either A_p (lag -11), SW_d (lag -8), β (lag -8), or *CR* (lag -9) as the independent measure while individually controlling for the remaining space weather variables. The annual β value lagged by 8 years was the only variable to remain significantly correlated with *HM* when controlling for all other measures (Table 9). This led to the conclusion that the ratio of plasma pressure to magnetic pressure of solar wind (β) was the central source of variance regarding the previously observed bivariate correlations with *HM*.

Table 8: Matrix of Pearson correlation (r) coefficients between heliophysical parameters which displayed the greatest relationships with hypertensive mortality (*HM*) with SE values in parentheses; all values are significant at $p < 0.05$; all correlations were also significant for zero-lag variables

	A_p (lag -11)	SW_d (lag -8)	β (lag -8)	CR (lag -9)
A_p (lag -11)		0.507 (0.203)	0.682 (0.172)	0.662 (0.177)
SW_d (lag -8)	0.507 (0.203)		0.562 (0.181)	0.473 (0.197)
β (lag -8)	0.682 (0.172)	0.562 (0.181)		0.801 (0.134)
CR (lag -9)	0.662 (0.177)	0.473 (0.197)	0.801 (0.134)	

A_p = geomagnetic activity, SW_d = solar wind proton density, β = solar wind plasma beta, CR = cosmic rays

Table 9: Partial correlation (r) coefficients for solar wind plasma beta (β) lagged by 8 years with hypertensive mortality (*HM*), individually controlling for other heliophysical parameters

***HM* with β (lag -8) controlling for**	**Partial r**	**p**
A_p (lag -11)	0.568	< 0.05
SW_d (lag -8)	0.639	0.001
CR (lag -9)	0.581	< 0.01

A_p = geomagnetic activity, SW_d = solar wind proton density, CR = cosmic rays

A series of analyses were conducted in order to discern potential cyclicity of *HM* in range of those observed for heliophysical parameters. An exploratory least-squares spectral analysis of *HM* revealed a relative amplitude peak for a cycle of ∼10 years overlapping with A_p index (Figure 24), along with a secondary peak at approximately 17 years. However, only the shorter cyclicity in range of heliophysical parameters was chosen as the focus for guiding further exploration. The major periodicity observed for both β and *CR* was ∼11 years. The dominant SW_d cycle was much shorter at approximately 4.6 years.

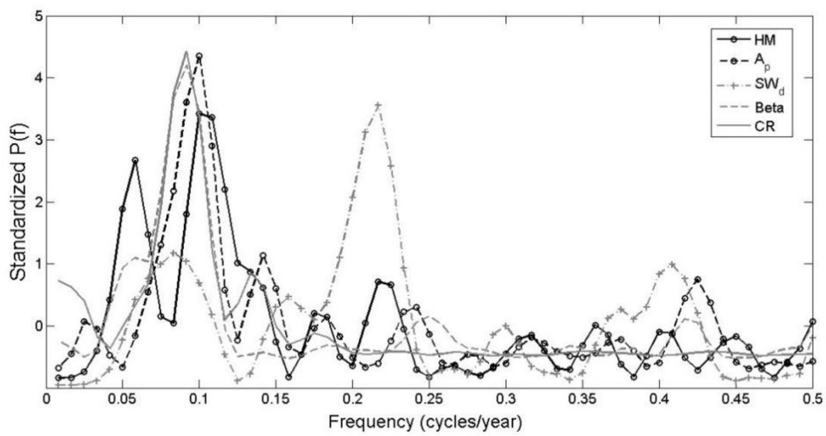

Figure 24: Periodogram for least-squares spectral analysis of hypertensive mortality (*HM*) and linearly related heliophysical factors with standardized (*z*-scores) power; geomagnetic activity (A_p index), solar wind proton density (SW_d), solar wind plasma beta (β), and cosmic rays (*CR*)

Annual *HM* was further analyzed with periodic regression (Dimitrov 1993) by manually computing a series of cosine and sine waves over a short band of nearby cycle lengths (T_c=∼9 to 11) at simple increasing increments of 0.1 years. The resulting values within each period T_c were fit to the annual *HM* totals through a series of cosinor analyses. Results suggested a significant *HM* rhythm (R^2 = 34%, p < 0.01) centered on ∼9.6 years (Figure 25) defined by:

$$HM(\mathrm{t}) = 1591.014 + (-42.40)\cos\left(\frac{2\pi \mathrm{t}}{9.60}\right) + (-41.636)\sin\left(\frac{2\pi \mathrm{t}}{9.60}\right)$$

The amplitude, which reflects half of the predicted change for an observed cycle (Cornélissen 2014), indicated a value of *Amp* = 59.424. Additionally, one can see a general reduction in both amplitude and general conformity to the cyclic trend during polarity reversal of solar cycle 22 (March, 1986 to June 1996) compared to the preceding cycle 21 or the following cycle 23. However, this apparently declining incidence also reflects the previously observed ∼17-year periodicity.

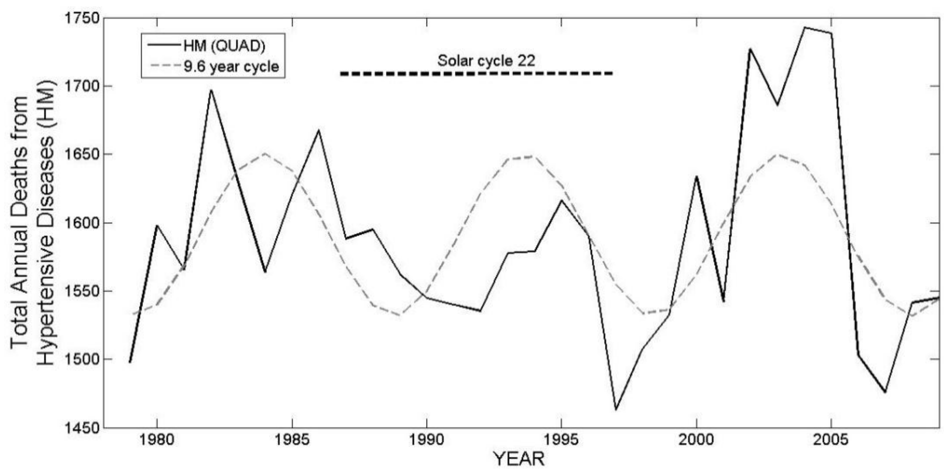

Figure 25: Annual hypertensive mortality (*HM*) after detrending with superposed 9.6-year cyclicity; note the dark dashed line indicating polarity reversal during solar cycle 22

Further investigation employed a series of short-band periodic regression analyses for correlated space weather variables beginning with the observed *HM* cycle length of T_c = 9.6 to the standard solar cycle of ∼11 years. The annual A_p index was best fit (R^2 = 46%, p < 0.01) with a 10.1-year cycle (Figure 26) and the regression model:

$$A_{\mathrm{p}}(\mathrm{t}) = 13.968 + (-3.365)\cos\left(\frac{2\pi\mathrm{t}}{10.10}\right) + 1.834 \cdot \sin\left(\frac{2\pi\mathrm{t}}{10.10}\right)$$

which revealed an amplitude (*Amp*) of 3.832 with a gradual overall peak increase observed over each subsequent solar cycle. No cyclicity in the examined range of rhythms could be significantly fit to SW_d. The annual β values revealed a 10.9-year cycle after normalized rank transformation (R^2 = 58%, $p < 0.001$) fit with the equation:

$$\beta(\mathrm{t}) = -0.013 + (-0.426)\cos\left(\frac{2\pi\mathrm{t}}{10.90}\right) + (-0.914)\sin\left(\frac{2\pi\mathrm{t}}{10.90}\right)$$

and non-zero *Amp* = 1.008 (Figure 27). Finally, the annual *CR* values achieved the greatest fit (R^2 = 65%, $p < 0.001$) at the maximum (T_c = 11) cycle length examined (Figure 28) with *Amp* = 586.108 and the overall equation:

$$CR(\mathrm{t}) = 8756.641 + (-471.580)\cos\left(\frac{2\pi\mathrm{t}}{11}\right) + (-348.045)\sin\left(\frac{2\pi\mathrm{t}}{11}\right)$$

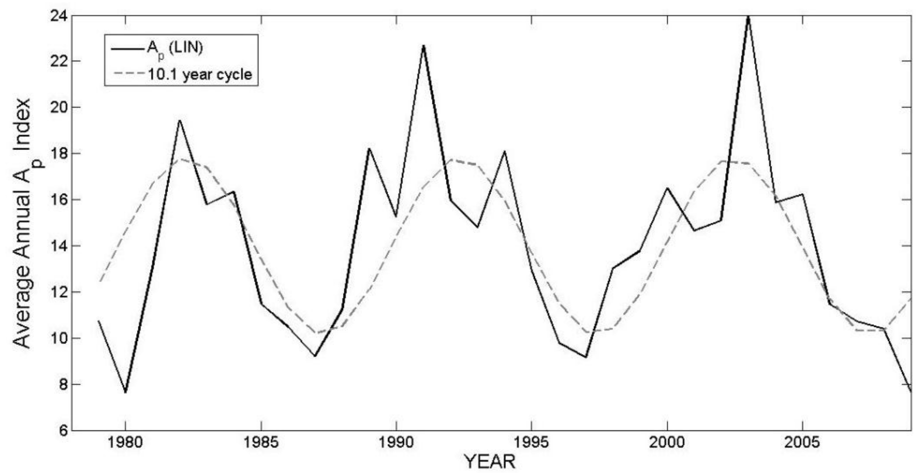

Figure 26: Average annual geomagnetic activity (A_p index) after detrending with superposed 10.1-year cyclicity

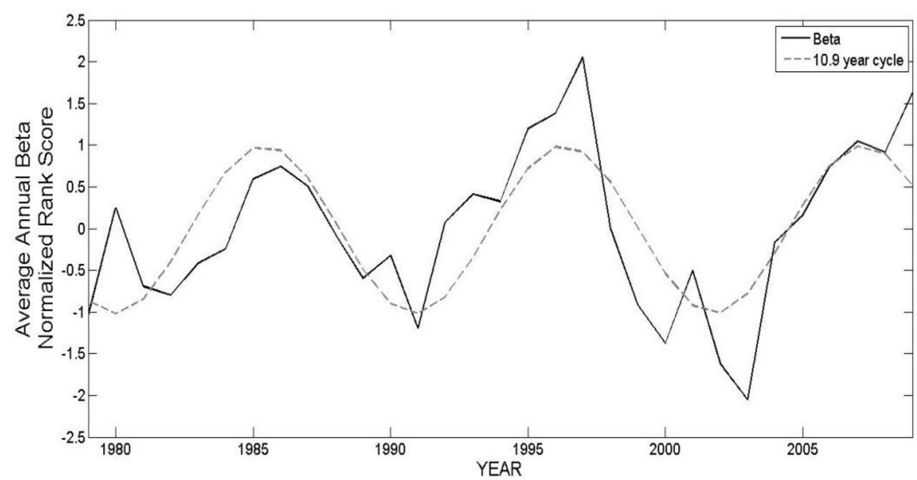

Figure 27: Annual average solar wind plasma beta (β) with superposed 10.9-year cyclicity

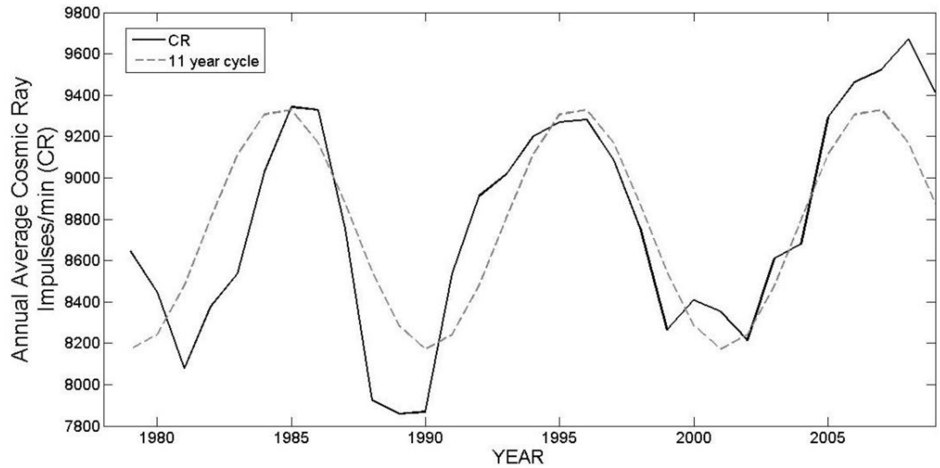

Figure 28: Annual average cosmic ray (*CR*) impulses per minute with superposed 11-year cyclicity

The 7- to 8-year phase shift seemingly has no general association with heliobiological factors or local fluctuations in the sociological setting. It was posited that this relationship between β and *HM* may signify an inherent, rhythmic perturbation of the boundaries of the magnetosphere and magnetopause. In this manner, we approximated the general particle density of a defined area associated with the β function for solar wind. This measure represents the ratio between plasma and magnetic pressures and can be expressed as:

$$\beta = \frac{(nk\mathrm{K})}{\left(\frac{B^2}{2\mu}\right)}$$

where n = particle density (particles·m^{-3}), k = Boltzmann constant (~1.38·10^{-23} J·K^{-1}), K = absolute temperature in Kelvin, B = strength of the magnetic field, and μ = permeability of free space. Here, we assume that the effective range of β (i.e., the range in value that could directly influence the mortality rate) is contingent upon direct application to the human heart and brain, the former of which shall be explored here. The human heart contains ~2 to 3 billion electrically active cells (Alder & Costabel, 1974) that constitute a general volume of 10^{-6} m^3 (assuming that the volume of a single cell is 10^{-15} m^3, derived from the linear dimension of 10 μm). The strength of the magnetic field related to the energy stored in the magnetic field is expressed by the following equation:

$$\mathrm{J} = \left(\frac{B^2}{4\pi\mu}\right) \cdot \mathrm{m}^3$$

where J = energy in Joules. This can be re-arranged to solve for the strength of the magnetic field, given that we have an average of $2.5 \cdot 10^9$ cells operating at an energy of 10^{-20} J per cell (Persinger, 2010) within the described volume, and the resultant field strength would be in the order of 10^{-5} T (Tesla). Consider the relationship described by β where, in order for the ratio to be equivalent, we must set the plasma and magnetic pressures to be equal to each other. Thus, the relationship becomes:

$$nk\mathrm{K} = \left(\frac{B^2}{2\mu}\right)$$

This can then be re-arranged again to solve for the limit of particle density that would affect the human heart. Provided that all the particles are heated to the temperature at the surface of the sun (~$5.778 \cdot 10^3$ K), the solution becomes $1.25 \cdot 10^{15}$ particles$\cdot$m^{-3}. Similarly, if we assume that the quintessential activation within the cortex as a single "thought" is associated with the simultaneous stimulation of 10^7 neurons (Dotta & Rouleau, 2014; Levy et al., 2004) each operating at 10^{-20} J, then the strength of the magnetic field would be in the order of 10^{-8} T. This magnitude is well within the geomagnetic ranges which have been shown to interfere with endorphinergic pathways (Murugan et al., 2014) where chronic fluctuations can lead to accumulation of stress responses intimately tied to arterial blood pressure and vascular tone homeostasis (Deanfield et al., 2007; Guyenet, 2006; McCubbin et al., 1989). We continued with our previous assumptions of temperature and the threshold of mortality when β is set such that plasma and magnetic pressures are equal, and the effective particle density would be in the order of $1.25 \cdot 10^{10}$ particles$\cdot$m^{-3}. In these calculations, we have neglected the coefficients as they would not significantly alter the magnitude of the calculated densities.

5.4. Discussion

While there may not be a direct causality deduced from the current analyses, the results nonetheless present a number of intriguing potential heliobiological links to mortality associated with hypertensive diseases (*HM*) in Canada, which are supported by previous research (Cornélissen et al., 2002; Dimitrova et al., 2004; 2009; Papailiou et al., 2011; 2012; Stoupel et al., 2006). With regard to the linear relationships observed, there was a great deal of consistency revealed for geomagnetic activity (A_p index), solar wind plasma beta (β), and cosmic ray impulses (*CR*), even in the context of their respective relationships with *HM*. This was partially suggested by the strongest linear phase shifts between *HM* and space weather (range of ~8 to 11 years) and even more strongly suggested by the common ~10.67-year periodicity shown for lag/lead correlation coefficients between *HM* and space weather. This could indicate that the linear relationships between variables observed over time might oscillate as a function of the related solar cycle, which was an average of 10.6 years for the current data. Further analysis into the potential source of these relationships suggested that the correlations obtained could be driven by the annual average β value. Based on the relationship observed for *HM* with both A_p

index and β, we further hypothesized a potential congruence between space weather-mediated occurrences of *HM* and sudden infant death syndrome (SIDS) with β, given the similar effects of heliogeophysical activity on SIDS incidence (O'Connor & Persinger 1997), as well as the apparent overlap between a secondary 1- to 2-year phase shift time for the relationship between *HM* with β and the typical age of onset for SIDS (e.g., 1 to 2 years of age).

Despite the results regarding β as the most likely shared source of variance, a strong linear correlation was observed between annual *HM* with A_p index phase shifted by the typical solar cycle length of 11 years. This particular relationship became more apparent upon subsequent investigation of cyclicity. Specifically, annual geomagnetic activity was the only heliophysical parameter to share a distinct overlapping peak periodicity with *HM* of approximately 10 years, while β and *CR* demonstrated cycles closer to that of the typical solar cycle length of ~11 years. Cosinor rhythms were applied to identify more specific cycles, with A_p index (10.1 years) closest to that observed for *HM* (9.6 years). The dominant cyclicity of annual *HM* in Canada was closest in length to the middle solar cycle in the current data examined (cycle 22), which was 9.7 years. However, there was a distinct depression in overall *HM* totals and a general disruption of the 9.6-year rhythm during the polarity reversal associated with solar cycle 22 (~1986 to 1996). This particular pattern in mortality was further accounted for by the secondary ~17-year periodicity revealed for *HM*. Furthermore, the 9.6-year rhythm of *HM* also appears to be reflected within the dominant periodicity observed for the lag/lead correlation coefficients between *HM* and SW_d. Although the raw data for *HM* in Canada displayed an overall quadratic trend, generally increasing over time, the rhythmic features of this specific cause of mortality appeared to at least coincide with those found for associated space weather factors.

Taken together, these data suggest a rhythmic relationship with a range of heliobiological factors contributing to the complex nature of human mortality, at least with regard to hypertensive diseases. Here, we have identified prominent solar periodicities, such as the 11-year solar cycle, as being correlated with *HM*. These variables may interact at a fundamental level of development associated with the evolutionary progression of the human species, as delineated in previous calculations, such that under specific circumstances (e.g., during discrete sectors of the solar periods), powerful relationships might emerge.

On an even more interesting note, we suggest here that the phase relationship of *HM* with the β function shares a level of congruence with the incidence of SIDS. The data presented here suggest that there is a relationship between the incidence of *HM* and β that demonstrated a dominant 7- to 8-year lagged phase shift with secondary peak correlations for 1 to 2 years. The 1- to 2-year phase relationship is congruent with the typical age of onset for SIDS (Kinney et al., 1992), which generally occurs around 1 to 2 years of age. First, we assumed that the correlation between β with *HM* coincides with the earliest gestation period of human embryological development (e.g., developing within the womb during a period of increased solar wind β values). According to the model provided, a subsequent increase in SIDS would occur 1 to 2 years after initial insemination (i.e., between 1 and 2 years of age), coinciding with the identified timeframe for the typical occurrence of SIDS mortality. The resultant resonance between dynamic pressure systems and human biological development may encourage a specific course of reactions that inevitably lead to the dissolution of the organism. A related hypothesis has been put forth by additional authors (Dimitrov, 2000; Ekbom et al., 1992; Ryabykh & Bodrova, 1992) who suspect a form of "heliogeophysical imprinting" on the developing organism through which cyclic environmental factors may preferentially affect certain tissue types during early ontogenesis. Furthermore, subsequent emergence of the related environmental phenomenon and associated periodicities may produce a form of “resonance” with the organism, promoting the development of a particular biological dysfunction (e.g., disease) later in life. It has also been previously demonstrated that the relationship between the incidence of SIDS and geomagnetic perturbations (O’Connor & Persinger, 1997) shows a similar type of link as that presented with *HM* in the current study. Perhaps it is not only the direct influence of local geomagnetic perturbations that are associated with the onset of SIDS (and *HM*), but the overall relationship between solar wind plasma and magnetic pressures that can account for the distinct source of variance which may help explain space weather-driven increases in either *HM* or SIDS.

As per the demonstrated calculations derived through dimensional analysis, we have proposed an intrinsic limitation between the effective fluctuations within the distribution of particle densities within a given space. It is suggested that any alteration to the system that enhances or depresses the overall normal distribution of particles would be enough to stimulate both the brain and the heart to respond preferentially to this deviation and alter the likelihood of mortality associated with physiological dysfunction. The deviations in particle density are contingent upon either the injection or removal of particles within a fixed boundary or the relative dynamic alterations of the boundary in which the particles reside. This may suggest an inherent expansion and contraction of the magnetosphere and magnetopause that follows a predictable periodicity. This local hypothetical contraction or expansion of the magnetosphere and magnetopause converge at the level of the human being and can alter the normal functioning of the organism. In this manner, subtle changes in activity may lead to an increase in the likelihood of mortality.

Through directly examining the relationship between β and *HM*, it is noted that an increase in β is strongly correlated with an increase in *HM* at the optimal time shift. We suggest that change in the local structure of the boundary conditions or particle densities may in fact contribute to annual *HM* in a dynamic manner. It should also be noted that the change in β can be driven by a decrease in the magnetic pressure or a fluctuation in the local temperature mechanics, outcomes which can occur with equal probability. It is not our intent to postulate the direction of this change or the underlying mechanism associated with dynamical alterations within the β function. Here, we merely interpret the relationship and offer a hypothesis, supported by quantitative analysis, that may occur at the level of the human body in response to these dynamic changes.

References

Alder, C. P., & Costabel, U. (1974). Cell number in human heart in atrophy, hypertrophy, and under the influence of cytostatics. *Recent Advancements in Studies of Cardiac Structure and Metabolism*, 6: 343-355.

Babayev, E. S., & Allahverdiyeva, A. A. (2007). Effects of geomagnetic activity variations on the physiological and psychological state of functionally healthy humans: Some results of Azerbaijani studies. *Advances in Space Research*, 40(12): 1941-1951.

Bertoia, M. L., Waring, M. E., Gupta, P. S., Roberts, M. B., & Eaton, C. B. (2012). Implications of new hypertension guidelines in the United States. *Hypertension*, 60(3): 639-644.

Blom, G. (1958). *Statistical Estimates and Transformed Beta Variables*. New York: Wiley.

Cornélissen, G. (2014). Cosinor-based rhythmometry. *Theoretical Biology and Medical Modelling*, 11(1): 16-40.

Cornélissen, G., Halberg, F., Breus, T., Syutkina, E. V., Baevsky, R.,Weydahl, A., Watanabe, Y., Otsuka, K., Siegelova, J., Fiser, B., & Bakken, E. E. (2002). Non-photic solar associations of heart rate variability and myocardial infarction. *Journal of Atmospheric and Solar-Terrestrial Physics*, 64: 707-720.

Cornélissen, G., Dimitrov, B. D., Carandente, F., & Halberg, F. (2011). Space and Earth weather mirrored in patterns of suicide incidence. *World Heart Journal*, 3(1): 31-42.

Deanfield, J. E., Halcox, J. P., & Rabelink, T. J. (2007). Endothelial function and dysfunction: Testing and clinical relevance. *Circulation*, 115: 1285-1295.

Dimitrov, B. D. (1993). Heliophysical activity and incidence variations of skin malignant melanoma in Czechoslovakia: A regional study. *International Journal of Biometeorology*, 37: 67-71.

Dimitrov, B. (1999). Malignant melanoma of the skin and non-Hodgkin's lymphoma in USA: A comparative epidemiological study. *Folia Medica*, 41(1): 121-125.

Dimitrov, B. D. (2000). Cyclic patterns of cancer incidence in males by body site: Data from the USA for the period 1973-1989. *Journal of the Balkan Union of Oncology*, 5: 81-84.

Dimitrov, B. D., Rachkova, M. I., & Atanassova, P. A. (2008). Cyclic patterns of incidence rate for skin malignant melanoma: Association with heliogeophysical activity. *Journal of Zheijang University Science B*, 9(6): 489-495.

Dimitrov, B. D., Atanassova, P. A., & Rachkova, M. I. (2009). Cyclicity of suicides may be modulated by internal or external ∼11-year cycles: An example of suicide rates in Finland. *Sun and Geosphere*, 4(2): 50-54.

Dimitrova, S., Stoilova, I., & Cholakov, I. (2004). Influence of local geomagnetic storms on arterial blood pressure. *Bioelectromagnetics*, 25(6): 408-414.

Dimitrova, S., Mustafa, F. R., Stoilova, I., Babayev, E. S., & Kazimov, E. A. (2009). Possible influence of solar extreme events and related geomagnetic disturbances on human cardiovascular state: Results of collaborative Bulgarian-Azerbaijani studies. *Advances in Space Research*, 43(4): 641-648.

Dotta, B. T., & Rouleau, N. Y. (2014). Electromagnetic fields as structure-function *zeitgebers* in biological systems: Environmental orchestrations of morphogenesis and consciousness. *Frontiers of Integrative Neuroscience*, 8: 84.

Dzvoník, O., Stetiarova, J., Kudela, K., & Daxner, P. (2006). A monitoring of space weather effects on some parameters of mental performance and health in aviation personnel. *Studia Psychologica*, 48(4): 273-291.

Ekbom, A., Trichopoulos, D., Adami, H. O., Hsieh, C. C., & Lan, S. J. (1992). Evidence of prenatal influences on breast cancer risk. *Lancet*, 340: 1015-1018.

Gee, M. E., Bienek, A., McAlister, F. A., Robitaille, C., Joffres, M., Tremblay, M. S.,

Johansen, H., & Campbell, N. R. C. (2012). Factors associated with lack of awareness and uncontrolled high blood pressure among Canadian adults with hypertension. *Canadian Journal of Cardiology*, 28(3): 375-382.

Guyenet, P. G. (2006). The sympathetic control of blood pressure. *Nature Reviews Neuroscience*, 7: 335-346.

Halberg, F. (1969). Chronobiology. *Annual Review of Physiology*, 31: 675-725.

Joffres, M. R., Ghadirian, P., Fodor, J. G., Petrasovits, A., Chockalingam, A., & Hamet, P. (1997). Awareness, treatment, and control of hypertension in Canada. *American Journal of Hypertension*, 10(10): 1097-1102.

Johnson, R. J., Kang, D. H., Feig, D., Kivlighn, S., Kanellis, J., Watanabe, S., Tuttle, K. R., Rodriguez-Iturbe, B., Hierra-Acosta, J., & Mazzali, M. (2003). Is there a pathogenetic role for uric acid in hypertension and cardiovascular and renal disease? *Hypertension*, 41: 1183-1190.

Kancírová, M., & Kudela, K. (2014). The relationship between suicide incidents in Slovakia and the Czech Republic and heliophysical parameters: Empirical results. *Journal of Astrobiology and Outreach*, 2(2).

Kaplan, M. S., Huguet, N., Feeny, D. H., & McFarland, B. H. (2010). Self-reported hypertension prevalence and income among older adults in Canada and the United States. *Social Science and Medicine*, 70(6): 844-849.

Kinney, H. C., Filiano, J. J., & Harper, R. M. (1992). The neuropathology of the sudden infant death syndrome: A review. *Journal of Neuropathology and Experimental Neurology*, 51(2): 115-126.

Levy, D., Larson, M. G., Vasan, R. S., Kannel, W. B., & Ho, K. K. L. (1996). The progression from hypertension to congestive heart failure. *Journal of the American Medical Association*, 275(20): 1557-1562.

Levy, I., Hasson, U., & Malach, R. (2004). One picture is worth at least a million neurons. *Current Biology*, 14(11): 996-1001.

Lloyd-Jones, D. M., Larson, M. G., Leip, E. P., Beiser, A., D'Agostino, R. B., Kannel, W. B., Murabito, J. M., Vasan, R. S., Benjamin, E. J., & Levy, D. (2002). Lifetime risk for developing congestive heart failure: The Framingham heart study. *Circulation*, 106: 3068-3072.

Lomb, N. R. (1976). Least-squares frequency analysis of unequally spaced data. *Astrophysics and Space Science*, 39(2): 447-462.

McCubbin, J. A., Surwit, R. S., Williams, R. B., Nemeroff, C. B., & McNeilly, M. (1989). Altered pituitary hormone response to naloxone in hypertension development. *Hypertension*, 14(6): 636-644.

Mulligan, B. P., & Persinger, M. A. (2012). Experimental simulation of the effects of sudden increases in geomagnetic activity upon quantitative measures of human brain activity: Validation of correlational studies. *Neuroscience Letters*, 516(1): 54-56.

Mulligan, B. P., Hunter, M. D., & Persinger, M. A. (2010). Effects of geomagnetic activity and atmospheric power variations on quantitative measures of brain activity: Replication of the Azerbaijani studies. *Advances in Space Research*, 45(7): 940-948.

Murugan, N. J., Karbowski, L. M., & Persinger, M. A. (2014). Weak burst-firing magnetic fields that produce analgesia equivalent to morphine do not initiate activation of proliferation pathways in human breast cells in culture. *Integrative Cancer Science and Therapeutics*, 1(3): 47-50.

O'Connor, R. P., & Persinger, M. A. (1997). Geophysical variables and behavior: LXXXH. A strong association between sudden infant death syndrome and increments of global geomagnetic activity: Possible support for the melatonin hypothesis. *Perceptual and Motor Skills*, 84(2): 395-402.

O'Leary, D. H., Polak, J. F., Kronmal, R. A., Manolio, T. A., Burke, G. L., & Wolfson, S. K. (1999). Carotid-artery intima and media thickness as a risk factor for myocardial infarction and stroke in older adults. *New England Journal of Medicine*, 340: 14-22.

Papailiou, M., Mavromichalaki, H., Kudela, K., Stetiarova, J., & Dimitrova, S. (2011). Effect of geomagnetic disturbances on physiological parameters: An investigation on aviators. *Advances in Space Research*, 48: 1545-1550.

Papailiou, M., Mavromichalaki, H., Kudela, K., Stetiarova, J., & Dimitrova, S. (2012). Cosmic radiation influence on the physiological state of aviators. *Natural Hazards*, 61: 719-727.

Persinger, M. A. (2010). 10^{-20} Joules as a neuromolecular quantum in medicinal chemistry: An alternative approach to myriad molecular pathways. *Current Medicinal Chemistry*, 17(27): 3094-3098.

Persinger, M. A. (2014). Infrasound, human health, and adaptation: An integrative overview of recondite hazards in a complex environment. *Natural Hazards*, 70: 501-525.

Robitaille, C., Dai, S., Waters, C., Loukine, L., Bancej, C., Quach, S., Ellison, J., Campbell, N., Tu, K., Reimer, K., Walker, R., Smith, M., Blais, C., & Quan, H. (2011). Diagnosed hypertension in Canada: Incidence, prevalence and associated mortality. *Canadian Medical Association Journal*, 184(1): 49-56.

Ryabykh, T. P., & Bodrova, N. B. (1992). Correlation of the risk of oncological breast disease and solar activity. *Biofizika*, 37: 710-715.

Saroka, K. S., & Persinger, M. A. (2014). Quantitative evidence for direct effects between Earth-ionosphere Schumann resonances and human cerebral cortical activity. *International Letters of Chemistry, Physics and Astronomy*, 20(2): 166-194.

Saroka, K. S., Caswell, J. M., Lapointe, A., & Persinger, M. A. (2014). Greater electroencephalographic coherence between left and right temporal lobe structures during increased geomagnetic activity. *Neuroscience Letters*, 560: 126-130.

Scargle, J. D. (1982). Studies in astronomical time series analysis. II. Statistical aspects of spectral analysis of unevenly spaced data. *Astrophysical Journal*, 263: 835-853.

Stoupel, E., Babayev, E. S., Mustafa, F. R., Abramson, E., Israelevich, P., & Sulkes, J. (2006). Clinical cosmobiology: Sudden cardiac death and daily/monthly geomagnetic, cosmic ray and solar activity - The Baku study (2003-2005). *Sun and Geosphere*, 1(2): 13-16.

Vaníček, P. (1971). Further development and properties of the spectral analysis by least-squares. *Astrophysics and Space Science*, 12: 10-33.

Williams, B., Lacy, P. S., Thom, S. M., Cruickshank, K., Stanton, A., Collier, D., Hughes, A. D., Thurston, H., & O'Rourke, M. (2006). Differential impact of blood pressure-lowering drugs on central aortic pressure and clinical outcomes. *Circulation*, 113: 1213-1225.

Wolf-Maier, K., Cooper, R. S., Kramer, H., Banegas, J. R., Giampaoli, S., Joffres, M. R., Poulter, N., Primatesta, P., Stegmayr, B., & Thamm, M. (2004). Hypertension treatment and control in five European countries, Canada, and the United States. *Hypertension*, 43: 10-17.

Yusuf, S., Hawken, S., Ounpuu, S., Dans, T., Avezum, A., Lanas, F., McQueen, M., Budaj, A., Pais, P., Varigos, J., & Lisheng, L. (2004). Effect of potentially modifiable risk factors associated with myocardial infarction in 52 countries (the INTERHEART study): Case-control study. *Lancet*, 364(9438): 11-17.

Chapter 6 – Exploring Spatial Trends in Canadian Incidence of Hospitalization due to Myocardial Infarction with Additional Determinants of Health

Published in Public Health

6. Abstract

An ecological study was conducted using aggregate data from the Canadian Institute for Health Information for age-standardized rates of myocardial infarction hospitalizations by health region in 2013. Exploratory spatial data analyses were applied to myocardial infarction hospitalization rates including Moran's *I* for detecting global spatial autocorrelation. Local spatial dependence was examined using local indicators of spatial autocorrelation to better identify the location of potential regional clusters. Linear and spatial regressions were applied to examine the role of additional health determinants. Significant spatial autocorrelation was observed for hospitalizations due to myocardial infarction for both sexes, independently and combined. This was largely present in the form of geographic disparities with cold spot clusters of low rates in the west, particularly British Columbia, and hot spot clusters of high rates moving east, especially in Ontario, Quebec, and New Brunswick. Additional disparities were observed with high rates clustered in Northern Ontario compared to clusters of low rates in Southern Ontario. Significant predictors included smoking, average income, education, and overweight or obesity and, after controlling for these, the central cold spot of low rates shifted east to Saskatchewan. This suggests a necessity for better geographic-based preventive measures as determined by the varied needs of particular regions' communities.

6.1. Introduction

The better understanding of cardiovascular disease such as myocardial infarction (*MI*) along with their associated determinants of health (e.g., smoking behavior, overweight and obesity, physical activity, etc.) is an integral component of health care systems given the overwhelming prevalence of associated medical issues such as hypertension. Within Canada, earlier research had suggested that up to ~20% of people in the country could present with hypertension placing them at increased risk for cardiovascular disease (Joffres et al., 1997). Another notable factor associated with this prevalence is that many cardiovascular diseases could be avoidable by adopting healthier lifestyle choices (McGill et al., 2008) including dietary concerns and greater physical activity. Obesity is one of many factors that contribute to detrimental health in this regard (National Institute of Health, 2004) and the feature of body weight is of particular relevance to Canadian populations (Katzmarzyk, 2002). Furthermore, spatial trends have been observed for overweight and obesity rates in Canada that vary across geographic regions administered by various health authorities (Pouliou & Elliott, 2009). Considering the link between issues of overweight and obesity with cardiovascular health (Eckel et al., 1998; Freedman et al., 2001; Williams et al., 2002), it is reasonable to assume that the incidence of *MI* might also demonstrate spatial homogeneity across the country that follows, to some extent, the spatial trends observed for obesity and other closely related health issues (Katzmarzyk, 2002; Pouliou & Elliott, 2009). Despite myriad suggestions related to lifestyle changes for improving cardiovascular health, the expense associated with *MI* incidence presents a persistent drain on available healthcare resources and personal finances (Azoulay et al., 2003; Cohen et al., 2014).

As previously identified by Pouliou and Elliott (2009), most Canadian studies of interest for this context have been conducted at the national or provincial level with relatively little research for smaller spatial scales (Katzmarzyk, 2002). This could be a particularly informative approach to geographic partitioning within spatial analyses given that each Canadian province defines its own health regions that each represents an administrative area served by a particular regional or district health authority responsible for administering public health programs and relevant information campaigns for their associated communities. One study of particular interest analyzed rates of hospitalization due to ischemic heart disease in Quebec's health regions over a 17 year period for which the authors (Bayentin et al., 2010) reported a significant degree of spatial variability that was also associated with extreme increases or decreases in temperature during summer and winter months respectively. An additional study investigating spatial dependence in Canadian overweight and obesity rates was conducted at the health region level from which the authors inferred better regional programs directed towards specific populations were required to combat the spatial trends and geographic disparity that were observed (Pouliou & Elliott, 2009). Examining *MI* trends elsewhere in the world, Ahmadi et al. (2015) recently found evidence of spatial dependence among *MI* rates throughout provinces of Iran. Therefore, the current ecological study was designed to explore the presence of spatial trends for recent Canadian *MI* rates at the health region level in order to better determine where future emphasis should be placed with regard to better health promotion programs and policies specifically designed for regional populations in order to help address issues of cardiovascular health that may vary by geography. Furthermore, additional regression techniques were applied in order to examine the associated role of independent predictor measures including socioeconomic and health factors.

6.2. Methods

A cartographic shapefile of Canadian health regions (2013 boundaries) was accessed from Statistics Canada (2015a) online. However, some areas with smaller populations have since been collapsed into fewer health regions due to sampling and other issues (Statistics Canada, 2015b) and these changes were accommodated by merging relevant health regions within Quantum GIS v.2.12.3 software prior to analysis (i.e., Mamawetan, Keewatin, and Athabasca regional health authorities in Saskatchewan have been merged and Nova Scotia areas were combined into six zones). Prince Edward Island (PEI), which was contiguously neighborless in the accessed shapefile, has been changed from four zones into a single administrative area so that data are only available at the provincial level. Data for PEI were therefore excluded from the current analysis according to their inconsistency with the current spatial scale of interest, along with Northwest Territories, Nunavut, and Yukon, which largely represent reduced samples and culturally unique Inuit populations (Pouliou & Elliott, 2009). Quebec regions of Nunavik and Terres-Cries-de-la-Baie-James were also excluded from the current study given particularly small samples, missing data from the dependent measure of interest, and similar density of Inuit populations. This process resulted in a total of N = 106 health regions for analysis. Publically available annual data regarding the incidence of hospitalization due to myocardial infarction (*MI*) in 2013 were obtained from the Canadian Institute for Health Information (CIHI; http://www.cihi.ca/) and calculated as age-standardized rate per 100,000 population for males and females combined and separately. Data were merged with the health region shapefile in GeoDa v1.6.7 software for further analysis. Additional independent variables (in population proportions) acquired from Statistics Canada (2015c) included access to regular medical doctor

(*%Doc*), high perceived life stress (*%LifeStr*), high blood pressure (*%HBP*), high (five or more times per day) consumption of fruits and vegetables (*%FruVeg*), current (daily or occasional) smoking (*%Smoke*), heavy drinking according to World Health Organization and Health Canada guidelines (*%Drink*), as well as overweight or obesity determined by body mass index (BMI) among those aged ≥ 18 years and excluding pregnant women (*%BMI*). Further information on these measures can be found at the relevant Statistics Canada (2015c) website. The latest data from the National Household Survey (Statistics Canada, 2015d) were only available for 2011, however, the average income (in Canadian $) was acquired for the current study (*AvInc*) along with the ratio of the population ≥ 15 years of age with a high school diploma or greater to those without a high school education (*Edu*) for which higher values indicate relatively more people with a secondary education at minimum.

A spatial weight matrix (w_{ij}) can be used to quantify the spatial relationships that exist among a set of data for which the row and column (i and j) of each combination of values denotes the spatial relationship for a given set of regions where areas closer to one another present relatively greater weights (Anselin, 1994) when w_{ij} values are row-standardized in order to better control for varied region size and associated number of neighbors. Statistical spatial weights were computed according to the queen contiguity rule (first order) for which health regions were considered neighbors when they shared a common border. Standard techniques for exploratory spatial data analysis (ESDA) were employed including preliminary mapping of spatial distributions for *MI* rates followed by calculation of Moran's (1950) *I* values and local indicators of spatial association (LISA). The global Moran's *I* statistic is a common method of examining spatial dependence for a variable of interest according to:

$$I = \frac{\mathrm{n}}{\sum_i \sum_j w_{ij}} \cdot \frac{\sum_i \sum_j w_{ij}(y_i - \mu)(y_j - \mu)}{\sum_i (y_i - \mu)^2}$$

where n = number of cases or units in a spatial matrix, y = variable under investigation, and μ = average value of y. Values range from +1 to -1 where zero is an indication that the spatial pattern of the data is completely random. Testing of the null hypothesis was accommodated using Monte Carlo simulation where an empirical distribution of results was derived from testing multiple permutations of the data and statistically comparing the actual result of interest to this distribution by standardized z-score calculation. For the current study, 999 random permutations were used for estimating probabilities where $p < 0.05$ was considered statistically significant. One of the limitations of Moran's *I* is the inability to determine where spatial dependence could be occurring (between which regions) and the associated directions of these spatial relationships (i.e., high-high or hot spots = high rates with high rates in neighboring regions, and low-low or cold spots = low rates with low rates in neighboring regions). Therefore, LISA maps were also assessed in order to identify local clusters of spatial dependence (Anselin, 1995) where statistical significance ($p < 0.05$) was similarly estimated using a Monte Carlo simulation method with 999 random data permutations. LISA statistics were computed for each health region according to:

$$I_i = \frac{\mathrm{n}}{(\mathrm{n}-1)\sigma^2}(y_i - \mu)\sum_{j=1}^{\mathrm{n}} w_{ij}(y_j - \mu)$$

where summing all of the local *I* values for each region *i* also indicates the global Moran's *I* (Sparks & Sparks, 2010). Along with previously mentioned hot spots and cold spots, high-low and low-high relationships can also be identified with this technique (so-called spatial outliers which are not outliers in the traditional statistical sense). Although the primary research question concerned the spatial properties of *MI* rates, differences between males and females were also noted according to statistical analyses carried out with SPSS v17 software. This included assessment of distribution properties with Shapiro-Wilks test and comparison between sexes facilitated by either paired *t*-test or Wilcoxon signed rank test as determined by the presence or absence of normal distributions. Exploration of global Moran's *I* for spatial autocorrelation was also undertaken for all independent measures of interest.

After preliminary ESDA, all variables with non-normal distributions were transformed to their natural logarithm (LN) and reassessed with Shapiro-Wilks test prior to subsequent parametric analyses. Where both LN and square root transformations failed to correct distribution issues Blom's (1958) method for computing normalized rank scores (BN) was used as a last resort. Note that variables transformed in this manner remained perfectly correlated with their original values according to nonparametric Spearman correlations ($\rho = 1.0$). All variables were then standardized (*z*-scores) prior to regression analyses to make subsequent units consistent across measures and to allow direct interpretation of regression coefficients (Sparks & Sparks, 2010) ($B = \beta$ for standardized variables). Estimation of ordinary least-squares (OLS) regression for *MI* as the dependent measure was conducted with stepwise variable entry of predictors in SPSS software with calculation of variance inflation factors (VIF) for assessment of potential multicollinearity where the standard linear model follows:

$$y = A + B_1 x_1 +, \dots, B_i x_i + \varepsilon$$

where A = regression intercept, B = ith coefficient, x = ith independent variable, and ε = error or residuals. Maximum likelihood estimation was also employed to compute Akaike information criteria (AIC) to further facilitate direct comparison between models.

Residuals derived from OLS were tested for normality using the Shapiro-Wilks method (SPSS) and for heteroscedasticity using Breusch-Pagan test (GeoDa). Standardized residuals were then assessed for spatial autocorrelation with global Moran's I to detect remaining spatial association after controlling for significant predictor variables. Lagrange multiplier tests were also applied to the OLS residuals with the constructed spatial weight matrix w_{ij} in order to better determine whether a spatial lag or spatial error model would likely best describe the data (Sparks & Sparks, 2010). The significant predictors identified through OLS were entered into spatial lag and spatial error regressions in GeoDa to better determine their effect on overall regional MI after accounting for spatial processes. The spatial lag model describes a scenario in which an indicator of health in one region is associated with that factor in neighboring region(s) and follows the form:

$$y = \lambda w_{ij} y + B_1 x_1 +, \ldots, + B_i x_i + \varepsilon$$

where λ = spatial autoregressive parameter (Sparks & Sparks, 2010). This places the spatial term on the dependent measure (MI) although, as indicated by Sparks and Sparks (2010), this particular model better reflects scenarios involving, for example, infectious disease where the spread of the infection may diffuse across space into neighboring areas and would likely require a much more discrete spatial scale at the local level. Conversely, the spatial error model includes a spatial term on the regression error according to:

$$y = B_1x_1 +, \dots, +B_ix_i + u$$

for which u is defined by:

$$u = \lambda w_{ij}(\varepsilon + h)$$

where h = uncorrelated homoscedastic errors. This analysis reflects potential independent variables including those that are not included in the model rather than diffusion of the process under consideration and better indicates spatial associations of the independent measures which could be responsible for spatial clustering of the dependent variable (Sparks & Sparks, 2010; Morenoff, 2003). As with OLS results, spatial regression residuals were assessed for homoscedasticity using Breusch-Pagan test with additional likelihood ratio tests applied to better determine the statistical significance of regression differences between OLS and spatial models.

6.3. Results

Because *MI* rates for both males and females were not normally distributed ($p < 0.05$), nonparametric testing was first employed. Wilcoxon signed rank test indicated that males consistently demonstrated significantly ($z = 8.938$, $p < 0.001$) higher rates of hospitalization due to *MI* in 2013 (*mean* = 329.991, *sd* = 87.485) compared to females (*mean* = 153.708, *sd* = 54.927). Despite this relative difference, the spatial distribution observed with choropleth maps colored by quartile (Figure 29) tended to qualitatively demonstrate a degree of overlap between sexes with the lowest rates of *MI* hospitalization observed to the far western province of British Columbia with a graded increase moving east, and additional disparities observed between north and south.

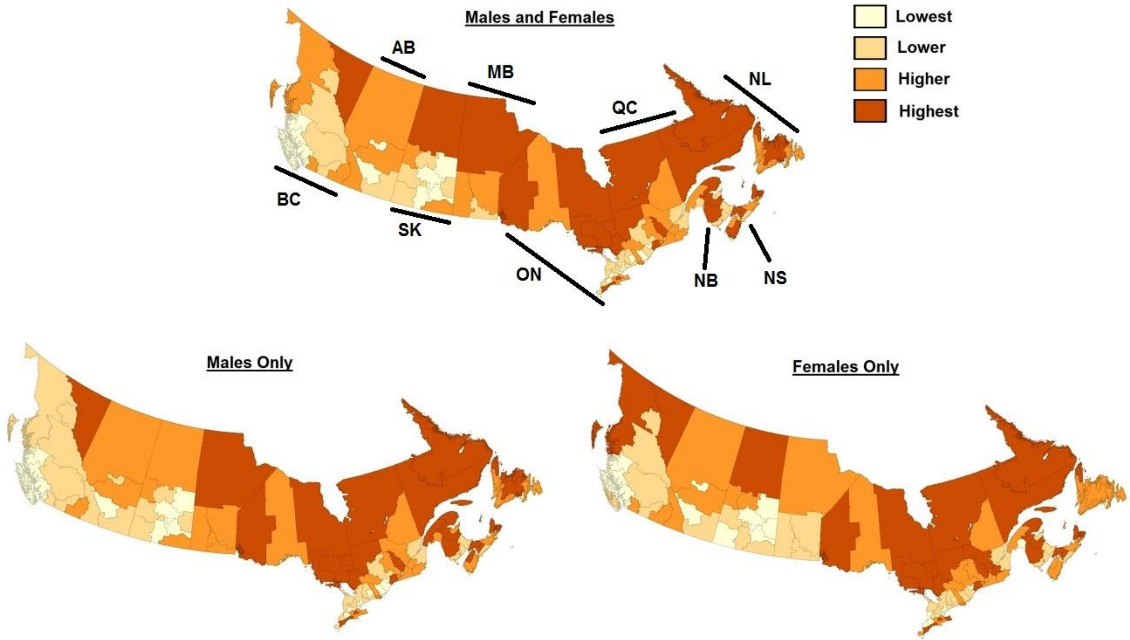

Figure 29: Choropleth maps colored by quartile of myocardial infarction (*MI*) hospitalization rates for males and females together and separately from Canada in 2013; provinces are indicated in top figure where BC = British Columbia, AB = Alberta, SK = Saskatchewan, MB = Manitoba, ON = Ontario, QC = Quebec, NB = New Brunswick, NS = Nova Scotia, and NL = Newfoundland

Testing for global spatial autocorrelation using Moran's *I* indicated significantly positive autocorrelation among the total population (I = 0.384, z_I = 5.501, p < 0.001). The same overall positive spatial dependence was also observed for males (I = 0.407, z_I = 5.954, p < 0.001) with a relatively weaker but nonetheless statistically significant result for females (I = 0.307, z_I = 4.513, p < 0.001). Significant (p < 0.001) global spatial autocorrelation was also identified for all independent variables including *%Doc* (I = 0.314, z_I = 4.733), *%LifeStr* (I = 0.373, z_I = 5.494), *%HBP* (I = 0.361, z_I = 5.354), *%FruVeg* (I = 0.553, z_I = 7.932), *%Smoke* (I = 0.384, z_I = 5.446),

%Drink (I = 0.321, z_I = 4.859), *%BMI* (I = 0.504, z_I = 7.622), and *AvInc* (I = 0.378, z_I = 5.565), as well as weak but statistically significant autocorrelation for *Edu* (I = 0.191, z_I = 2.828, p = 0.004). Choropleth maps for many independent measures qualitatively demonstrated spatial patterns similar to those for *MI*, particularly with regard to spatial clusters of high values in Northern Ontario and Quebec.

To better investigate the local spatial autocorrelations, LISA maps were plotted after significance testing. Results for total population revealed clusters of low *MI* rates related to low neighboring rates, or cold spots, primarily in British Columbia and Southern Ontario. Conversely, hot spots of high *MI* rates related to high neighboring rates were observed for Northern Ontario, Quebec, and New Brunswick. All results derived from the LISA technique are mapped in Figure 30. Among the most consistent cold spots for males, females, and both sexes combined were the regions covered by the Central Vancouver Island health service (total 181/100,000 *MI* rate) along with the North Shore and Garibaldi Coast region (total 144/100,000 *MI* rate). An additional cold spot for low *MI* rates was also consistently observed in Southern Ontario including the Wellington-Dufferin-Guelph area (total 213/100,000 *MI* rate), Toronto (total 145/100,000 *MI* rate), Peel (total 181/100,000 *MI* rate), and York (total 156/100,000 *MI* rate). A final low-low cluster was found in Saskatchewan, but for females only, and included Five Hills (total 183/100,000 *MI* rate), Heartland (total 199/100,000 *MI* rate), Regina (total 164/100,000 *MI* rate), and Sunrise health regions (total 212/100,000 *MI* rate). Conversely, a consistent hot spot was revealed beginning in Northern Ontario and moving east. The Ontario areas that appeared for all conditions included Porcupine (total 363/100,000 *MI* rate), Sudbury (total 293/100,000 *MI* rate), Thunder Bay (total 264/100,000 *MI* rate), and Timiskaming health regions (total 331/100,000 *MI* rate) while associated hot spot areas in Quebec included Région de la Mauricie et du Centre-du-Québec (total 261/100,000 *MI* rate), de l'Abitibi-Témiscamingue (total 347/100,000 *MI* rate), Côte-Nord (total 298/100,000 *MI* rate), and Nord-du-Québec (total 514/100,000 *MI* rate). Of particular note, Région du Saguenay – Lac-Saint-Jean demonstrated relatively lower rates surrounded by high neighboring rates for males while the same region was part of the Quebec hot spot cluster for females (total 241/100,000 *MI* rate). Although Zone 5 from New Brunswick (total 450/100,000 *MI* rate) was included for every result, the similarly significant neighboring regions in the province were only particularly prominent for the male population. The regions that demonstrated the most consistent spatial clustering across samples are listed in Table 10.

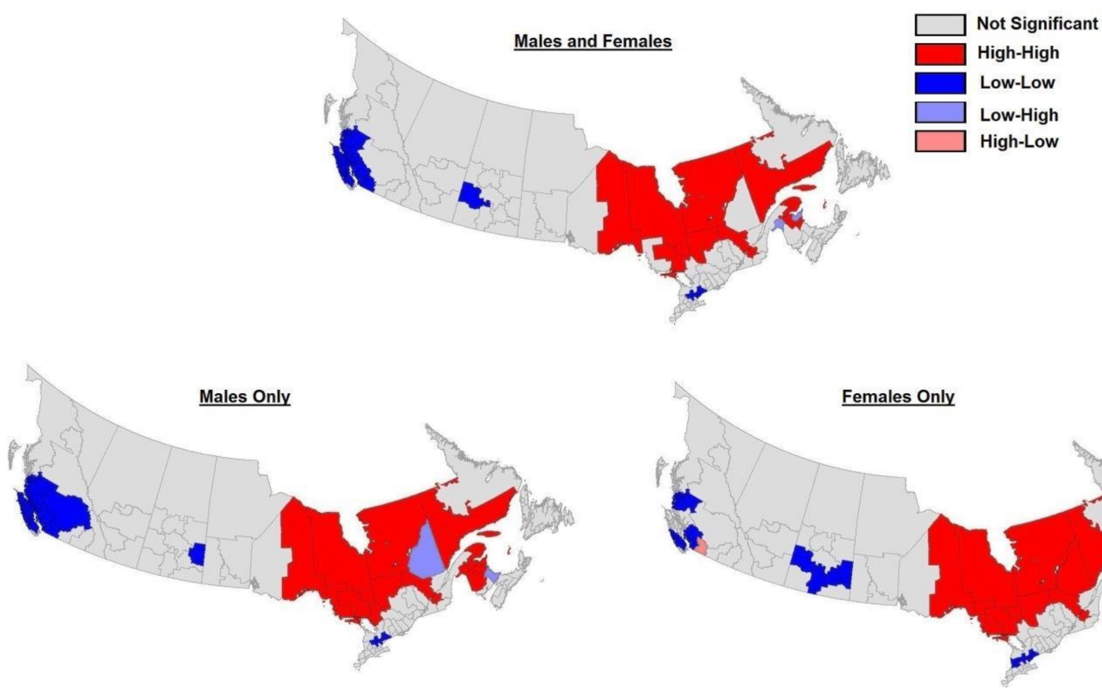

Figure 30: Local indicators of spatial autocorrelation (LISA) maps of myocardial infarction (*MI*) for both sexes, males only, and females only for Canada in 2013

Table 10: Significantly spatially clustered health regions by province according to high-high hot spots or low-low cold spots that remained consistent across samples (total, males, females)

	AB	BC	MB	NB	NL	NS	ON	QC	SK
High-High	-	-	-	(1) Zone 5	-	-	(1) Porcupine (2) Sudbury (3) Thunder Bay (4) Timiskaming	(1) Mauricie et du Centre-du-Québec (2) l'Abitibi-Témiscamingue (3) Côte-Nord (4) Nord-du-Québec	-
Low-Low	-	(1) Central Vancouver Island (2) North Shore and Garibaldi Coast	-	-	-	-	(1) Wellington-Dufferin-Guelph (2) Toronto (3) Peel (4) York	-	-

Shapiro-Wilks testing for normal distributions indicated transformation was necessary ($p < 0.05$) for *MI*, *%Doc*, *%HBP*, *%BMI*, and *AvInc*, where the natural logarithm (LN) was adequate for only the first three variables. Neither LN nor square root transforms were adequate for the remaining variables and Blom's method for normalized rank scores (BN) was applied to *%BMI* and *AvInc* to accommodate parametric testing after which all variables were standardized (*z*-scores). Estimation of the OLS regression was conducted with stepwise variable entry for which calculated VIF did not indicate issues of multicollinearity. The final model ($F_{(4, 105)} = 31.286$, $p < 0.001$, $R^2 = 0.553$) included significant predictors *%Smoke*$_z$ ($\beta = 0.293$, SE = 0.079, $p < 0.001$), BN_*AvInc*$_z$ ($\beta = -0.313$, SE = 0.070, $p < 0.001$), *Edu*$_z$ ($\beta = -0.258$, SE = 0.083, $p = 0.002$), and BN_*BMI*$_z$ ($\beta = 0.170$, SE = 0.082, $p = 0.041$). Model residuals were normally distributed as determined by Shapiro-Wilks test ($p > 0.05$) and there were no issues of heteroscedasticity according to Breusch-Pagan test ($p > 0.05$). Maximum likelihood estimation was also employed to compute information criteria (AIC = 224.368) for subsequent model comparisons. Lagrange multiplier tests indicated that spatial lag or spatial error models could potentially fit the data equally well (*p*s ~0.0001).

Residual values obtained through OLS were analyzed using global Moran's *I* in order to explore spatial autocorrelation of *MI* after controlling for significant predictor variables (*%Smoke*$_z$, BN_*AvInc*$_z$, *Edu*$_z$, and BN_*BMI*$_z$) for which Monte Carlo simulation showed an expected *I* statistic of $E_I = -0.001$. Significant spatial autocorrelation was detected for OLS residuals ($I = 0.272$, $z_I = 3.987$, $p < 0.001$), with LISA results of corrected rates mapped in Figure 31, and thus additional spatial regression models were assessed. Note that the primary low-low cold spot appeared to shift from British Columbia to Saskatchewan after OLS. For the preliminary spatial lag regression, *%BMI*$_z$ was no longer statistically significant ($p > 0.05$) although the overall model (AIC = 213.697) presented issues of heteroscedasticity according to Breusch-Pagan test ($p < 0.05$). However, spatial error regression did not demonstrate this issue and additional results are therefore presented in detail. This model was statistically significant for the autoregressive spatial term ($\lambda = 0.412$, $p < 0.001$) and for all entered predictors including *%Smoke*$_z$ ($\beta = 0.303$, SE = 0.076, $p < 0.001$), BN_*AvInc*$_z$ ($\beta = -0.262$, SE = 0.072, $p < 0.001$), *Edu*$_z$ ($\beta = -0.228$, SE =

0.076, p = 0.003), and BN_BMI_z (β = 0.187, SE = 0.085, p = 0.027) with a significant difference from the OLS model according to likelihood ratio test (LR = 13.023, p < 0.001) and slightly reduced information criteria compared to both of the other examined models (AIC = 211.345). The residuals computed through spatial error regression were finally assessed with Moran's *I* for global spatial autocorrelation which was no longer significant, as should be expected (I = -0.019, z_I = -0.104, p > 0.05). Note that results for *MI* values of males and females, including LISA maps and regressions, were practically identical to those delineated in the preceding discussion. The only major difference observed was the absence of BN_BMI_z from the female regression models. Independent variable statistics are provided for the male and female *MI* OLS and spatial error models in Table 11.

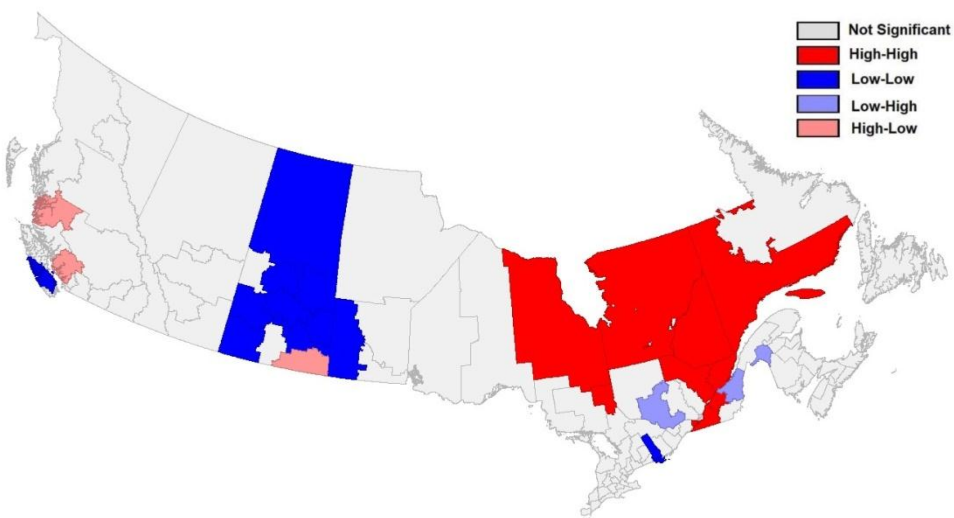

Figure 31: Local indicators of spatial autocorrelation (LISA) map of total myocardial infarction (*MI*) hospitalization rate regression residuals after controlling for smoking (*%Smoke*), overweight and obesity (*%BMI*), average income (*AvInc*), and education (*Edu*)

Table 11: Independent variable coefficients (β) with their standard errors (SE) and probabilities (p) from male and female myocardial infarction (*MI*) regression models for predictors including education (Edu_z), average income (BN_$AvInc_z$), smoking ($\%Smoke_z$), and overweight or obesity (BN_BMI_z)

	β*	SE	p
Males – OLS			
Edu_z	-0.294	0.085	0.001
BN_$AvInc_z$	-0.284	0.072	< 0.001
$\%Smoke_z$	0.238	0.081	0.004
BN_BMI_z	0.189	0.084	0.027
Males – Spatial Error			
Spatial Component	0.437	0.102	< 0.001
Edu_z	-0.271	0.077	< 0.001
$\%Smoke_z$	0.249	0.078	0.001
BN_$AvInc_z$	-0.213	0.074	0.004
BN_BMI_z	0.249	0.087	0.035
Females – OLS			
$\%Smoke_z$	0.388	0.082	< 0.001
BN_$AvInc_z$	-0.349	0.073	< 0.001
Edu_z	-0.206	0.082	0.013
Females – Spatial Error			

	β*	SE	*p*
Spatial Component	0.342	0.111	0.002
%*Smoke*$_z$	0.387	0.082	< 0.001
BN_*AvInc*$_z$	-0.330	0.077	< 0.001
***Edu*$_z$**	-0.196	0.076	0.010

*β is equivalent to the autoregressive spatial error parameter (λ) for the *Spatial Component* terms

6.4. Discussion

The results of the current study suggest a regional disparity among rates of hospitalization due to *MI* which demonstrated spatial dependence and clustering, particularly for high rates of *MI* in Northern Ontario, Quebec, and New Brunswick, while Southern Ontario showed a cold spot of low *MI* incidence similar to that revealed in Western British Columbia. This general trend of greater prevalence in the northeast compared to the southwest of the country was similarly indicated (Pouliou & Elliott, 2009) by indices of overweight and obesity aggregated over health regions from 2005 and the observed pattern of *MI* hospitalizations may in part reflect this particular spatial trend. It should also be noted that spatial trends in *MI* rates have similarly been observed for areas outside of Canada (Ahmadi et al., 2015). However, after controlling for significant socioeconomic and other health factors, the larger cold spot previously observed in British Columbia became less prominent and instead was centralized across Saskatchewan. Because cardiovascular health is mediated by myriad contributing social and environmental factors and current spatial regression results suggested additional spatial processes could be involved, it may be that the current results also reflect the different major sectors of the Canadian workforce to an extent (e.g., mining industry in Northern Ontario) and their associated environmental contributors which itself is an additional consideration for future research in order to properly implement optimal public health programs that address specific issues relevant to each community.

After OLS regression of *MI* using predictor variables typically associated with cardiovascular health including socioeconomic factors and health-related behaviors it was determined that regular smoking (*%Smoke*) and overweight or obesity (*%BMI*) were significantly and positively associated with *MI*, while average income (*AvInc*) and education (*Edu*) were negatively related to *MI*, all of which are known contributors to cardiovascular health (Eckel et al., 1998; Ockene & Miller, 1997; Winkleby et al., 1992). However, the role of overweight or obesity was not as prominent for female *MI* results as opposed to those observed for total rates or males only and did not enter the tested regression models. No other independent variables were statistically significant. Application of ESDA techniques to OLS residuals also revealed significant spatial autocorrelation for which LISA results demonstrated similar spatial patterns to those observed for a number of independent measures with hot spots of corrected *MI* mostly revealed among the health regions of Northern Ontario and Quebec although low-low clusters moved further east from British Columbia to the health regions of Saskatchewan when controlling for significant independent factors.

One of the potential issues inherent to any study of this type is the modifiable areal unit problem (MAUP) as originally identified by Gehlke and Biehl (1934) whereby the aggregation level at which data is grouped can affect statistical results. However, there remains no satisfactory solution to this problem (Horner & Murray, 2002; King, 1979; Openshaw, 1983), although the data currently employed were for the smallest spatial scale available. In addition to this, the potential insight gleaned from the present results remains relevant to the scale of analysis which is administered by regional and district health authorities that can then more effectively design health promotion efforts. As a specific example from the current results, Région du Saguenay – Lac-Saint-Jean in the province of Quebec was identified with particularly low *MI* hospitalization rates for males compared to neighboring regions while the same health region was clustered within a hot spot for high *MI* rates among females. The gender disparity of extreme lows and highs within spatial autocorrelations could serve as further insight for programs specifically designed to address the most relevant section of the population.

Identification of spatial homogeneity and clustering of *MI* rates indicates the necessity for better geographic-based preventive measures as determined by the varied needs of particular regions overall, especially for sub-regional communities with lower socioeconomic status. Spatial associations identified after controlling for significant predictor measures (*%Smoke*, *AvInc*, and *Edu*, as well as *%BMI* for males and total rates) remained statistically significant and maintained an indication of east-west and north-south disparities with hot spots of high *MI* rates observed toward the northeast, especially in Northern Ontario and Quebec. Finally, the spatial error specification for the latter analyses further suggested that spatial processes among independent variables or potentially unmeasured independent factors could be responsible for the spatial patterns found for *MI*. Overall, the demonstration that space matters with regard to *MI* rates indicates that spatial dependence should be included in further statistical investigation of related factors with appropriate spatial methods employed for general public health surveillance while unique environmental factors associated with varied geographic regions may also contribute a great deal to the observed spatial trends. Further research is required to better assess the myriad potential contributors to cardiovascular health in this respect.

References

Ahmadi, A., Soori, H., Mehrabi, Y., & Etemad, K. (2015). Spatial analysis of myocardial infarction in Iran: National report from the Iranian myocardial infarction registry. *Journal of Research in Medical Sciences*, 20(5): 434-439.

Anselin, L. (1994). Exploratory spatial data analysis and geographic information systems. In: Longley, P., Brooks, S., Macmillan, B., McDonnell, R. (eds.) *GeoComputation: A Primer* (pp. 77-94). New York: Wiley.

Anselin, L. (1995). Local indicators of spatial association – LISA. *Geographical Analysis*, 27: 93-115.

Azoulay, A., Pilote, L., Filion, K. B., & Eisenberg, M. J. (2003). Costs of treatment of acute myocardial infarction in Canadian and US hospitals. *Cardiovascular Reviews and Reports*, 24(11).

Bayentin, L., El Adlouni, S., Ouarda, T. B. M. J., Gosselin, P., Doyon, B., & Chebana, F. (2010). Spatial variability of climate effects on ischemic heart disease hospitalization rates for the period 1989-2006 in Quebec, Canada. *International Journal of Health Geographics*, 9(5).

Blom, G. (1958). *Statistical Estimates and Transformed Beta Variables*. New York.

Cohen, D., Manuel, D. G., Tugwell, P., Sanmartin, C., & Ramsay, T. (2014). Direct healthcare costs of acute myocardial infarction in Canada's elderly across the continuum of care. *Journal of the Economics of Ageing*, 3: 44-49.

Eckel, R. H., Krauss, R. M., & AHA Nutrition Committee. (1998). American Heart Association call to action: Obesity as a major risk factor for coronary heart disease. *Circulation*, 97(21): 2099-2100.

Freedman, D. S., Kettel-Khan, L., Dietz, W. H., Srinivasan, S. R., & Berenson, G. S. (2001). Relationship of childhood obesity to coronary heart disease risk factors in adulthood: The Bogalusa Heart Study. *Pediatrics*, 108(3): 712-718.

Gehlke, C. E., & Biehl, K. (1934). Certain effects of grouping upon the size of the correlation coefficient in census tract material. *Journal of the American Statistical Association*, 29(185A): 169-170.

Horner, M. W., & Murray, A. T. (2002). Excess commuting and the modifiable areal unit problem. *Urban Studies*, 39(1): 131-139.

Joffres, M. R., Ghadirian, P., Fodor, J. G., Petrasovits, A., Chockalingam, A., & Hamet, P. (1997). Awareness, treatment, and control of hypertension in Canada. *American Journal of Hypertension*, 10(10): 1097-1102.

Katzmarzyk, P. T. (2002). The Canadian obesity epidemic, 1985-1998. *Journal of the Canadian Medical Association*, 166: 1039-1040.

King, P. E. (1979). Problems of spatial analysis in geographical epidemiology. *Social Science and Medicine*, 13D: 249-252.

McGill, H. C., McMahan, C. A., & Gidding, S. S. (2008). Preventing heart disease in the 21st century: Implications of the Pathobiological Determinants of Atherosclerosis in Youth (PDAY) study. *Circulation*, 117(9): 1216-1227.

Moran, P. A. P. (1950). Notes on continuous stochastic phenomena. *Biometrika*, 37(1): 17-23.

Morenoff, J. D. (2003). Neighborhood mechanisms and the spatial dynamics of birth weight. *American Journal of Sociology*, 108: 976-1017.

National Institute of Health. (2004). *A Report of the NIH Obesity Research Task Force*. U.S. Department of Health and Human Services, Bethesda, MD.

Ockene, I. S., & Miller, N. H. (1997). Cigarette smoking, cardiovascular disease, and stroke. *Circulation*, 96: 3243-3247.

Openshaw, S. (1983). *The Modifiable Areal Unit Problem*. Norwick: GeoBooks.

Pouliou, T., & Elliott, S. J. (2009). An exploratory spatial analysis of overweight and obesity in Canada. *Preventive Medicine*, 48: 362-367.

Sparks, P. J., & Sparks, C. S. (2010). An application of spatially autoregressive models to the study of US county mortality rates. *Population, Space and Place*, 16: 465-481.

Statistics Canada. (2015a). *82-402-X: Health Region Boundary Files*. Retrieved from http://www.statcan.gc.ca/pub/82-402-x/2013002/reg-eng.htm

Statistics Canada. (2015b). *Table 7-e: Summary of Changes to Health Region Codes, Names and Boundaries, 2011 and 2013*. Retrieved from http://www.statcan.gc.ca/pub/82-402-x/2015001/regions/tbl/tbl7e-eng.htm

Statistics Canada. (2015c). *Data Tables, Maps and Fact Sheets*. Retrieved from http://www.statcan.gc.ca/pub/82-221-x/2013001/tbl-eng.htm

Statistics Canada. (2015d). *NHS Profile, 2011*. Retrieved from https://www12.statcan.gc.ca/nhs-enm/2011/dp-pd/prof/index.cfm?Lang=E

Williams, C. L., Hayman, L. L., Daniels, S. R., Robinson, T. N., Steinberger, J., & Paridon, S. (2002). Cardiovascular health in childhood: A statement for health professionals from the Committee on Atherosclerosis, Hypertension, and Obesity in the Young (AHOY) of the Council on Cardiovascular Disease in the Young, American Heart Association. *Circulation*, 106(1): 143-160.

Winkleby, M. A., Jatulis, D. E., Frank, E., & Fortmann, S. P. (1992). Socioeconomic status and health: How education, income, and occupation contribute to risk factors for cardiovascular disease. *American Journal of Public Health*, 82(6): 816-820.

Chapter 7 – Prevalence of Reported High Blood Pressure in Canada: Investigation of Demographic and Spatial Trends

Published in Journal of Public Health

7. Abstract

The current study sought to investigate recent demographic and spatial trends of self-reported high blood pressure in Canada, including influence of age, gender, and household income, as well as the identification of global spatial autocorrelations and local spatial clustering within gender/income groups. Data acquired from the Canadian Community Health Survey 2014 were analyzed using both categorical response variables and age-standardized prevalence estimates. Inferential statistical procedures were assessed along with exploratory spatial statistics at the health region scale. All demographic variables contributed to reports of high blood pressure. Significant differences between genders and income quintiles were observed with a linear decrease in high blood pressure with increased household income for females, whereas income gradation was nonlinear for males. Local spatial clustering of high rates was observed, particularly in the eastern provinces. Income dependence on spatial parameters was found to vary by gender. Both spatial and non-spatial analyses outlined specific cross-sections of the Canadian population that may be at high risk for developing additional cardiovascular health issues related to hypertension. Spatial results demonstrated specific health regions that may be in greater need of public health efforts toward promoting cardiovascular fitness that are tailored to particular regional and cross-sectional requirements.

7.1. Introduction

Matters of cardiovascular health remain a prominent concern for public health systems where associated issues of high blood pressure (*HBP*) and heart disease account for large proportions of global burdens of disease, particularly in industrialized nations including Canada where *HBP* is a leading risk for premature death and disability (Campbell et al., 2012). Specifically in Canada, an earlier study by Joffres et al. (1997) identified approximately 4.1 million potentially hypertensive individuals across the country (~20%) with an inordinately high proportion of people unaware of their condition (64% and 19% of men and women respectively). Later research similarly demonstrated that two thirds to three quarters of the Canadian hypertensive population were untreated, which was actually greater than that observed for the United States (Wolf-Maier et al., 2004). One of the most important points related to the prevalence of *HBP* and subsequent heart disease is that many cases would be preventable through healthier lifestyle choices (McGill et al., 2008). An example in the context of dietary concerns is reducing the intake of sodium additives in order to decrease blood pressure which previous researchers (Joffres et al., 2007) have suggested could also reduce annual health care costs associated with current hypertension prevalence by approximately $430 million.

Along with statistical investigation of the influence of demographic factors on *HBP* (e.g., gender and income), the use of spatial techniques for the analysis of population and geographic data present an interesting perspective that may provide alternative insights into myriad research questions in epidemiology (Auchincloss et al., 2012) and demography (Sparks et al., 2013) which can be useful for public health surveillance. Ahmadi et al. (2015) recently applied spatial methods to the analysis of hospitalizations due to myocardial infarction throughout Iran in order to help identify which regions of the country appeared to present “hot spots” or spatially clustered groups of neighboring regions with high rates of hospitalization. This procedure was subsequently applied to the study of myocardial infarction hospitalizations in Canada, which indicated low prevalence clusters in the west and south with high rates clustered in the north and east (Caswell, 2016). The spatial scale of sub-provincial health regions has previously been considered for the exploration of spatial trends among overweight and obesity rates in Canada (Pouliou & Elliott, 2009), similarly indicating low rates clustered in the west and south with hot spots in the north and east, a pattern that emerged for both males and females. There are, of course, many additional determinants of cardiovascular health including socioeconomic factors, and an area’s income level may be associated with spatial trends for specific cross-sections of a population (Guessous et al., 2014). For example, indicators of neighborhood deprivation were much more strongly associated with hypertension among females in Canada compared to their male counterparts (Matheson et al., 2009).

The primary aim of the present study was to explore the non-spatial influence of standard demographic factors on recent *HBP* reporting in Canada including gender, income, and age, as well as potential spatial clustering of *HBP* prevalence throughout the country. Although data were self-reported, the utility of *HBP* rates derived from self-reports has been examined and present a useful means for the study of health determinants (Atwood et al., 2013). The spatial scale of interest, similar to previous research (Pouliou & Elliott, 2009), was that of sub-provincial health regions. Each is defined by a regional health unit and its associated geographic or operational boundaries and may be responsible for various health promotion programs, administering health care services, or other community health roles (Statistics Canada, 2015).

National survey data were employed to study the influence of gender, age, and household income on the occurrence of *HBP*, as well as the spatial trends (i.e., global spatial autocorrelation and local spatial clustering) of age-standardized *HBP* prevalence for males and females overall and within each income quintile.

7.2. Methods

Data from the Canadian Community Health Survey (CCHS) 2014 annual component (Statistics Canada, 2016) were accessed from odesi (http://search1.odesi.ca) through the Data Liberation Initiative (DLI) at Laurentian University for a cross-sectional ecological study of reported *HBP* prevalence throughout the country. The CCHS is a voluntary cross-sectional survey for the collection of health-related data across Canada at the sub-provincial level of health regions that examines respondents 12 years of age and older with the exception of those living on Aboriginal reserves, armed forces, institutionalized persons, and those living in specific areas of Quebec with high-density Inuit populations and small total populations (Région du Nunavik and Région des Terres-Cries-de-la-Baie-James). Altogether this criteria excluded less than 3% of the population within the specified age range (12 years and older) and there were n = 63,522 total respondents available from 2014. However, only those ≥ 20 years of age (n = 57,041 respondents) were examined. Where regions with small total populations (< 20,000) were identified, data were combined according to updated health region aggregation (e.g., Statistics Canada, 2015) or removed from the analysis following previous research (Pouliou & Elliott, 2009). Yukon, Nunavut, and the Northwest Territories were also removed given their relatively small populations and large proportion of culturally unique Inuit peoples (Pouliou & Elliott, 2009). Furthermore, Prince Edward Island (PEI) now disseminates relevant information at the provincial level only (Statistics Canada, 2015) making this data inconsistent with the current spatial scale of interest. Therefore, PEI was excluded from the current study.

A series of statistical weights was also provided in the accessed public use microdata file (PUMF) indicating how many individuals each respondent represented in the relevant population. Weights were summed accordingly for categorical data and rate calculations to more accurately reflect the covered population. Variables of interest included respondents' health region, gender, household income quintile, and age bracket (5-year groups), while the primary variable of interest was derived from CCHS question *CCC_071* which asked whether or not the respondent had high blood pressure (*HBP*), which is commonly defined by blood pressure of 140/90 mm Hg or above (≥ 140 systolic or ≥ 90 diastolic). Note that the term high blood pressure (*HBP*) is deliberately employed throughout the current study as this was the terminology used for the CCHS rather than hypertension. The distribution of *HBP* "Yes" respondents were plotted as histograms for males and females in Figure 32. It should also be noted that the current sample may have overestimated or, more likely, underestimated the actual prevalence of *HBP* given the voluntary nature of the CCHS. The potential likelihood of underestimation is further supported by previous results for a study conducted in Vietnam (Van Minh et al., 2006) which found that 17.4% of hypertensive individuals were unaware of their condition and earlier results from Canada (Joffres et al., 1997) found that 41% were unaware of their high arterial blood pressure. Despite this issue, the CCHS has a history of use for similar studies of hypertension or hypertensive awareness (Joffres et al., 2007; Veenstra, 2013) and correlated health issues (Pouliou & Elliott, 2009).

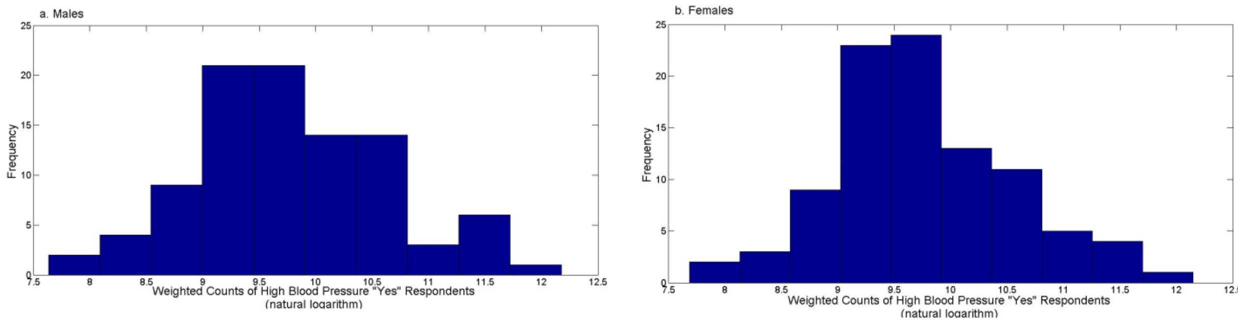

Figure 32: Histograms for distribution of *HBP* “Yes” respondents for (a) males and (b) females

Preliminary non-spatial data analyses employed raw survey responses weighted by the appropriate values computed by Statistics Canada (2016) with the binary response for *HBP* (no/yes) as the dependent measure of interest and categorical independent measures (gender, age in 5-year brackets, and household income quintile). There were n = 56,830 adult participants (≥ 20 years of age) who provided valid responses to all survey items of interest. Although sets of categorical variables (i.e., nominal and ordinal) are often analyzed using log-linear analysis, there is no distinction made between dependent and independent measures for this technique. However, any data assessed with log-linear methods can also be analyzed using logistic regression (binomial or multinomial) given the mathematical relationships between these models which are all essentially generalized linear models. Properly coded dummy variables were created for categorical variables (gender and income) in order to determine non-spatial influence of gender, age, and income on the odds of reporting *HBP* with binary logistic regression analysis (backward conditional variable entry) which follows the logit form:

$$\text{logit}_{p_y} = \log\left(\frac{p_y}{1-p_y}\right) = a + B_1x_1 +, \ldots, +B_ix_i$$

where *a* = constant, *B* = coefficients, *y* = *HBP*, and *x* = independent variables. The exponentiated regression coefficients $exp(\beta_i)$ represent the odds ratio (OR) of *HBP* between group x_i = 1 and group x_i = 0 when other independent variables are controlled at the same level. The model constant *a* is the log of odds for the baseline group with all variables *x* equal to zero (0). Regression analysis was accomplished with SPSS v17 software.

Weighted counts of *HBP* and total population were summed within each gender and age bracket combination for all relevant health regions. Population demographics from the 2006 census table corresponding to 2013 health regions (Statistics Canada, 2013) were downloaded from odesi and exported with Beyond 20/20 v7 software for use as a standard population in further rate calculations. Age standardization procedures were conducted using Excel 2010 software. Age-specific rates of *HBP* responses from the CCHS 2014 were computed per 10,000 within each health region. Next, the fraction of the population within each combination from the 2006 census (standard population) was identified and direct age-standardized rates of *HBP* responses from the 2014 CCHS were obtained as the summed products of the age-specific rates, multiplied by the fraction of the appropriate standard population. This procedure helps minimize the influence of age on prevalence rates according to a standard age structure (Sparks & Sparks, 2010) where we would expect more individuals reporting *HBP* within older age groups. The entire procedure was also conducted for each subgroup combination within each household income quintile. A cartographic shapefile of Canadian health regions as of 2013 was accessed from Statistics Canada (2013). Relevant regions were merged according to updated boundaries and aggregation (Statistics Canada, 2015) using Quantum GIS v2.12.3 software and data were merged with the shapefile using GeoDa v1.6.7 software for exploratory spatial data analysis (ESDA). Those regions with missing data were subsequently removed from the shapefile; the final number of health regions for investigation was n = 95.

For ESDA procedures, a spatial weight matrix (*w*) was first constructed. This matrix is used to quantify spatial relationships among geographic data (i.e., health regions) where each point (row and column combination *i* and *j*) indicates the particular weight w_{ij} for the associated features which are typically binary (i.e., 0 = non-neighboring features, 1 = neighboring features). The five closest regions as indicated by their relative distance between centroids were identified as neighbors $w_{ij} = 1$ and all others were $w_{ij} = 0$. The diagonal elements will always be $w_{ij} = 0$ (Zhou & Lin, 2008). However, the spatial weights can also be row standardized (i.e., each weight is divided by the sum of its row) to better account for uneven regional areas and potentially biased distribution due to sampling or aggregation (Anselin, 1994). Since the removal of certain regions from the source shapefile caused non-contiguities, a distance-based weighting scheme was selected based on preliminary histogram testing with contiguity rules (*k*-nearest neighbors with $k = 5$) rather than the more typical contiguity-based rook or queen spatial weights. This method measures the distance between the centroid (approximate center) of a region to the centroids of all other regions and selects the five nearest as neighbors. Preliminary ESDA examined global spatial autocorrelation using the global Moran's *I* test (Moran, 1950). Values of *I* range from -1 to +1 where zero indicates a random spatial pattern of the data, negative values suggest that high and low values are very widely dispersed, and positive values reflect positive spatial autocorrelation such that regions with high values cluster together and those with low values also occur in close proximity to each other. The index of global spatial autocorrelation derived through this procedure is computed according to:

$$I = \frac{\mathrm{n}}{\sum_i \sum_j w_{ij}} \cdot \frac{\sum_i \sum_j w_{ij}(y_i - \mu)(y_j - \mu)}{\sum_i (y_i - \mu)^2}$$

where n = number of spatial units, y = variable of interest, and μ = average of y. Note that variables are standardized (z-scores) prior to calculation in order to avoid unit dependence. The subsequent value of I itself can be converted to a standardized z-score through Monte Carlo simulation to produce an empirical distribution for comparison and probability estimation. For the current study, 999 random data permutations were used to test the null hypothesis in each case with $p < 0.05$ considered statistically significant. However, an inherent limitation of techniques for global spatial autocorrelation is that results cannot be used to determine where spatial dependence might be occurring. Local indicators of spatial association (LISA) are generally employed for helping to determine where spatial associations might be present, often through calculation of local Moran's I_i values (Anselin, 1995). Since spatial weights in the current study were derived from distance rather than contiguity, it was instead decided to use Getis and Ord's (1992; Ord & Getis, 1995) local G_i statistics of spatial clustering for assessment similar to the LISA technique as this method uses centroid-based distances and does not include additional spatial parameters beyond local clustering. Local G_i values measure the association that is present among a concentration of region centroids (Getis & Ord, 1992) originally calculated using traditional binary spatial weights with:

$$G_i(d) = \frac{\sum_j w_{ij}(d) y_j}{\sum_j y_j}$$

where d = distance (note that distance in the current study was not a defined value but instead used to identify the k = 5 relatively nearest neighbors). However, the authors updated this method to allow for row standardized weights with additional considerations (Ord & Getis, 1995) that can be applied to normally distributed or skewed data. Positive values of G_i significantly larger than zero indicate spatial clustering of high rates among the k = 5 nearest neighbors, while negative values lower than zero reflect clustering of low rates. Similar to global Moran's *I* testing, probability estimates for local G_i results were derived from Monte Carlo simulation with 999 random data permutations in the current study with $p < 0.05$ considered statistically significant, although sensitivity was examined with results filtered for $p < 0.01$ to better indicate central sites of interest. It should also be noted that there are two variants of local *G* where standard G_i excludes the value at point *i* while the G_i^* variant includes *i* in the summation steps (Ord & Getis, 1995). The latter G_i^* was employed in the present study since this variant is generally applied to exploration of spatial clustering rather than a diffusive process. However, only those groups which demonstrated significant global spatial autocorrelation were further assessed for local clustering (Gruebner et al., 2011). Finally, the ratio of individuals within lower household income quintiles (1 and 2) to the numbers of people from middle to upper incomes (3 to 5) was computed as a crude estimate of income disparity and assessed using bivariate Moran's *I* with the spatially lagged prevalence of reported *HBP* from neighboring health regions in order to better determine potential spatial relationships between variables (Gruebner et al., 2011).

All ESDA techniques were assessed using GeoDa software. Standard descriptive statistics and inferential procedures for age-standardized rates were conducted using SPSS v17 software including distribution testing with visual techniques (histogram and Q-Q plot) along with Shapiro-Wilks tests. Since many variables, such as natural logarithms, tended not to display normal distributions even after data transformation, nonparametric techniques were employed for paired comparisons. These included Friedman tests for assessing multiple repeated measures and Wilcoxon signed rank tests for post hoc comparisons with false discovery rate (FDR) linear step-up probability correction (Benjamini & Hochberg, 1995) applied with Matlab v7.12 software to adjust for multiple testing between income quintiles at $\alpha = 0.05$. It should be noted that when data are normally distributed, the nonparametric Wilcoxon method only presents ~5% reduced statistical power compared to standard *t*-tests and that the power exceeds that of parametric counterparts when data are not normally distributed. Comparisons were examined between males and females and between income quintiles within gender. Nonparametric Spearman (ρ) correlations were also used for investigation of non-spatial linear relationships. Spatial trends were investigated for total male and female rates of reported *HBP* as well as for each income quintile within each gender where income groups (total household income from all sources in Canadian dollars $) included (1) < $20,000 (n = 6,473), (2) $20,000 to $39,999 (n = 13,658), (3) $40,000 to $59,999 (n = 11,564), (4) $60,000 to $79,999 (n = 9,120), and (5) ≥ $80,000 (n = 22,641). Note that all presented n values are before application of statistical weights.

7.3. Results

The initial analyses of non-spatial categorical data employed binary logistic regression with dummy coded independent variables and were conducted using weighted survey responses. All predictors entered the model with significant ($p < 0.001$) OR values for which the odds of *HBP* were 1.292 greater for males compared to females and an increase in the odds of *HBP* was observed with increasing age (OR = 1.424). A linear increase in the odds of *HBP* for income quintiles 2 to 4 compared to quintile 1 was observed while decreased odds of *HBP* were revealed for the highest income quintile (5) compared to the lowest (1). All model coefficients, OR values, and their 95% confidence intervals (CI) are provided in Table 12.

Table 12: Model coefficients (*B*) and odds ratios (OR) with their 95% confidence intervals (CI) for logistic regression of high blood pressure (*HBP*)

Independent Variable	***B***	**OR**	**CI 95%**
Model Constant	-5.158	0.006*	-
Males (vs. Females)	0.256	1.292	1.289 to 1.295
Age (5-year brackets)	0.353	1.424	1.423 to 1.425
Income 2 (vs. Income 1)	0.058	1.059	1.055 to 1.064
Income 3 (vs. Income 1)	0.014	1.014	1.009 to 1.018
Income 4 (vs. Income 1)	0.030	1.031	1.026 to 1.036
Income 5 (vs. Income 1)	-0.172	0.842	0.839 to 0.846

*baseline odds

After calculation of age-standardized rates for reported *HBP* in each group within each health region, descriptive statistics were computed (Table 13) with males presenting higher average prevalence (mean of 2056.150 per 10,000) compared to females (mean of 1902.807 per 10,000). Total rates for males and females were compared using Wilcoxon signed rank testing which indicated that the prevalence of *HBP* among males tended to be significantly higher than that of females (z = 2.743, p = 0.006, es = 0.199). A preliminary Friedman test for multiple paired comparisons was conducted for prevalence among males within each household income quintile which suggested a significant overall difference ($\chi^2_{(4)}$ = 10.922, p = 0.027, ϕ = 0.152) where the mean rank order from lowest to highest prevalence was lowest income (1), highest income (5), second highest (4), middle income (3), and second lowest (2) as initially shown by descriptive statistics (Table 13). A series of Wilcoxon signed rank tests between each pair of income brackets was conducted. Although four results were initially significant at $p < 0.05$, only a single test remained marginally significant ($z = 2.725$, $p = 0.006$, $es = 0.198$) after FDR probability correction ($p = 0.06$) for which *HBP* prevalence among males was higher in the second lowest household income quintile (2) compared to the highest income (5). All male results are shown in Figure 33. Results from Friedman testing of female rates also indicated a significant difference of *HBP* prevalence between income quintiles ($\chi^2_{(4)} = 46.543$, $p < 0.001$, $\phi = 0.313$) with rates following a linear trend in which the highest prevalence was observed for the lowest income (1) and the lowest prevalence was observed for the highest income (5) as shown by preliminary descriptive statistics (Table 13), a linearity that was not present for males. Wilcoxon signed rank tests were again employed for *post hoc* comparisons and all significant results ($p < 0.05$) remained significant after FDR probability correction which determined the only groups that were not significantly different from each other were income levels 1 and 2, as well as income levels 2 and 3 where the magnitude of the difference among the other brackets increased according to the degree of income disparity and included the following results: income 1 and 3 ($z = 2.223$, $p = 0.026$, $es = 0.161$), income 1 and 4 ($z = 4.016$, $p < 0.001$, $es = 0.291$), income 1 and 5 ($z = 5.234$, $p < 0.001$, $es = 0.380$), income 2 and 4 ($z = 3.883$, $p < 0.001$, $es = 0.282$), income 2 and 5 ($z = 5.939$, $p < 0.001$, $es = 0.431$), income 3 and 4 ($z = 2.346$, $p = 0.019$, $es = 0.170$), income 3 and 5 ($z = 4.670$, $p < 0.001$, $es = 0.339$), and income 4 and 5 ($z = 2.261$, $p = 0.024$, $es = 0.164$). All female results are visualized in Figure 34.

Table 13: Descriptive statistics for age-standardized 2014 rates of reported high blood pressure (*HBP*) per 10,000 across n = 95 health regions and reported by household income quintile within each gender; includes mean, median, standard deviation (st. dev.), minimum (min.), and maximum (max.)

Group	Mean	Median	St. Dev.	Min.	Max.
Males (total)	2056.150	1998.819	517.703	1077.123	3330.269
Females (total)	1902.807	1787.544	497.461	1023.670	3422.097
Males					
(1) < $20,000	1810.448	1772.834	915.122	211.325	4186.754
(2) $20,000 to $39,999	2126.960	2030.86	824.723	674.411	4721.327
(3) $40,000 to 59,999	2064.931	2059.674	757.785	605.410	4752.710
(4) $60,000 to $79,999	1947.741	1860.381	893.850	100.346	4287.360
(5) ≥ $80,000	1841.307	1861.634	622.513	379.742	3370.581
Females					
(1) < $20,000	2103.798	1918.446	953.278	542.204	4737.650
(2) $20,000 to $39,999	2037.357	2026.384	661.178	659.794	4131.420
(3) $40,000 to 59,999	1861.0	1818.748	667.720	552.773	3492.797
(4) $60,000 to $79,999	1630.413	1569.266	671.626	146.902	3310.825
(5) ≥ $80,000	1468.086	1347.151	560.968	34.598	3047.183

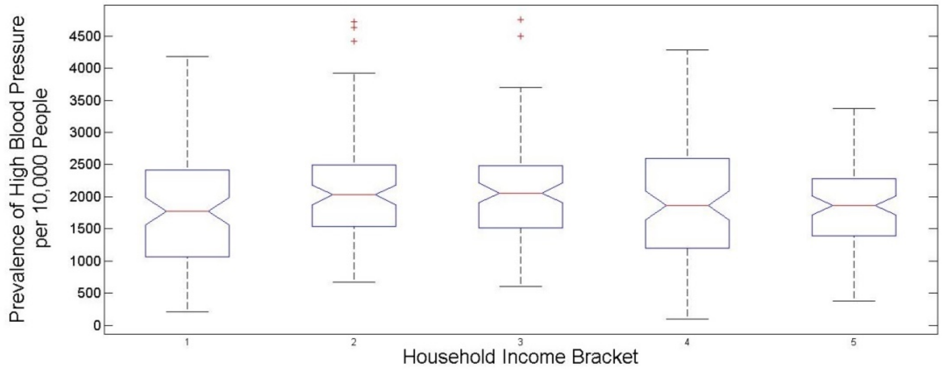

Figure 33: Notched box-and-whisker plot of high blood pressure (*HBP*) prevalence for males by household income bracket (quintile); notched areas of boxes indicate medians with 95% confidence intervals, whiskers indicate minimum and maximum values, and '+' signs indicate outliers

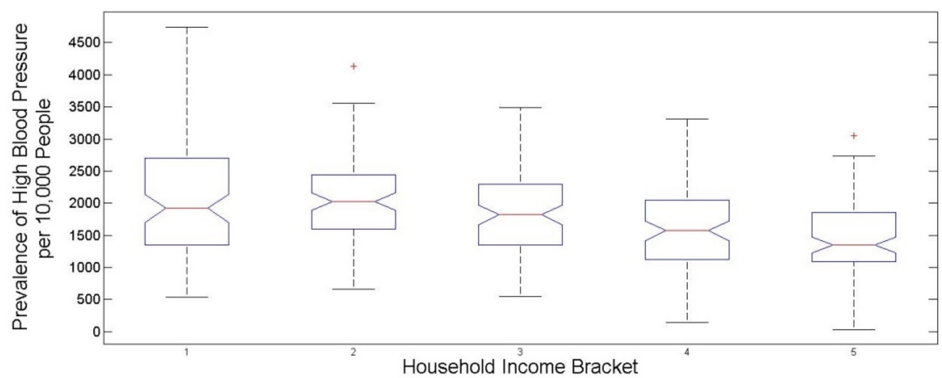

Figure 34: Notched box-and-whisker plot of high blood pressure (HBP) prevalence for females by household income bracket (quintile); notched areas of boxes indicate medians with 95% confidence intervals, whiskers indicate minimum and maximum values, and '+' signs indicate outliers

Total rates for both males and females were each plotted with choropleth maps according to quartile (Figure 35 and Figure 36). Qualitative inspection suggested that lower prevalence of reported *HBP* tended to be found within the western provinces with an uneven gradient moving east. Small pockets of higher rates were observed for central provinces while increasing prevalence was more apparent within the eastern provinces. Potential disparities between north and south were not as immediately apparent upon visual inspection. Application of global Moran's *I* testing demonstrated statistically significant spatial autocorrelation for total prevalence among both males and females, although the associated coefficient was much stronger for females (Table 14). Within each household income quintile, only the two lowest income levels revealed significant spatial autocorrelation for males, while all female groups were spatially autocorrelated with the exception of the middle income quintile (Table 14). The ratio of lower (1 and 2) to higher income (3 to 5) populations of each health region were not found to be correlated with reported *HBP* prevalence for males, although a moderate significant linear relationship was observed for female prevalence with regional income ratio ($\rho = 0.491$, $p < 0.001$). Bivariate implementation of Moran's *I* testing was applied to total male and female regional prevalence with associated regional income ratios to estimate spatial correlations with neighboring rates of *HBP*. Significant results were identified for both males ($I = 0.160$, $z = 3.410$, $p < 0.001$) and females ($I = 0.255$, $z = 5.543$, $p < 0.001$).

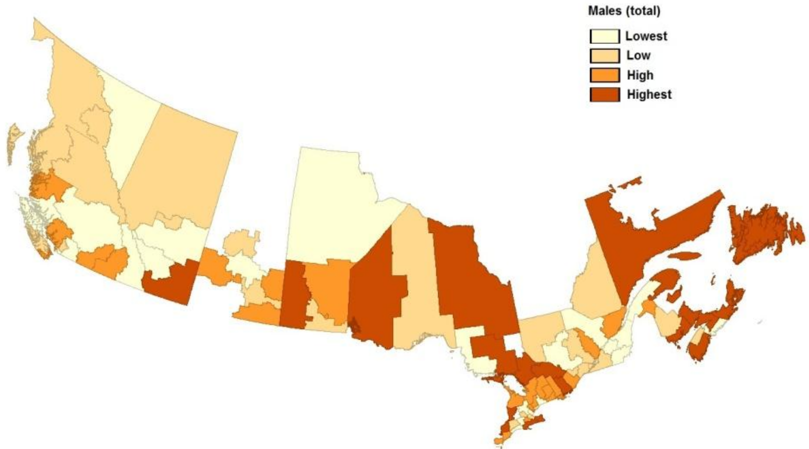

Figure 35: Choropleth map of reported high blood pressure (*HBP*) prevalence among males in 2014, shaded by quartile

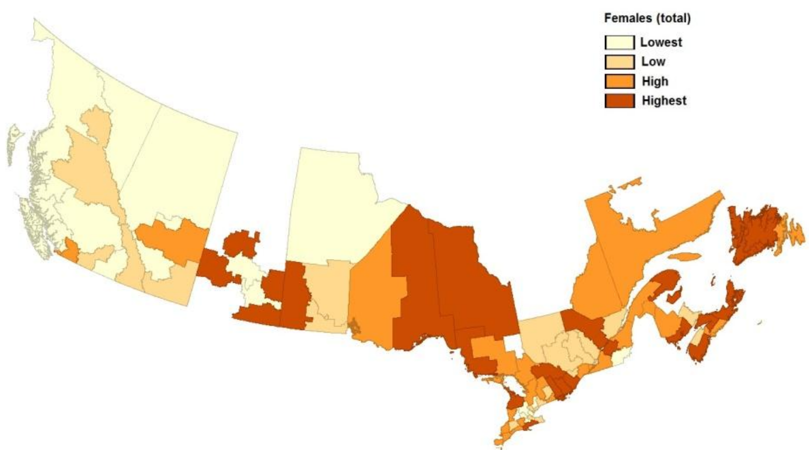

Figure 36: Choropleth map of reported high blood pressure (*HBP*) prevalence among females in 2014, shaded by quartile

Table 14: Results from all Moran's *I* tests for global spatial autocorrelation with *z*-score derived from Monte Carlo simulation (999 permutations) and associated two-tailed probability values (n.s. = not significant, $p > 0.05$)

Group	***I***	***z***	***p***
Males (total)	0.115	2.107	0.036
Females (total)	0.347	6.139	$8.311 \cdot 10^{-10}$
Males			
(1) < $20,000	0.183	3.348	$8.140 \cdot 10^{-4}$
(2) $20,000 to $39,999	0.133	2.436	0.014
(3) $40,000 to 59,999	0.052	1.093	n.s.
(4) $60,000 to $79,999	-0.064	-0.948	n.s.
(5) ≥ $80,000	-0.050	-0.697	n.s.
Females			
(1) < $20,000	0.280	5.117	$3.106 \cdot 10^{-7}$
(2) $20,000 to $39,999	0.107	2.055	0.040
(3) $40,000 to 59,999	0.012	0.356	n.s.
(4) $60,000 to $79,999	0.123	2.519	0.012
(5) ≥ $80,000	0.118	2.298	0.022

Initial G_i^* statistics for local spatial clustering revealed cold spots of low reported *HBP* rates in British Columbia for both males and females, as well as in Alberta and southern Ontario for females only. Conversely, hot spots of high rates were clustered in western Ontario, New Brunswick, Nova Scotia, Newfoundland, and Quebec for males (Figure 37) and in Saskatchewan, New Brunswick, Newfoundland, and Quebec for females (Figure 38). After checking sensitivity of results at $p < 0.01$, health regions with the strongest clustering association included hot spots of high rates for males in New Brunswick (1302 and 1303) and Newfoundland, particularly region 1011, as well as for Nova Scotia for the lower income quintiles with the most consistent contribution from region 1269, as well as for Quebec in region 2411. All individual health regions associated with significant spatial clustering for both low and high rates of reported *HBP* for males overall and by (significantly spatially autocorrelated) household income quintile are provided in Table 15. Clustered hot spot regions for females that remained significant at $p < 0.01$ and were most consistently identified across subgroups included health regions of Newfoundland (1011, 1012, and 1013) and areas of Saskatchewan, especially regions 4704 and 4706. The clustered health regions after checking sensitivity of results are provided for females overall and by income quintile in Table 16.

Table 15: Health regions (four-digit codes) that displayed the strongest significant local spatial clustering for male 2014 total rates of reported high blood pressure (*HBP*) at $p < 0.01$ within each investigated province (AB = Alberta, BC = British Columbia, MB = Manitoba, NB = New Brunswick, NL = Newfoundland, NS = Nova Scotia, ON = Ontario, QC = Quebec, and SK = Saskatchewan) with indication of high or low prevalence clustering

	AB	BC	MB	NB	NL	NS	ON	QC	SK

	AB	BC	MB	NB	NL	NS	ON	QC	SK
Males (total)	-	5912, 5913, 5914, 5921, 5952 (low)	-	1303 (high)	1011 (high)	-	-	2411 (high)	-
Income (1)	-	-	-	1302 (high)	1011, 1013 (high)	1269 (high)	3551 (low)	-	-
Income (2)	5952 (low)	-	-	1302 (high)	-	1223, 1258, 1269 (high)	3534 (low), 3562 (high)	2403, 2412 (low), 2411 (high)	-

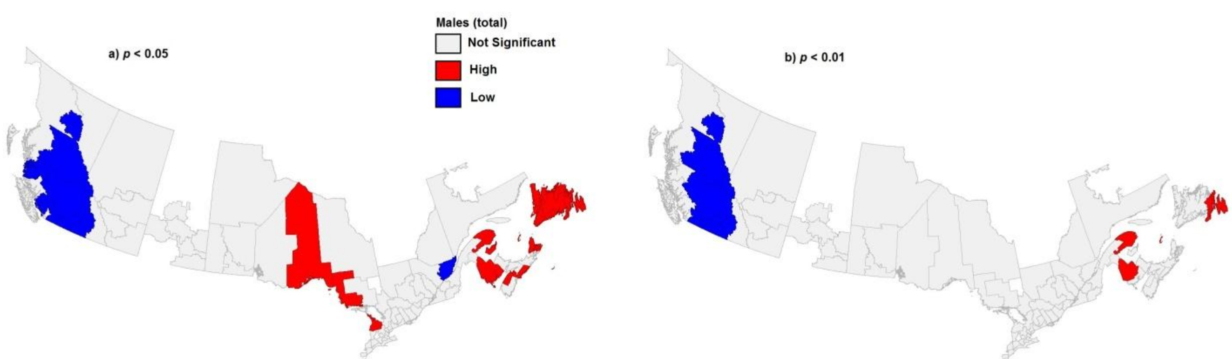

Figure 37: Spatial clusters (local G_i^*) for low or high prevalence of high blood pressure (*HBP*) in 2014 among males at (a) $p < 0.05$ and (b) $p < 0.01$

Table 16: Health regions (four-digit codes) that displayed the strongest significant local spatial clustering for female 2014 total rates of reported high blood pressure (*HBP*) at $p < 0.01$ within each investigated province (AB = Alberta, BC = British Columbia, MB = Manitoba, NB = New Brunswick, NL = Newfoundland, NS = Nova Scotia, ON = Ontario, QC = Quebec, and SK = Saskatchewan) with indication of high or low prevalence clustering

	AB	BC	MB	NB	NL	NS	ON	QC	SK
Females (total)	-	5921, 5922, 5923, 5931, 5932, 5933, 5941, 5942, 5943, 5951 (low)	-	-	1011, 1012, 1013 (high)	-	3537 (low)	2411 (high)	4704, 4706 (high)
Income (1)	-	5921, 5952 (low)	-	-	1012 (high)	-	3530, 3539, 3547, 3553, 3570 (low), 3540 (high)	-	-
Income (2)	-	5922, 5923, 5932, 5933, 5941, 5942, 5943, 5952 (low)	-	-	-	-	-	-	4704, 4706 (high)
Income (4)	-	5942, 5951 (low)	-	-	1012 (high)	-	-	-	-
Income (5)	-	-	-	-	1011, 1013 (high)	-	-	2412 (low)	4704, 4705, 4706 (high)

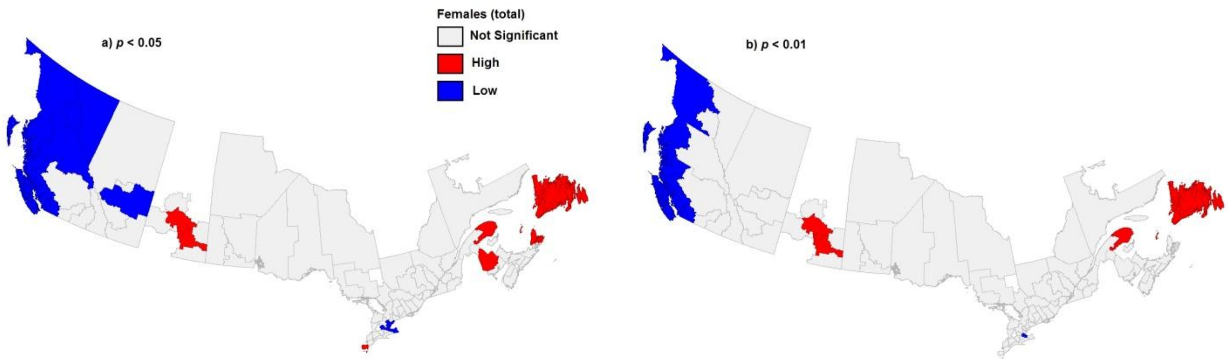

Figure 38: Spatial clusters (local G_i^*) for low or high prevalence of high blood pressure (*HBP*) in 2014 among females at (a) $p < 0.05$ and (b) $p < 0.01$

7.4. Discussion

From the initial non-spatial analysis of raw categorical response data, a number of expected demographic trends emerged including increased odds of reporting *HBP* for males by ~1.3 compared to females in Canada, along with a fairly straightforward increase in the odds of reporting *HBP* with age (OR = 1.424). Conversely, the second through fourth lowest income quintiles (2 to 4) actually had small but statistically significant increases in odds of *HBP* compared to the lowest income range (OR = 1.014 to 1.059), while the highest income quintile (5) showed decreased odds of *HBP* compared to the lowest income group (OR = 0.842). That the influence of age on the prevalence of self-reported *HBP* was the strongest statistical effect observed in the preliminary non-spatial analysis was not surprising considering the general decline in health typically observed with aging and, in the particular context of cardiovascular health, the age-related development of arterial stiffness that may contribute to hypertension (McEniery et al., 2007).

Some authors (Johnston et al., 2009) have criticized the use of self-reported measures of *HBP* for investigation of an income gradient as they found no evidence of such a relationship after analysis compared to the health disparity observed when using objective measurements of hypertension. Kaplan et al. (2010) also identified an even distribution of self-reported *HBP* across income bands in Canada. Although the income quintile effects from analysis of categorical data in the present study were relatively small, the within-subjects analyses for reported *HBP* prevalence after age standardization at the health region level also identified clear differences by income. Along with the significant increase in *HBP* prevalence for males compared to females, the lowest relative rates of *HBP* for males were observed for the lowest income quintile. Conversely, the lowest ranges of household income demonstrated the highest *HBP* prevalence among females. This is actually consistent with previous research which found a greater impact of neighborhood deprivation measures on female hypertension compared to males (Matheson et al., 2009) as well as a greater influence of socioeconomic factors on female hypertension compared to males (Leng et al., 2015; Loucks et al., 2007; Van Minh et al., 2006). Furthermore, the decrease in *HBP* with increasing income was found to be linear for females while prevalence for males was nonlinear, with the highest rates of reported *HBP* observed for income quintiles 2 and 3.

Spatial analyses also revealed a number of discrepancies between household income ranges and between males and females with age-standardized rates of *HBP*. Total rates for males and females demonstrated statistically significant global spatial autocorrelation that was positive in both cases although the associated effect size was much greater for females (standardized difference of z ~4), suggesting stronger overall spatial associations compared to males. After computing age-standardized rates for each income quintile, only the two lowest ranges (1 and 2) were spatially autocorrelated for males whereas the spatial distribution of reported *HBP* prevalence was random for middle and upper income households. Although further research is required, this could be an indicator of the association between income and housing mobility with subsequent indicators of public health (Acevedo-Garcia et al., 2004; Dohmen, 2005). For females, however, only the middle income quintile (3) was not spatially autocorrelated which again appears to reflect the greater contribution of place of residence to *HBP* for females compared to males (Matheson et al., 2009). Consistent with this conclusion, non-spatial linear correlation between *HBP* prevalence and income ratio for each health region was statistically significant for females but not for males, although the spatial correlation between income ratio and neighboring *HBP* prevalence was significant in both cases. Previous results from the USA also indicated that hourly-employment ("blue-collar work") was related to increased risk of *HBP* for females only (Clougherty et al., 2011). Further evidence for the varying influence of interactions between gender and socioeconomic factors with hypertension has been observed in Vietnam (Van Minh et al., 2006) which indicated that lower education and occupational status, as well as higher income was associated with increased *HBP* in males. Conversely, lower occupational status and income were associated with *HBP* for females (Van Minh et al., 2006). In a study of metabolic syndrome, which includes elevated blood pressure, Loucks et al. (2007) found that a low (< 1) poverty to income ratio was related to *HBP* in females but not men, with a similar influence of socioeconomic position on *HBP* for females only. A meta-analysis also revealed that an increased risk of *HBP* associated with low socioeconomic status was stronger for females than males, particularly in high-income nations (Leng et al., 2015).

With regard to the local features of spatial clustering that were observed, both males and females showed consistent cold spots of low *HBP* prevalence in the western province of British Columbia, with hot spots of high rates in the east of the country, particularly in Newfoundland. Central health regions within consistent hot spot clusters were specifically revealed for the Eastern Regional Integrated Health Authority (Newfoundland) for both genders. Other central clustering sites for males consistently included Zone 2 or the Saint John area (New Brunswick), Région de la Gaspésie-Îles-de-la-Madeleine (Quebec), and the former Capital District Health Authority (Nova Scotia). The additional hot spot centers for females included other sites in Newfoundland such as the Central Regional Integrated Health Authority and the Western Regional Integrated Health Authority, as well as those in Saskatchewan, especially the Regina Qu'Appelle Regional Health Authority and the Saskatoon Regional Health Authority. These regional variations according to larger provincial boundaries were also consistent with previous research examining spatial clustering of overweight and obesity among Canadian health regions with similarly lower rates in the west and hot spots of clustered high rates in the north-east (Pouliou & Elliott, 2009).

One of the main limitations of this and similar spatial studies is the modifiable areal unit problem (MAUP) as originally outlined by Gehlke and Biehl (1934) from which it has been recognized that the level of aggregation (i.e., spatial scale) chosen for analysis can influence the observed results. While there is no universally satisfactory solution to the MAUP (Horner & Murray, 2002; King, 1979; Openshaw, 1983), the data in the present study were acquired for the smallest spatial scale available and should nonetheless appropriately reflect the specific context of this scale. Furthermore, the level of health regions has been considered important for spatial analyses in previous research (Pouliou & Elliott, 2009), particularly for general public health surveillance. Additionally, there were a number of regions removed from the analysis according to the various exclusion criteria previously discussed. While the excluded regions tended to coincide with those removed in earlier research (Pouliou & Elliott, 2009), an additional potential issue for the current study was the removal of the province of PEI. Although this was not done in similar studies, earlier work in this area was conducted with data obtained during a time when PEI still disseminated census and survey data at the regional level, whereas more recent data such as that employed in the current study are now only reported at the provincial level. As previously noted, it was felt that this was inconsistent with the spatial scale of interest. An additional limitation does not necessarily negatively impact the present results, but may affect the potential implementation of future analyses. Since *k*-nearest neighbour distance-based spatial weights were used in the current study, these data would be incompatible with many spatial statistical techniques beyond ESDA, including various forms of spatial regression, which tend to rely on symmetrical spatial weight matrices for accurate results. If the cartographic shapefile were to be further edited and neighborless regions joined in an appropriate manner based on a standard recommendation, then contiguity-based weights could be accommodated. However, this was beyond the scope of the present study. Finally, although other local spatial methods such as LISA are capable of providing further insight into spatial data properties including identification of spatial outliers (i.e., low rates surrounded by high rates or vice versa) (Anselin, 1995), the current interest was in distance-based local clustering.

The present study provides a number of insights into more recent trends in Canadian prevalence of (self-reported) *HBP* which reflect contributions from demographic factors such as gender and age, as well as household income differences that differed by gender when controlling for age. The spatial results also presented a more novel account of recent Canadian *HBP* from a geographic perspective which indicated a number of regional hot spots for high rates of *HBP* reporting, particularly in Newfoundland, with additional clusters more dispersed in the east of the country for males and localized to Newfoundland and Saskatchewan for females. The use of spatial methods provides further insight for trends or other statistical relationships in the population sciences, especially epidemiology (Auchincloss et al., 2012), and should continue to be included as a tool for general public health surveillance. In particular, the present study suggests that specific regional health units in Canada, particularly in the North Atlantic, should provide information on hypertensive counselling to their administered populations with an emphasis on those in lower socioeconomic status. In light of these results and those suggesting an alarming rate of Canadian individuals unaware of their hypertensive condition (Joffres et al., 1997), information regarding the importance of blood pressure monitoring by a health professional can be utilized in a context most relevant to the at-risk populations identified.

References

Acevedo-Garcia, D., Osypuk, T. L., Werbel, R. E., Meara, E. R., Cutler, D. M., Berkman, L. F. (2004). Does housing mobility policy improve health? *Housing Policy Debate*, 15(1): 49-98.

Ahmadi, A., Soori, H., Mehrabi, Y., & Etemad, K. (2015). Spatial analysis of myocardial infarction in Iran: National report from the Iranian myocardial infarction registry. *Journal of Reseach in Medical Sciences*, 20(5): 434-439.

Anselin, L. (1994). Exploratory spatial data analysis and geographic information systems. In: Longley, P., Brooks, S., Macmillan, B., & McDonnell, R. (eds.) *Geocomputation: A Primer* (pp. 77-94). Wiley: New York.

Anselin, L. (1995). Local indicators of spatial association – LISA. *Geographical Analysis*, 27: 93-115.

Atwood, K. M., Robitaille, C. J., Reimer, K., Dai, S., Johansen, H. L., & Smith, M. J. (2013). Comparison of diagnosed, self-reported, and physically-measured hypertension in Canada. *Canadian Journal of Cardiology*, 29(5): 606-612.

Auchincloss, A. H., Gebreab, S. Y., Mair, C., & Diez Roux, A. V. (2012). A review of spatial methods in epidemiology, 2000-2010. *Annual Review of Public Health*, 33: 107-122.

Benjamini, Y., & Hochberg, Y. (1995). Controlling the false discovery rate: A practical and powerful approach to multiple testing. *Journal of the Royal Statistical Society*, 57: 289-300.

Campbell, N., Young, E. R., Drouin, D., Legowski, B., Adams, M. A., Farrell, J., Kaczorowski, J., Lewanczuk, R., Lum-Kwong, M. M., & Tobe, S. (2012). A framework for discussion on how to improve prevention, management, and control of hypertension in Canada. *Canadian Journal of Cardiology*, 28(3): 262-269.

Caswell, J. M. (2016). Exploring spatial trends in Canadian incidence of hospitalization due to myocardial infarction with additional determinants of health. *Public Health*, in press.

Clougherty, J. E., Eisen, E. A., Slade, M. D., Kawachi, I., & Cullen, M. R. (2011). Gender and sex differences in job status and hypertension. *Occupational and Environmental Medicine*, 68: 16-23.

Dohmen, T. J. (2005). Housing, mobility, and unemployment. *Regional Science and Urban Economics*, 35(3): 305-325.

Gehlke, C. E., & Biehl, K. (1934). Certain effects of grouping upon the size of the correlation coefficient in census tract material. *Journal of the American Statistical Association*, 29(185A): 169-170.

Getis, A., & Ord, J. K. (1992). The analysis of spatial association by use of distance statistics. *Geographical Analysis*, 24(3): 189-206.

Gruebner, O., Khan, M. M. H., Lautenbach, S., Müller, D., Kraemer, A., Lakes, T., & Hostert, P. (2011). A spatial epidemiological analysis of self-rated mental health status in the slums of Dhaka. *International Journal of Health Geographics*, 10(36).

Guessous, I., Joost, S., Jeannot, E., Theler, J.-M., Mahler, P., Gaspoz, J.-M., & GIRAPH Group (2014). A comparison of the spatial dependence of body mass index among adults and children in a Swiss general population. *Nutrition and Diabetes*, 4(e111).

Horner, M. W., & Murray, A. T. (2002). Excess commuting and the modifiable areal unit problem. *Urban Studies*, 39(1): 131-139.

Joffres, M. R., Campbell, N. R. C., Manns, B., & Tu, K. (2007). Estimate of the benefits of a population-based reduction in dietary sodium additives on hypertension and its related health care costs in Canada. *Canadian Journal of Cardiology*, 23(6): 437-443.

Joffres, M. R., Ghadirian, P., Fodor, J. G., Petrasovits, A., Chockalingam, A., & Hamet, P. (1997). Awareness, treatment, and control of hypertension in Canada. *American Journal of Hypertension*, 10(10): 1097-1102.

Johnston, D. W., Propper, C., & Shields, M. A. (2009). Comparing subjective and objective measures of health: Evidence from hypertension for the income/health gradient. *Journal of Health Economics*, 28(3): 540-552.

Kaplan, M. S., Huguet, N., Feeny, D. H., & McFarland, B. H. (2010). Self-reported hypertension prevalence and income among older adults in Canada and the United States. *Social Science and Medicine*, 70(6): 844-849.

King, P. E. (1979). Problems of spatial analysis in geographical epidemiology. *Social Science and Medicine*, 13D: 249-252.

Leng, B., Jin, Y., Li, G., Chen, L., & Jin, N. (2015). Socioeconomic status and hypertension: A meta-analysis. *Journal of Hypertension*, 33(2): 221-229.

Loucks, E. B., Rehkopf, D. H., Thurston, R. C., & Kawachi, I. (2007). Socioeconomic disparities in metabolic syndrome differ by gender: Evidence from NHANES III. *Annals of Epidemiology*, 17(1): 19-26.

Matheson, F. I., White, H. L., Moineddin, R., Dunn, J. R., & Glazier, R. H. (2009). Neighbourhood chronic stress and gender inequalities in hypertension among Canadian adults: A multilevel analysis. *Journal of Epidemiology and Community Health*, jech-2008.

McEniery, C. M., Wilkinson, I. B., & Avolio, A. P. (2007). Age, hypertension and arterial function. *Clinical and Experimental Pharmacology and Physiology*, 34(7): 665-671.

McGill, H. C., McMahan, C. A., & Gidding, S. S. (2008). Preventing heart disease in the 21st century: Implications of the Pathobiological Determinants of Atherosclerosis in Youth (PDAY) study. *Circulation*, 117(9): 1216-1227.

Moran, P. A. P. (1950). Notes on continuous stochastic phenomena. *Biometrika*, 37(1): 17-23.

Openshaw, S. (1983). *The Modifiable Areal Unit Problem*. GeoBooks: Norwick.

Ord, J. K., & Getis, A. (1995). Local spatial autocorrelation statistics: Distributional issues and an application. *Geographical Analysis*, 27(4): 286-306.

Pouliou, T., & Elliott, S. J. (2009). An exploratory spatial analysis of overweight and obesity in Canada. *Preventive Medicine*, 48(4): 362-367.

Sparks, P. J., & Sparks, C. S. (2010). An application of spatially autoregressive models to the study of US county mortality rates. *Population, Space and Place,* 16: 465-481.

Sparks, P. J., Sparks, C. S., & Campbell, J. J. A. (2013). Poverty segregation in nonmetro counties: A spatial exploration of segregation patterns in the US. *Spatial Demography*, 1(2): 162-177.

Statistics Canada. (2013). *Health Regions: Boundaries and Correspondence with Census Geography, 2013 (hreg-82F0082-E-2013)*. Ottawa, ON.

Statistics Canada. (2015). *Summary of Changes to Health Region Codes, Names and Boundaries, 2011 and 2013*. Retrieved from http://www.statcan.gc.ca/pub/82-402-x/2013003/regions/hrt7e-eng.htm

Statistics Canada. (2016). *Canadian Community Health Survey, 2014: Annual Component (cchs-82M0013-E-2014-Annual-component)*. Ottawa, ON.

Van Minh, H., Byass, P., Chuc, N. T. K., & Wall, S. (2006). Gender differences in prevalence and socioeconomic determinants of hypertension: Findings from the WHO STEPs survey in a rural community of Vietnam. *Journal of Human Hypertension*, 20: 109-115.

Veenstra, G. (2013). Race, gender, class, sexuality (RGCS) and hypertension. *Social Science and Medicine*, 89: 16-24.

Wolf-Maier, K., Cooper, R. S., Kramer, H., Banegas, J. R., Giampaoli, S., Joffres, M. R., Poulter, N., Primatesta, P., Stegmayr, B., & Thamm, M. (2004). Hypertension treatment and control in five European countries, Canada, and the United States. *Hypertension*, 43: 10-17.

Zhou, X., & Lin, H. (2008). Spatial weights matrix. In *Encyclopedia of GIS* (pp. 1113). Springer US.

Chapter 8 – Regional Hypertension among Older Adult Canadians and Association with Education: An Ecological Study

8. Abstract

A cross-sectional, ecological study was conducted to explore the potential role of socioeconomic factors on self-reported high blood pressure (i.e., hypertension) among older adult Canadians (≥ 65 years of age) at the health region scale from 2014. After controlling for additional determinants of health, linear regression analyses demonstrated a significant negative relationship between regional proportions of hypertension and the ratio of older adults with a high school diploma or higher to those without a secondary education. Although variables including overweight or obesity and heavy drinking also contributed positively to regional hypertension proportions for older adult females, only education was statistically significant for older adult males after relevant adjustments. Generalized estimating equations were used to assess the composite dataset of both genders combined which similarly indicated significant correlations between proportions of high blood pressure reports with regional variables for overweight or obesity and education. There were no spatial associations among health regions for older adult male hypertension data while a weak spatial trend for females was removed after regression analysis. Potential implications for public health of older adults and cardiovascular care are discussed with a focus on improving regional health literacy and education.

8.1. Introduction

Given the publically funded healthcare system in Canada, socioeconomic gradients of cardiovascular health should be relatively minimal, although there is evidence for income-associated trends in Canadian high blood pressure (i.e., hypertension) prevalence and the nature of these trends may differ by gender and geography (Caswell, 2016a). However, Kaplan et al. (2010) found no indication of a similar effect when specifically examining older adults (≥ 65 years of age) in Canada rather than overall age-standardized rates. Various risk factors for heart disease, including high blood pressure, were previously examined using the Canadian Heart Health Survey for which an inverse relationship was identified for heart disease risk factors with socioeconomic status (Choinière et al., 2000). It was also determined that education demonstrated a stronger effect on health than income (Choinière et al., 2000). The high prevalence of cardiovascular diseases in Canada is also complicated by the alarmingly high number of individuals unaware of associated issues with their own health, such as hypertension (Joffres et al., 1997).

Further complicating the nature of socioeconomic contributions to cardiovascular health in Canada are the myriad interactions with gender, age, and geography (Bayentin et al., 2010; Caswell, 2016b; Tanuseputro et al., 2003). Although an association with income may be present for cardiovascular health concerns (Guessous et al., 2014), this specific relationship may differ by gender where a previously observed income-hypertension gradient was nonlinear for male age-standardized rates and linear for females (Caswell, 2016a). Furthermore, geospatial clustering for high rates of hypertension was also markedly different for males and females by income quintile. Interactions between gender and socioeconomic factors with respect to hypertension have also been observed elsewhere in the world where stronger effects have typically been revealed for females (Leng et al., 2015; Loucks et al., 2007; Van Minh et al., 2006). For example, Van Minh et al. (2006) found that the lowest rates of hypertension for males in Vietnam occurred in relation to the lowest income groups, while lower income for females was associated with the highest rates of hypertension. An ecological study using Canadian data has similarly indicated lower age-standardized hypertension rates related to lower income for males, while the reverse was true for females with high rates of hypertension associated with low income (Caswell, 2016a). Finally, a meta-analysis using data from many countries found that the correlation between socioeconomic status and high blood pressure was more pronounced for females than their male counterparts, especially in developed nations (Leng et al., 2015).

An additional consideration for public health is geography for which previous spatial analyses have indicated relationships with cardiovascular health. Earlier research applied exploratory spatial statistics to an ecological study of overweight and obesity rates in Canada at the sub-provincial health region scale for which the authors suggested improved geographic-based preventive measures were required after identification of clustered high rates, particularly in the North Atlantic (Pouliou & Elliott, 2009). Caswell (2016b) has previously identified significant spatial clusters of Canadian hospitalizations due to myocardial infarction with a graded increase from west to east and with the highest neighboring rates observed in Northern Ontario and Quebec. Ahmadi et al. (2015) have similarly noted significant spatial trends for myocardial infarction hospitalizations throughout the provinces of Iran. Spatial clustering within specific regions previously revealed for self-reported high blood pressure prevalence in Canada after age standardization was found to vary by gender and income (Caswell, 2016a) and, specifically within the province of Quebec, climate effects on ischemic heart disease hospitalizations were also shown to vary by geography (Bayentin et al., 2010). The identification of and control for geospatial processes in the study of socioeconomic determinants of cardiovascular health may be particularly important when considering the relevant effects of neighborhood-level deprivation and housing mobility (Acevedo-Garcia et al., 2004; Dohmen, 2005; Matheson et al., 2009).

As noted by Lakatta (1990), aging and hypertension appear similar in many respects and, as a result, hypertension is often referred to as “accelerated aging”. Many factors associated with aging influence the cardiovascular system and potential hypertension including increased arterial stiffness (McEniery, 2007) and oxidative stress (Monahan, 2007), as well as a decrease in capacity for the autonomic-mediated baroreflex to properly maintain blood pressure (Monahan, 2007). Additional factors that may exacerbate aging-related decline in cardiovascular health include higher dietary sodium intake (Gates et al., 2004), reduced physical activity (Arbab-Zadeh et al., 2004; Madden et al., 2009), and psychological depression (Simonsick et al., 1995). Higher levels of visceral fat are also positively associated with stiffening of the aorta and hypertension in older adults (Sutton-Tyrrell et al., 2001). Beyond the more intuitive association between hypertension and subsequent cardiovascular disease, high blood pressure among older adults may indicate a concomitant reduction in the volume of brain matter and associated decline in cognitive function (Nagai et al., 2008).

The current ecological study sought to investigate proportions of high blood pressure among older adult Canadians for cross-sectional associations with socioeconomic factors including income, housing suitability, and education, as well as any potential relationship with reporting a high sense of community belonging, while also adjusting for additional determinants of health.

Analyses were conducted separately for males and females, along with a combined analysis using alternate statistical methods. Furthermore, hypertension data were assessed for the presence of spatial trends and controlled where necessary.

8.2. Methods

Data were acquired at the health region scale from the 2014 Canadian Community Health Survey (CCHS) through an open-source online database of Statistics Canada (2016a) for a cross-sectional, ecological study. The CCHS is a cross-sectional, voluntary national survey that is representative of the Canadian population at the health region level. The dependent measure of interest was the proportion of older adult males or females (≥ 65 years of age) reporting high blood pressure (i.e., hypertension) diagnosed by a health professional (*HBP*) which is commonly defined by blood pressure ≥ 140/90 mm Hg. However, a recent recommendation for older adults indicated that blood pressure should be maintained < 150/90 mm Hg (James et al., 2014). Similar proportions of older adult males or females with overweight or obesity (*BMI*), high sense of community belonging (*Belong*), and regular doctor access (*Doc*) were also obtained from the same source (Statistics Canada, 2016a). Data from the latest available National Household Survey (NHS 2011) (Statistics Canada, 2016b) were used to calculate the ratio of those living in suitable housing to those in unsuitable dwellings (*Housing*), ratio of those with at least a high school diploma to those without (*Edu*), and average income (*AvInc*). According to NHS definitions (Statistics Canada, 2016c), housing suitability is based on the National Occupancy Standard for which housing is considered suitable when the dwelling contains an adequate number of bedrooms for the tenant composition. Overall proportions of daily or occasional smokers (*Smoke*) and heavy drinkers (*Drink*) for each region were also obtained although these were not available for gender or age-specific groups and thus present much stronger limitations compared to other independent measures of interest. It should be noted that the use of voluntary, self-reported data may result in over- or, more likely, underestimation of the true prevalence. This is particularly true for the study of *HBP* rates when considering that many individuals may be unaware of their hypertensive condition, both in Canada and abroad (Joffres et al., 1997; Van Minh et al., 2006). Despite this potential caveat, the CCHS is considered representative of the sampled population at the health region level (Statistics Canada, 2016a) and has a history of use for the study of cardiovascular health and correlated issues (Caswell, 2016a; Joffres et al., 2007; Pouliou & Elliott, 2009; Veenstra, 2013).

The cartographic shapefile accessed for the current study (Statistics Canada, 2015) was based on 2013 health region boundaries where some areas were merged according to updated guidelines following previous research (Caswell, 2016a; 2016b) using Quantum GIS v2.12.3 software. Additionally, the province of Prince Edward Island (PEI) now only disseminates data at the provincial scale rather than the current spatial scale of interest and this area was thus removed from the current analyses. Areas with high proportions of culturally unique Inuit populations were excluded from the current study, including Northwest Territories, Nunavut, and Yukon, following previous work (Caswell, 2016a; 2016b; Pouliou & Elliott, 2009). Finally, regions with missing data were also removed from the shapefile by gender. For males, regions removed for this reason included 3547, 3552, 4710, 4714, and 5953, for a final total n = 101 health regions. For females, areas removed due to missing data included 4714 and 5931 for a total n = 104 health regions. To better accommodate parametric techniques, variables were assessed for normal distributions using Shapiro-Wilks test and transformed using natural logarithm or square root functions where necessary. Where standard data transformation failed to remedy distribution properties, Blom's (1958) method of normalized rank scores was applied. All measures were standardized (z-score) to prevent unit dependence of subsequent model parameters and to allow direct interpretation of regression coefficients.

Prior to exploratory spatial data analysis (ESDA), a spatial weight matrix (Anselin, 1994) was constructed for the cartographic shapefile of Canadian health regions with GeoDa v1.6.7 software to determine which areas were considered neighbors according to the queen (first order) contiguity rule. The queen rule considers regions to be neighbors when they share a common point along their boundaries where neighbors = 1 and non-neighbors = 0. Spatial weights were then row-standardized by dividing each weight by their respective row sum. Each *HBP* variable for both males and females was analyzed for global spatial autocorrelation using Moran's I (1950) with probabilities computed through Monte Carlo simulation with 999 random permutations. Moran's (1950) test follows:

$$I = \frac{\mathrm{n}}{\sum_i \sum_j w_{ij}} \cdot \frac{\sum_i \sum_j w_{ij} \, (y_i - \mu)\left(y_j - \mu\right)}{\sum_i (y_i - \mu)^2}$$

where w = spatial weight matrix value at row i column j, and μ = mean of outcome y. Obtained I values were standardized and compared to an empirical distribution of results from randomization with $p < 0.05$ considered statistically significant. The values of I can range between +1 and -1 with zero indicating that a variable of interest is randomly distributed across the spatial units under consideration. Values significantly greater than or less than zero are indicative of spatial autocorrelation where like-values cluster together in space more than would be expected by chance (positive) or are separated by space more than would be expected (negative).

Linear regressions were fit to all data with SPSS v23 software using ordinary least-squares (OLS) for *HBP* as the dependent measure and block entry of independent variables under consideration according to the standard linear model:

$$y = \alpha + \beta_1 x_1 +, \ldots, + \beta_i x_i + \varepsilon$$

where y = dependent variable, α = model intercept, β = regression coefficients, x = independent variables, and ε = error term or residuals. Two blocks were used for variable entry with nested models. The first block consisted of automatically entering primary health-related variables BMI_z, $Smoke_z$, $Drink_z$, Doc_z, while the second block consisted of stepwise variable entry for Edu_z, $Housing_z$, $AvInc_z$, and $Belong_z$. Variance inflation factors (VIF) were calculated for final male and female OLS models in order to detect multicollinearity among predictors. This process involved fitting separate regressions for each independent variable x_i with all other independent variables x as predictors. The VIF for a given variable was then obtained by:

$$\mathrm{VIF}_i = \frac{1}{1 - R_i^2}$$

where R^2 = coefficient of determination for independent variable x_i. Values of VIF > 10 indicate potential issues related to multicollinearity. Standard Shapiro-Wilks test was applied to the model residuals in SPSS for assessing the assumption of normality, with Breusch-Pagan testing in GeoDa used to confirm the presence of homoscedasticity. For regression models presenting issues of heteroscedasticity, the HC3 estimation method (Davidson & MacKinnon, 1993) was used to compute heteroscedastic-consistent standard errors with an SPSS macro created by Hayes and Cai (2007). Residuals were also analyzed for any remaining spatial autocorrelation with Moran's *I* after OLS regression.

As a final stage of analysis, regional HBP_z among older adult males and females were also combined in a composite dataset for further analysis with generalized estimating equations (GEE) in SPSS, with gender as a within-subject factor and HBP_z residuals as the repeated measure within health regions, in order to determine the independent variable effects on the population-level mean. Residual values (HBP_ε) for male and female HBP_z were derived after adjusting for regional smoking ($Smoke_z$) and heavy drinking prevalence ($Drink_z$) with linear regression according to the formula:

$$HBP_\varepsilon = HBP_z - \left(\alpha + \beta_{Smoke_z}(Smoke_z) + \beta_{Drink_z}(Drink_z)\right)$$

This was done prior to analysis with GEE given the lack of available data for gender-specific rates of smoking and heavy drinking. Subsequent values were standardized (*z*-score). The GEE specification of a generalized linear model is semiparametric in nature which allows for regression analyses that incorporate dependence between repeated measures acquired from a within-subjects design context (Liang & Zeger, 1986) which follows:

$$U(\beta) = \sum_{i=1}^{\mathrm{N}} \frac{\partial \mu_{ij}}{\partial \beta_k} V_i^{-1}\{y_i - \mu_i(\beta)\}$$

where ∂ = partial differential, μ = mean model for case *i* repeated measure *j*, *y* = outcome measure to be modelled, β = regression parameter for variable *k*, and *V* = variance structure.

Regression parameters are computed using the Newton-Raphson (NR) algorithm (Ypma, 1995) to solve for $U(\beta) = 0$ with a form of covariance specified for the repeated measures to better model an unknown correlation between within-subjects outcomes. The NR algorithm is employed to obtain the best approximation of a function's roots (i.e., a zero-input that produces a zero-output). A covariance structure is specified within GEE analysis which may be unknown. An independent correlation structure was chosen for the current analysis to account for repeated measures between males and females while estimating the overall population-level effect of all independent variables on *HBP* among older adults after adjusting for smoking and drinking (HBP_ε). Testing of GEE error normality was conducted using Shapiro-Wilks test in SPSS while homoscedasticity was evaluated using Breusch-Pagan test in Matlab v7.12.

8.3. Results

Prior to data standardization, it was determined that most older adult male variables were normally distributed according to Shapiro-Wilks test ($p > 0.05$) although *Belong*, *Doc*, and *AvInc* were transformed to normalized rank scores using Blom's method (log and square root were inadequate). Older adult male HBP_z was not spatially autocorrelated according to global Moran's *I* with Monte Carlo simulation, contrary to total male age-standardized rates previously explored (Caswell, 2016b). Standardized values for males are plotted in Figure 39 including non-spatial box plot and spatial box map.

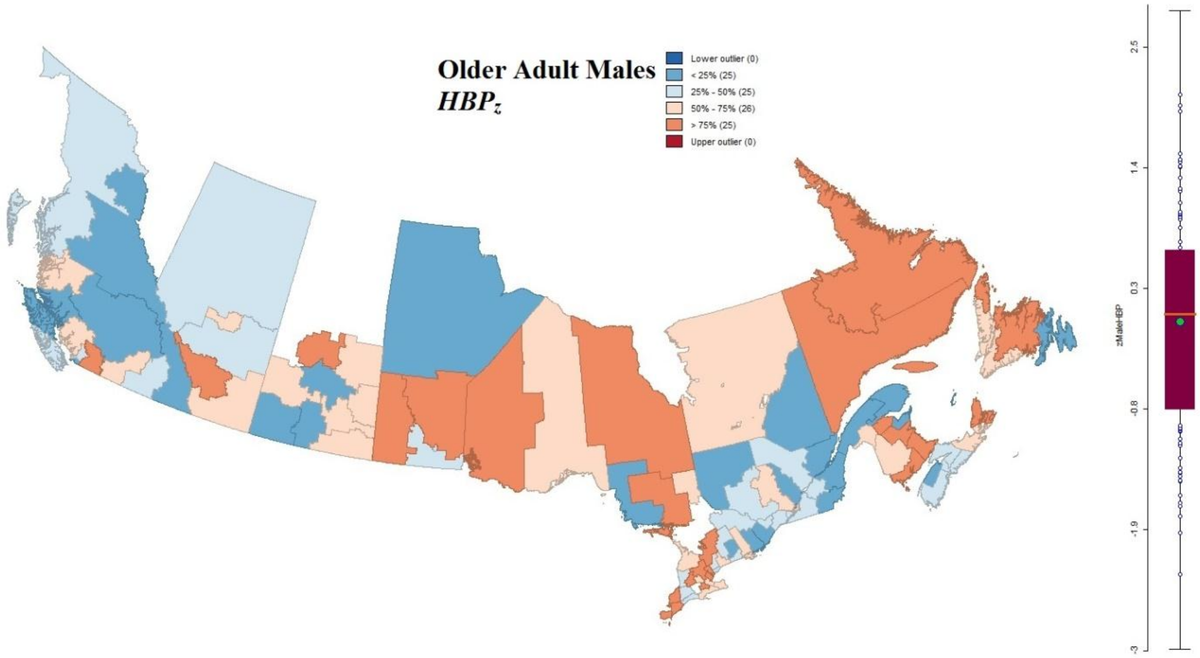

Figure 39: Box map (hinge = 1.5) of standardized (*z*-score) high blood pressure prevalence (HBP_z) among older adult males in Canada (2014) with standard box plot on right side of figure (horizontal line and dot within box indicate mean and median); excluded regions have been removed from map

A linear regression was fit to all male data by OLS with HBP_z as the dependent measure and block independent variable entry for which the final model was statistically significant ($F_{(6, 100)}$ = 3.433, p = 0.004, R^2 = 0.180). While holding other independent measures constant, significant (p < 0.05) predictors for older adult male HBP_z included $Drink_z$ (β = 0.216), Doc_z (β = 0.198), $Housing_z$ (β = -0.276), and Edu_z (β = -0.262). Calculated VIF did not reveal multicollinearity (all VIF < 10) and Shapiro-Wilks test indicated normally distributed residuals (p > 0.05). Model residuals were not spatially autocorrelated according to Moran's I (p > 0.05). However, there were potential issues of heteroscedasticity according to Breusch-Pagan test (p < 0.05).

Heteroscedastic-consistent parameter estimates were computed for the male OLS model without assuming homoscedasticity of errors after which statistically significant predictors included only Edu_z (β = -0.262). Standard errors (SE) and their probabilities for significant independent measures are included in Table 17.

Table 17: Significant ($p < 0.05$) independent variables for linear regression predicting Canadian (2014) older adult male high blood pressure (HBP_z) with standardized coefficients (β), standard errors (SE) and probabilities (p) from both standard ordinary least-squares (OLS) and heteroscedastic-consistent estimates (HC3)

Variable	β	OLS – SE (p)	HC3 – SE (p)
$Drink_z$	0.216	0.102 (0.037)	n.s.
Doc_z	0.198	0.099 (0.048)	n.s.
$Housing_z$	-0.276	0.106 (0.011)	n.s.
Edu_z	-0.262	0.115 (0.026)	0.106 (0.016)

n.s. = not significant ($p > 0.05$)

As observed for males, older adult female variables tended to be normally distributed ($p > 0.05$) with the exception of *AvInc*, which was transformed to a natural logarithm, and *Doc*, which was transformed to normalized rank scores. All data were standardized prior to analysis. Female HBP_z was weakly spatially autocorrelated according to global Moran's I test with Monte Carlo simulation for one-tailed probability (I = 0.120, z = 1.952, p = 0.027) in contrast to older adult male HBP_z. Standardized values for females are plotted in Figure 40.

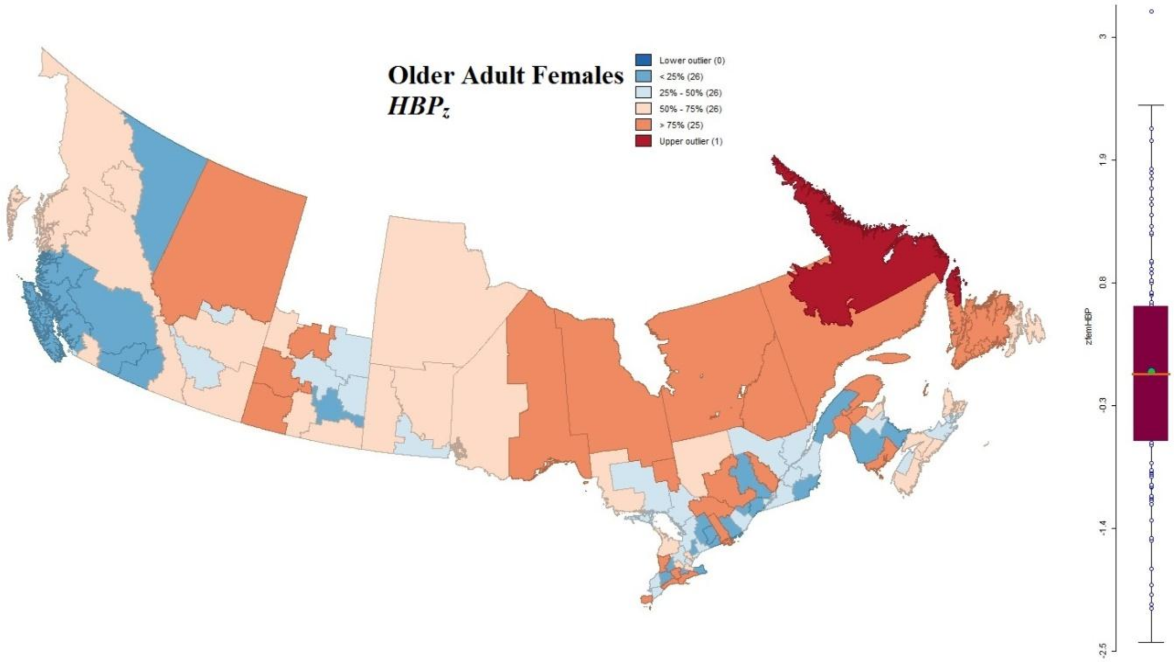

Figure 40: Box map (hinge = 1.5) of standardized (*z*-score) high blood pressure prevalence (HBP_z) among older adult females in Canada (2014) with standard box plot on right side of figure (horizontal line and dot within box indicate mean and median) ; excluded regions have been removed from map

The female OLS regression model was statistically significant ($F_{(5, 103)} = 7.995$, $p < 0.001$, $R^2 = 0.290$) with no issues of multicollinearity (VIF < 10). Residual values derived from OLS were also normally distributed ($p > 0.05$). While holding other independent variables constant, statistically significant ($p < 0.05$) results for older adult females included $Drink_z$ ($\beta = 0.181$), BMI_z ($\beta = 0.235$), and Edu_z ($\beta = -0.290$). Model residuals were not spatially autocorrelated after controlling for independent measures according to Moran's I ($p > 0.05$). However, Breusch-Pagan testing detected potential issues of heteroscedasticity ($p < 0.05$). After computing HC3 parameter estimates, all significant predictors were retained by the model including $Drink_z$ ($\beta =$

0.181), BMI_z (β = 0.235), and Edu_z (β = -0.290). Standard errors (SE) and their probabilities are provided for significant independent variables in Table 18.

Table 18: Significant ($p < 0.05$) independent variables for linear regression predicting Canadian (2014) older adult female high blood pressure (HBP_z) with standardized coefficients (β), standard errors (SE) and probabilities (p) from both standard ordinary least-squares (OLS) and heteroscedastic-consistent estimates (HC3)

Variable	β	OLS – SE (p)	HC3 – SE (p)
$Drink_z$	0.181	0.089 (0.046)	0.089 (0.045)
BMI_z	0.235	0.095 (0.015)	0.088 (0.009)
Edu_z	-0.290	0.102 (0.005)	0.109 (0.009)

Because there were repeated measures for each available health region (i.e., males and females), the GEE method was used to conduct linear regression analysis on the composite dataset while incorporating dependence between repeated measures from the within-subjects aspect of the study design (i.e., health regions were considered subjects in the current design). This allowed for estimation of population-level mean effects of the covariates of interest with an independent correlation structure chosen to account for repeated measures between males and females within each health region. Note that male and female residual values of the dependent measure (HBP_ε) after adjusting for regional $Smoke_z$ and $Drink_z$ were used for GEE analysis. After controlling for all other independent measures of interest, significant predictors included BMI_z (β = 0.20, SE =

0.064, $p = 0.002$) and Edu_z ($\beta = -0.254$, SE = 0.072, $p < 0.001$). Residual values were assessed for normal distribution and homoscedasticity with no issues identified ($p > 0.05$).

8.4. Discussion

The current results demonstrate that the socioeconomic correlates and spatial trends associated with Canadian *HBP* at the health region level markedly differed for older adults compared to total age-standardized prevalence. Specifically for older adult males (≥ 65 years of age), there was a distinct lack of spatial dependence for regional *HBP* proportions despite the strongly significant spatial autocorrelations and clustering previously identified (Caswell, 2016a) using age-standardized *HBP* prevalence for all adult males (≥ 20 years of age). Whereas earlier studies had also shown a relationship between cardiovascular health and socioeconomic factors (Caswell, 2016a; 2016b; Guessous et al., 2014; Leng et al., 2015; Loucks et al., 2007; Matheson et al., 2009; Van Minh et al., 2006), current analyses of older adult Canadian males only identified *Edu* as a statistically significant predictor of *HBP* after adjusting for heteroscedasticity. Specifically, health regions with lower numbers of high school graduates were associated with higher regional proportions of *HBP* among older adult males. Although education has previously been identified as a correlate of cardiovascular health (Choinière et al., 2000; Van Minh et al., 2006; Winkleby et al., 1992), it is interesting to note that this was the only significant predictor of *HBP* for older adult males when holding other independent variables constant and after additional statistical adjustment.

A negative relationship between *HBP* and *Edu* was also revealed for older adult females, although additional statistically significant relationships were observed including an increase in *HBP* for regions with higher proportions of heavy drinkers (*Drink*), and for regions with higher proportions of older adult females with overweight or obesity (*BMI*). The addition of *BMI* for the female model but not males in the current study was in contrast to results for Canadian myocardial infarction hospitalizations where *BMI* entered the age-standardized male regression models but not those for females (Caswell, 2016b). Note that, after controlling for additional determinants of health and computing heteroscedastic-consistent parameter estimates, a relationship with income was not apparent for older adult Canadians contrary to age-standardized rates of either *HBP* or myocardial infarction hospitalizations (Caswell, 2016a; 2016b). Although regional *HBP* of older adult females was weakly spatially autocorrelated, the strength of this relationship may cast doubt over the validity of any further inferences from this perspective. Furthermore, the potential spatial association was removed after computing model residuals through linear regression indicating that, if any spatial dependence exists for *HBP* of older adult females, this could be accounted for by the correlation with *Drink*, *BMI*, and *Edu*. Again, this is in contrast to previous analyses of age-standardized rates in Canada which identified particularly strong spatial associations among regional *HBP*, even after controlling for additional determinants of health (Caswell, 2016a). Finally, analysis of the composite dataset similarly indicated that *Edu* was a consistent predictor of *HBP* with a negative relationship, although *BMI* was also statistically significant for GEE analysis of males and females combined with a positive correlation.

The potential role of education as a health determinant has been established through myriad methods and in many areas of the world (Chen et al., 2015; Smith et al., 2014; van der Heide et al., 2013; von dem Knesebeck et al., 2006; Winkleby et al., 1992), though it is interesting to note the prominent role of education in association with *HBP* specifically among older adults in

Canada for which a number of possible explanations exist. An earlier study in the USA indicated that education was the strongest socioeconomic predictor of risk factors for cardiovascular disease including cigarette smoking and elevated blood pressure (Winkleby et al., 1992). In the Canadian province of Saskatchewan, Chen et al. (2015) observed that those with lower education were also at higher risk of obesity. Furthermore, many patients with chronic diseases, including hypertension, were more likely to have less knowledge of their condition associated with lower health literacy, suggesting further need for continuing patient education as well as preventive education (Gazmararian et al., 2003). Although research in France did not identify a relationship between compulsory education and mortality rates (Albouy & Lequien, 2009), low education was associated with individuals' health literacy and subsequent low self-reported health in the Netherlands (van der Heide et al., 2013). Consistent with these conclusions, there has recently been an emphasis on improving health literacy for disease management in Canada (Poureslami et al., 2016). However, it should also be noted that international research indicated the correlation between lower education and increased risk of low self-reported health was stronger for the age range of 25 to 55 years compared to older adults, although the authors' conclusions maintained an effect of education on health with variations by country, age, and gender (von dem Knesebeck et al., 2006). To briefly address the compounded issue of education in association with health awareness rather than actual disease occurrence, Smith et al. (2014) have shown that those with lower education tended to demonstrate greater difficulty making informed decisions regarding bowel cancer screening, which may also be relevant to screening for other health conditions such as hypertension and subsequent awareness.

Continuing education relevant to improving health literacy should be readily available to older adults in Canada, especially for regions with lower levels of general education, in order to increase awareness of cardiovascular health concerns, allow better informed decisions and motivation related to medical screening, and subsequent treatment options where necessary. The need for improving awareness is particularly important in Canada (Joffres et al., 1997), although additional improvements conducive to better cardiovascular health among older adults can be implemented including those related to dietary concerns, particularly reducing sodium intake (Gates et al., 2004), regular exercise (Arbab-Zadeh et al., 2004; Madden et al., 2009), and pharmacological treatment of blood pressure variations (Kazuomi et al., 2003; Nagai et al., 2008). However, it should also be noted that adherence to antihypertensive medication among older adults may present additional behavioral variations and limitations regarding treatment efficacy (Krousel-Wood et al., 2009).

Although the possibility for over- or underestimation of *HBP* prevalence has been discussed, an additional limitation of the current study concerns the ecological fallacy which reflects the fact that correlations among aggregate data may not necessarily represent individual-level correlations given the absence of cross-sectional effects in the latter (Robinson, 1950; Freedman, 2002). Thus, a statistical relationship between relevant variables (i.e., *HBP* and *Edu*) can be inferred at the health region level but not for inferences related to risks of individuals or for smaller aggregate units such as cities. However, the currently employed health region scale indicates the administrative boundaries of operation for sub-provincial health units in Canada and, therefore, the current results should still be relevant at this particular scale. A related caveat concerns the modifiable areal unit problem (MAUP) which indicates that the level of aggregation can impact subsequent statistical results in spatial analyses (Gehlke & Biehl, 1934; Horner & Murray, 2002; King, 1979). However, as with previous studies (Caswell, 2016a; Pouliou & Elliott, 2009), the current results were obtained employing the smallest spatial scale available for the CCHS (i.e., sub-provincial health regions).

The correlation between *Edu* and *HBP* in the current study further indicates that education may have a stronger link to hypertension among older adult Canadians at the health region scale compared to age-standardized prevalence (Caswell, 2016a), particularly when considering the absence of any significant effect for other socioeconomic factors examined, including income or housing suitability. An increased emphasis on hypertensive counseling and education for older adults through public health units administering the health regions of Canada may be particularly important when considering the potential role of health literacy in public health outcomes (Gazmararian et al., 2003; Poureslami et al., 2016; van der Heide et al., 2013) and the apparent regional influence of education for *HBP* among older adults. Additional research is required to further address the concerns related to socioeconomic influence of cardiovascular health at the individual level while also accounting for relevant variations in gender and age across geographic space.

References

Acevedo-Garcia, D., Osypuk, T. L., Werbel, R. E., Meara, E. R., Cutler, D. M., & Berkman, L. F. (2004). Does housing mobility policy improve health? *Housing Policy Debate*, 15(1): 49-98.

Ahmadi, A., Soori, H., Mehrabi, Y., & Etemad, K. (2015). Spatial analysis of myocardial infarction in Iran: National report from the Iranian myocardial infarction registry. *Journal of Research in Medical Sciences*, 20(5): 434-439.

Albouy, V., & Lequien, L. (2009). Does compulsory education lower mortality? *Journal of Health Economics*, 28(1): 155-168.

Anselin, L. (1994). Exploratory spatial data analysis and geographic information systems. In: Longley, P., Brooks, S., Macmillan, B., & McDonnell, R. (eds.) *GeoComputation: A Primer* (pp. 77-94). New York: Wiley.

Arbab-Zadeh, A., Dijk, E., Prasad, A., Fu, Q., Torres, P., Zhang, R., Thomas, J. D., Palmer, D., & Levine, B. D. (2004). Effect of aging and physical activity on left ventricular compliance. *Circulation*, 110(13): 1799-1805.

Bayentin, L., El Adlouni, S., Ouarda, T. B. M. J., Gosselin, P., Doyon, B., & Chebana, F. (2010). Spatial variability of climate effects on ischemic heart disease hospitalization rates for the period 1989-2006 in Quebec, Canada. *International Journal of Health Geographics*, 9(5).

Blom, G. (1958). *Statistical Estimates and Transformed Beta Variables*. New York.

Caswell, J. M. (2016a). Prevalence of reported high blood pressure in Canada: Investigation of demographic and spatial trends. *Journal of Public Health*. DOI: 10.1007/s10389-016-0761-4

Caswell, J. M. (2016b). Exploring spatial trends in Canadian incidence of hospitalization due to myocardial infarction with additional determinants of health. *Public Health*. DOI: 10.1016/j.puhe.2016.07.006

Chen, Y., Rennie, D. C., Karunanayake, C. P., Janzen, B., Hagel, L., Pickett, W., Dyck, R., Lawson, J., Dosman, J. A., Pahwa, P., & Saskatchewan Rural Health Study Group. (2015). Income adequacy and education associated with the prevalence of obesity in rural Saskatchewan, Canada. *BMC Public Health*, 15.

Choinière, R., Lafontaine, P., & Edwards, A. C. (2000). Distribution of cardiovascular disease risk factors by socioeconomic status among Canadian adults. *Canadian Medical Association Journal*, 162(9): S13-S24.

Davidson, R., & MacKinnon, J. G. (1993). *Estimation and Inference in Econometrics*. Oxford: Oxford University Press.

Dohmen, T. J. (2005). Housing, mobility, and unemployment. *Regional Science and Urban Economics*, 35(3): 305-325.

Freedman, D. A. (2002). *The Ecological Fallacy*. California: University of California Press.

Gates, P. E., Tanaka, H., Hiatt, W. R., & Seals, D. R. (2004). Dietary sodium restriction rapidly improves large elastic artery compliance in older adults with systolic hypertension. *Hypertension*, 44: 35-41.

Gazmararian, J. A., Williams, M. V., Peel, J., & Baker, D. W. (2003). Health literacy and knowledge of chronic disease. *Patient Education and Counseling*, 51(3): 267-275.

Gehlke, C. E., & Biehl, K. (1934). Certain effects of grouping upon the size of the correlation coefficient in census tract material. *Journal of the American Statistical Association*, 29(185A): 169-170.

Guessous, I., Joost, S., Jeannot, E., Theler, J.-M., Mahler, P., Gaspoz, J.-M., & GIRAPH Group. (2014). A comparison of the spatial dependence of body mass index among adults and children in a Swiss general population. *Nutrition and Diabetes*, 4(e111).

Hayes, A. F., & Cai, L. (2007). Using heteroskedasticity-consistent standard error estimators in OLS regression: An introduction and software implementation. *Behavior Research Methods*, 39(4): 709-722.

Horner, M. W., & Murray, A. T. (2002). Excess commuting and the modifiable areal unit problem. *Urban Studies*, 39(1): 131-139.

James, P. A., Oparil, S., Carter, B. L., Cushman, W. C., Dennison-Himmelfarb, C., Handler, J., Lackland, D. T., LeFevre, M. L., MacKenzie, T. D., Ogedegbe, O., Smith Jr., S. C., Svetkey, L. P., Taler, S. J., Townsend, R. R., Wright Jr., J. T., Narva, A. S., & Ortiz, E. (2014). 2014 evidence-based guideline for the management of high blood pressure in adults: Report from the panel members appointed to the Eight Joint National Committee (JNC 8). *Journal of the American Medical Association*, 311(5): 507-520.

Joffres, M. R., Campbell, N. R. C., Manns, B., & Tu, K. (2007). Estimate of the benefits of a population-based reduction in dietary sodium additives on hypertension and its related health care costs in Canada. *Canadian Journal of Cardiology*, 23(6): 437-443.

Joffres, M. R., Ghadirian, P., Fodor, J. G., Petrasovits, A., Chockalingam, A., & Hamet, P. (1997). Awareness, treatment, and control of hypertension in Canada. *American Journal of Hypertension*, 10(10): 1097-1102.

Kaplan, M. S., Huguet, N., Feeny, D. H., & McFarland, B. H. (2010). Self-reported hypertension prevalence and income among older adults in Canada and the United States. *Social Science and Medicine*, 70(6): 844-849.

Kario, K., Shimada, K., & Pickering, T. G. (2003). Abnormal nocturnal blood pressure falls in elderly hypertension: Clinical significance and determinants. *Journal of Cardiovascular Pharmacology*, 41: S61-S66.

King, P. E. (1979). Problems of spatial analysis in geographical epidemiology. *Social Science and Medicine*, 13D: 249-252.

Krousel-Wood, M. A., Muntner, P., Islam, T., Morisky, D. E., & Webber, L. S. (2009). Barriers to and determinants of medication adherence in hypertension management: Perspective of the Cohort Study of Medication Adherence among Older Adults. *Medical Clinics of North America*, 93(3): 753-769.

Lakatta, E. G. (1990). Similar myocardial effects of aging and hypertension. *European Heart Journal*, 11: 29-38.

Leng, B., Jin, Y., Li, G., Chen, L., & Jin, N. (2015). Socioeconomic status and hypertension: A meta-analysis. *Journal of Hypertension*, 33(2): 221-229.

Liang, K.-Y., & Zeger, S. (1986). Longitudinal data analysis using generalized linear models. *Biometrika*, 73(1): 13-22.

Loucks, E. B., Rehkopf, D. H., Thurston, R. C., & Kawachi, I. (2007). Socioeconomic disparities in metabolic syndrome differ by gender: Evidence from NHANES III. *Annals of Epidemiology*, 17(1): 19-26.

Madden, K. M., Lockhart, C., Cuff, D., Potter, T. F., & Meneilly, G. S. (2009). Short-term aerobic exercise reduces arterial stiffness in older adults with type 2 diabetes, hypertension, and hypercholesterolemia. *Diabetes Care*, 32(8): 1531-1535.

Matheson, F. I., White, H. L., Moineddin, R., Dunn, J. R., & Glazier, R. H. (2009). Neighbourhood chronic stress and gender inequalities in hypertension among Canadian adults: A multilevel analysis. *Journal of Epidemiology and Community Health*, jech-2008.

McEniery, C. M., Wilkinson, I. B., & Avolio, A. P. (2007). Age, hypertension and arterial function. *Clinical and Experimental Pharmacology and Physiology*, 34(7): 665-671.

Monahan, K. D. (2007). Effect of aging on baroreflex function in humans. *American Journal of Physiology*, 293(1): R3-R12.

Moran, P. A. P. (1950). Notes on continuous stochastic phenomena. *Biometrika*, 37(1): 17-23.

Nagai, M., Hoshide, S., Ishikawa, J., Shimada, K., & Kario, K. (2008). Ambulatory blood pressure as an independent determinant of brain atrophy and cognitive function in elderly hypertension. *Journal of Hypertension*, 26(8): 1636-1641.

Pouliou, T., & Elliott, S. J. (2009). An exploratory spatial analysis of overweight and obesity in Canada. *Preventive Medicine*, 48(4): 362-367.

Poureslami, I., Rootman, I., Pleasant, A., & FitzGerald, J. M. (2016). The emerging role of health literacy in chronic disease management: The response to a call for action in Canada. *Population Health Management*, 19(4).

Robinson, W. S. (1950). Ecological correlations and the behavior of individuals. *American Sociological Review*, 15(3): 351-357.

Simonsick, E. M., Wallace, R. B., Blazer, D. G., & Berkman, L. F. (1995). Depressive symptomatology and hypertension-associated morbidity and mortality in older adults. *Psychosomatic Medicine*, 57(5): 427-435.

Smith, S. K., Simpson, J. M., Trevena, L. J., & McCaffery, K. J. (2014). Factors associated with informed decisions and participation in bowel cancer screening among adults with lower education and literacy. *Medical Decision Making*, 34(6): 756-772.

Sutton-Tyrrell, K., Newman, A., Simonsick, E. M., Havlik, R., Pahor, M., Lakatta, E., Spurgeon, H., & Vaitkevicius, P. (2001). Aortic stiffness is associated with visceral adiposity in older adults enrolled in the Study of Health, Aging, and Body Composition. *Hypertension*, 38: 429-433.

Statistics Canada. (2015). *82-402-X: Health Region Boundary Files*. Retrieved from http://www.statcan.gc.ca/pub/82-402-x/2013002/reg-eng.htm

Statistics Canada. (2016a). *Table 105-0501: Health Indicator Profile, Annual Estimates, by Age Group and Sex, Canada, Provinces, Territories, Health Regions (2013 Boundaries) and Peer Groups*. Retrieved from http://www5.statcan.gc.ca/cansim/a05?lang=eng&id=01050501

Statistics Canada. (2016b). *NHS Profile, 2011*. Retrieved from https://www12.statcan.gc.ca/nhs-enm/2011/dp-pd/prof/index.cfm?Lang=E

Statistics Canada. (2016c). *Housing Reference Guide, National Household Survey, 2011*. Retrieved from https://www12.statcan.gc.ca/nhs-enm/2011/ref/guides/99-014-x/99-014-x2011007-eng.cfm

Tanuseputro, P., Manuel, D. G., Leung, M., Nguyen, K., & Johansen, H. (2003). Risk factors for cardiovascular disease in Canada. *Canadian Journal of Cardiology*, 19(11): 1249-1259.

van der Heide, I., Wang, J., Droomers, M., Spreeuwenberg, P., Rademakers, J., & Uiters, E. (2013). The relationship between health, education, and health literacy: Results from the Dutch Adult Literacy and Life Skills Survey. *Journal of Health Communication: International Perspectives*, 18(S1): 172-184.

Van Minh, H., Byass, P., Chuc, N. T. K., & Wall, S. (2006). Gender differences in prevalence and socioeconomic determinants of hypertension: Findings from the WHO STEPs survey in a rural community of Vietnam. *Journal of Human Hypertension*, 20: 109-115.

Veenstra, G. (2013). Race, gender, class, sexuality (RGCS) and hypertension. *Social Science and Medicine*, 89: 16-24.

von dem Knesebeck, O., Verde, P. E., & Dragano, N. (2006). Education and health in 22 European countries. *Social Science and Medicine*, 63(5): 1344-1351.

Winkleby, M. A., Jatulis, D. E., Frank, E., & Fortmann, S. P. (1992). Socioeconomic status and health: How education, income, and occupation contribute to risk factors for cardiovascular disease. *American Journal of Public Health*, 82(6): 816-820.

Ypma, T. J. (1995). Historical development of the Newton-Raphson method. *SIAM Review*, 37(4): 531-551.

Chapter 9 – Discussion

9. General Overview

Cardiovascular health is associated with an enormous range of factors across both physical and social sciences. Therefore, interdisciplinary approaches are increasingly necessary to better accommodate various relevant perspectives and their associated variables of interest. The current series of studies investigated a number of issues related to cardiovascular health, including hypertension, myocardial infarction, arrhythmia, and environmental electrophysiology, from a range of interdisciplinary perspectives focusing on overall frameworks of biomedical signal processing, heliobiology, and public health, all of which emphasized diverse quantitative methodologies. Although many significant results were identified and interpreted throughout the preceding chapters, the following discussion concerns the most prominent findings and their potential implications.

9.1. Biomedical Signal Processing Results

The development of new tools for measurement and quantification of biological signals plays an important role in clinical and other medical settings. The potential to apply these tools to sources of so-called “big data” and personal quantification through both current and future developments in technology may also allow improved means of general public health surveillance and self-monitoring of personal health. The framework of biomedical signal processing employed in Chapter 2 focused on clinical utility, signal processing, information theory, and physiology. Electrocardiograph (ECG) recordings acquired from human participants, including healthy and arrhythmic records, were transformed to various indices of heart rate variability (HRV). A number of nonlinear indices derived from signal processing and information theory approaches were also employed.

The commonly used Poincaré plot analysis (PPA) appeared to overlap with standard measures of HRV and, although some researchers continue to use PPA for inferences of nonlinear dynamics (Kemp et al., 2012; Saranya et al., 2015; Stein et al., 2005), this characteristic of overlap has been identified in previous studies (Brennan et al., 2001; Hoshi et al., 2013). However, factor analysis demonstrated that only HRV values derived from wavelet entropy stood out among all variables as potentially reflecting information not contained within standard HRV indices. In order to discern if this apparent "information novelty" might present some preliminary clinical utility, logistic models were used to investigate the capacity to discriminate between healthy and arrhythmic records using various indices of HRV. After controlling for participant age, only the addition of wavelet entropy demonstrated statistically significant predictive power to identify arrhythmic records according to their relatively decreased time-frequency complexity.

Although the use of soft computing techniques has often been applied to the study of objectively more urgent cardiovascular concerns, including sudden cardiac death (Gang, 2013; Fujita et al., 2016), the currently explored technique of HRV wavelet entropy may provide some basis to the development of automated arrhythmia detection by combining live signal processing of ECG recordings with simple artificial learning algorithms to analyze relevant data (i.e., fuzzy logic controllers or artificial neuro-fuzzy inference systems, as determined by hardware capacity) and help determine the most appropriate course of action. While the detection of cardiovascular arrhythmia may be a relatively simple matter for a cardiologist, the advent of increasingly ubiquitous self-quantification technologies or activity monitors that measure physiological parameters including ECG (e.g., Fitbit Tracker, QardioCore, Samsung Gear Fit) may also allow enhanced personal tracking of health parameters. More advanced algorithms could be integrated such that likelihood of arrhythmia or other concerns would be identified automatically according to live feedback provided to the device.

9.2. Heliobiological Results

Beginning with the earlier investigations of Alexander Chizhevsky (1926; 1936), many scientific disciplines have been involved in the study of heliobiology or cosmobiology and related fields (i.e., biometeorology) from physical and social perspectives. The studies discussed in Chapter 3 and Chapter 4 included matters of biology and physics, although the results may also have relevance to psychology (Appelhans & Luecken, 2006; Brosschot et al., 2007; Durantin et al., 2014; Kemp et al., 2012; Sakuragi et al., 2002) and associated aggregate population dynamics. The role of environment in cardiovascular health has been investigated although more common environmental variables such as temperature are often the focus (Bayentin et al., 2010; Lim et al., 2012; Madrigano et al., 2013). However, there are myriad results that appear to indicate a relationship between cardiovascular physiology and solar-geophysical processes (Cornélissen et al., 2002; Dimitrova et al., 2004; 2009; 2013; Kleimenova et al., 2007; Oinuma et al., 2002; Otsuka et al., 2001; Papailiou et al., 2011; Stoupel, 1999). While these studies are often inherently correlational given the nature of the independent measures, there is some experimental support for heliobiological effects in general (Mulligan & Persinger, 2012; Mitsutake et al., 2004; Murugan et al., 2013), although there remains a prominent need to further verify the diverse effects identified by biophysicists.

The experimental study conducted in Chapter 3 addressed the issue of experimental verification in heliobiology through artificial simulation of fast-frequency (~5.5 to 5.7 s) sudden geomagnetic impulses within a laboratory setting. Measurements of ECG and HRV were acquired from human participants during both baseline (no field) and geomagnetic simulation conditions in a counterbalanced repeated-measures design. Significant increases in HRV were identified during the geomagnetic field condition compared to baseline recordings, specifically for the low frequency (0.04 to 0.15 Hz) component of HRV and the low frequency to high frequency (0.15 to 0.40 Hz) ratio which may indicate an autonomic effect on cholinergic input to the cardiovascular system (Billman, 2013). The pilot case study conducted in Chapter 4 investigated the presence of similar relationships associated with geomagnetic storms for a single person's HRV over a period of 54 days. Similar findings were acquired where specific frequency components increased with concomitant occurrences of geomagnetic storms but not with solar activity or local temperature. However, the longitudinal nature of this particular study also allowed assessment of nonlinear features associated with a cardiovascular-geomagnetic dynamic for which a depression in HRV frequency components was observed with moderate geomagnetic activity compared to relative increases during either quiet or storm conditions.

The foremost implication of these results is, of course, the verification of HRV effects related to fast-frequency geomagnetic impulses. Although there are many correlational studies that have converged upon similar conclusions (Cornélissen et al., 2002; Dimitrova et al., 2004; 2009; 2013; Kleimenova et al., 2007; Oinuma et al., 2002; Otsuka et al., 2001; Papailiou et al., 2011; Stoupel, 1999), the application of experimental procedures contributes much greater confidence in current interpretation of such results. Furthermore, it has become increasingly apparent that variations in these dynamics may exist between geographies (Cornélissen et al., 2002; Zenchenko et al., 2014) and according to individual biology (Dimitrova et al., 2013). As such, additional verification of heliobiological effects through experimental methods should be pursued further in future studies with varied parameters. Although there were a number of drawbacks associated with the current longitudinal case study, these pilot results appeared to strongly confirm the inferences derived from experimental findings and suggest additional quantitative avenues for future investigation with particular emphasis on nonlinear features.

The additional heliobiological study featured in Chapter 5, while also integrating biology and physics, further included perspectives from epidemiology. Annual counts of mortalities associated with hypertensive diseases were acquired for all of Canada from 1979 to 2009. Time-lagged linear relationships were observed between hypertensive mortalities and a number of space weather factors including geomagnetic activity, cosmic rays, interplanetary magnetic field, and solar wind parameters. The time-varying correlation strengths also demonstrated a rhythmicity of ~10.6 years, or approximately the average solar cycle length for the period under consideration. However, additional analyses suggested that the most likely source of variance for these correlations was the solar wind beta, which indicates the ratio of magnetic to plasma pressure, predominantly from eight years prior to hypertensive mortality counts. Time series analyses also identified a significant cycle of ~9.6 years for mortalities after removing a dominant quadratic trend, which was most similar to the ~10.1 year periodicity observed for concomitant geomagnetic activity, although measures of frequency domain coherence were not pursued given the relatively small dataset. Finally, dimensional analyses suggested that the rhythmic cycles of increasing hypertensive mortalities over ~10 year increments could be associated with expansion and contraction of the magnetosphere and magnetopause due to solar wind pressure variations.

Although much more rigorous statistical methods and detailed data should be employed to better discern the potential influence of heliogeophysical dynamics on cardiovascular mortalities associated with hypertensive diseases, the current study nonetheless provides a basis for such investigations at an aggregate scale. While correlation may not reflect causation, the inferences derived from the perspective of physical dimensional analysis could support the contentions regarding potential for such an effect. Furthermore, the identification of temporal dynamics including periodicities may also provide additional benefits to public health surveillance and general healthcare administration (Ayala et al., 2013; Cantwell et al., 2015; Čulić, 2014; Halberg et al., 1990; Lemmer, 2012; Levandovski et al., 2012), while the potential association between relevant periodicities and those observed for environmental factors may enhance such applications (Cornélissen et al., 2002; Dimitrov et al., 2013; Syutkina et al., 1997).

9.3. Public Health Results

Although epidemiology is one of the primary sciences involved in public health, there are contributions from myriad disciplines across the spectrum of physical and social sciences, including general physiology, (epi)genetics, biochemistry, and pharmacology from the former, as well as psychology, sociology, economics, and geography from the latter. Cardiovascular public health is particularly important when considering the burden of disease represented by poor cardiovascular health in Canada (Campbell et al., 2012; Joffres et al., 1997; 2007). The current series of public health-oriented studies focused on an ecological social epidemiology perspective for the investigation of myocardial infarction hospitalizations and hypertension across Canada, most prominently integrating demography and geospatial sciences.

The first of these studies (Chapter 6) examined age-standardized rates of Canadian hospitalizations due to myocardial infarction in 2013 aggregated at the sub-provincial health region scale. A number of additional demographic, socioeconomic, and behavioral determinants of health were also included as independent variables. Exploratory spatial data analysis (ESDA) demonstrated highly significant global spatial autocorrelation for all variables under consideration. Local indicators of spatial association (LISA) showed hot spots of high hospitalization rates in Northern Ontario, Quebec, and New Brunswick, with cold spots of low rates in British Columbia and Southern Ontario. Linear models further indicated that regional education and household income were both negatively related to myocardial infarction hospitalization rates, while regional smoking was positively related to hospitalizations. Although a positive association was also observed with overweight and obesity rates, this was for males only and not statistically significant for female rates. Spatial regressions showed significant model improvement compared to ordinary least-squares and all independent measures identified with previous analyses remained significant after controlling for an appropriate spatial error term. However, subsequent residual values demonstrated a slight shift in local spatial clusters with hot spots of high hospitalization rates localized in Northern Ontario and Quebec, and cold spots of low rates clustered in Saskatchewan.

The results of Chapter 6 demonstrate the prominent ecological role of socioeconomic factors and lifestyle (i.e., issues of overweight and obesity as well as smoking behavior) on regional rates of myocardial infarction hospitalizations and thus the particularly strong ecological link between education, income, and cardiovascular disease. Although the overall relationships among these variables are well-established (Choinière et al., 2000; Guessous et al., 2014; Leng et al., 2015; Van Minh et al., 2006), it is interesting to note the significance and magnitude of the currently observed socioeconomic effects compared to more physical measures directly associated with health. Note, however, that socioeconomically disadvantaged positions are also related to poorer health-related behaviors in general (Chen et al., 2015; Winkleby et al., 1992). In particular, the role of education and literacy has been shown to affect various health outcomes which could be related to a person's health literacy and thus better monitoring and informed decision making (Gazmararian et al., 2003; van der Heide et al., 2013; von dem Knesebeck et al., 2006; Poureslami et al., 2016). The spatial trends observed in the present study are among the more significant results and reveal prominent geographic disparity for myocardial infarctions among the health regions of Canada where areas in the Northeast were associated with high hospitalization clusters even after controlling for additional determinants of health. As previously noted by Pouliou & Elliott (2009), this type of spatial disparity could suggest a need for improved geographic-based preventive public health measures and, furthermore, indicates the relevance of integrating spatial processes in the study of Canadian cardiovascular public health.

The second study from the public health investigations (Chapter 7) looked at Canadian age-standardized rates of self-reported high blood pressure (i.e., hypertension) from 2014. Preliminary non-spatial analyses at the individual level indicated expected relationships with hypertension, age, and gender, where the odds of reporting high blood pressure increased with age and for males more than females. However, the relationship with income quintile, while statistically significant, appeared to be nonlinear according to individual coefficients for dummy coded variables. After aggregation of data at the health region level and for each income quintile for each gender separately, additional nonparametric analyses indicated nonlinearity for males with the second ($20,000 to $39,999 in Canadian $) and third ($40,000 to $59,999 in Canadian $) income quintiles demonstrating the highest relative rates of regional hypertension reports. Conversely, the income gradient for self-reported high blood pressure among females was linear and negative where regional hypertension rates increased for the lowest income groups and decreased for the highest income groups. As with the study on myocardial infarctions, there was significant global spatial autocorrelation for male and female hypertension rates with a similar East-West and North-South gradation. However, the prominent hot spot for high rates of regional hypertension was observed in Newfoundland according to LISA statistics. Additionally, the global spatial autocorrelations varied by income quintile and gender for which only the two lowest income groups demonstrated significant spatial trends for males. The middle income quintile ($40,000 to $59,999 in Canadian $) was the only group to not demonstrate significant geospatial trends for females.

Although education was not included in this particular study, the role of socioeconomic factors nevertheless appears significant for Canadian hypertension at the health region scale with respect to household income differences. Furthermore, similar interactions between gender and income have been noted previously (Leng et al., 2015; Loucks et al., 2007; Van Minh et al., 2006) and this may relate to the relatively greater sensitivity to neighborhood-environment and associated factors on females' health compared to males (Clougherty et al., 2011; Leng et al., 2015; Matheson et al., 2009). While this remains consistent with results of the previous study, the spatial trends observed in Chapter 7 varied from those of myocardial infarctions with regard to the particular regions identified within significant clusters. Specifically, a small segment of the North Atlantic in Newfoundland was identified as the prominent hot spot for clusters of high hypertension rates for both males and females and across income brackets, while British Columbia was consistently among the provinces to present cold spots of low rates. As previously noted, this geospatial disparity and its interaction with both gender and income could indicate a necessity for better geographic-based preventive medicine and cardiovascular public health with a focus on socioeconomically disadvantaged areas. The current spatial scale of analysis may be of particular relevance for public health endeavors given that the regional boundaries for each area are defined by administrative boundaries of local public health units.

While the previous two investigations employed total age-standardized rates, the study in Chapter 8 instead focused on older adult Canadians (≥ 65 years of age) and the proportion of those from each health region reporting high blood pressure (i.e., hypertension). Additional determinants of health were also employed including socioeconomic and behavioral factors. After properly accounting for model heteroscedasticity, the only statistically significant predictor of regional hypertension among older adult males was education and, as expected, this relationship was negative. However, a number of independent measures were significant for older adult female hypertension rates including regional drinking habits and older adult overweight or obesity, which were both positively related, as well as education, which was negative. Generalized modeling for both males and females combined further indicated a significant relationship between aggregate rates of self-reported hypertension with both education and overweight or obesity. Contrary to the preceding two studies of total age-standardized rates associated with cardiovascular health, including hypertension, the results from Chapter 8 did not indicate any strong spatial trends for older adult males or females.

Although the absence of any significant geospatial clustering for older adult hypertension rates was contrary to those found for total age-standardized rates, this should be unsurprising after considering the strong age-related components of hypertension (Lakatta, 1990; McEniery et al., 2007; Monahan, 2007) and, thus, that the presence of high blood pressure reports among older adults was evenly distributed across Canadian geography. However, the particularly strong relationship with regional education among older adults and rates of hypertension among this population was notable given that this stood out as one of the only significant linear predictors and, for males, was actually the only significantly associated variable. As previously noted, this could be related to an influence of health literacy (Gazmararian et al., 2003; van der Heide et al., 2013; von dem Knesebeck et al., 2006; Poureslami et al., 2016) which, according to the present results, could be a primary ecological concern for management of regional high blood pressure rates among aging populations in Canada.

9.4. Conclusions

While the methods and applications from the current series of studies were diverse in focus, the findings and associated inferences converge upon central themes relevant to cardiovascular health management; the varied roles of socioeconomic and environmental factors with applied quantitative methodologies for clinical and public health settings. To succinctly summarize, continued investigation of signal processing tools can enhance medical applications in electrophysiological measurement, space weather may contribute to this electrophysiology in a number of ways, this potential influence of space weather could extend to cardiovascular disease factors, and cardiovascular disease states are predominantly associated with socioeconomic and geographic factors at the ecological level. There remain many additional considerations to incorporate into future research that follow the current studies, however, the present results contribute to the growing interdisciplinary endeavors in cardiovascular health and provide a strong basis for further research employing greater resources.

References

Appelhans, B. M., & Luecken, L. J. (2006). Heart rate variability as an index of regulated emotional responding. *Review of General Psychology*, 10(3): 229-240.

Ayala, D. E., Hermida, R. C., Mojón, A., & Fernández, J. R. (2013). Cardiovascular risk of resistant hypertension: Dependence on treatment-time regimen of blood pressure-lowering medications. *Chronobiology International*, 30(1-2): 340-352.

Bayentin, L., El Adlouni, S., Ouarda, T. B. M. J., Gosselin, P., Doyon, B., & Chebana, F. (2010). Spatial variability of climate effects on ischemic heart disease hospitalization rates for the period 1989-2006 in Quebec, Canada. *International Journal of Health Geographics*, 9(5).

Billman, G. E. (2013). The LF/HF ratio does not accurately measure cardiac sympatho-vagal balance. *Frontiers in Physiology*, 4(26): 1-5.

Brennan, M., Palaniswami, M., & Kamen, P. (2001). Do existing measures of Poincaré plot geometry reflect nonlinear features of heart rate variability? *IEEE Transactions on Biomedical Engineering*, 48(11): 1342-1347.

Brosschot, J. F., van Dijk, E., & Thayer, J. F. (2007). Daily worry is related to low heart rate variability during waking and the subsequent nocturnal sleep period. *International Journal of Psychophysiology*, 63(1): 39-47.

Campbell, N., Young, E. R., Drouin, D., Legowski, B., Adams, M. A., Farrell, J., Kaczorowski, J., Lewanczuk, R., Lum-Kwong, M. M., & Tobe, S. (2012). A framework for discussion on how to improve prevention, management, and control of hypertension in Canada. *Canadian Journal of Cardiology*, 28(3): 262-269.

Cantwell, K., Morgans, A., Smith, K., Livingston, M., & Dietze, P. (2015). Temporal trends in cardiovascular demand in EMS: Weekday versus weekend differences. *Chronobiology International*, 32(6): 731-738.

Chen, Y., Rennie, D. C., Karunanayake, C. P., Janzen, B., Hagel, L., Pickett, W., Dyck, R., Lawson, J., Dosman, J. A., Pahwa, P., & Saskatchewan Rural Health Study Group. (2015). Income adequacy and education associated with the prevalence of obesity in rural Saskatchewan, Canada. *BMC Public Health*, 15.

Chizhevsky, A. L. alternately Tchijevsky, A. L. (1926). Physical factors of the historical process. *Annual Meeting of the American Meteorological Society*, 1926.

Chizhevsky, A. L. alternately Tchijevsky, A. L. (1936). *The Terrestrial Echo of Solar Storms* (translated). Moscow: Mysl'Press.

Choinière, R., Lafontaine, P., & Edwards, A. C. (2000). Distribution of cardiovascular disease risk factors by socioeconomic status among Canadian adults. *Canadian Medical Association Journal*, 162(9): S13-S24.

Clougherty, J. E., Eisen, E. A., Slade, M. D., Kawachi, I., & Cullen, M. R. (2011). Gender and sex differences in job status and hypertension. *Occupational and Environmental Medicine*, 68: 16-23.

Cornélissen, G., Halberg, F., Breus, T., Syutkina, E. V., Baevsky, R., Weydahl, A., Watanabe, Y., Otsuka, K., Siegelova, J., Fiser, B., & Bakken, E. E. (2002). Non-photic solar associations of heart rate variability and myocardial infarction. *Journal of Atmospheric and Solar-Terrestrial Physics*, 64(5-6): 707-720.

Čulić, V. (2014). Chronobiological rhythms of acute cardiovascular events and underlying mechanisms. *International Journal of Cardiology*, 174(2): 417-419.

Dimitrov, B. D., Valev, D., Werner, R., Atanassova, P. A. (2013). Cyclic patterns of malaria admissions in Papua New Guinea for the years 1987-1996. *Epidemiology and Infection*, 141(11): 2317-2327.

Dimitrova, S., Stoilova, I., & Cholakov, I. (2004). Influence of local geomagnetic storms on arterial blood pressure. *Bioelectromagnetics*, 25(6): 408-414.

Dimitrova, S., Mustafa, F. R., Stoilova, I., Babayev, E. S., & Kazimov, E. A. (2009). Possible influence of solar extreme events and related geomagnetic disturbances on human cardio-vascular state: Results of collaborative Bulgarian-Azerbaijani studies. *Advances in Space Research*, 43(4): 641-648.

Dimitrova, S., Angelov, I., & Petrova, E. (2013). Solar and geomagnetic activity effects on heart rate variability. *Natural Hazards*, 69(1): 25-37.

Durantin, G., Gagnon, J.-F., Tremblay, S., & Dehais, F. (2014). Using near infrared spectroscopy and heart rate variability to detect mental overload. *Behavioural Brain Research*, 259: 16-23.

Fujita, H., Acharya, U. R., Sudarshan, V. K., Ghista, D. N., Sree, S. V., Eugene, L. W. J., & Koh, J. E. W. (2016). Sudden cardiac death (SCD) prediction based on nonlinear heart rate variability features and SCD index. *Applied Soft Computing*, 43: 510-519.

Gang, Y. (2013). Heart rate variability: Measurements and risk stratification. In Gussak, I., & Antzelevitch, C. (eds.) *Electrical Diseases of the Heart*. London: Springer-Verlag.

Gazmararian, J. A., Williams, M. V., Peel, J., & Baker, D. W. (2003). Health literacy and knowledge of chronic disease. *Patient Education and Counseling*, 51(3): 267-275.

Guessous, I., Joost, S., Jeannot, E., Theler, J.-M., Mahler, P., Gaspoz, J.-M., & GIRAPH Group (2014). A comparison of the spatial dependence of body mass index among adults and children in a Swiss general population. *Nutrition and Diabetes*, 4(e111).

Halberg, F., Cornélissen, G., & Bakken, E. (1990). Caregiving merged with chronobiologic outcome assessment, research and education in health maintenance organizations (HMOs). *Progress in Clinical Biology Research*, 341B: 491-549.

van der Heide, I., Wang, J., Droomers, M., Spreeuwenberg, P., Rademakers, J., & Uiters, E. (2013). The relationship between health, education, and health literacy: Results from the Dutch Adult Literacy and Life Skills Survey. *Journal of Health Communication: International Perspectives*, 18(S1): 172-184.

Hoshi, R. A., Pastre, C. M., Vanderlei, L. C. M., & Godoy, M. F. (2013). Poincaré plot indexes of heart rate variability: Relationships with other nonlinear variables. *Autonomic Neuroscience: Basic and Clinical*, 177: 271-274.

Joffres, M. R., Ghadirian, P., Fodor, J. G., Petrasovits, A., Chockalingam, A., & Hamet, P. (1997). Awareness, treatment, and control of hypertension in Canada. *American Journal of Hypertension*, 10(10): 1097-1102.

Joffres, M. R., Campbell, N. R. C., Manns, B., & Tu, K. (2007). Estimate of the benefits of a population-based reduction in dietary sodium additives on hypertension and its related health care costs in Canada. *Canadian Journal of Cardiology*, 23(6): 437-443.

Kemp, A. H., Quintana, D. S., Felmingham, K. L., Matthews, S., & Jelinek, H. F. (2012). Depression, comorbid anxiety disorders, and heart rate variability in physically healthy, unmedicated patients: Implications for cardiovascular risk. *PLoS ONE*, 7(2).

Kleimenova, N. G., Kozyreva, O. V., Breus, T. K., & Rapoport, S. I. (2007). Pc1 geomagnetic pulsations as a potential hazard of the myocardial infarction. *Journal of Atmospheric and Solar-Terrestrial Physics*, 69(14): 1759-1764.

von dem Knesebeck, O., Verde, P. E., & Dragano, N. (2006). Education and health in 22 European countries. *Social Science and Medicine*, 63(5): 1344-1351.

Lakatta, E. G. (1990). Similar myocardial effects of aging and hypertension. *European Heart Journal*, 11: 29-38.

Lemmer, B. (2012). The importance of biological rhythms in drug treatment of hypertension and sex-dependent modifications. *ChronoPhysiology and Therapy*, 2: 9-18.

Leng, B., Jin, Y., Li, G., Chen, L., & Jin, N. (2015). Socioeconomic status and hypertension: A meta-analysis. *Journal of Hypertension*, 33(2): 221-229.

Levandovski, R., Harb, A., Bernardi, F., Allebrandt, K. V., & Paz Loayza Hidalgo, M. (2012). A chronobiological policy to decrease the burden of hypertension and obesity in low- and middle-income population. *Biological Rhythm Research*, 43(1): 81-102.

Lim, Y.-H., Hong, Y.-C., & Kim, H. (2012). Effects of diurnal temperature range on cardiovascular and respiratory hospital admissions in Korea. *Science of the Total Environment*, 417-418: 55-60.

Loucks, E. B., Rehkopf, D. H., Thurston, R. C., & Kawachi, I. (2007). Socioeconomic disparities in metabolic syndrome differ by gender: Evidence from NHANES III. *Annals of Epidemiology*, 17(1): 19-26.

Madrigano, J., Mittleman, M. A., Baccarelli, A., Goldberg, R., Melly, S., von Klot, S., & Schwartz, J. (2013). Temperature, myocardial infarction, and mortality: Effect modification by individual and area-level characteristics. *Epidemiology*, 24(3): 439-446.

Matheson, F. I., White, H. L., Moineddin, R., Dunn, J. R., & Glazier, R. H. (2009). Neighbourhood chronic stress and gender inequalities in hypertension among Canadian adults: A multilevel analysis. *Journal of Epidemiology and Community Health*, jech-2008.

McEniery, C. M., Wilkinson, I. B., & Avolio, A. P. (2007). Age, hypertension and arterial function. *Clinical and Experimental Pharmacology and Physiology*, 34(7): 665-671.

Mitsutake, G., Otsuka, K., Oinuma, S., Ferguson, I., Cornélissen, G., Wanliss, J., & Halberg, F. (2004). Does exposure to an artificial ULF magnetic field affect blood pressure, heart rate variability and mood? *Biomedical Pharmacotherapy*, 58: 20-27.

Monahan, K. D. (2007). Effect of aging on baroreflex function in humans. *American Journal of Physiology*, 293(1): R3-R12.

Mulligan, B. P., & Persinger, M. A. (2012). Experimental simulation of the effects of sudden increases in geomagnetic activity upon quantitative measures of human brain activity: Validation of correlational studies. *Neuroscience Letters*, 516(1): 54-56.

Murugan, N. J., Karbowski, L. M., Lafrenie, R. M., & Persinger, M. A. (2013). Temporally-patterned magnetic fields induce complete fragmentation in planaria. *PLOS One*. http://dx.doi.org/10.1371/journal.pone.0061714

Oinuma, S., Kubo, Y., Otsuka, K., Yamanaka, T., Murakami, S., Matsuoka, O., Ohkawa, S., Cornélissen, G., Weydahl, A., Holmeslet, B., Hall, C., & Halberg, F. (2002). On behalf of the "ICEHRV" Working Group: Graded response of heart rate variability associated with an alteration of geomagnetic activity in a subarctic area. *Biomedical Pharmacotherapy*, 56: 284-288.

Otsuka, K., Cornélissen, G., Weydahl, A., Holmeslet, B., Hansen, T. L., Shinagawa, M., Kubo, Y., Nishimura, Y., Omori, K., Yano, S., & Halberg, F. (2001a). Geomagnetic disturbance associated with decrease in heart rate variability in a subarctic area. *Biomedical Pharmacotherapy*, 55: 51-56.

Papailiou, M., Mavromichalaki, H., Kudela, K., Stetiarova, J., & Dimitrova, S. (2011). Effect of geomagnetic disturbances on physiological parameters: An investigation on aviators. *Advances in Space Research*, 48: 1545-1550.

Pouliou, T., & Elliott, S. J. (2009). An exploratory spatial analysis of overweight and obesity in Canada. *Preventive Medicine*, 48: 362-367.

Poureslami, I., Rootman, I., Pleasant, A., & FitzGerald, J. M. (2016). The emerging role of health literacy in chronic disease management: The response to a call for action in Canada. *Population Health Management*, 19(4).

Sakuragi, S., Sugiyama, Y., & Takeuchi, K. (2002). Effects of laughing and weeping on mood and heart rate variability. *Journal of Physiological Anthropology and Applied Human Science*, 21(3): 159-165.

Saranya, K., Pal, G. K., Habeebullah, S., & Pal, P. (2015). Analysis of Poincaré plot of heart rate variability in the assessment of autonomic dysfunction in patients with polycystic ovary syndrome. *International Journal of Clinical and Experimental Physiology*, 2(1): 34-39.

Stein, P. K., Domitrovich, P. P., Huikuri, H. V., & Kleiger, R. E. (2005). Traditional and nonlinear heart rate variability are each independently associated with mortality after myocardial infarction. *Journal of Cardiovascular Electrophysiology*, 16(1): 13-20.

Stoupel, E. (1999). Effect of geomagnetic activity on cardiovascular parameters. *Journal of Clinical and Basic Cardiology*, 2(1): 34-40.

Syutkina, E. V., Cornélissen, G., Grigoriev, A. E., Mitish, M. D., Turti, T., Yatsyk, G. V., Pimenov, K., Breus, T. K., Studenikin, M. Y., Siegelova, J., Fiser, B., Dusek, J., Johnson, D., & Halberg, F. (1997). Neonatal intensive care may consider associations of cardiovascular rhythms with local magnetic disturbance. *Scripta Medica*, 70: 217-226.

Van Minh, H., Byass, P., Chuc, N. T. K., & Wall, S. (2006). Gender differences in prevalence and socioeconomic determinants of hypertension: Findings from the WHO STEPs survey in a rural community of Vietnam. *Journal of Human Hypertension*, 20: 109-115.

Winkleby, M. A., Jatulis, D. E., Frank, E., & Fortmann, S. P. (1992). Socioeconomic status and health: How education, income, and occupation contribute to risk factors for cardiovascular disease. *American Journal of Public Health*, 82(6): 816-820.

Zenchenko, T. A., Jordanova, M., Poskotinova, L. V., Medvedeva, A. A., Alenikova, A. E., & Khorseva, N. I. (2014). Synchronization between human heart rate dynamics and Pc5 geomagnetic pulsations at different latitudes. *Biophysics*, 59(6): 965-972.